MACROMOLECULAR PERMEABILITY OF FENESTRATED CAPILLARIES IN THE RABBIT SUBMANDIBULAR GLAND

by

Peter David Spencer

A thesis presented towards the
degree of Doctor of Philosophy
in the University of London,
Faculty of Science.

Department of Physiology
Charing Cross Hospital
Medical School
London

April 1984

CHARING CROSS & WESTMINSTER
CHARING CROSS
MEDICAL SCHOOL LIBRARY

ABSTRACT

Organs with fenestrated capillaries, in general, are those in which large transcapillary fluxes of water and solutes occur. In the past, fenestrated capillaries have been regarded as having 'giant pores', possibly located at the fenestrae, which allowed relatively free passage of all molecular species. In recent years, however, evidence has been accumulating that fenestrated capillaries do restrict the passage of solutes on the basis of molecular size.

The experiments described in this thesis were designed to extend previous work in the submandibular gland, an organ whose capillaries are all of the fenestrated type. Two approaches were used:

a) transcapillary passage of radiolabelled albumin was followed in the in situ gland by taking tissue samples at various times after intravenous injection of the isotope, in both resting and secreting glands.

b) filtration coefficients and osmotic reflexion coefficients of raffinose, inulin and albumin were determined in the isolated perfused gland, using the osmotic transient method of Vargas and Johnson (1964).

The first technique yielded an albumin reflexion coefficient of at least 0.999. A mathematical model designed to interpret the results of the osmotic transient experiments showed that errors would arise in determining the reflexion coefficients of each of the test molecules, but for different reasons. Values for some of the important parameters used in the model are not currently available. Nevertheless, estimates of coefficients were made as follows:

filtration coefficient - 1 ml min^{-1} 100 g^{-1} mm^{-1} Hg

reflexion coefficient - raffinose - 0.05 - 0.2

- inulin - 0.3 - 0.4

- albumin - 0.8

These data indicate that the submandibular gland capillaries are at least as selective as capillaries of the continuous type.

ACKNOWLEDGEMENTS

"There are minds so impatient of inferiority that their gratitude is a species of revenge, and they return benefits, not because recompense is a pleasure, but because obligation is a pain."

(Samuel Johnson - The Rambler, 1751)

Clearly, it is not always a pleasure to publicly record a debt of gratitude. That it is so for me owes more to the manner in which that debt was accumulated than to any "patience of inferiority" which I might possess. Three people have been so influential on the course of this thesis that without any one of them I would not have been able to start, continue or complete it.

First, my supervisor Laurence Smaje, who always managed to find time to listen to my outrageous ideas, and brought me back to reality when I thought I had the answer to Life's problems.

John Gamble must the hardest working person I know. In between a punishing schedule of experiments and teaching, he takes on major singing roles and still manages to make time to sail his yacht at the weekend. It is to John that I am grateful for performing the lion's share of the work for the experiments described in Chapter 4.

Does a husband ever appreciate his wife's talents? Gill has uncomplainingly combined the roles of wife, mother, secretary, student, bringer of cups of coffee and many others besides. It is mainly due to her encouragement that the thesis was completed at all, and to her typing skill that it is presentable.

Of the many other people who have played a part, I would particularly like to mention Bill Penn, Chief Technician in the Physiology Department at Charing Cross, whose friendly and expert manner made it a pleasure to do experiments; and Gerry Rayman, who always reminded me that there was more to Physiology than animal experiments. To them and everyone else - thank you.

TABLE OF CONTENTS

	Page
Abstract	2
Acknowledgements	4
List of Figures	13
List of Tables	18
Chapter 1 - Introduction	20
1.1. Anatomy of Salivary Glands	23
1.1.1. Secretory Apparatus	23
1.1.2. Blood Supply	28
1.1.3. Nerve Supply	32
1.1.4. Lymphatics	33
1.2. The Secretion of Saliva	34
1.2.1. Vasodilatation	34
1.2.2. Epithelial Transport	36
1.3. Quantitative Description of Transport Properties of Membranes	39
1.3.1. Phenomenological Equations and Membrane Coefficients	40
1.3.2. Convection, Diffusion and Solvent Drag	42
1.3.3. Pores, Fibres and Vesicles	45
1.4. Techniques for Studying Solute Transport Particularly in Whole Organs	49
1.4.1. Ultrastructural Studies	51

Page

1.4.2. Indicator Diffusion Methods 52

1.4.3. Osmotic Transient Method, 55

1.4.4. Tissue Uptake Methods 59

1.4.5. Analysis of Lymph 61

1.5. Aims of the Present Studies 65

Chapter 2 - Transcapillary Passage of Radiolabelled Albumin and EDTA in the Rabbit Submandibular Gland 67

2.1. Introduction 68

2.2. Mathematical Model of Extravascular Albumin Accumulation 70

2.2.1. Model System 70

2.2.2. Assumptions of the Model 70

2.2.3. Equations Used 76

2.2.4. Iteration Technique 78

2.2.5. Values Used 79

2.2.6. Estimation of Permeability-Surface Area Product and Reflexion Coefficient of Albumin from Initial Rates of Extravascular Albumin Accumulation 81

2.3. Methods 84

2.3.1. Animals and Anaesthesia 85

2.3.2. Cannulations, Blood Pressure and Rectal Temperature Monitoring 85

2.3.3. Parasympathetic Nerve Stimulation 85

2.3.4. Counting of Radioisotope Activity 87

		Page
2.3.5.	Labelling of Rabbit Erythrocytes with ^{51}Cr	89
2.3.6.	Determination of Protein-Bound ^{125}I-labelled Albumin in Blood and Tissue Samples	89
2.3.7	Determination of the Amount of Cellular Binding of ^{51}Cr-EDTA and ^{125}I-HSA	91
2.3.8.	Measurement of Venous and Arterial Haematocrit	92
2.3.9.	Determination of Dynamic Intravascular Haematocrit	93
2.3.10.	Measurement of Transvascular Escape Rate of ^{125}I-labelled Albumin	95
2.3.11.	Measurement of Volumes of Distribution of Labelled Molecules	96
2.3.12.	Calculation of Volumes of Distribution of Labelled Molecules in Submandibular Glands	97
2.4.	Results	102
2.4.1.	Transvascular Escape Rate of ^{125}I-HSA	102
2.4.2.	Intraglandular Haematocrit	104
2.4.3.	Intravascular Volume	105
2.4.4.	Interstitial Volume	105
2.4.5.	Extravascular Accumulation of ^{125}I-labelled Albumin	108

Page

2.5. Comparison of Mathematical Model with Experimental Data 108

2.6. Discussion 118

2.6.1. Use of ^{125}I-HSA and ^{51}Cr-EDTA as Markers for the Various Volumes of Distribution in the Salivary Gland 118

2.6.2. Disappearance of Labelled Albumin from Plasma 120

2.6.3. Dynamic Haematocrit in Control and Stimulated Glands 124

2.6.4. Intravascular Volume, Capillary Surface Area and Capillary Recruitment During Nerve Stimulation 126

2.6.5. Exclusion of Albumin in the Interstitium 129

2.6.6. Permeability and Reflexion Coefficients of Albumin 134

Chapter 3 - A Model for Osmotically-Induced Weight Changes in the Submandibular Gland 138

3.1. Introduction 139

3.2. Description of the Model 144

3.2.1. Model System 144

3.2.2. Assumptions of the Model 146

3.2.3. Equations Used 147

3.2.4. Iteration Procedure 152

3.2.5. Testing the Model 158

3.2.6. Values of Parameters Used in the Model 161

Page

3.3. Correction of Estimate of Solute Reflexion Coefficient Obtained by 'Initial Slope' Method 164

3.4. Model Results 165

3.4.1. Venous Pressure Elevation 166

3.4.2. Osmotic Transient Using Albumin as the Test Solute 179

3.4.3. Osmotic Transient Using Inulin as the Test Solute 185

3.4.4. Osmotic Transient Using Raffinose as the Test Solute 196

3.5. Discussion 205

3.5.1. Transcellular Water Flux 206

3.5.2. Solute Buffering 207

3.5.3. Venous Pressure Elevation 208

3.5.4. Assumptions of the Model 213

Chapter 4 - Filtration and Reflexion Coefficients in the Isolated Perfused Rabbit Submandibular Gland 219

4.1. Introduction 220

4.2. Methods 221

4.2.1. Animals and Anaesthesia 221

4.2.2. Isolation of the Submandibular Gland and Transfer to Perfusion Circuit 221

4.2.3. Perfusion Circuits 223

4.2.4. Perfusing Solutions 226

Page

4.2.5. Measurement of Changes in Gland Weight 227

4.2.6. Measurement of Venous Pressure and Flow Rate 227

4.2.7. Experimental Protocol 228

4.2.8. Statistical Comparisons 230

4.3. Results 230

4.3.1. Measurement of Capillary Filtration Coefficient (K_f) 230

4.3.2. Reflexion Coefficient of Albumin 237

4.3.3. Reflexion Coefficients of Inulin and Raffinose 243

4.4. Discussion 249

4.4.1. Capillary Filtration Coefficient 249

4.4.2. Apparent Rectification of Volume Flux 251

4.4.3. Reflexion Coefficient of Albumin 256

4.4.4. Reflexion Coefficients of Inulin and Raffinose 258

4.4.5. Transport Pathways Across Capillary Endothelium in the Rabbit Submandibular Gland; Equivalent Pores and Fibre Matrix 260

Chapter 5 - Summary and Concluding Remarks 268

References 272

Appendix 1 - List of Symbols Used in Text 290

Page

Appendix 2 - Computer program for model of extravascular albumin accumulation 293

Appendix 3 - Computer program for osmotic transient model. 295

LIST OF ILLUSTRATIONS

		Page
Fig. 1.1.	Light microscope appearance of secretory apparatus in rat submandibular gland.	24
Fig. 1.2.	Dissection of the neck of a rabbit to show the major blood vessels supplying the parotid and submandibular gland.	29
Fig. 1.3.	Transport pathways across fenestrated capillaries.	50
Fig. 2.1.	Schematic diagram of model of extravascular albumin accumulation.	71
Fig. 2.2.	Cross channel correction formula for 3 isotopes.	88
Fig. 2.3.	Summary of experimental protocols - 2-isotope experiments	98
Fig. 2.4.	Summary of experimental protocols - 3-isotopes.	99
Fig. 2.5.	Schematic diagram of volumes of distribution of a solute in the gland and a blood sample.	100
Fig. 2.6.	Plasma concentration of ^{125}I-HSA as a function of time after the initial injection.	103
Fig. 2.7.	Extravascular volume of distribution of ^{125}I-HSA at various times after the initial injection, in control and in stimulated glands.	110
Fig. 2.8.	Model predictions of albumin accumulation - $\sigma_{alb}^{cap} = 0.99$.	111
Fig. 2.9.	Model predictions of albumin accumulation - $\sigma_{alb}^{cap} = 0.999$.	112

		Page
Fig. 2.10.	Model predictions of albumin accumulation - effect of changing PS_{alb}^{cap} and $V_{alb}^{int}(\infty)$ - control conditions.	115
Fig. 2.11.	Model predictions of albumin accumulation - effect of changing PS_{alb}^{int} and $V_{alb}^{int}(\infty)$ - stimulated conditions.	116
Fig. 2.12.	Model predictions of albumin accumulation - effect of changing lymph flow.	117
Fig. 2.13.	Pore size distribution of a fibre matrix.	132
Fig. 3.1.	Schematic diagram of components of osmotic transient model.	145
Fig. 3.2.	Normalized gland weight vs time following venous pressure elevation.	167
Fig. 3.3.	$\Delta w/\Delta t$ plotted against $\Delta \bar{P}^{cap}$ for venous pressure elevations.	168
Fig. 3.4.	$\Delta w/\Delta t$ vs time after venous pressure elevation of 10 mm Hg. $\Delta w/\Delta t$ plotted on a logarithmic scale to allow extrapolation to zero time.	170
Fig. 3.5.	Changes in intracapillary albumin and NaCl concentration along the length of the capillary during a 10 mm Hg venous pressure elevation.	172
Fig. 3.6.	$\Delta w/\Delta t$ and π^{cap} vs time following a 10 mm Hg venous pressure elevation.	174
Fig. 3.7.	10 mm Hg venous pressure elevation - effect of changing interstitial compliance.	175
Fig. 3.8.	10 mm Hg venous pressure elevation - effect of changing σ_{alb}^{cap}	177

Page

Fig. 3.9. 10 mm Hg venous pressure elevation - effects of changing σ_{alb}^{cap} on the time course of interstitial colloid osmotic pressure. 178

Fig. 3.10. Normalized weight changes produced by changing the perfusate albumin concentration to 8 g 100 ml^{-1} and 2 g 100 ml^{-1}. 180

Fig. 3.11. $\Delta w/\Delta t$ plotted against π^{cap} for the model runs illustrated in Fig. 3.10. 181

Fig. 3.12. Capillary pressure required to keep the gland isogravimetric when the albumin concentration of the perfusate is changed. 183

Fig. 3.13. Time course of gland weight when 10 mM inulin is added to the perfusate. 186

Fig. 3.14. 10 mM inulin transient - changes in interstitial and cell volumes. 187

Fig. 3.15. 10 mM inulin transient - effect of changing K_{cell}. 189

Fig. 3.16. Transcapillary osmotic pressure differences due to inulin, albumin and NaCl during a 10 mM inulin transient. 190

Fig. 3.17. 10 mM inulin transient - effect of changing σ_{alb}^{cap}. 194

Fig. 3.18. 10 mM inulin transient - $\Delta w/\Delta t$ plotted on a logarithmic scale to allow extrapolation to zero time. 195

Fig. 3.19. Time course of gland weight when 50 mM raffinose is added to the perfusate. Two values of K_{cell} are shown. 197

Fig. 3.20. 50 mM raffinose transient - changes in interstitial and cell volumes. 198

Page

Fig. 3.21. Transcapillary osmotic pressures due to raffinose, albumin and NaCl during a 50 mM raffinose transient. 199

Fig. 3.22. 50 mM raffinose transient - $\Delta w/\Delta t$ plotted on a logarithmic scale to allow extrapolation to zero time. 202

Fig. 3.23. 50 mM raffinose transient - effect of changing σ_{alb}^{cap}. 204

Fig. 4.1. Diagram of perfusion circuit for isolated submandibular gland. 224

Fig. 4.2. Arterial and venous pressures plotted against flow in the isogravimetric gland. 232

Fig. 4.3. Experimental record of gland weight changes in response to venous pressure elevation and depression. 235

Fig. 4.4. Rate of change of gland weight plotted against capillary pressure. 236

Fig. 4.5. Experimental record of gland weight changes in response to elevation and depression of perfusate albumin concentration. 238

Fig. 4.6. Rate of change of gland weight plotted against intravascular colloid osmotic pressure. 239

Fig. 4.7. Experimental record of weight changes during an inulin osmotic transient, with model fits of the data. 244

Fig. 4.8. Experimental record of weight changes during a raffinose osmotic transient, with model predictions using σ_{raff}^{cap} determined by the 'initial slope' method. 246

Page

Fig. 4.9. Same experimental record as Fig. 4.8. - model parameters adjusted to give better fits to the data. 247

Fig. 4.10. Model predictions of weight changes in response to an increase of venous pressure with subsequent return of pressure to baseline to illustrate apparent rectification. 253

Fig. 4.11. Reflexion coefficient as a function of molecular radius according to Drake and David (1978). 262

Fig. 4.12. Reflexion coefficient of a fibre matrix as a function of molecular radius - effect of changing r_f. 263

Fig. 4.13. Reflexion coefficient of a fibre matrix as a function of molecular radius - effect of changing ε. 264

LIST OF TABLES

		Page
Table 2.1.	Values of parameters used in model of extravascular albumin accumulation.	80
Table 2.2.	Arterial concentrations of ^{125}I-HSA at various times after injection of isotope.	102a
Table 2.3.	Intravascular volume, measured by ^{131}I-HSA injected 5 minutes before removal of the gland, in animals which had previously been given ^{125}I-HSA.	106
Table 2.4.	Volumes of distribution of ^{51}Cr-EDTA in control and stimulated glands, at various times after the injection of isotope.	107
Table 2.5.	Volumes of distribution of ^{125}I-HSA in control and stimulated glands, at various times after injection of isotope.	109
Table 2.6.	Capillary surface area in various organs.	128
Table 3.1.	Equations describing volume and solute fluxes between specific compartments in the model of osmotically induced weight changes.	149
Table 3.2.	Tests of the model - results of inserting 'extreme' conditions for various parameters on the output of the program.	159
Table 3.3.	Values of parameters used in the osmotic transient model.	162
Table 4.1.	Pre- and post-capillary resistance and filtration coefficients in the isolated, perfused submandibular gland.	231

Page

Table 4.2. Filtration and albumin reflexion coefficients determined by taking the fast and slow components of the albumin osmotic transient. 242

CHAPTER 1

Introduction

INTRODUCTION

A salivary gland may be defined as any tissue that discharges a secretion into the oral cavity (Young and van Lennep, 1978a). This definition will include many 'minor' glands which lie in the submucosa of the oral cavity and open to it via short ducts, as well as the 'major' glands, which lie at some distance from the mouth, and communicate via extraglandular ducts. The functions of saliva include lubrication of food, provision of digestive enzymes, wetting of fur to increase heat loss, and secretion of venom. Saliva was also believed to have magical, strength-giving properties; a vestige of this belief still remains in the practice of spitting on the hands before performing an arduous task. However, the main requirement for saliva is that there be plenty of it. Since the maximal salivation rate exceeds the resting plasma flow, there must be a substantial increase in blood flow to provide the water for the secretion. In addition, the barriers between blood and saliva (capillary endothelium, interstitium and salivary epithelium) must have the required properties to allow the rapid transport of water and nutrients for the secretory cells.

Until recently, most studies concerning transport in salivary glands have concentrated on the epithelial barrier, the fenestrated endothelium and short interstitial

diffusion distances being considered to offer negligible hindrance to solute movement. The fact that organs which can have high rates of water flux (eg kidney, intestine) generally have fenestrated capillaries has led to the belief that this type of endothelium is highly permeable to all solutes; indeed, it has been claimed in one student textbook of physiology (Selkurt, 1976) that fenestrated capillaries have 'giant pores' which allow molecules of any size to pass with relative ease.

All the capillaries of the submandibular gland are of the fenestrated type (Mohammed, 1975) and this organ has been used by Smaje and his colleagues to investigate the permeability properties of this type of endothelium. Certainly the permeability to small solutes, such as NaCl, sucrose, EDTA, vitamin B_{12} and inulin is very high (Mann, Smaje and Yudilevich, 1979a, b), but the authors were able to demonstrate restricted diffusion of the largest molecules through the endothelium. Koo, Smaje, Dzielgielewska, Spencer and Penn (1980) measured the concentrations of endogenous albumin and IgG in lymph from the cat submandibular gland and concluded that the permeability to these molecules was no higher than that found in organs in which the capillaries have a continuous endothelium.

In this introduction, the general anatomy and physiology of salivary glands is briefly reviewed, but the emphasis is on the structure of the capillary endothelium and the methods available to investigate solute transport across it.

1.1. Anatomy of Salivary Glands

1.1.1. Secretory Apparatus

Salivary glands are compound (ie the ducts are branched) and the ducts are specialized for secretion. Originally, glands were classified as mucous, serous or seromucous, according to the nature of the secretion and the histological appearance of the gland using the simple dyes then available (see Quintarelli (1963) for historical aspects). Newer histochemical techniques have shown that the the situation is much more complicated with, for example, a continuously variable ratio of carbohydrate to protein in secretory substances and changes with time in sialic acid and sulphate content. A reclassification of the cell types in strict histochemical terms "however commendable in principle ....., has only resulted in greater confusion, each author using his own interpretation of the terms ..." (Young and van Lennep, 1978b). In view of these complexities, Young and van Lennep have suggested using the terms, serous, mucous and seromucous in the 'classical' sense based on cell morphological characteristics as a convenient way of identifying cell types.

A diagrammatic representation of the secretory epithelium of the rat submandibular gland is shown in Fig. 1.1. Using the studies of Materazzi, Bondi, Beldoni and Maraldi (1976) and following the classification of Shackleford and Wilborn (1968), it is possible to identify the following structures in the rabbit submandibular gland:

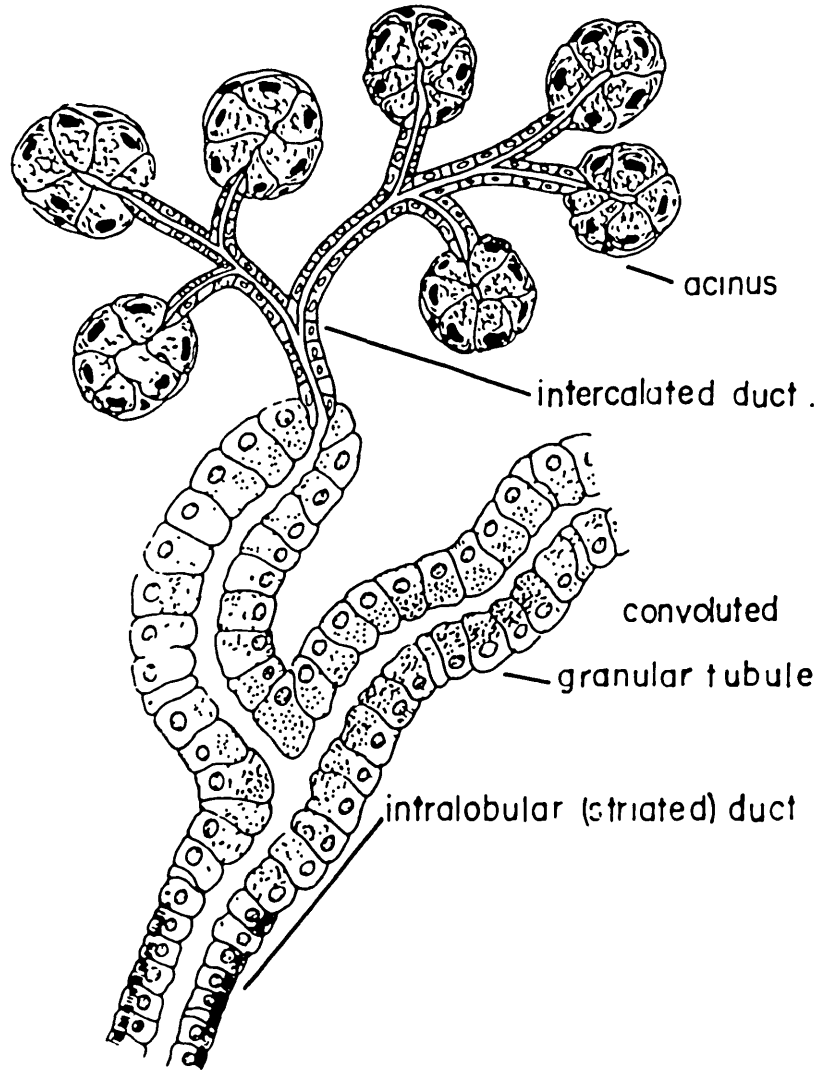


Fig. 1.1. Light microscope appearance of secretory apparatus in rat submandibular gland (from Leeson, 1959).

1. Secretory endpiece - central serous tubules with terminal and peripheral seromucinous acini; serous and seromucous cells.
2. Intercalated ducts - cuboidal epithelium surrounding a narrow lumen.
3. Striated ducts - these have a distinctive radial eosinophilic striation covering the basal third of the cell.

Ultrastructurally, serous endpiece cells have a broad base and a narrow apex, being described as pyramidal in shape. Each cell is surrounded by a plasma membrane which may have microvilli at the apex and which interdigitates laterally with the membrane of the neighbouring cells. The membrane at the base of the cell is smooth in the rabbit submandibular gland, although in some species there may be extensive infolding (eg Tandler and Poulsen, 1977).

The size, shape and density of the secretory granules in the acinar cells may vary considerably (eg Dorey and Bhoola, 1972) and depend on the fixative used. They are surrounded by a membrane which appears to be similar to the cell membrane, discharge of secretion taking place by fusion of the two membranes and establishment of discharge channels. Ichikawa (1965) noticed that the granules of the stimulated pancreatic acinus appeared to form 'chains' in which one granule fused with the cell membrane and others fused with the first to form a discharge channel. Whether this is a general feature of exocrine

glands is not known, but Amsterdam, Ohad and Schramm (1969) have noticed a similar phenomenon in rat parotid glands. It is not clear what causes enhancement of membrane fusion during stimulation. Although secretory granules are found close to the apical membrane in unstimulated glands, they apparently show little tendency to fuse. It has been suggested (Selinger, Sharoni and Schramm, 1974) that the granules form pseudopodia, and that this is inhibited when cyclic AMP is absent. Young and van Lennep (1978b) point out that pseudopod formation is likely to be due to the activity of actin filaments on the outside of the secretion granule, particularly since the pseudopodia are formed at the side of the granule facing the cell membrane.

The short intercalated ducts contain a flattened epithelium with a roughly spheroidal nucleus. In the rabbit submandibular gland, cells contain large granules that are believed to contain kallikrein and amylase (Dorey and Bhoola, 1972). Young and van Lennep (1978b) consider that these cellsshould be designated as part of the secretory endpiece. More recent immunocytochemical techniques have localized kallikrein largely in the striated duct cells of rat (Brandtzaeg, Gautvik, Nustad and Pierce, 1976), cat (Maranda, Rodriguez, Schachter, Shnitka and Weinberg, 1978), guinea-pig (Schachter, Maranda and Moriwaki, 1978) mouse (Simson, Chao and Margolius, 1978) dog and man (Matsuda, Moriwaki, Peret,

Schachter and Shnitka, 1979). Schachter (1980) believes that the studies demonstrating kallikrein-localization in the secretory endpiece were invalid "probably due to difficulties with earlier methods" but he concèdes that exceptions to an exclusively ductal location may be found.

Striated ducts have extensive infoldings of the basal cell membranes and numerous ellipsoidal mitochondria are found in the folds, with their long axes perpendicular to the duct lumen (eg Pease, 1956). The presence of plasma membrane infolding and an abundance of mitochondria strongly suggest an epithelium which transports water and electrolytes.

Cells lining the excretory ducts also have basal infoldings and numerous mitochondria. Several investigators (eg Knauf, 1972; Martin, Fromter, Gebner, Knauf and Young, 1973) have used the isolated excretory duct of the rabbit submandibular gland to investigate water and electrolyte transport, and it appears that the excretory ducts may play a role in determining the final composition of the salivary secretion.

Myoepithelial cells lie between the cell membrane of the secretory epithelium and the basement membrane. They are either multipolar or spindle-shaped, depending on whether they surround the secretory endpiece or the intercalated duct (Tamarin, 1966), and have a central cell body with a variable number of branching processes.

They have longitudinal cytoplasmic filaments. A contractile function in expelling secretion has been established in sweat glands (Hurley and Shelley, 1954) and mammary glands. Moreover, myoepithelial cells do resemble smooth muscle cells and do contain myosin (Archer and Kao, 1968). Also, rises in pressure in salivary ducts can be induced by pharmacological means (eg Emmelin, Garrett and Ohlin, 1968), and these are associated with neither vasodilatation nor secretion, so seem to have been produced by a contractile element in or around the secretory apparatus.

1.1.2. Blood Supply

The arterial blood supply to the rabbit submandibular gland is via a branch of the external maxillary artery, itself a branch of the external carotid artery (Figure 1.2). The artery enters the gland, together with the main venous drainage, nerves and excretory duct, at the hilus of the gland and then divides. The vessels generally follow the intralobular ducts and break up into the capillary networks which surround the acini and ducts. All the capillaries in the rabbit submandibular gland have a fenestrated endothelium (Mohammed, 1975).

There has been a controversy over whether the acinar and ductal circulations are arranged in series or in parallel, and also over the possible presence of arterio-

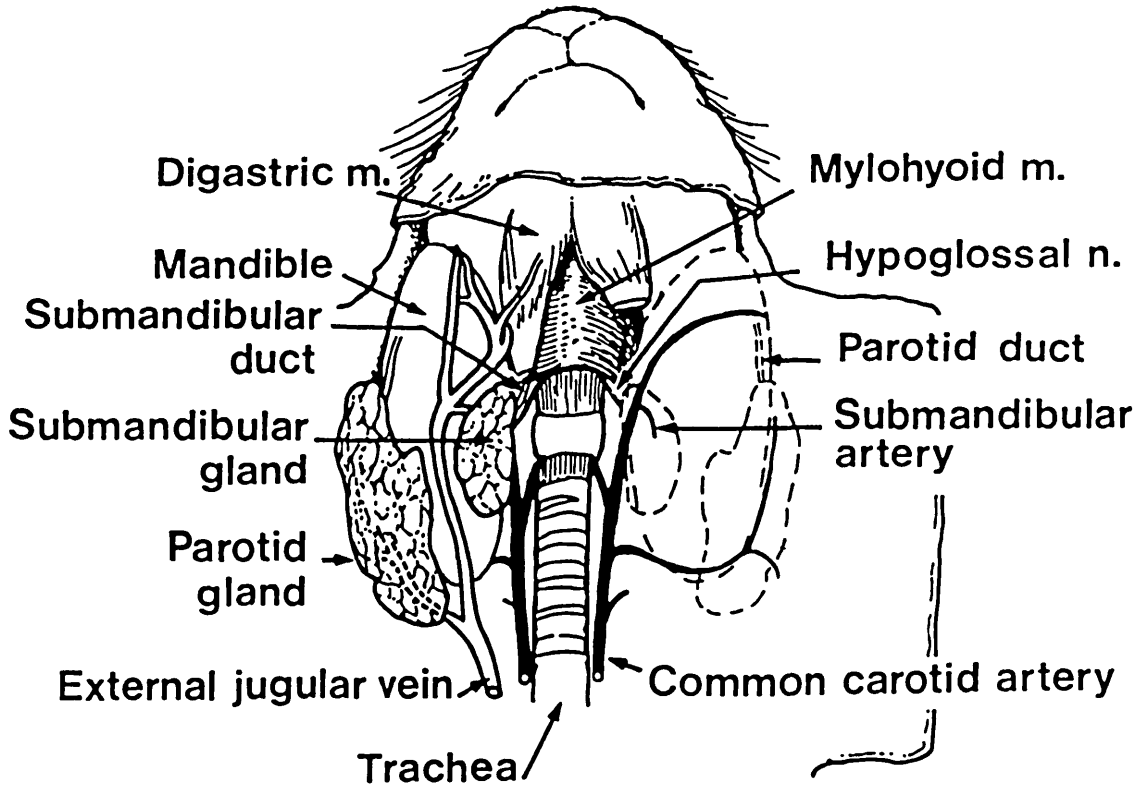


Fig. 1.2. Dissection of the neck of a rabbit to show the major blood vessels supplying the parotid and submandibular salivary glands. (Smaje and Henderson, 1984).

venous anastomoses in the gland. Kowalewsky (1885) first suggested that the acinar and ductal circulations were in parallel, a conclusion supported by the more recent work of Fraser and Smaje (1977). The latter authors found that parasympathetic nerve stimulation elicited different patterns of blood flow in the two circulations, flow in the whole gland increasing at the same time as acinar flow was decreasing and ductal flow was increasing. Also, 16 μm microspheres injected close-arterially were trapped in both acinar and ductal capillaries, and were absent from the venous effluent. The conclusions drawn from these studies were that the acinar and ductal circulations were arranged in parallel, and that arteriovenous anastomoses were not present in large numbers.

Suddick and Dowd (1969), using injections of silicone rubber and of India ink in the rat submandibular gland described structures which "may represent arteriovenous anastomoses" (their words, my underlining). This conclusion is arrived at by the observation of a network of vessels, referred to as the "intermediate arteriolar plexus", which is composed of "arteriole and metarteriole-sized vessels; interconnections were observed between larger vessels in the plexus".

Burgen and Seeman (1958) argued that the two circulations were in series with blood flowing counter-current to the flow of saliva. This is in contrast to the report of Blair-West, Coghlam, Denton et al (1969),

who agreed that the circulations were in series but concluded that the blood flow was concurrent with the saliva flow.

Recently, Ohtani and his colleagues (Ohtani, Kikuta, Ohtsuka et al, 1983; Ohtani, Ohtsuki, Lipsett and Gannon, 1983) have used corrosion casting and scanning electron microscopy to investigate the microvascular organisation of the salivary glands of the rat. They found that the intralobular duct capillaries receive blood from the acinar capillaries through portal venules (ie a concurrent series arrangement) but that the interlobular excretory ducts receive blood directly from the interlobular arteries (ie the excretory duct circulation is in parallel with that of the acini and striated ducts). They observed no arteriovenous anastomoses, but a number of arterio-arterial and veno-venous anastomoses were seen along the excretory duct. Ohtani, Ohtsuka, Lipsett and Gannon (1983) argue that the results of Fraser and Smaje (1977) are consistent with the scanning electron-microscope observations, and the difference between the conclusions "are only in the distance down the salivary duct system that a circulation independent of that around the acini begins". This statement appears to ignore the fact that Fraser and Smaje (1977) found differences in flow responses in acini and <u>intralobular</u> ducts. Whether the differences are due to interspecies variation or whether some other explanation (such as acinar capillary recruitment without ductal recruitment in response to parasympathetic nerve

stimulation) is responsible awaits a scanning electron-microscope study in the rabbit submandibular gland.

The arrangement of the salivary gland microcirculation has important implications for the site of water transport in stimulated glands (Fraser, 1976) and also for the interpretation of permeability studies, particularly the single-passage indicator dilution technique (Mann, Smaje and Yudilevich, 1979a). A portal arrangement of vessels would lead to greater heterogeneity of capillary lengths (and hence transit times). Levitt (1970) has argued that this could lead to major errors in determination of the permeability-surface area product (PS). This would be particularly serious if precession of small solutes occurred between the two sets of capillaries.

1.1.3. Nerve Supply

The salivary glands of all animals receive innervation from both the parasympathetic and sympathetic divisions of the autonomic nervous system, but while parasympathetic stimulation consistently evokes a copious secretion, sympathetic stimulation does so only in some species.

Parasympathetic fibres to the submandibular gland leave the cranium in the facial nerve and run in the chorda tympani. This joins the lingual nerve and in some species the submandibular fibres enter the submandibular ganglion. Only a few fibres synapse here, and so the

fibres passing along the salivary duct to enter the gland at the hilus are both pre- and post-ganglionic. Within the gland the fibres follow the subdivisions of the ductal and vascular tree.

Ultrastructural studies reveal a variable density of innervation around ducts and secretory endpieces (eg Garrett, 1972), with both cholinergic and adrenergic endings being present. Recently, Lundberg (1981) has provided evidence that some nerve endings contain both acetylcholine and vasoactive intestinal peptide (VIP); this may have an important bearing on the relationship between vasodilatation and secretion (see Sections 1.2.1 and 1.2.2 of this thesis).

1.1.4. Lymphatics

Very little is known about the intraglandular lymphatic arrangement in salivary glands. In the human parotid, Sviridova (1970) concludes that the lymphatics originate in the interstitium around "primary lobules", which are defined as containing secretory endpieces, intercalated ducts and terminal striated ducts. In the rabbit submandibular gland Wensel (1967 - quoted in Young and van Lennep, 1978b) found that there were no lymphatic capillaries around secretory endpieces or intercalated ducts. A periductal sheath of fine lymphatic capillaries anastamoses with a network surrounding the blood vessels, the whole system following the branching system of ducts

and blood vessels. Eventually, the lymphatics leave the gland, usually along the main blood vessels.

1.2. The Secretion of Saliva

1.2.1. Vasodilatation

It has been known for well over a hundred years (Bernard, 1858) that salivary secretion induced by parasympathetic nerve stimulation is accompanied by a marked increase in gland blood flow and a reddening of the venous outflow. It has been known for almost as long (Heidenhain, 1872) that atropine blocks salivation. In some glands, such as cat and dog submandibular glands, the vasodilatation persists, but in others, eg rabbit submandibular gland the vasodilatation is blocked also.

A special set of vasodilator nerves was postulated to explain the atropine-resistant vasodilatation. Barcroft (1914), however, thought that the vasodilatation was due to metabolites. Terroux, Sekelj and Burgen (1959) found that atropine largely inhibited the rise in oxygen consumption induced by parasympathetic nerve stimulation in the dog submandibular gland. Ungar and Parrot (1936) suggested that the vasodilatation was due to a substance kallikrein which was also a hypotensive agent. Kallikrein was subsequently shown to be a proteolytic enzyme which split polypeptides such as bradykinin from plasma kininogens (see Schachter, 1980). The work of Hilton and Lewis (1955a,b)

supported this proposal. However, Ferreira and Smaje (1976) found that the vasodilatation in the dog submandibular gland persisted after atropine but that kinins disappeared from the venous effluent, despite the infusion of bradykinin-potentiating peptides. Maranda et al (1978) found that stimulation of the sympathetic nerve supply to the cat submandibular gland caused most of the kallikrein-containing granules of the ductal cells to discharge into the lumen of the secretory system; parasympathetic stimulation caused no such discharge, despite the production of copious quantities of saliva and a large increase in gland blood flow. In the cat submandibular gland Darke and Smaje (1972) found a biphasic increase in blood flow, with the second (maintained) phase increasing with increasing stimulation frequency. At low stimulation frequencies (1 - 5 Hz) both phases were reduced by atropine whereas at high stimulation frequencies (10 - 20 Hz) the maintained phase was not inhibited.

A recent development in the cat submandibular gland has been the demonstration of the coexistence of acetylcholine and vasoactive intestinal peptide (VIP) in the same neurone (Lundberg, 1981). VIP was released during parasympathetic nerve stimulation of the gland. The venous concentration of VIP increased with increasing stimulation frequency, but at any single frequency did not reach a maximum until about 5 minutes after the beginning of stimulation. Lundberg (1981) confirmed the observations

of Darke and Smaje (1972) concerning the dependence of both the vasodilator response and the effect of atropine upon stimulation frequency, but also found that VIP output was increased by atropine administration. Infusion of VIP antiserum reduced both vasodilatation and salivary secretion in response to nerve stimulation while infusion of exogenous VIP produced an atropine-resistant vasodilation but no secretion. VIP also potentiated the secretion induced by infusion of acetylcholine. From these findings, Lundberg (1981) concluded that VIP acted as a neuromodulator for secretion and as a neurotransmitter for vasodilatation, whereas acetylcholine acted as a neurotransmitter for both secretion and vasodilatation. It appears that the wheel has turned full circle and we are back to the concept of vasodilator nerves, at least in the cat submandibular gland.

1.2.2. Epithelial Transport

A vast literature has arisen concerning the transport of water, electrolytes and proteins into saliva, and it would be inappropriate to review this in any detail in this thesis. Essentially, the two stage-hypothesis of Thaysen, Thorn and Schwartz (1954) has become accepted by most investigators. The essential points of this hypothesis are:-

1. An isotonic primary fluid rich in sodium is produced by the salivary endpiece.

2. The primary fluid is modified by the duct system, by sodium and chloride reabsorption in excess of water and potassium secretion, rendering the final saliva hypotonic.

Although Thaysen et al (1954) proposed this hypothesis, their experimental work did not provide direct evidence for it. The fact that, for example, the sodium content of human parotid saliva increases with increasing flow rate is consistent with the hypothesis but not proof of it. However, subsequent micropuncture studies have indicated that the mechanism proposed by Thaysen et al does indeed occur in the glands so far investigated.

Since the osmolality of the primary fluid appears to be largely independent of its rate of formation, it is thought likely that secretion occurs via secretory canaliculi with the creation of standing osmotic gradients (Diamond and Bossert, 1967). This implies the existence of an epithelium with a relatively high hydraulic conductivity. Although the primary fluid appears not to be simply a modified ultrafiltrate of plasma (as suggested by Shannon, Suddick and Dowd, 1974), yet it would be wrong to totally disregard any effect of hydrostatic or osmotic pressure upon the rate of fluid secretion. After all, unless water is actively transported, the fluid flux across the epithelium will depend upon the balance of hydrostatic and osmotic pressures across it. A rise in interstitial hydrostatic pressure due to increased capillary filtration, or a fall in intraductal pressure after expulsion of the

initial preformed saliva, will cause a greater trans-epithelial fluid flux for the same osmotic gradient. This is supported by the demonstration of an inverse relationship between salivation rate and colloid osmotic pressure in the solution perfusing the isolated rabbit submandibular gland (Gamble, Smaje and Young, 1983). However, in the same preparation there was an inverse relationship between venous hydrostatic pressure and salivation rate. This latter result may have been due to lack of substrate for the epithelial cells, since perfusate flow rate slowed during venous pressure elevation.

The proposed ductal modification of the primary secretion implies an epithelium with a very low hydraulic conductivity. This point could be investigated by measuring the concentrations of a substance which is either freely filtered or secreted in known concentrations in the acini, and is not reabsorbed or secreted in the ducts (in a manner analogous to inulin in the mammalian kidney). In the rabbit parotid gland, Mangos, McSherry, Irwin and Hong (1973) found that the concentration of amylase, an endogenous secretory macromolecule, did not change from primary fluid to final saliva for flow rates above 90 $\mu l\ min^{-1}g^{-1}$. Below this flow rate the amylase concentrations in final saliva were higher than that in the primary fluid, implying some reabsorption of water. Mangos et al (1973) calculated that almost 20% of the secreted water was reabsorbed at the lowest flow rate ($7.8\ \mu l\ min^{-1}g^{-1}$). Amylase is not secreted by the rabbit

submandibular gland in high enough concentrations to allow determination of concentration in the very small sample volumes obtained, and so Mangos et al (1973) perfused the main duct with hypotonic saliva containing ^{14}C-inulin. Their results indicated that at very low flow rates, 15% of the water delivered to the duct was reabsorbed.

These results confirm the low hydraulic conductivity of the ductal epithelium and suggest that water reabsorption along the ducts is unimportant when the gland is stimulated to secrete.

For a fairly recent review of the literature on epithelial transport in salivary glands, see Young and van Lennep (1978a) or Young and Schneyer (1981).

1.3. Quantitative Description of Transport Properties of Membranes

Experimentally, information about the permeability properties of membranes is obtained by measuring fluxes of water and/or solutes in relationship to differences in concentration, hydrostatic pressure or electrochemical potential across the membranes. In order to interpret the experimental data in terms of membrane structure and the nature of the transport process a model must be set

up. Such a model may be one of two basic types:

a) phenomenological - this relates the fluxes to the forces which produce them via a set of "membrane coefficients". Such an approach cannot, of course, give any information about the microscopic mechanisms of transport but it may help in excluding some mechanisms.

b) mechanistic - such an approach tries to throw light on the molecular mechanisms of transport, eg vesicles, large and small pores, active transport. A mechanistic model must be consistent not only with the phenomenological model set up for the particular experimental situation, but also with morphological data and other mathematical and thermodynamic constraints.

1.3.1. Phenomenological Equations and Membrane Coefficients

Kedem and Katchalsky (1958) are generally credited with providing the first description of flux equations, based on the applications of irreversible thermodynamics to solute and water flow across membranes. It is important to note (Katchalsky and Curran, 1965) that the system has to be not too far from equilibrium and the processes have to be slow in order for the dissipation function ϕ (which represents the rate of decrease of free energy due to the irreversible process) to be equal to the sum of the products of the fluxes and their appropriate driving forces.

It is generally held that three membrane coefficents are sufficient to characterise the permeability properties of a particular membrane; the hydraulic conductivity (L_p), the solute permeability coefficient (P), and the solute reflexion coefficient (σ_s). These coefficients can be related by a pair of equations known as the Kedem-Kalchalsky equations, although they were first derived by Staverman (1951):

$$J_v = L_p S(\Delta P - \sigma_s \Delta \pi) \qquad 1.1$$

$$J_s = PS\Delta C + J_v(1 - \sigma_s)\bar{C}_s \qquad 1.2$$

where J_v and J_s are respectively transmembrane volume and solute flux; S is the membrane surface area; ΔP, $\Delta \pi$ and ΔC are respectively the difference in hydrostatic pressure osmotic pressure and solute concentration across the membrane, and $\bar{C}_s$ is the average concentration of solute in the membrane. These equations have been widely used, but are subject to several criticisms (eg Hill, 1979; Ogston and Michel, 1978). In particular, the meaning of $\bar{C}_s$ is unclear. It has been taken as the average concentration of solute (either arithmetic or logarithmic) between the solutions on either side of the membrane, but the actual membrane concentration will depend upon the exclusion of solute from the membrane and the flow regime.

It is usually assumed that σ_s is the same in both equations 1.1. and 1.2. For this to be true, "Onsager reciprocity" must hold, which itself assumes that osmotic volume flow and hydrostatic pressure-driven flow are

similar processes. Hill (1979) has pointed out that Onsager symmetry can never be proved until we have "a full description of osmosis in physical terms (hydrostatic and kinetic)".

An alternative expression for solute flux has been employed by several authors (eg Brace, Granger and Taylor, 1978; Katz, 1980; Patlak, Goldstein and Hoffman, 1963).

$$J_s = J_v(1 - \sigma_s)C_1 + \frac{J_v(1 - \sigma_s)\Delta C}{(e^{\lambda} - 1)} \qquad 1.3.$$

where C_1 is the solute concentration on the side of the membrane from which net water flux occurs and $\lambda = J_v(1 - \sigma_s)/PS$. This is in fact the more general expression of solute flux from which equation 1.2. may be obtained by a linearization procedure (Thomas and Mikulecky, 1978), and so is subject to the same criticisms as the linear equation. However it does not assume a particular form of concentration profile through the membrane, and so "as soon as the actual profile differs significantly from the diffusion profile, the Kedem-Katchalsky linearization becomes a poor approximation to the actual, nonlinear, solute flow." (Thomas and Mikulecky, 1978).

1.3.2. Convection, Diffusion and Solvent Drag

Much effort has gone into determining whether convection or diffusion is the major mechanism for transcapillary exchange of solutes, particularly macromolecules.

The linear equation 1.2. can be divided conveniently into separate contributions of diffusion ($J_s^d = PS\ \Delta C$) and solvent drag ($J_s^c = (1 - \sigma_s)J_v\bar{C}_s$) to solute flux, so the ratio of diffusive to convective flow may be expressed as:

$$\frac{J_s^d}{J_s^c} = \frac{PS\Delta C}{(1 - \sigma_s)J_v\bar{C}_s} \qquad 1.4.$$

Even a brief glance at this equation shows that the ratio of diffusive to convective solute flux depends upon the solute concentrations on either side of the membrane and the volume flux as well as on the membrane coefficients. A common experimental approach is to inject a tracer at time zero and follow its disappearance from the blood and its appearance in the tissue of interest. It is evident that at zero time, there is no solute outside the capillaries, and so the term $\Delta C/\bar{C}_s$ reduces to 2 or ∞ depending upon the expression used for $\bar{C}_s$ [either $(C_1 + C_2)/2$ or $\ln (C_1 - C_2)/C_1/C_2$, where C_2 is the solute concentration on the side of the membrane into which net water flux occurs]. Also, at higher J_v, convection will make a larger contribution to solute flux. It will also be seen from Eqn. 1.4. that net solute flux may be zero or negative (ie in the opposite direction to J_v) if J_v is in the direction opposite to that of the downhill concentration gradient. For $J_s = 0$

$$J_v = \frac{PS\Delta C}{(1 - \sigma_s)\bar{C}_s} \qquad 1.5.$$

Noer and Lassen (1979) attempted to show that filtration was the dominant mechanism for albumin transport in human muscle and subcutaneous tissue. They injected radiolabelled albumin into these tissues in the leg and followed the disappearance of label from the injection site and its appearance in the plasma. They found that when the leg was about 25 cm below heart level, so as to retard lymphatic return, very little tracer was found in the blood. They assumed that because there was little backflux in the leg down position, the same applied to the horizontal position. Their interpretation of this result was that albumin crosses the capillary wall mainly by filtration through "big leaks". However, the leg down position, by increasing capillary pressure and hence J_v, is just the condition required to oppose diffusional albumin flux from the interstitium to the capillaries. Also, there appears to be no good justification for assuming a retardation of lymph flow in the leg down position; indeed, with the increased filtration, lymph flow might even increase. Thus their ratio of 0.01 for (local back transport)/(out transport) is likely to be an underestimate.

The problem with determining the dominant mechanism for macromolecular transport is that PS is of the same order as $(1 - \sigma_s)J_v$ and so the dominance of diffusion or convection will depend crucially upon J_v and measurements of J_v, PS and σ_s. In the discussion after the paper by Noer and Lassen (1979), Renkin points out that diffusion dominates in macromolecular transport at low lymph flows,

and convection is predominant at high lymph flows. The figure he presents (see also Renkin, Joyner, Sloop and Watson, 1977) appears to show that the data for albumin from lymph protein clearance in the dog paw can be fitted quite well by $\sigma = 0.83$ and $PS = 0.47 \times 10^{-4}$ ml.s^{-1}, using the analysis of Perl (1975). However, a careful inspection of this figure reveals that the lymph protein clearance appears to be reaching a plateau up to a lymph flow of about 4×10^{-4} ml.s^{-1}, and then rises again at higher lymph flows. This effect is least noticeable for albumin but more marked for globulin, Dextran-110 and fibrinogen-macroglobulin. Renkin himself admitted that a permeability change could occur above 45 mm Hg venous pressure, with "a big step in protein transport and lowering of discrimination", and it could be argued that diffusion would predominate even at high lymph flows if it were not for this alteration in permeability. For example, the albumin data of Renkin et al (1977) could be fitted by $PS = 0.8$, $\sigma = 1$ for lymph flows up to 4×10^{-1} ml.s^{-1} and the data for the other macromolecules can similarly be fitted by an alteration in PS with $\sigma = 1$ up to the same lymph flow.

1.3.3. Pores, Fibres and Vesicles

The idea of 'pores' as minute channels to allow the passage of materials between compartments is not new. Harvey (1628) surmised that there were "porosities in the

flesh and solid parts which are pervious to the blood ", when wondering how blood travelled from arteries to veins. However, Virchow (1859) stated that "Even the minute pores, which have recently been observed in different parts, have not, upto the present time, met with their counterparts in the capillary membrane, and when the porosity of this membrane is spoken of, the expression can only be admitted in a physical sense, as applying to invisible, really molecular, interstices. A film of collodion is not more homogenous, nor more continuous, than the membrane of a capillary." This view of the capillary could not really be changed until the electron microscope revealed that "molecular interstices" really did exist. This, together with the work of Starling (1896) and Landis (1927) on filtration, and Pappenheimer, Renkin and Borrero (1951) on filtration and diffusion, led capillary physiologists to regard intercellular channels as the major pathway for solute transport. Until recently, the permeability properties of capillaries have been attributed to one or more systems of water-filled pores connecting the capillary lumen with the interstitium. The geometry, size and density (number per unit capillary surface area) of the pores have been the subject of debate for the past 30 years. Pappenheimer et al (1951) envisaged a single "equivalent pore radius" for cylindrical channels, but Grotte (1956), using much larger tracer molecules, introduced the idea of large pores through which macromolecules could pass. The "two-pore" idea has enjoyed much popularity and the

debate concerning the size and location of the pores continues. "Three-pore" models (Taylor and Granger, 1983) or continuous distributions of pore sizes (eg Johnson, Levitt, Wangensteen and Bloom, 1975) have been put forward to explain data obtained by a variety of physiological methods.

However, the electron microscope revealed other potential candidates for transport pathways, including vesicles and fenestrae. There was also a complication in that the 'simple' capillary membrane appeared to be lined by a glycoprotein 'endocapillary layer' (Luft,1966) and was enclosed by a condensation of collagen, the basement membrane (Bennet, Luft and Hampton, 1959).

The electron microscope has also been used to follow the pathways followed by electron-dense tracers across the capillaries. Most of the tracer electron micrograph studies have employed large molecules, and these have clearly been shown to enter vesicles (Palade, Simionescu and Simionescu, 1979). Simionescu, Simionescu and Palade (1972) found that molecules 10 - 30 nm in diameter could pass through fenestral diaphragms. Small solutes can of course pass through most of these pathways, but there is evidence (eg Curry, Mason and Michel, 1976) that some water passes through an 'exclusive' channel (presumably the cell membrane). In fenestrated capillaries this pathway cannot account for a large fraction of the total water transport, since the capillaries are so highly permeable to small solutes.

The endocapillary layer described by Luft (1966) and the intercellular cement idea of Chambers and Zweifach (1947) have recently been given a quantitative form by the fibre matrix theory (Curry and Michel, 1980). In essence this states that the permeability properties of the capillary wall are determined by a fibrous lining rather than the size of any pores. This could explain why fenestrated capillaries are highly permeable to small molecules (Mann, Smaje and Yudilevich, 1979a) yet retain their impermeability to macromolecules (Koo et al, 1981; Granger and Taylor, 1980). A similar situation could exist, however, if there were a log-normal distribution of pore sizes (Johnson et al, 1975) or if each pore varied in size with time.

Until fairly recently, the interstitium has been ignored as a structure which could exert any influence on exchange of substances. However the demonstration by Guyton (1963) that 'tissue pressue' could change markedly with interstitial fluid volume led to its recognition. The fact that the interstitium could exclude molecules from a portion of the space available to water, and could retard the movement of molecules across it (see Comper and Laurent, 1979 for review) led Watson (1980) to argue that it was the interstitial matrix, and not the capillary wall, which was the major barrier to water and solute movement. Watson states that restricted diffusion across capillary walls has not been demonstrated using the single-passage indicator technique, which gives the best estimate of capillary wall permeability. This appears not be the

case for the cat submandibular gland (Mann, Smaje and Yudlilevich, 1979a,b). Also, while the interstitium may form a major barrier in such tissues as mesentery and dog paw, where the interstitial distances are large, this may not be the case for the salivary glands, where the distances involved are comparable to the diameter of a capillary.

Figure 1.3. is a schematic diagram of the possible pathways for solute transport across fenestrated endothelium.

1.4. Techniques for Studying Solute Transport, Particularly in Whole Organs

A wide variety of techniques has been used to study transcapillary movement of water and solutes, both in single capillaries and in whole organs; each approach has its particular advantages and limitations. Apart from electron-microscope studies, the single capillary approach has not been widely applied in organs with fenestrated capillaries; for this reason, and also because the experiments described in this thesis were performed on entire salivary glands, this section concentrates on 'whole-organ'techniques.

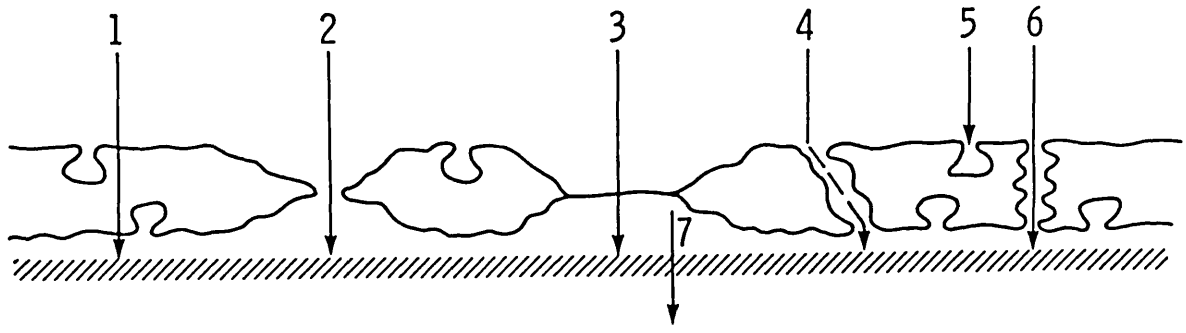


Fig. 1.3. Transport pathways across fenestrated capillaries

1. Cell membrane
2. open fenestrae
3. diaphragmed fenestrae
4. intercellular junctions
5. pinocytotic vesicles
6. transendothelial channels
7. basement membrane

(After Granger and Barrowman, 1983)

1.4.1. Ultrastructural Studies

As mentioned in Section 1.3., electron-dense tracers have been used to follow the pathways taken by the tracers across the capillary wall. Quantitation in a limited way has been possible by looking at the time course of vesicular labelling or concentration gradients in the intercellular junctions. In fenestrated capillaries, horseradish peroxidase (diameter $\sim$ 5 nm) leaves the plasma through the fenestrae and reaches the pericapillary spaces within 1 min (Clementi and Palade, 1969). In muscle capillaries, Karnovsky (1967, 1970) showed that molecules the size of horseradish peroxidase (5 nm) and cytochrome C (3 nm) could pass through the intercellular junctions, whereas Bruns and Palade (1968) and Simionescu Simionescu and Palade (1973, 1975) found that the junctions were impermeable to molecules ranging in diameter from heme-peptides (2 nm) to ferritin (11 nm), while the vesicles were labelled. This controversy is not yet resolved.

Although a number of investigators have determined how tracers cross the capillary wall, far less attention has been paid to their subsequent fate. Published photographs seem to show tracer accumulation in the pericapillary spaces, usually between the capillary and the basement membrane. Bruns and Palade (1968) and Clementi and Palade (1969) concluded that the basement membrane of muscle and intestinal capillaries was freely permeable to ferritin.

Johansson (1979), using interstitially injected ferritin in rat skeletal muscle found a large concentration difference across the basement membrane. Johansson (1979) also found rapid labelling of abluminal vesicles with interstitially injected horseradish peroxidase. An interesting additional finding in this study was that perfusion of the muscle with a venous outflow pressure of +10 cm H_2O resulted in a decrease in the density of abluminal vesicles and a diminished endothelial cell thickness as compared with perfusion with a venous outflow pressure of -4 cm H_2O.

1.4.2. Indicator Diffusion Method

Chinard, Vosburgh and Enns (1955) first proposed that transcapillary solute exchange could be assessed using a modification of the Stewart-Hamilton dye-dilution technique for measuring whole-organ blood flow. They argued that a tracer which crossed the capillary wall would be 'extracted' relative to one that remained in the vasculature, and so its concentration in the venous effluent would be lower than if it had remained in the vessels. Assuming that the solute crosses the capillary wall solely by diffusion, the extravascular concentration of solute is negligible and there is no backflux of solute into the circulation during the passage of the bolus, it can be argued (Kety, 1951) that the intracapillary concentration of solute falls according to a simple exponential.

Using the above argument, together with Fick's law of diffusion and the expression for the extraction (E) of the solute

$$E = 1 - \frac{C_{test}}{C_{ref}} \qquad 1.6$$

where C_{test} and C_{ref} are respectively the venous concentrations of a diffusible test solute and a reference intravascular marker solute, normalised to the arterial concentration of the solute, it is a relatively simple matter to arrive at the equation

$$PS = -F \ln(1 - E) \qquad 1.7$$

where F is the flow of blood or perfusate through the system (eg Renkin, 1959; Crone, 1963).

There are several comments worthy of note in the use of this method. Firstly, the assumption must be made that the tissue solute concentration is zero. The very fact that the solute crosses the capillary wall makes this assumption invalid. The fall of solute concentration along the capillary will then follow a double exponential. The amount of error will depend on the extravascular volume of distribution of the solute (EVV). Levitt (1970) has argued that if the EVV is at least three times the intravascular volume, then reasonable estimates for PS are obtained.

The analysis assumes no tracer backflux, ie unidirectional movement of solute out of the capillary. Backflux is an inevitable consequence of tracer diffusion, and Martin de Julian and Yudilevich (1964) have developed an analysis in which the whole of the venous outflow curve is used and extraction extrapolated to zero time (E_o) where it was assumed that backflow would be negligible. However, a more serious criticism is not merely tracer backflux into the same capillary, but 'precession' of the diffusible tracer directly from the arterial end of one capillary to the venous end of another. This would mean that the diffusible tracer appeared earlier than the intravascular tracer in the venous effluent. Thus the initial extraction, and hence PS, would be underestimated.

Levitt (1970) has discussed the implications of heterogeneity of flow and capillary lengths on the estimation of PS. He concludes that PS may be seriously underestimated, particularly for more highly diffusible tracers. It has been reported that high flow rates may minimise capillary heterogeneity (eg Alvarez and Yudilevich, 1969; Vargas and Johnson, 1967); however, these high flow rates accentuate the effect of solvent drag on the transport of tracer, an effect which is completely ignored in the analysis. This will lead to overestimation of PS, particularly for the larger molecules where convection is more important for exchange. In the cat submandibular gland, Mann et al (1979a) characterised a PS vs flow relationship for a series of lipid-insoluble molecules

with molecular radii ranging from 0.23 to 1.5 nm. They found that the permeability to the molecules studies was very high, and that the smaller molecules were flow limited even at the highest flows used. In spite of this high permeability, Mann et al (1979a) were able to demonstrate restricted diffusion for the larger molecules, and the arguments presented above would only tend to increase the degree of restriction.

1.4.3. Osmotic Transient Methods

The work of Pappenheimer, Renkin and Borrero (1951) provided the first detailed quantitative investigation of both filtration and diffusion across capillary walls. They used isolated perfused hindlimbs of cats or dogs and added a known amount of an osmotically active test solute to the perfusing solution. The resulting tendency of fluid to shift from the tissues to the blood (and hence for the limb to lose weight) was exactly counterbalanced by an increase in venous, and hence capillary, pressure. Arterial pressure was adjusted so as to keep the perfusate flow rate constant. Pappenheimer et al (1951) argued that as the test solute diffused across the capillary walls, the osmotic tendency for fluid shift would be reduced, and so the venous pressure necessary to maintain the limb at constant weight would fall; this is exactly what was observed. The change in venous and arterial pressures (Pappenheimer, and Soto-Rivera, 1948) was a measure of

the osmotic pressure exerted by the test solute across the cell membrane.

Pappenheimer et al (1951) used three well-known relationships to estimate the permeability of the capillaries to the test solute:

1. $J_s = F(Ca - Cv)$ 1.8

Where J_s is the flux across the vascular wall, F is the blood flow and Ca and Cv are the arterial and venous concentrations of the solute. This is an expression of the Fick principle for estimating loss or gain of a substance passing through an organ.

2. $$J_s = \frac{DA_s\Delta C}{\Delta x}$$ 1.9

where D is the free diffusion coefficient of the molecule, A_s is the fractional area of the membrane available for diffusion, ΔC is the mean solute concentration difference across the capillary wall, and Δx is the path length for diffusion through the membrane.

3. $\Delta P = \Delta CRT$ 1.10

where ΔP is the osmotic pressure exerted by the molecules across the capillary wall, R is the gas constant and T the absolute temperature.

Eliminating J_s from (1) and (2) and solving for $A_s/\Delta x$, they obtained

$$\frac{A_s}{\Delta x} = \frac{F(Ca - Cv)RT}{D.\Delta P} \qquad 1.11$$

Experimentally, the only variables are (Ca - Cv) and ΔP (since F is maintained constant) and these are readily measurable. If $A_s/\Delta x$ is to be constant for a given solute, then $(Ca - Cv)/\Delta P$ must be constant, and this is what was found. On the basis of a falling $A_s/\Delta x$ with increasing molecular size, they proposed that a restriction to progressively larger molecules was occurring. They modified available theories on corrections to Stoke's law in systems where the particle size is comparable with the dimensions of the sedimentation chambers, and concluded that uniform cylindrical pores of radius 30 Å would successfully account for the data.

The work of Pappenheimer et al (1951) has been criticised on the grounds that their measurments of osmotic pressure did not account for the reflexion coefficient (σ) of the molecule at the capillary wall. Pappenheimer et al (1951) can hardly be blamed for this omission since the theoretical work of Staverman (1951) relating to the reflexion coefficient was not published until after the acceptance of their paper. Pappenheimer et al (1951) did note, however, that the initial osmotic pressures obtained by extrapolation to zero time were only a fraction of the osmotic pressure corresponding to concentrations of test molecules in blood, and that this fraction increased with increasing molecular weight.

Another serious objection to the isogravimetric technique is related to the compliance of the vessels and connecting tubing. Fig. 3 of Pappenheimer and Soto-Rivera (1948) indicates that a rise in venous pressure of 4 mm Hg increases vascular volume by approximately 0.5 ml in a leg weighing 274 g. This gives a compliance of approximately 0.05 ml. 100 g^{-1} mm^{-1} Hg. The average filtration coefficient of the limbs was less than 0.02 ml. min^{-1} 100 $g^{-1}.mm^{-1}$ Hg. and so the pressure change required for a given change in weight will be much less than that required to counterbalance the osmotic pressure. This means that there will still be a tendency for the tissue to lose weight, and so the next venous pressure decrease will have to be smaller than would be expected from the fall in the transcapillary osmotic pressure gradient. The net result is that the time course of the measured venous pressure is lengthened, while that of the arteriovenous concentration difference is unaffected. Pappenheimer et al (1951) imply that the time course of the osmotic pressure exerted by the test solute follows a decreasing monoexponential. In order for the quotient (Ca - Cv)/ΔP to be a constant, (Ca - Cv) must also follow a decreasing monoexponential with the same time constant. If compliance plays a significant part in these experiments, as described above, then this cannot be the case. A compliance effect could also explain the long time course of equilibration of both D_2O and haemoglobin described in the paper.

A different osmotic transient method was described by Vargas and Johnson (1964) using the rabbit heart. Since this is the main subject of Chapters 3 and 4 of this thesis it will not be described in detail here, but in essence the tissue was allowed to lose weight in response to addition of the test solute and the permeability coefficients calculated from the rate of change of tissue weight. This method does not suffer from the compliance problems mentioned above, but has a number of problems of its own. For a further discussion of these problems and of attempts at their solution, see particularly Chapter 3 of this thesis.

1.4.4. Tissue Uptake Methods

The idea that if a solute crosses the capillary wall, then it must accumulate in the extracapillary space has led many investigators to determine capillary permeability by adding a test solute to the arterial blood and measuring its concentration in the tissue at various times after the initial addition. A particular advantage of the method is that low-permeability solutes can be studied easily, by extending the time periods over which accumulation is measured. A major disadvantage is that only one value at a given time point can be determined, so that many experiments must be performed. One way of overcoming this problem is to indirectly monitor tissue concentration by external counting of a radiolabelled test solute. Another feature of the technique is that volumes of

distribution may be determined, as well as capillary permeability, by allowing sufficient time for the test solute to equilibrate in its distribution volume.

Despite the widespread use of this technique for measuring small solute permeability (see Crone and Levitt, 1983 for review), relatively little use has been made of it for determinations of macromolecular permeability. This may be due to the long time periods required for a single experimental point, or to the use of the lymph sampling technique (Section 1.4.4.). Friedman (1957) determined vascular - extravascular equilibration of iodinated serum albumin in mice, but did not frame his results in terms of permeabilities. Studer and Pochen (1971) used labelled serum albumin and red cells to determine an extravascular albumin volume of distribution in various tissues of the rat at various times after the injection of tracer, and Triffit and Owen (1973) performed similar experiments in the rabbit. None of these authors used a specific model to determine permeabilities, preferring to use the rate of extravascular albumin accumulation as an index with which to compare the various tissues. This neglects the effect of changing intravascular isotope concentration and the removal of isotope in the lymph. Johnson (1966) formulated a model which accounted for lymphatic removal of solute, but his analysis assumed a constant intracapillary solute concentration. The technique is discussed in more detail in Chapter 2 of this thesis.

1.4.5. Analysis of Lymph

Renkin (1964) was the first to give quantitative form to the concept that the analysis of lymph could provide estimates of capillary permeability. Previous workers (eg Mayerson, Wolfram, Shirley and Wasserman, 1960) had realised that ratio of solute concentration in the lymph to that in the plasma (L/P ratio, also termed R) would fall as permeability fell, and had used this information to postulate the existence of "leaks" (Grotte, 1956) or "large pores" (Mayerson et al, 1960), which allowed macromolecules to pass through. Using the Kedem and Katchalsky (1955) equations, Renkin (1964) derived an equation by which the PS product of a macromolecule could be determined

$$PS_i^{cap} = \frac{J_v^L R_i}{1 - R_i} \qquad 1.12$$

where PS_i^{cap} represents the PS product of solute i at the capillary wall, J_v^L is the lymph flow rate and R_1 is the L/P ratio for solute i. It is clear that this analysis ignores the effect of convective transport of the molecule by assuming that the reflexion coefficient of the capillary membrane to the molecule is 1. If this assumption is not made, the complete expression for R becomes

$$R_i = \frac{\frac{1}{2}(1 - \sigma_i^{cap}) + PS_i^{cap}/J_v^L}{\frac{1}{2}(1 + \sigma_i^{cap}) + PS_i^{cap}/J_v^L} \qquad 1.13$$

where σ_i^{cap} represents the reflexion coefficents of solute i at the capillary wall. The non-linear transport equation can be solved for R_i (Granger and Taylor, 1980) to yield

$$R_i = \frac{1 - \sigma_i^{cap}}{1 - \sigma_i^{cap} e^{-\lambda}} \qquad 1.14$$

where $\lambda = \frac{(1 - \sigma_i^{cap}) J_v^L}{PS_i^{cap}}$

Both the linear and non-linear equations may be used to determine σ_i^{cap} by increasing the lymph flow rate and allowing R_i to approach a limit. In the case of the linear equation the limit is

$$\lim_{J_v^L \to \infty} R_i = \frac{(1 - \sigma_i^{cap})}{(1 + \sigma_i^{cap})} \qquad 1.15$$

while the non linear equation gives

$$\lim_{J_v^L \to \infty} R_i = 1 - \sigma_i^{cap} \qquad 1.16$$

The most important assumption made in arriving at the expression for R_i is that $J_v^{cap} = J_v^L$, where J_v^{cap} represents the net filtration across the capillary wall. This is likely to be the case in tissues such as heart and

skeletal muscle, but is unlikely to be the case in absorbing or secreting intestine, and is certainly not true in the secreting salivary gland. There are basically 2 ways in which J_v^{cap} may be increased in the salivary gland:

a) raising capillary hydrostatic prssure (or lowering capillary colloid osmotic pressure). This increases J_v^{cap} without increasing J_v^{sal}. The gland gains weight until fluid transudes across the capsule (Gamble, unpublished observations).

b) parasympathetic nerve stimulation. This increases J_v^{sal} by almost the same amount as J_v^{cap}. In the isolated perfused salivary gland preparation described in Chapter 4 of this thesis, the lymphatic vessels were cut and lymph allowed to accumulate in the gland holder; significant lymph flow would thus have caused a measurable gain in weight of the system. Addition of acetylcholine in this preparation caused a copious secretion of saliva but no tendency to a continued weight gain (Gamble, unpublished observations).

Thus, neither method of increasing J_v^{cap} increases J_v^L by the same amount. This would not affect the issue as long as J_v^L could be increased so that R_i becomes filtration-independent (Granger and Taylor, 1980).

A more serious objection is the fact that saliva is essentially free of proteins derived directly from the blood. The transport equations then have to be written with the expression $J_v^{cap} = J_v^L + J_v^{sal}$ substituted for $J_v^{cap} = J_v^L$ but protein clearance in lymph is still equal

to $J_v^L.C_i^L$, where C_i^L is the lymphatic concentration of solute i. Equation 1.13 then becomes

$$R_i = \frac{\frac{1}{2}(1 - \sigma_i^{cap}) + PS_i^{cap}(J_v^L + J_v^{sal})}{(J_v^L + PS_i^{cap})/(J_v^L + J_v^{sal}) - \frac{1}{2}(1 - \sigma_i^{cap})} \qquad 1.17$$

and equation 1.14 becomes

$$R_i = \frac{(1 - \sigma_i^{cap})(J_v^L + J_v^{sal})}{J_v^L(1 - \sigma_i^{cap}e^{-\lambda}) + J_v^{sal}(1 - \sigma_i^{cap})e^{-\lambda}} \qquad 1.18$$

and the limits become

$$\lim_{J_v^L \to \infty} R_i = \frac{\frac{1}{2}(1 - \sigma_i^{cap})}{J_v^L/(J_v^L + J_v^{sal}) - \frac{1}{2}(1 - \sigma_i^{cap})} \qquad 1.19$$

using the linear equation and

$$\lim_{J_v^L \to \infty} R_i = (1 - \sigma_i^{cap})(1 + J_v^{sal}/J_v^L) \qquad 1.20$$

using the non-linear equation. It may easily be seen that equations 1.19 and 1.20 reduce to equation 1.15 and 1.16 respectively, if $J_v^{sal} = 0$. More importantly, the limits to R_i depend on both J_v^{sal} and J_v^L, even if the gland is isogravimetric. When the gland is actively secreting, J_v^{sal} is much greater than J_v^L and a small error in measuring

J_v^L will produce a much greater error in the estimation of σ_i^{cap}. Also the increase in J_v^{cap} occurs mainly via an increase in J_v^{sal} and so a constant limiting value for R is never reached whichever equation is used. This means that σ_i^{cap} cannot be estimated using this method in the secreting salivary gland.

1.5. Aims of the Present Studies

Previous work in this laboratory provided the first comprehensive studies of the permeability coefficients of the salivary gland capillaries to small molecules. It was hoped to extend this work in two main directions:

1. To determine the capillary permeability coefficient of a macromolecule, albumin.
2. To determine the osmotic reflexion coefficients of a series of solutes with a wide range of molecular sizes.

In this way, it was hoped to characterize more fully the properties of the salivary gland capillary wall.

Two methods were used; first, an *in vivo* study of the rate of extravascular accumulation of radiolabelled albumin in the gland (Chapter 2); second, an *in vitro* study using the osmotic transient technique of Vargas and Johnson (1964) in the isolated perfused gland (Chapters 3 and 4). It was necessary to contruct mathematical models

for both methods; a simple model appeared to be adequate for the isotope accumulation study, but a more complex model was required for the osmotic transient experiments. The model is described in Chapter 3, and its application to the experimental work is described in Chapter 4.

CHAPTER 2

Transcapillary Passage of Radiolabelled Albumin and EDTA in the Rabbit Submandibular Gland

TRANSCAPILLARY PASSAGE OF RADIOLABELLED ALBUMIN AND EDTA IN THE RABBIT SUBMANDIBULAR GLAND

2.1. Introduction

In most tissues, there is a small but steady passage of proteins from the blood into the interstitial space; the proteins may then be metabolised or be returned to the bloodstream either directly or via the lymphatic system. The mechanisms underlying the transcapillary passage of proteins are, however, incompletely understood. As indicated in Chapter 1 (Section 1.3.2), the dominant mechanism may depend on the conditions of the experiment; in particular, raising venous pressure to enhance fluid filtration may cause an unwanted increase in the capillary permeability to the proteins under investigation.

The rabbit submandibular gland is particularly suited to the study of protein transport during variations in the rate of fluid filtration. By stimulating the parasympathetic nerve supply to the gland, the net filtration rate across the gland capillaries may be increased by at least two orders of magnitude without a large increase in venous pressure. The gland may be exposed with a relatively small amount of dissection, and the nerve supply may be prepared for stimulation without touching the gland itself.

The two most commonly used approaches for determining protein permeability in organs are the tissue uptake technique and the analysis of lymph; both techniques were mentioned in Chapter 1. Two reasons dictated the use of the tissue uptake technique in these experiments: (1) the theoretical objection outlined in Section 1.4 related to the secretion of protein-free fluid in the saliva; (2) the technical difficulty of identifying and cannulating a lymph vessel from the gland, particularly when it was important not to damage the gland.

If the tracer molecules traversed a single membrane separating two well mixed compartments, a simple analytical solution could be found to calculate the required coefficients. However, the real situation is much more complicated and so a mathematical model is required which is solved numerically using a computer. With the use of such a model, determination of the accumulation rate of a tracer protein molecule under control conditions and with nerve stimulation, together with measurement of accumulation of a low molecular weight extracellular marker, can yield the following information:

1. PS product and reflexion coefficient of the protein.
2. Extravascular volume of distribution of the protein. This together with the extravascular volume of distribution of the extracellular marker, can provide information on exclusion in the interstitial space.
3. Capillary surface area. Using an appropriate value

for capillary radius, measurement of the intravascular volume of the tissue allows estimation of the capillary surface area, which can be compared with morphometric analysis. Measurement of the intravascular volume during nerve stimulation supplies information on capillary recruitment.

4. Measurements of the various volumes of distribution yield values essential to the model developed for the osmotic transient experiments (Chapter 3).

2.2. Mathematical Model of Extravascular Albumin Accumulation

2.2.1. Model System

A schematic diagram of the model is shown in Fig. 2.1. The central element in the system is a 'typical capillary' surrounded by interstitial space. A lymphatic vessel originates in the interstitium and carries fluid and protein away. An acinus and salivary duct form the secretory apparatus which transports fluid into the main duct system.

2.2.2. Assumptions of the Model

1. Albumin is not metabolised in the tissue to a measurable extent within the time course of the experiment.

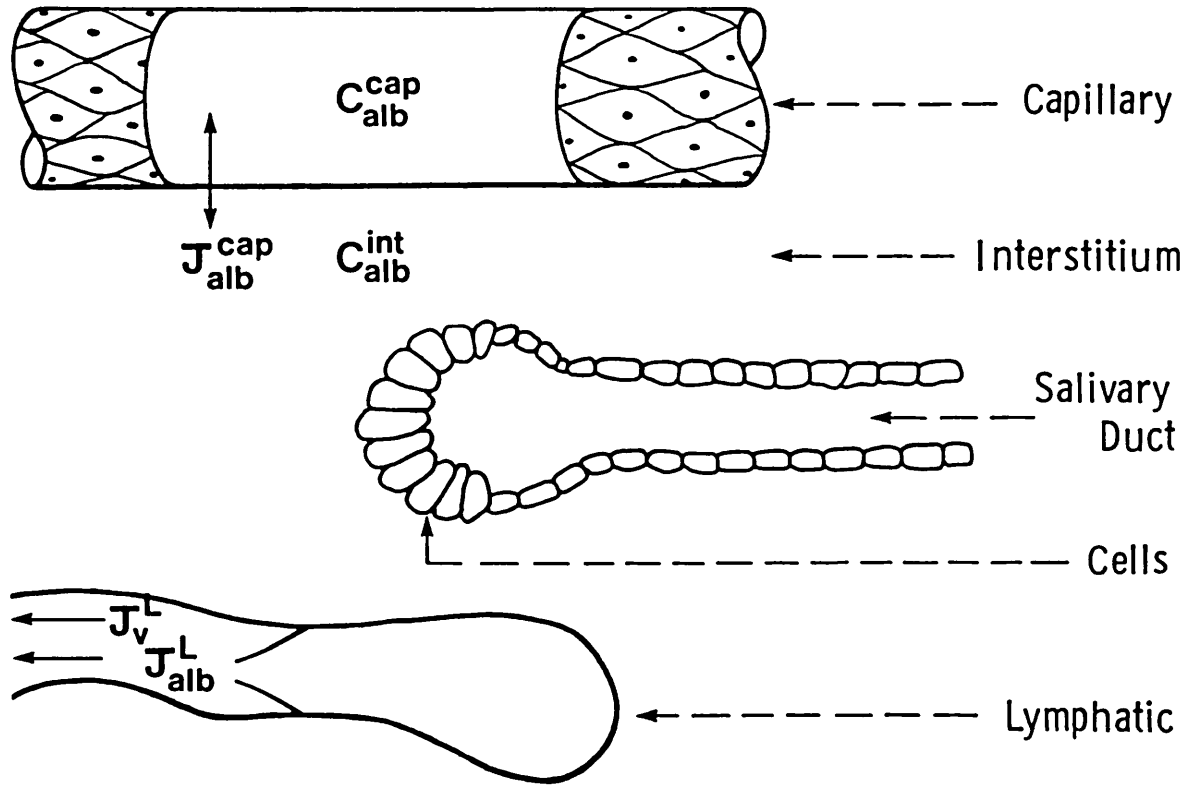


FIGURE 2.1. Schematic diagram of model of extravascular albumin accumulation. Note that no protein enters the saliva, ie $J_{alb}^{sal} = 0$. The equations governing the fluxes between compartments are given in Section 2.3.3., and a list of symbols used is given in Appendix 1.

2. Passive processes only are involved in albumin transport. For the purposes of the model, vesicular transport can be considered to be a passive process as long as protein transport is proportional to the concentration difference between the capillary lumen and the interstitium.

3. Albumin crosses the capillary wall, but does not enter the cells during the experiment.

4. Instantaneous mixing of albumin occurs in the interstitium - ie the interstitium can be considered to be a single compartment. Indirect justification for this assumption comes from the work of Fox and Wayland (1979) who measured the interstitial diffusion of macromolecules in rat mesentery. Using a semi-infinite slab geometry to model interstitial concentration profiles their figures indicate that the interstitial concentration of albumin 5 μm away from the capillary wall was approximately 95% of the value at the interstitial side of the capillary wall. Measurements of interstitial space presented in the results of the present experiments (see Section 2.4.4.) are equivalent to a ring of interstitium less than 3 μm thick surrounding the capillary.

5. Albumin concentration in lymph is equal to interstitial concentration (eg Renkin, 1979). This assumption is a contentious one, and depends upon the value taken for the interstitial volume of

distribution of albumin. If albumin is excluded from a part of the interstitium then the albumin concentration in the volume in which it distributes will be higher than the concentration given by the ratio of interstitial amount of albumin to interstitial volume. Also, if the interstitium behaves like a gel filtration column (eg Wiederhielm and Black, 1976; Watson, Bell and Renkin, 1980), then the albumin will travel more quickly into the lymph It has further been suggested (eg.Watson, 1980) that the interstitium forms the major barrier in blood-to-lymph solute movement, implying that significant concentration gradients occur in the interstitium. If this is so for the salivary gland, then assumption 4 above would not hold. However, Watson (1980) supports his hypothesis with examples taken from experiments in skin and mesentery, tissues in which distances in the interstitial space are large. The argument given here in support of assumption 4 indicates that the interstitium does not form a significant barrier to albumin movement in the salivary gland.

6. No albumin appears in the saliva.(see Section 2.3.3)

7. The tissue is isogravimetric, ie $J_v^{cap} = J_v^{L} + J_v^{sal}$. This appears to be the case in the resting gland. However, Lundvall and Holmberg (1978) showed that in the first minute after the onset of parasympathetic nerve stimulation the gland lost weight and

thereafter gradually returned towards pre-stimulation weight. The initial rapid loss of weight was assumed to be due to ejection of preformed saliva, perhaps by contraction of myoepithelial cells around the ducts. In the series of experiments described in this thesis, the weight of stimulated glands at the end of a period of nerve stimulation was not significantly different from that of the control contralateral glands.

8. There are no axial or radial concentration gradients in the capillary. Radial concentration gradients in the bulk of the plasma are unlikely due to stirring by red cells. However, the possibility exists that there is an unstirred layer of fluid adjacent to the capillary wall. As filtration proceeds, the albumin concentration in this layer would increase, thus opposing filtration but favouring diffusion of albumin into the interstitium. It is impossible to estimate this in the present model and so it has been ignored. A few preliminary experiments designed for a different purpose indicated that axial concentration gradients could be ignored. These experiments were unsuccessful in following albumin accumulation but they did show that albumin concentrations in the artery supplying the gland were not significantly different from those in the venous effluent.

9. ^{125}I-labelled human albumin behaves in an identical manner to endogenous rabbit albumin. This is unlikely for at least two reasons - species difference and method of labelling the albumin. Experiments on albumin movement into the rat peritoneal cavity showed differences between rat and human albumins which were labelled in an identical manner (Gamble, Hawkins, Penn and Spencer, 1982a). There were also differences in the electrophoretic mobility of these species, indicating a difference in molecular charge. Of the various methods of albumin iodination, the one employed by Amersham is the Chloramine-T method (Greenwood, Hunter and Glover, 1963; Lee and Ryan, 1973). This method of labelling causes an increase in albumin permeability in the rat peritoneal dialysis model (Gamble, Hawkins, Penn and Spencer, 1982b), and an increased rate of albumin degradation after endocytosis by oocytes (Opresko, Wiley and Wallace, 1980). This would suggest that the permeability coefficients using albumin labelled with Chloramine-T would be higher than those of the endogenous molecule.

10. The test molecule does not contribute to osmotic water flows but acts only as a tracer. The concentration of albumin in the isotope solution used was 2 g 100 ml^{-1}. Using the Landis-Pappenheimer (1963) equation for osmotic pressure of an albumin solution, this albumin concentration would give an osmotic pressure of approximately 4.9 mm Hg. Since about

1 ml of isotope solution was distributed in a plasma volume of approximately 70 ml, the osmotic pressure contribution of the labelled albumin would be approximately 0.06 mm Hg. With a filtration coefficient of 1 ml min^{-1} 100 $g^{-1}mm^{-1}$Hg (see Chapter 4) the extra osmotic pressure would cause a tendency to reabsorb 6 x 10^{-4} ml $min^{-1}g^{-1}$ if the albumin reflexion coefficient were 1. This value is comparable to the value used for filtration rate when the gland is not secreting, but with the high reflexion coefficient found for albumin in these experiments, very little difference is made to the solvent drag component of albumin flux by ignoring the osmotic contribution of the tracer.

2.2.3. Equations Used

It was decided to use the non-linear form of the transport equation (eg Patlak et al, 1963; Brace et al, 1977) since the Kedem and Katchalsky (1958) linear formulation was derived for systems close to equilibrium. Initially there is no labelled albumin in the interstitium yet the linear equation predicts an average membrane concentration of 50% of the plasma labelled albumin concentration. One form of the non-linear equation is

$$J_{alb}^{cap} = J_v^{cap}(1 - \sigma_{alb}^{cap})C_{alb}^{cap} + \frac{J_v^{cap}(1 - \sigma_{alb}^{cap})(C_{alb}^{cap} - C_{alb}^{int})}{(e^{\lambda} - 1)} \qquad 2.1$$

where $\lambda = J_v^{cap}(1 - \sigma_{alb}^{cap})/PS_{alb}^{cap}$, C_{alb}^{cap}, C_{alb}^{int} are respectively the intracapillary and interstitial albumin concentrations, J_{alb}^{cap} is the net transcapillary albumin flux, σ_{alb}^{cap} is the capillary reflexion coefficient of albumin and PS_{alb}^{cap} is the PS product of albumin across the capillary.
In order to calculate net albumin flux into the interstitium (J_{alb}^{net}) it is necessary to correct for protein loss in the lymph. This is given by $J_v^L.C_{alb}^{int}$ (assumption 5, Section 2.2.2). Thus

$$J_{alb}^{net} = J_{alb}^{cap} - J_v^L.C_{alb}^{int} \qquad 2.2$$

J_v^{cap} was found using the relationship (assumption 7)

$$J_v^{cap} = J_v^L + J_v^{sal} \qquad 2.3$$

and assigning J_v^L and J_v^{sal} according to the experimental conditions.

With a numerical solution such as employed in this model it is unnecessary to assume a constant concentration of labelled albumin in the plasma. Bill (1977) tried to achieve this by periodic infusions of labelled albumin. However, this would lead to a 'saw-tooth' pattern of concentration, rather than the constancy expected. It was thought better to let the albumin concentration fall and know the time course of the fall so that allowance could be made for it in the iterations.

2.2.4. Iteration Technique

It is first necessary to assign values to J_v^L and J_v^{sal} (and hence J_v^{cap}, Eqn. 2.3), PS_{alb}^{cap} and the equilibrium volume of distribution for albumin, $V_{alb}^{int}(\infty)$. Note that

1) it is unnecessary to have a value for K_f since values for filtration rates have already been assigned

2) $V_{alb}^{int}(\infty)$ will in general not be equal to the interstitial space measured by ^{51}Cr-EDTA, due to steric exclusion. (see Section 2.6.5)

Initial plasma concentration of labelled albumin is set at 100% (expressed in the same manner as the experimental results) and initial interstitial labelled albumin concentration at 0.

Using the values assigned, J_{alb}^{net} is calculated over a known time interval Δt (Eqn. 2.2). Since J_{alb}^{net} is very small, Δt can be relatively long without leading to instability in the solution. C_{alb}^{int} is then recalculated

$$C_{alb}^{int} = \frac{A_{alb}^{int}}{V_{alb}^{int}(\infty)} \qquad 2.4$$

where A_{alb}^{int} is the interstitial amount of labelled albumin.

The measured extravascular volume of distribution at time t, $V_{alb}^{int}(t)$, will then be given by

*$V_{alb}^{int}(\infty)$ is a thermodynamic equilibrium value, and not a steady state value.

$$V_{alb}^{int}(t) = \frac{C_{alb}^{int} \times V_{alb}^{int}(\infty)}{C_{alb}^{cap}} \qquad 2.5$$

With the new value of C_{alb}^{int} and a new value of C_{alb}^{cap} determined from experimental results using a double exponential equation to fit the data (Section 2.4.1), the process can be repeated. After n iterations

$$(C_{alb}^{int})_n = (C_{alb}^{int})_{n-1} + \frac{(J_{alb}^{net})_n}{V_{alb}^{int}(\infty)} \qquad 2.6$$

and

$$(V_{alb}^{int})_n = \frac{(C_{alb}^{int})_n \times V_{alb}^{int}(\infty)}{(C_{alb}^{cap})_n} \qquad 2.7$$

where subscripts n and n-1 refer to values obtained after n and n-1 iterations respectively.

2.2.5. Values Used

This model requires values for J_v^{cap}, $V_{alb}^{int}(\infty)$, Δt, PS_{alb}^{cap} and σ_{alb}^{cap} as well as the equation for the fall of plasma albumin concentration. Table 2.1 shows the values used.

The values for J_v^L were based on the value found by Koo et al (1980) in the resting cat submandibular gland. This was found to be approximately 10^{-3} ml $min^{-1}g^{-1}$, and

	Control Gland	Stimulated Glands	Units
J_v^{sal}	2×10^{-4}	2×10^{-2}	ml. min^{-1} g^{-1}
J_v^{L}	$- 10^{-4}, 10^{-3}, 10^{-2} -$		
Δt	- 1 -		min
PS_{alb}^{cap}	$- 10^{-5} - 10^{-3} -$		ml. min^{-1} g^{-1}
σ_{alb}^{cap}	- 0.8 - 1 -		
$V_{alb}^{int}(\infty)$	- 2 - 5 -		ml. 100 g^{-1}

TABLE 2.1. Values used for model of extravascular albumin accumulation. (See Section 2.2.5. for details of how the values were chosen).

values one order of magnitude greater and smaller than this were tried in the model to determine the influence of errors in the estimation of J_v^L on the time course of interstitial albumin accumulation. The value for J_v^{sal} in the resting gland was taken from Smaje (1973), and that in the stimulated gland based on flow rates found during the present experiments. The values for PS_{alb}^{cap} and σ_{alb}^{cap} were estimated using the analysis outlined in Section 2.2.6 and that for $V_{alb}^{int}(\infty)$ assumed to lie between 2 and 5 ml 100 g^{-1}.

2.2.6. Estimation of Permeability-Surface Area Product and Reflexion Coefficient of Albumin from Initial Rates of Extravascular Albumin Accumulation

The non-linear transport equation (2.1) can be used to estimate PS_{alb}^{cap} and σ_{alb}^{cap} without the use of a mathematical model. At early times, the interstitial concentration of labelled albumin is low and is zero at time zero. Due to the low PS product of albumin the assumption of zero (or negligible) interstitial albumin concentration is valid for a relatively long time. Also, the assumption of negligible interstitial albumin concentration implies that protein removal via the lymphatics may be ignored, and so $J_{alb}^{net} = J_{alb}^{cap}$. Substituting $C_{alb}^{int} = 0$ in equation 2.1 gives

$$J_{alb}^{cap} = \frac{J_v^{cap}(1 - \sigma_{alb}^{cap})\ C_{alb}^{cap}}{1 - e^{-\lambda}} \qquad 2.8$$

If λ is small ($\lambda<0.1$), $(1 - e^{-\lambda})$ is approximately equal to λ and thus

$$J_{alb}^{cap} = PS_{alb}^{cap}.C_{alb}^{cap} \qquad 2.9$$

If λ is large ($\lambda>5$), $(1 - e^{-\lambda})$ approaches unity and

$$J_{alb}^{cap} = J_v^{cap}(1 - \sigma_{alb}^{cap})C_{alb}^{cap} \qquad 2.10$$

In a given time period, the amount of albumin transported into the interstitium is given by J_{alb}^{cap} (ml $min^{-1}g^{-1}$) multiplied by the time interval Δt (min). Since C_{alb}^{cap} is not constant, it is not possible to simply use $J_{alb}^{cap}.\Delta t$; an average value ($\bar{C}_{alb}^{cap}$) must be taken, given by

$$\bar{C}_{alb}^{cap} = \int_o^{t_1} C_{alb}^{cap}(t)dt \qquad 2.11$$

where 0 and t_1 are the time boundaries, $\Delta t = t_1 - 0$ and $C_{alb}^{cap}(t)$ is the intracapillary albumin concentration at time t ($t_1>t>0$). When λ is small, the amount of albumin transported across the capillary wall, J_{alb}^{cap}, is given by

$$A_{alb}^{cap} = PS_{alb}^{cap}\int_0^{t_1} C_{alb}^{cap}(t)dt \qquad 2.12$$

Since the extravascular volume of distribution at time t_1 ($V_{alb}^{int}(t_1)$) assuming no loss of albumin, is given by

$$V_{alb}^{int}(t_1) = \frac{A_{alb}^{cap}}{C_{alb}^{cap}(t_1)} \qquad 2.13$$

it follows that

$$V_{alb}^{int}(t_1) = \frac{PS_{alb}^{cap}\int_0^{t_1} C_{alb}^{cap}(t)dt}{C_{alb}^{cap}(t_1)} \qquad 2.14$$

Thus

$$PS_{alb}^{cap} = \frac{V_{alb}^{int}(t_1).C_{alb}^{cap}(t_1)}{\int_0^{t_1} C_{alb}^{cap}(t)dt} \qquad 2.15$$

Since PS_{alb}^{cap} and σ_{alb}^{cap} are relatively constant, the main way in which λ can be changed is by changing J_v^{cap}. This was done in the present experiments by stimulation of the parasympathetic nerve supply to the gland.

When λ is large, a similar analysis to that outlined above gives

$$V_{alb}^{int}(t_1) = \frac{J_v^{cap}(1 - \sigma_{alb}^{cap})\int_0^{t_1} C_{alb}^{cap}(t)dt}{C_{alb}^{cap}(t_1)} \qquad 2.16$$

Thus

$$\sigma_{alb}^{cap} = 1 - \frac{V_{alb}^{int}(t_1).C_{alb}^{cap}(t_1)}{J_v^{cap}\int_o^{t_1} C_{alb}^{cap}(t)\ dt} \qquad 2.17$$

2.3. Methods

The experiments described in this Chapter were designed to enable determinations to be made of volumes of distribution of the tracers under various conditions. The major potential sources of error in the measurement of these volumes of distribution were:-

1. Dissociation of radiolabel from the tracer (particularly important for albumin)
2. Binding of the tracer molecule to cells
3. Differences in haematocrit between blood in the gland and peripheral blood.

The following sections describe attempts to overcome these sources of error and so estimate more accurately the relevant distribution volumes.

2.3.1. Animals and Anaesthesia

New Zealand White Rabbits of either sex, weighing between 1.6 and 4.5 kg were used. Anaesthesia was induced with ethyl carbamate (urethane; Sigma Chemical Co, St Louis, Missouri) made up to a concentration of 25 g 100 ml^{-1} in sterile 0.9 g 100 ml^{-1} NaCl. The initial dose was approximately 1.8 g kg^{-1}. Additional urethane was administered as required to maintain anaesthesia.

2.3.2. Cannulations; Blood Pressure and Rectal Temperature Monitoring

The trachea and a femoral artery and vein were cannulated in each animal. Systemic arterial blood pressure was monitored via the arterial cannula using a Bell and Howell type 4-422-0001 Physiological Pressure Transducer connected to a Devices MX2 pen recorder. Isotopes and additional anaesthetic were administered via the venous cannula. Rectal temperature was maintained between 37^{o} and 38^{o}C using a servo-controlled animal heating system (CFP 8185; C F Palmer and George Washington, Sheerness, Kent).

2.3.3. Parasympathetic Nerve Stimulation

Since the parasympathetic nerve fibres to the submandibular gland run along the submandibular duct, the gland can be stimulated using stimulating electrodes

placed around the duct. The duct on one side was exposed and gently freed from the surrounding connective tissue, taking care not to handle the duct or the gland directly. A pair of platinum electrodes was placed around the duct. A small quantity of warm liquid paraffin was poured into the hollow containing the duct and electrodes; this served as an electrical insulator and to prevent drying of the tissue. The nerve was stimulated using square wave pulses of 2 ms duration and amplitude 8-10 V, at a frequency of 10 Hz.

Gland blood flow was not measured directly and so adequate stimulation was detected by a marked reddening of the gland. In some experiments a laser-doppler flowmeter ("Periflux"; Perimed, Stockholm, Sweden) was used to check that nerve stimulation did indeed increase blood flow through the gland. The probe of the instrument was placed about 1 mm from the surface of the gland and flow monitored during a control period and during a period of nerve stimulation. In all cases reddening of the gland was associated with an increased output signal from the instrument (see Tenland, 1982, for review of instrumentation and applications of the laser-doppler flowmeter).

Although salivary flow rate was not accurately measured by cannulating the salivary duct, in some experiments a crude estimate of salivary flow rate was made by collecting the saliva issuing from the animal's mouth.

The collected saliva was also counted for radioactivity to determine whether any of the tracers had entered the saliva. In 6 experiments the mean saliva flow rate was 2.3×10^{-2} ml $min^{-1}g^{-1}$, and a rounded value of 2×10^{-2} ml $min^{-1}g^{-1}$ was used in the model (Table 2.1). In the same 6 experiments, no saliva sample contained albumin or EDTA radioactivity distinguishable from background, thus supporting the assumption that none of the tracer albumin enters the saliva (assumption 6, Section 2.2.2).

2.3.4. Counting of Radioisotope Activity

All the radioisotopes used were gamma emitters, and counting was performed in a Packard "Modumatic" Model 5330 3-channel spectrometer. Since the energy spectra of different isotopes overlap, appropriate corrections were made for cross-channel contamination (Fig. 2.2.). The energy spectrum for each isotope was determined by using a narrow bandwidth setting and scanning over the range 0-1 MeV. The gain and energy bandwidths for each channel were chosen to maximise the count rate of the desired tracer while minimising contamination from the other tracer(s).

Standards containing only one of the isotopes in a given mixture were counted simultaneously in all channels in order to determine the degree of cross-channel contamination, and empty tubes counted to determine the background activity.

		Channel		
		1	2	3
	A	1	c	e
Isotope	B	a	1	f
	C	b	d	1
		x	y	z

$$A = \frac{x(1 - df) - a(y - dz) - b(z - fy)}{1 - ac - be - df + bcf + ade}$$

FIGURE 2.2. Calculation of activity of a given isotope by correcting for activity due to other isotopes used (cross-channel correction). Channels 1, 2 and 3 of the gamma counter are set to maximise the counts of isotopes A, B and C respectively while minimizing counts due to the other isotopes. The letters a - f in the upper part of the figure represent the counts obtained in each channel when a single isotope is counted (normalized so that isotope A gives a count of 1 in channel 1, etc), and x, y and z represent the counts obtained in channels 1, 2 and 3 respectively when a mixture of isotopes is counted. In the lower part of the figure, A represents the corrected counts of isotope A. Similar formulae may be derived for isotopes B and C.

2.3.5. Labelling of Rabbit Erythrocyte with ^{51}Cr

Rabbit erythrocytes were labelled with ^{51}Cr immediately before the experiment in which they were to be used. 4 ml of blood from the experimental animal were taken from a marginal ear vein and mixed with 1 ml acid citrate dextrose (Travenol Laboratories, Thetford, Norfolk) to prevent coagulation. The mixture was centrifuged at 3000 rpm (1000 G) in a BTL centrifuge (Baird and Tatlock Ltd, Chadwell Heath, Essex) for 10 minutes and the supernatant discarded. ^{51}Cr labelled sodium chromate (10 µCi in approx 0.2 ml) was added to the erythrocytes, the tube gently inverted a few times to ensure mixing, and the cells were allowed to equilibrate with the isotope for 30 minutes at room temperature (usually 20-23°C). The labelled cells were then washed with 10 ml of sterile 0.9% NaCl (Travenol Laboratories), the suspension centrifuged and the supernatant removed. The washing and centrifuging process was repeated until the supernatant contained a negligible amount of radioactivity, 4 washings usually sufficing. The labelled cells were then resuspended in 2 ml of sterile 0.9% NaCl.

2.3.6. Determination of Protein-Bound ^{125}I-labelled Albumin in Blood and Tissue Samples

In all batches of ^{125}I or ^{131}I-labelled albumin there is a small but variable percentage of radioisotope which is not bound to the protein. In these studies it

was important to measure only the radioactivity associated with the protein since free iodide would cross the capillary wall quickly and distort the figures for both transvascular escape rate and permeability of albumin. In order to determine the level of free radio-iodide, the protein was precipitated using trichloroacetic acid (TCA).

2 ml of 30% TCA was added directly to each 0.5 ml blood sample. Each gland (weighing approximately 0.5 g) was first homogenised in a Silverson mixer-emulsifier, using 2 ml 0.9% NaCl to aid the homogenizing process, and then 4 ml of 30% TCA was added to the homogenate. All samples were thoroughly mixed, left for 15 minutes and then centrifuged at 1000 G for 15 minutes. 0.5 ml of supernatant from each sample was counted for free ^{125}I activity (FI). Protein-bound ^{125}I activity (PBI) was calculated from the relationship

$$PBI = \text{Total } ^{125}I \text{ activity} - FI \times \frac{w + y}{0.5} \qquad 2.18$$

where w = weight of blood or gland sample

y = volume of liquid added to sample (2 ml for blood, 6 ml for gland)

2.3.7. Determination of the Amount of Cellular Binding of ^{51}Cr-EDTA and ^{125}I-HSA

It is important to establish whether the markers used to determine extracellular volumes of distribution are incorporated into cells to an extent that might affect the calculations. It was only possible to do this with blood cells. If the labels are bound to or incorporated into the cells then the "haematocrit" estimated from the distribution of label between cells and plasma will be lower than that measured by centrifugation.

5 ml of blood was taken from each of 4 experimental animals and placed in a tube containing a small amount of heparin. 0.1 ml of a mixture of labelled albumin and EDTA (containing approximately 0.1 μCi and 1 μCi ^{51}Cr-EDTA) was added to the sample and the resulting mixture incubated at 37°C for 60 minutes. After this time, the sample was gently shaken to evenly distribute the erythrocytes, an aliquot of 0.1 ml was taken for determination of haematocrit, and the remainder centrifuged at 1000 G for 15 minutes. The radioactivity of the sample was used to determine the haematocrit in two ways:

1. The whole centrifuged sample was counted. 0.1 ml of the supernatant was similarly counted. The haematocrit in the sample is given by

$$H = 1 - \frac{A}{10PV} \qquad 2.19$$

where H = haematocrit

A = activity of whole centrifuged sample (cpm)

P = activity of 0.1 ml of plasma supernatant (cpm)

V = volume of centrifuged sample (ml)

2. 0.1 ml of the mixture of radioisotopes was counted and 0.1 ml of the supernatant counted as in (1) above. In this case the haematocrit is given by

$$H = 1 - \frac{M}{PV} \qquad 2.20$$

where M = activity of 0.1 ml isotope mixture.

In 4 experiments, the haematocrit measured by centrifugation was 0.46 ± 0.01 (mean ± SEM). The haematocrit estimated from ^{125}I-radioactivity was 0.45 ± 0.01 using the first method and 0.46 ± 0.02 using the second method. The haematocrit estimated from ^{51}Cr radioactivity were respectively 0.48 ± 0.02 and 0.46 ± 0.02.

These results indicate that the isotopes do indeed remain in the extracellular space, at least in blood.

2.3.8. Measurement of Venous and Arterial Haematocrit

A small (0.5 ml) blood sample was obtained from the venous or arterial cannula as required and immediately a portion of the sample was transferred to a heparinized micro-haematocrit tube (MSE Ltd, Crawley, Sussex), the volume of which was approximately 0.1 ml. Both ends of

the tube were then sealed with tube sealing compound and the tube placed in a specially designed head in the centrifuge. The blood was centrifuged at 3000 rpm (1000 G) for 10 minutes and the haematocrit read in an MSE micro-haematocrit reader. To test the reproducibility of the system, 5 haematocrit tubes were filled from a larger (1 ml) venous sample, and centrifuged. Each tube was read 3 times. The maximum deviation was ± 2% of the mean (mean Hct = 0.47, range 0.46 - 0.48). The centrifugation and haematocrit readings were repeated to test whether or not the erythrocytes had packed down fully, but on no occasion was the second haematocrit reading more than 0.02 different from the first.

2.3.9. Determination of Dynamic Intravascular Haematocrit

It is well documented (eg Duling and Klitzman, 1979) that the haematocrit in micro vessels is in general lower than that in large vessels. It is essential to correct for this phenomenon when calculating volumes of distribution of tracers in the gland (Section 2.3.12). A mixture of ^{125}I-HSA and ^{51}Cr-labelled erythrocytes was injected intravenously. 5 minutes later an arterial blood sample was taken and both submandibular glands removed by tying 2 ligatures around the vascular bundle at the hilus of the gland and cutting between the ligatures. Blood and tissue samples were counted for protein-bound ^{125}I and ^{51}Cr activities as described earlier, and the

haematocrit of the arterial blood sample was measured by centrifugation. It was assumed that in the 5 minute period between injection of the isotope and collection of the samples, a negligible amount of labelled albumin had escaped into the interstitium of the gland.

If ^{51}Cr activity (A_{Cr}) is proportional to haematocrit and protein-bound ^{125}I activity (A_I) is proportional to (1 - haematocrit) then

$$A_{Cr} = K_{Cr}H \qquad 2.21$$

$$A_I = K_I\ (1 - H) \qquad 2.22$$

where K_{Cr} and K_I are constants of proportionality relating activity to concentration and H is the haematocrit. Dividing 2.21 by 2.22 gives

$$\frac{A_{Cr}}{A_I} = \frac{K_{Cr}}{K_I} \cdot \frac{H}{(1 - H)} \qquad 2.23$$

if $\frac{A_{Cr}}{A_I} = R$ and $\frac{K_{Cr}}{K_I} = K$, then

$$R = \frac{K.H}{(1 - H)} \qquad 2.24$$

Applying this relationship to blood (subscript b) and gland (subscript g) samples and noting that K is the

same for both, it is possible to eliminate K and solve the resulting equation for H_g. The result is

$$H_g = \frac{R_g H_B}{R_B(1 - H_B) + R_g H_B} \qquad 2.25$$

2.3.10. Measurement of Transvascular Escape Rate of ^{125}I-Labelled Albumin

Approximately 10 μCi of ^{125}I-HSA were injected intravenously at time zero. At known times after the initial injection, arterial blood samples of approximately 0.5 ml were obtained and placed in preweighed tubes. The weight of blood was determined by difference. The haematocrit of an additional 0.1 ml of each sample was measured as described in Section 2.2.8.

Total ^{125}I activity was determined in the whole blood samples and free ^{125}I activity measured in a known volume of the supernatant from trichloracetic acid precipitation (Section 2.2.6)

Blood samples were taken at 5, 10, 15, 30, 45, 60, 120, 180, 240 and 360 minutes after the initial injection. Protein-bound ^{125}I activity per unit weight of plasma of the 5 minutes sample was taken to be 100% and the values for subsequent samples normalized to this.

2.3.11. Measurement of Volumes of Distribution of Labelled Molecules

a) Intravascular Volume

It was assumed in the method for determining intraglandular haematocrit that there is negligible loss of labelled albumin from the vascular compartment in 5 minutes. The same assumption was made for determining intravascular volume. Arterial blood and gland samples were removed 5 minutes after the injection of ^{125}I or ^{131}I-HSA, weighed, processed and counted for protein-bound radioiodide activity.

b) Interstitial Volume

Both kidneys were ligated via a retroperitoneal incision in order to prevent renal excretion of the EDTA and approximately 50 μCi of ^{51}Cr-EDTA were injected intravenously. 5, 10, 60, 120 or 240 minutes after injection of the isotope, arterial blood and gland samples were removed, weighed and counted for ^{51}Cr activity.

c) Extravascular Accumulation of Labelled Albumin

10 μCi of ^{125}I-HSA were injected intravenously, and blood and gland samples were removed at 30, 60, 120 or 240 minutes after the injection, weighed, processed and counted for protein-bound ^{125}I activity.

All the measurements described above were made on both control and stimulated glands. In most experiments the gland on one side was stimulated and the contralateral gland left as a control. The measurements made 360 minutes

after injection of isotope followed a different protocol. In these experiments, the animal was not anaesthetized, and ^{125}I-HSA was injected via a marginal ear vein at time zero. 355 minutes later, ^{51}Cr-EDTA was injected intravenously. After a further 5 minutes, the animal was killed by an overdose of pentobarbitone ('Expiral'; May & Baker, Dagenham, Essex), a blood sample taken by cardiac puncture and the glands rapidly removed. Clearly, these experiments could be performed only on unstimulated glands.

Section 2.3.12 describes how the various volumes of distribution were calculated and Figs. 2.3 and 2.4 summarize the protocols of the experiments, some of which were designed to measure two or more volumes of distribution in the same animal.

2.3.12 Calculation of Volumes of Distribution of Labelled Isotopes in Submandibular Glands

A schematic diagram of the volumes of distribution in an idealised gland and blood sample is shown in Fig.2.5. The radioactivity is proportional to the amount of labelled molecule in the sample, and amount = concentration x volume.

Thus

$$A_g = C\left[(V^{pl})_g + (V^{int})_g\right] \qquad 2.26$$

TIME (min)	EXPERIMENT TYPE 1	2	3	4	5	6	7
0	EDTA HSA	HSA	EDTA HSA	EDTA HSA	EDTA HSA	HSA HSA	RBC HSA
5	B T				B	B	B T
10					B	B	
15					B	B	
20		EDTA					
30		B T			B	B	
45					B	B	
60			B T		B	B	
120				B T	B	B	
180					B	B	
240					B T	B	
355						EDTA	
360						B T	

FIGURE 2.3. Summary of protocols of experiments in which two radioisotopes were used.

EDTA = Time of injection of ^{51}Cr-EDTA

HSA = " " " " ^{125}I-HSA

RBS = " " " " ^{51}Cr-RBC

B = Time of blood sample

T = Time of tissue sample

Experiment types 1 - 6 are determinations of ^{125}I-HSA and ^{51}Cr-EDTA volumes of distribution at the times indicated. Experiment type 7 is a determination of intraglandular haematocrit.

TIME (min)	EXPERIMENT TYPE 1	2	3
0	^{125}I-HSA	^{125}I-HSA	^{125}I-HSA
25	EDTA ^{131}I-HSA		
30	B T		
55		EDTA ^{131}I-HSA	
60		B T	
115			EDTA ^{131}I-HSA
120			B T

FIGURE 2.4. Summary of Protocols in which three isotopes were used.

^{125}I-HSA - Time of injection of ^{125}I-HSA

^{131}I-HSA - Time of injection of ^{131}I-HSA

EDTA - Time of injection of ^{51}Cr-EDTA

B - Time of blood sample

T - Time of tissue sample

Experiment types 1 - 3 are determinations of ^{131}I-HSA, ^{125}I-HSA and ^{51}Cr-EDTA volumes of distribution at the times indicated.

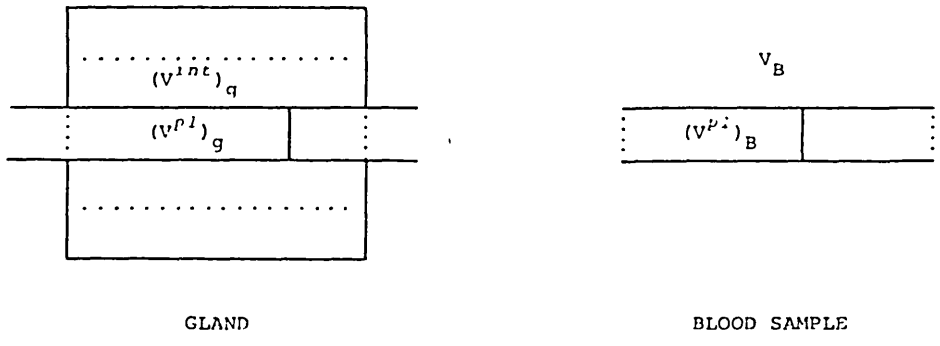


FIGURE 2.5. Schematic diagram of volumes of distribution of a solute in the gland and in a blood sample. See Section 2.3.12. for explanation of symbols.

CHARING CROSS & WESTMINSTER MEDICAL SCHOOL LIBRARY CHARING CROSS

$$A_B = C.(V^{pl})_B \qquad 2.27$$

But $$(V^{pl})_B = V_B(1 - H_B) \qquad 2.28$$

where A_g = total activity of isotope in gland

C = average concentration of isotope in its distribution volume

$(V^{pl})_g$ = intraglandular plasma volume

$(V^{int})_g$ = intraglandular interstitial volume

A_B = total activity of isotope in blood

$(V^{pl})_B$ = plasma volume of blood sample

V_B = total volume of blood sample

H_B = haematocrit of blood sample

Eliminating C and V_B^{pl} from equations 2.26 - 2.28 and expressing the result as volume per unit weight of gland gives

$$\frac{(V^{pl})_g + (V^{int})_g}{W_g} = \frac{A_g.V_B}{A_B.W_g}.(1 - H_B) \qquad 2.29$$

This is the total volume of distribution in the gland. The extravascular volume of distribution $(V^{int})_g$ is given by

$$(V^{int})_g = \text{Total volume of distribution} - (V^{pl})_g \qquad 2.30$$

From Fig. 2.5, it is easily seen that

$$(V^{pl})_g = (IVV)_g(1 - H_g) \qquad 2.31$$

where H_g is the intraglandular haematocrit, and IVV is the intravascular volume. Thus

$$\frac{(V^{int})_g}{W_g} = \left[\frac{A_g.V_B}{A_B.W_g} \cdot (1 - H_B)\right] - \left[\frac{(IVV)_g}{W_g} (1 - H_g)\right] \qquad 2.32$$

$(IVV)_g$ is readily calculated from this relationship, since, if $(V^{int})_g = 0$, eqn. 2.32 reduces to

$$\frac{(IVV)_g}{W_g} = \frac{A_g.V_B}{A_B.W_g} \cdot \frac{(1 - H_B)}{(1 - H_g)} \qquad 2.33$$

2.4. Results

2.4.1. Transvascular Escape Rate of ^{125}I-HSA

Table 2.2 shows the plasma ^{125}I-HSA concentration (expressed as a percentage of the 5 minute sample) as a function of time after the injection of labelled albumin. Fig. 2.6 displays the same data graphically, with ^{125}I-HSA concentration plotted on a logarithmic scale.

It was found that within the time of the experiment the data could be fitted by a bi-exponential curve,

TIME (min)	NORMALISED ^{125}I-HSA CONCENTRATION		
	MEAN	SEM	n
5	100	-	13
10	80.0	2.1	13
15	62.5	4.8	13
30	47.0	3.5	13
45	42.0	3.9	11
60	33.9	4.2	11
120	30.6	5.5	8
180	27.8	7.6	4
240	23.0	2.0	4
360	17.2	3.0	2

Table 2.2 Arterial concentrations of ^{125}-HSA at various times after injecting the isotope, expressed as a percentage of the 5 minute sample. n = number of samples. The data was fitted by a bi-exponential function

$$C(t) = C(5)\left[0.57e^{-(t-5)/12} + 0.43e^{-(t-5)/380}\right]$$

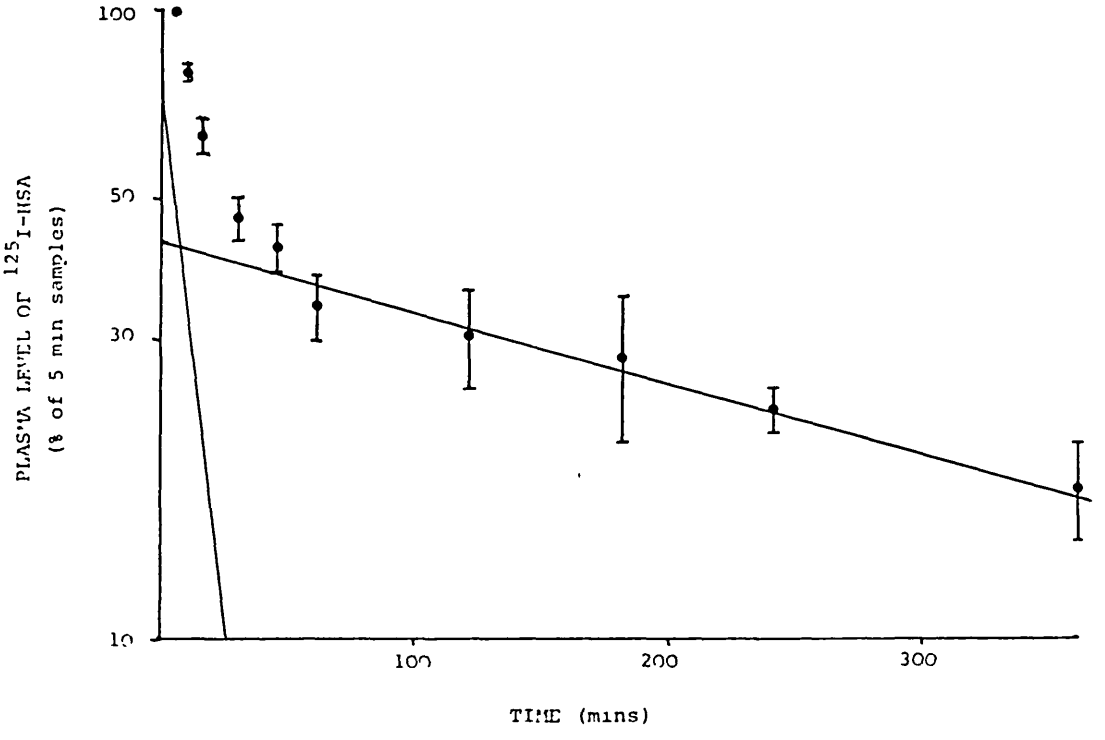


FIGURE 2.6. Plasma concentration of ^{125}I-HSA as a function of time after the initial intravenous injection. The sample taken 5 minutes after the injection was taken to be 100% and other values normalized to this. The solid lines represent the slopes of two exponentials derived from the curve as described in Section 2.4.1.

$$\text{ie} \quad C(t) = C(5)(a_1 e^{-t/\tau_1} + a_2 e^{-t/\tau_2}) \qquad 2.34$$

where C(5) and C(t) are the albumin concentrations after 5 and t minutes respectively, a_1 and a_2 are the ordinate intercepts, and τ_1 and τ_2 the time constants, of the two exponentials.

The procedure for determining a_1, a_2, τ_1, τ_2 was as follows; one monoexponential function was determined in the interval between 60 and 360 minutes using a least squares method. The line so obtained was extrapolated back to 5 minutes to give a_2. The fast exponential function was determined in the interval 10-30 minutes by subtracting the slow exponential from this part of the curve and fitting the resulting line by a least squares method. The values of a_1 and a_2 were normalised so that $a_1 + a_2 = 100 = C(5)$.

2.4.2. Intraglandular Haematocrit

Since most experiments were performed on animals in which one gland was stimulated whilst the other remained as a control it was not possible in this series of experiments to see whether there was any difference in large vessel haematocrit in the two situations. It is unlikely, however, that there should be a difference and in 2 animals in which both glands were unstimulated, large vessel haematocrit was 0.47 and 0.46.

In 38 experiments large vessel haematocrit was 0.47 ± 0.01 (mean ± SEM). In 6 control glands, dynamic intraglandular haematocrit was 0.20 ± 0.02 and in 6 glands stimulated for 5 minutes it was 0.29 ± 0.02.

2.4.3. Intravascular Volume

In the experiments in which 3 isotopes were used, it was possible todetermine the intravascular volume as well as the interstitial volume and the volume of distribution of albumin at various times. Table 2.3 shows that the stimulated glands had a higher intravascular volume than the control glands, but that there was no tendency for the intravascular volume to change with time. When the values for intravascular volume were pooled, the stimulated glands were found to have a significantly greater intravascular volume than the control glands ($p < 0.01$).

2.4.4. Interstitial Volume

Table 2.4 shows the ^{51}Cr-EDTA volumes of distribution at various times after the isotope injection, in both control and stimulated glands. It can be seen that in neither condition is there a tendency for the extravascular EDTA space to increase with time, suggesting that at 5 minutes the EDTA had fully equilibrated in its volume of distribution. Since the kidneys had been

TIME after ^{125}I-HSA (min)	INTRAVASCULAR VOLUME (ml.100 g^{-1})			
	MEAN	SEM	n	Difference from 30 min value
		CONTROL GLANDS		
30	5.5	0.20	4	-
60	5.3	0.27	4	NS
120	5.3	0.17	8	NS
Pooled	5.35*	0.12	16	
		STIMULATED GLANDS		
30	6.3	0.24	4	-
60	5.9	0.18	4	NS
120	5.9	0.21	4	NS
Pooled	6.03*	0.11	12	

TABLE 2.3 Intravascular volume, measured by ^{131}I-HSA injected 5 minutes before removal of the gland, in animals which had previously been given ^{125}I-HSA.

n = number of glands
NS = not significant

*The pooled values for intravascular volume in control and stimulated glands were significantly different ($p < 0.01$)

TIME (min)	^{51}Cr-EDTA VOLUME OF DISTRIBUTION ($ml.100\ g^{-1}$)			
	TOTAL		EXTRAVASCULAR	n
	CONTROL GLANDS			
	MEAN	SEM		
5	20.1	2.2	16.2	14
10	20.1	0.8	15.8	6
60	21.8	1.6	17.5	12
120	21.1	1.7	16.8	11
240	22.1	1.0	17.8	4
	pooled value		16.7 ± 0.4	
	STIMULATED GLANDS			
	MEAN	SEM		
5	19.9	1.0	15.6	6
10	20.5	1.4	16.2	5
60	21.2	2.0	16.9	8
120	21.1	1.8	16.8	4
240	22.2	2.0	17.9	4
	pooled value		16.6 ± 0.5	

TABLE 2.4. Volumes of distribution of ^{51}Cr-EDTA in control and stimulated glands, at various times after the injection of isotope. n = number of glands.
In neither control nor stimulated glands was there a tendency for the EDTA volume of distribution to increase with time, and so the values have been pooled. There is no sifnificant difference between the pooled estimates for control and stimulated glands.

ligated there was no tendency for plasma EDTA concentrations to fall once the molecule had equilibrated.

2.4.5. Extravascular Accumulation of ^{125}I-Labelled Albumin

Table 2.5 shows the extravascular ^{125}I-HSA volume of distribution at various times after the initial injection, and the same data is plotted in Fig. 2.7. In both stimulated and control glands, the extravascular albumin space slowly increased with time to reach a value of approximately 0.03 ml g^{-1} at 4-6 hrs.

At no time were the values for the control glands significantly different from those for the stimulated glands. The extravascular albumin space in control glands appeared to have reached a plateau after 240 minutes.

2.5. Comparison of Mathematical Model with Experimental Date

Figs. 2.8 and 2.9 show results of the model with different values of PS_{alb}^{cap} and σ_{alb}^{cap}. As expected, the extravascular volume of distribution of albumin gradually increases with time at a rate depending upon PS_{alb}^{cap} and σ_{alb}^{cap}. Closer inspection of Figs. 2.8 and 2.9 reveals

TIME (min)	^{125}I-HSA VOLUME OF DISTRIBUTION (ml.100 g^{-1})			
	TOTAL		EXTRAVASCULAR	
	CONTROL GLANDS			
	MEAN	SEM		p
5	4.4	0.3	0.1	-
30	4.7	0.4	0.4	NS
60	5.2	0.2	0.9	<0.005
120	5.8	0.2	1.5	<0.01
240	7.4	0.6	3.1	<0.001
360	7.3	0.4	3.0	<0.001
	STIMULATED GLANDS			
	MEAN	SEM		p
5	4.3	0.2	0	-
30	5.0	0.3	0.7	NS
60	5.5	0.5	1.2	<0.05
120	5.7	0.5	1.4	<0.05
240	7.6	0.5	3.3	<0.01

TABLE 2.5. Volumes of distribution of ^{125}I-HSA in control and stimulated glands, at various times after the injection of isotope. n = number of glands. The p values in the last column refer to the difference from the distribution volume at 5 minutes.
NS = not significant

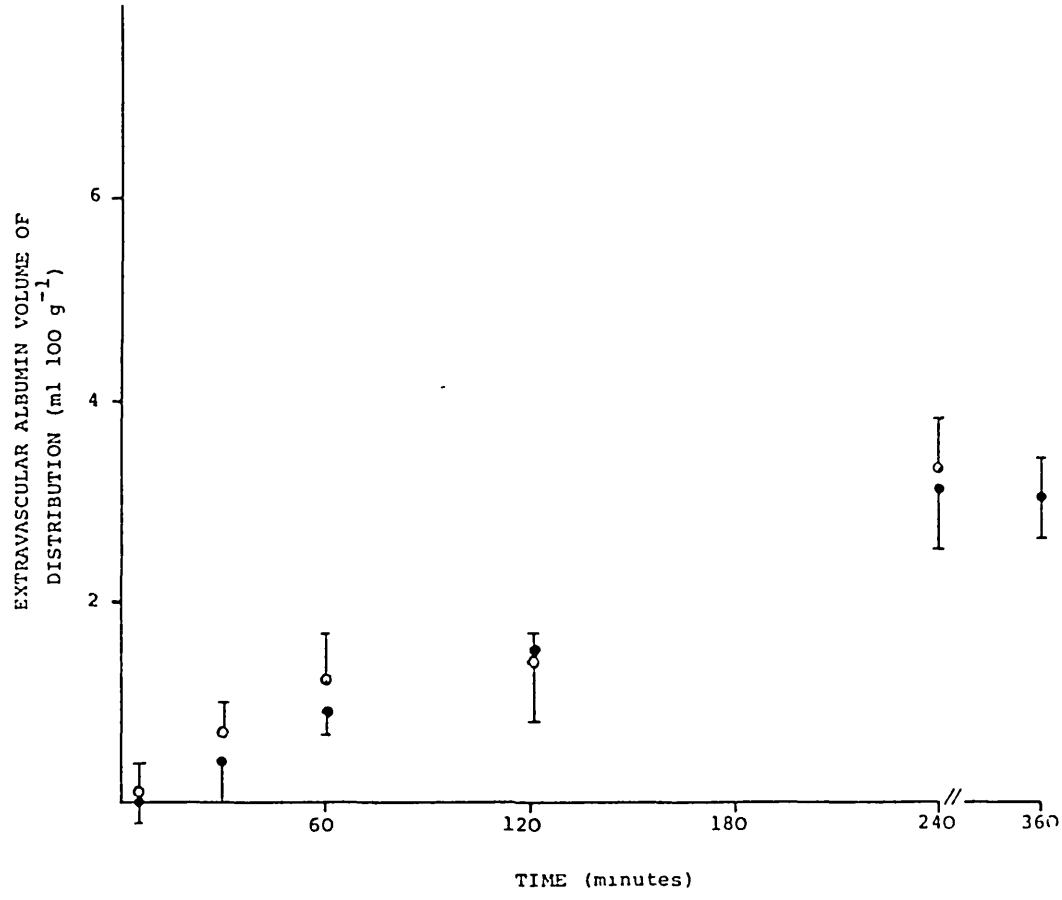


FIGURE 2.7. Extravascular volume of distribution of albumin at various times after injection of ^{125}I-HSA in control (●) and stimulated (o·) glands. Vertical bars represent one standard error of the mean.

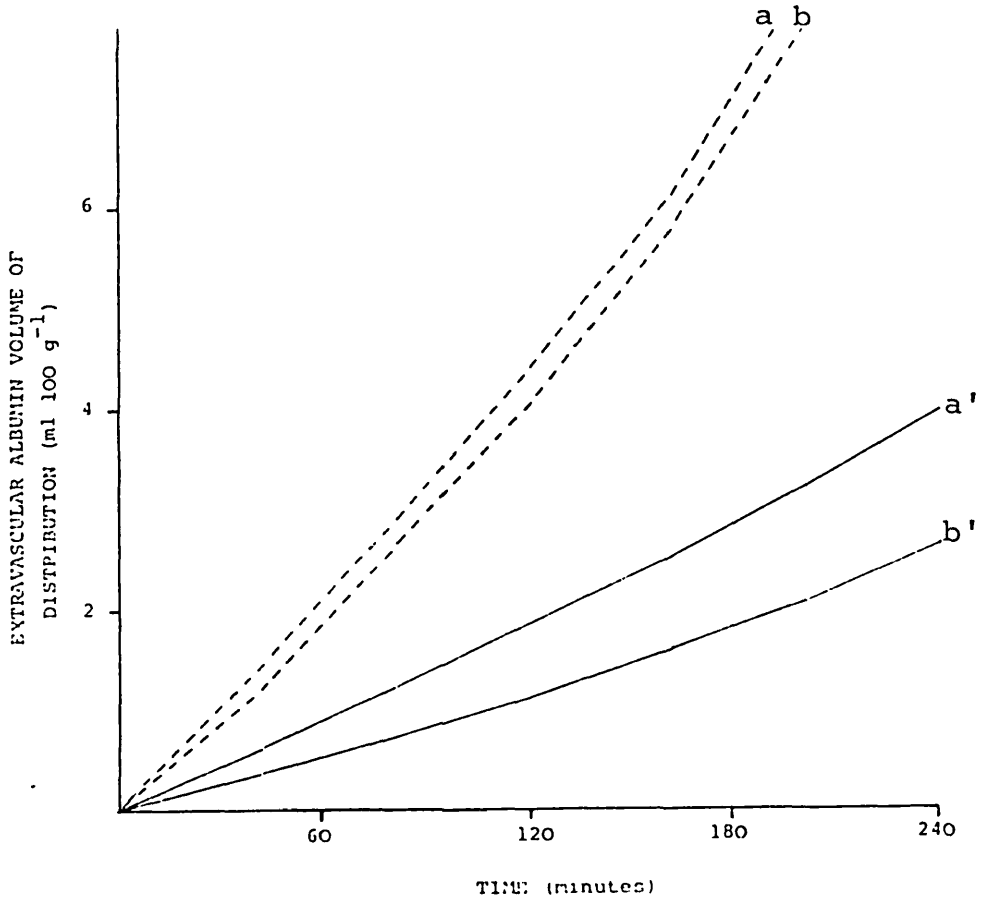


FIGURE 2.8. Extravascular accumulation of albumin predicted by computer model for control (——) and stimulated (---) glands; σ_{alb}^{cap} = 0.99. Note that even with this high value of σ_{alb}^{cap}, the high filtration rate causes a substantial movement of albumin into the interstitium.

Two values of PS_{alb}^{cap} are shown

a, a' PS_{alb}^{cap} = 1.1 x 10^{-4} ml min^{-1} g^{-1}

b, b' PS_{alb}^{cap} = 0.6 x 10^{-4} ml min^{-1} g^{-1}

V_{alb}^{int} (∞) = 4 ml 100 g^{-1}

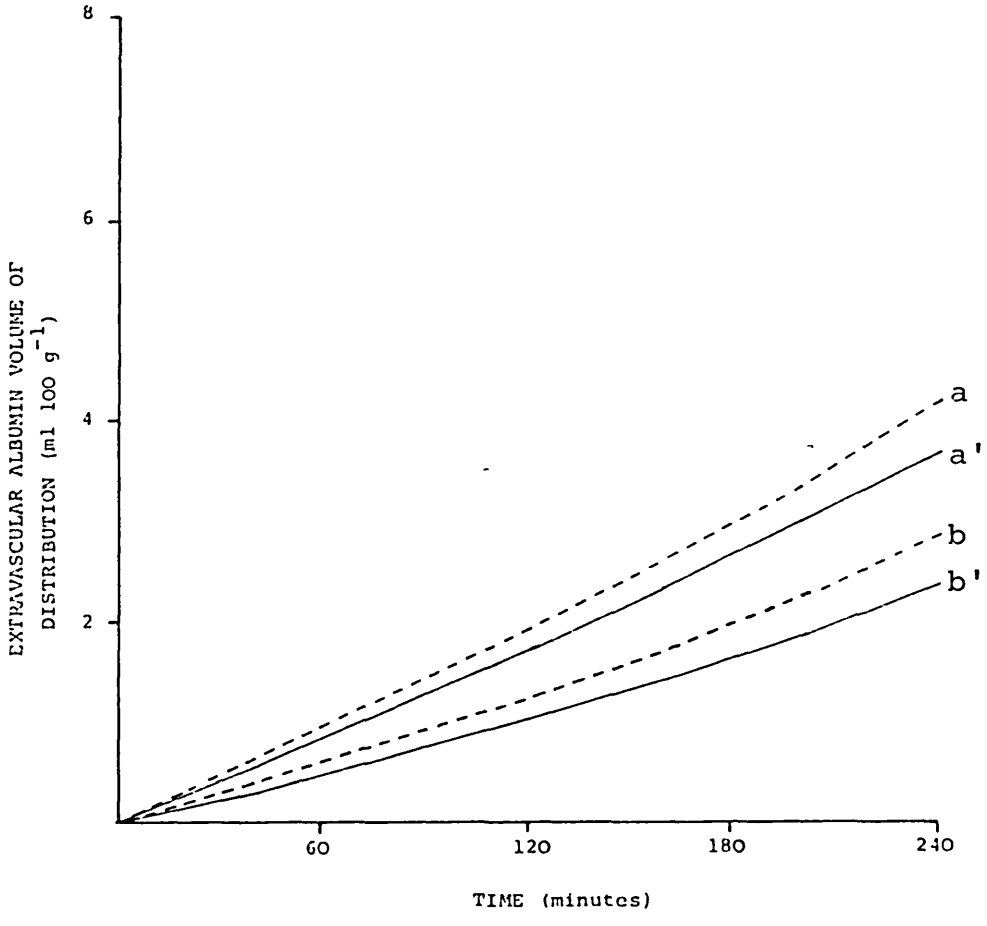


FIGURE 2.9. Extravascular accumulation of albumin predicted by computer model for control (——) and stimulated (- - -) glands; σ_{alb}^{cap} = 0.999. The values of PS_{alb}^{cap} shown are the same as in Fig. 2.8. Note that changing σ_{alb}^{cap} does not make much difference to the rate of accumulation in control glands but brings the rate in stimulated glands down almost to the level in control glands.

several interesting points:-

1. Perhaps the most striking feature of the results predicted by the model is the value of σ_{alb}^{cap}. In order to account for the data, this must be very close to 1. The pilot runs of the model used a value of 0.9 for σ_{alb}^{cap}, but it quickly became clear that a much higher value was required. Even a value for σ_{alb}^{cap} of 0.99 will result in a relatively large amount of albumin being transported into the interstitium under conditions when the filtration rate is high.
2. At low filtration rates, the rate of extravascular albumin accumulation depends more upon the value of PS_{alb}^{cap} than that of σ_{alb}^{cap}. This supports the assumption of low PS_{alb}^{cap} made in Section 2.3.6 and allows an estimate of PS_{alb}^{cap} to be made from the early times, using equation 2.15. This gives estimates of approximately 6×10^{-5} ml $min^{-1}g^{-1}$ for control gland and 8×10^{-5} ml $min^{-1}g^{-1}$ for the stimulated gland.
3. An estimate of σ_{alb}^{cap} may also be made from the rate of albumin accumulation at early times. Using the first 30 minutes, equation 2.17 predicts that $\sigma_{alb}^{cap} = 0.985$.
4. The values obtained for PS_{alb}^{cap} and σ_{alb}^{cap} using the 30 minute interstitial albumin volumes do not give good fits to the experimental values up to 240 minutes. Since the control and stimulated

accumulation rates are not significantly different, it is clear that σ_{alb}^{cap} must be very close to 1. Once this is fixed, PS_{alb}^{cap} and $V_{alb}^{cap}(\infty)$ may be varied to fit the experimental data. Figs. 2.10 and 2.11 show some pairs of PS_{alb}^{cap} and $V_{alb}^{int}(\infty)$ values in control and stimulated glands. It is clear that the estimate of PS_{alb}^{cap} increases, $V_{alb}^{int}(\infty)$ must decrease in order to fit the data. Putting PS_{alb}^{cap} equal to 6×10^{-5} ml $min^{-1} g^{-1}$ (point 2 of this Section) yields $V_{alb}^{int}(\infty) = 0.04$ ml g^{-1}.

5. At the high levels of reflexion coefficient required, varying lymph flow does not have an appreciable effect on the predictions of the model. Fig. 2.12 shows the effect of changing the lymph flow by a factor of 100 on the model predictions of albumin accumulation. The difference shown would not be detectable within the experimental errors.

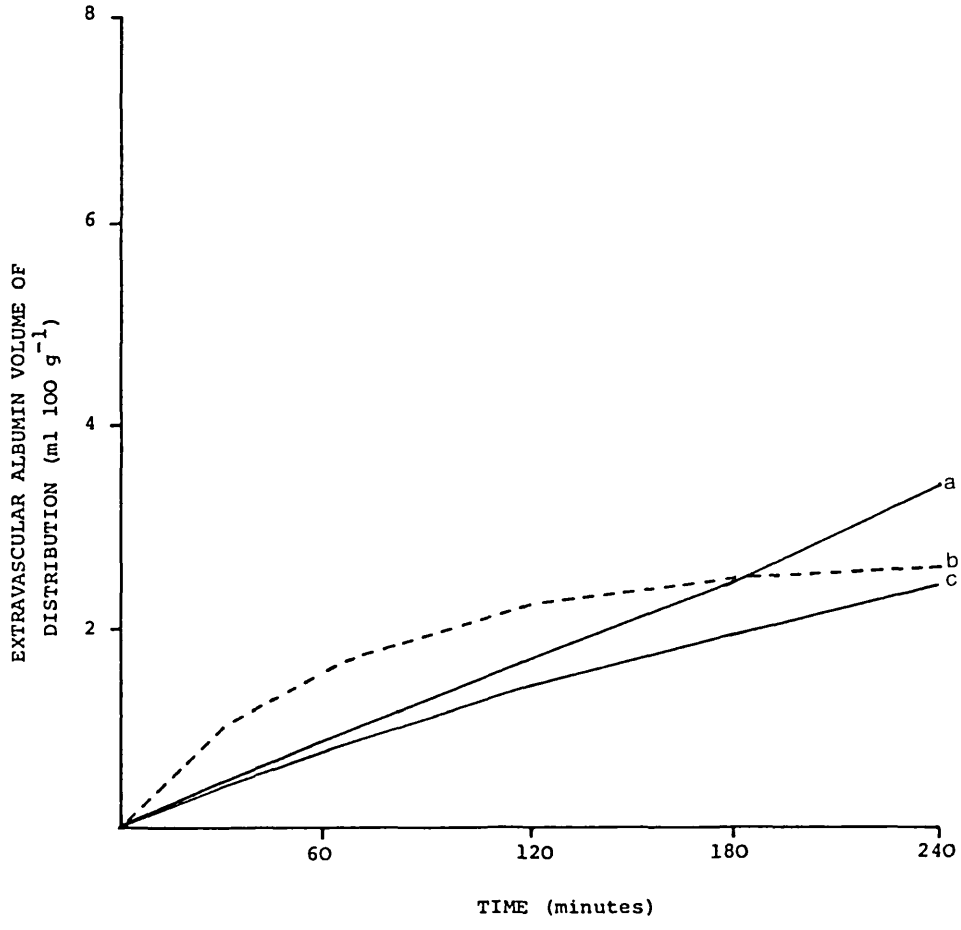


FIGURE 2.10. Effect of changing PS_{alb}^{cap} and $V_{alb}^{int}(\infty)$ (values indicated on figure) on computer predictions of extravascular albumin accumulation. Control conditions.

	PS_{alb}^{cap}	$V_{alb}^{int}(\infty)$
	ml min^{-1}g^{-1}	ml 100 g^{-1}
a	1.1 x 10^{-4}	3
b	3.1 x 10^{-4}	2
c	1.1 x 10^{-4}	2

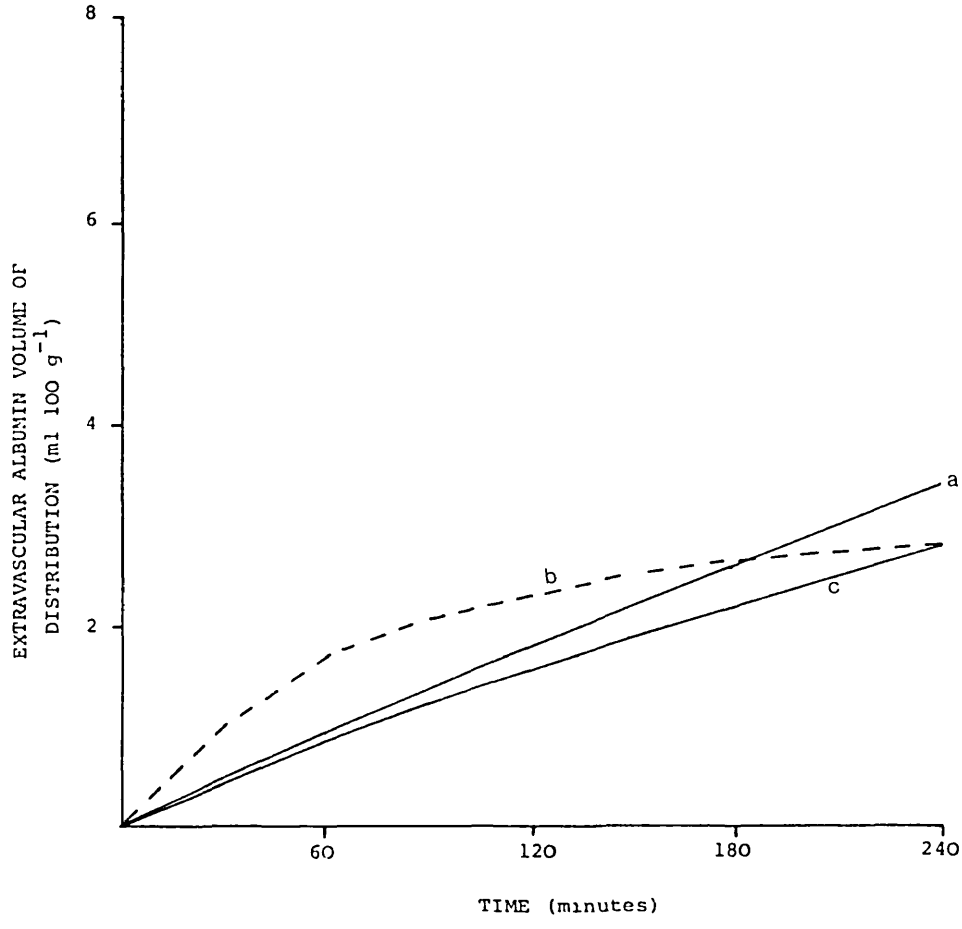


FIGURE 2.11. As for Fig. 2.10 but stimulated conditions are inserted into the model.

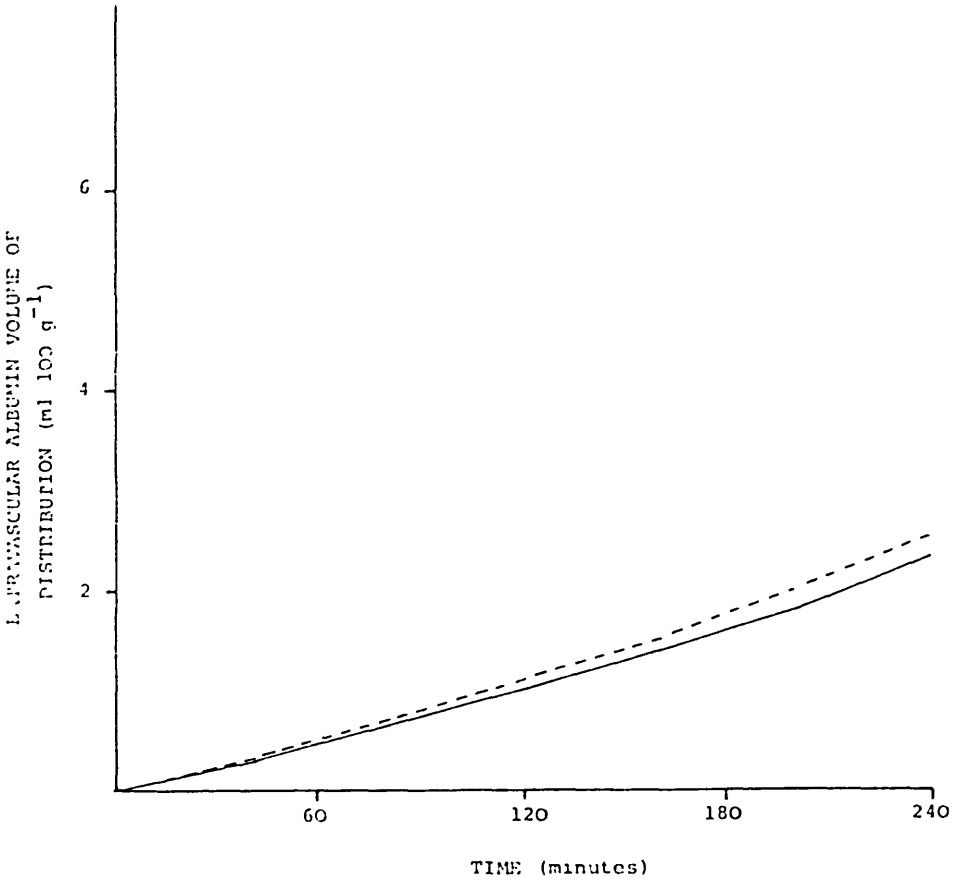


FIGURE 2.12. Effect of changing lymph flow by a factor of 100 on the computer predictions of extravascular albumin accumulation.

$J_v^L = 10^{-4}$ ml $min^{-1}g^{-1}$ (——)

$J_v^L = 10^{-2}$ ml $min^{-1}g^{-1}$ (- - -)

2.6. Discussion

2.6.1. Use of ^{125}I-HSA and ^{51}Cr-EDTA as Markers for the Various Volumes of Distribution in the Salivary Gland

In the studies of Mann et al (1979a, b), a high permeability was found to low and medium molecular weight substances in the cat submandibular gland. This raised the possibility that the intravascular marker albumin may not have remained in the vasculature during the time course of their experiments. Mann (1978) investigated this problem by injecting labelled erythrocytes and labelled albumin simultaneously and comparing the resulting indicator dilution curves. Although there was some variability in the recoveries of the tracers, there appeared to be no indication that a measurable quantity of ^{125}I-HSA was entering the extravascular space in the 5 - 10 seconds required for a dilution run. The results of the present experiments support this conclusion: 30 minutes after the injection of labelled albumin, its measured volume of distribution was not significantly different from that at 5 minutes. This could mean either a very rapid equilibration (high permeability) or a very slow accumulation (low permeability). The fact that the measured volume of distribution begins to rise after 30 minutes supports the latter interpretation. Owen and Triffit (1976), using a similar method in various tissues of the rabbit, found that the 5 minute ^{125}I-albumin space

was higher than the 5 minute ^{125}I-fibrinogen space in all tissues they studied. The authors proffered no explanation for this phenomenon, but it is of course possible that some albumin has escaped from the vasculature. Another possible interpretation is that the labelled albumin has been taken up by the endothelial cells in the gland, causing the albumin space to be overestimated. The experiments described in Section 2.3.7 suggests that the labelled albumin does not bind to erythrocytes, and so the possibility of endothelial cell uptake of albumin is less likely. Owen and Triffitt (1976) did not state whether their albumin and fibrinogen volumes of distribution were calculated using only precipitable ^{125}I activity. If they were not, then a larger proportion of unbound ^{125}I in the albumin samples could also account for the result.

EDTA has been used as an extracellular marker in various tissues and the results of the in vitro experiments described in Section 2. support the conclusion that EDTA does not penetrate cells in any measureable amount within the time course of the experiments. Further support for this interpretation comes from the fact that the measured extravascular EDTA space is far smaller than the total extravascular gland water content, but does not tend to increase with time. The values for EDTA volume of distribution agree well with those obtained by Mann, (1978), using the multiple tracer indicator

dilution technique in the cat submandibular gland.

2.6.2. Disappearance of Labelled Albumin from Plasma

The continuous fall in plasma concentration of radiolabelled albumin necessitated a correction in the mathematical analysis. The physiological significance of this fall is not clear, but it has been assumed that the early phase (approximately 1 - 2 hours) represents transcapillary passage of the albumin into the interstitium. The plasma albumin concentration is plotted logarithmically as a function of time, and the slope of the resulting line is equal to the 'transcapillary escape rate' Clearly, the assumed transcapillary passage of albumin depends crucially on the time constants of the plasma albumin concentration. It was thus disappointing to note that the time constants found in the present experiments were different from those found in rabbits by Owen and Triffit (1976) and Bill (1977). However, Owen and Triffit (1976) measured plasma albumin at only three times during the first 24 hours and so it is difficult to estimate the time constants in the first 4 - 6 hours. Bill (1977) tried to maintain a constant plasma concentration by intermittent injection of small quantities of ^{131}I-HSA; his plasma samples were taken only at intervals of 60 minutes, and so it is again difficult to estimate time constants within 4 - 6 hours. Paaske (1983) sampled every 15 seconds for the first 10 minutes and then every

5 minutes up to the 60th minute. His short time constant of 4 minutes is much shorter than that found in the present experiments but may partly reflect intravascular mixing of the albumin; the long time constant of approximately 450 minutes agrees reasonably well with that of 380 minutes found in the experiments described in this Chapter.

The transcapillary escape rate method has been employed and subjected to extensive analysis by a number of authors (eg Lassen, Parving and Rossing, 1974; Perl, 1975; Paaske, 1983) in order to elucidate the mechanism of albumin transport in the whole organism. One of the most recent contributions to the subject has been that of Paaske (1983) who obtained results identical to those of Perl (1975) for γ (the solvent drag component of unidirectional tracer outflux relative to the permeative component), j_{sc}/j_{sp} (the convective component of net albumin flux) and j_{12}/j_{21} (the pure permeation ratio of influx to outflux). In his analysis Paaske uses the following equation (his Eqn. 9) from Perl (1975; Eqn. 12)

$$R = \frac{PS_{alb}^{cap} + \frac{1}{2}(1 - \sigma_{alb}^{cap}).J_v^L}{PS_{alb}^{cap} + \frac{1}{2}(1 + \sigma_{alb}^{cap}).J_v^L} \qquad 2.35$$

where

$$R = \frac{\text{interstitial albumin concentration}}{\text{plasma albumin concentration}} \qquad 2.36$$

Rearranging gives

$$\frac{J_v^L}{PS_{alb}^{cap}} = \frac{2(1-R)}{R(1+\sigma_{alb}^{cap})J_v^L} \qquad 2.36$$

Since

$$\gamma = \frac{\frac{1}{2}(1-\sigma_{alb}^{cap})J_v^L}{PS_{alb}^{cap}} \qquad \text{(Perl, 1975;Eqn 36)}$$

we obtain

$$\gamma = \frac{(1-R)(1-\sigma_{alb}^{cap})}{R(1+\sigma_{alb}^{cap}) - (1-\sigma_{alb}^{cap})} \qquad 2.37$$

The solution to this equation thus depends only upon the values of R and σ_{alb}^{cap} chosen. Also, since

$$\frac{j_{sc}}{j_{sp}} = \frac{(1+R)}{(1-R)}\gamma \qquad 2.38$$

and

$$\frac{j_{12}}{j_{21}} = \frac{R(1-\gamma)}{(1+\gamma)} \qquad 2.39$$

these ratios will also depend on the values chosen for R and σ_{alb}^{cap}. The values R = 0.61, σ_{alb}^{cap} = 0.9 were used by both Paaske (1983) and Perl (1975). Using these values, we obtain

$$\gamma = 0.037$$

$$\frac{j_{sc}}{j_{sp}} = 0.153$$

$$\frac{j_{12}}{j_{21}} = 0.566$$

exactly the values obtained by Paaske, Paaske, however, arrived at these figures by calculating mean transit times for plasma albumin from the disappearance curves, and incorporating them into simultaneous equations which reduce to equations 2.37 - 2.39 above.

Paaske states that "the so-called transcapillary rate ..... cannot be attributed to reflect any physiological process, especially not the transcapillary exchange of albumin". Unfortunately, Paaske's analysis would seem to throw no further light on this statement as it is based on equations whose solutions do not depend on his experimental data but on assumed values taken from the literature.

In the present experiments the plasma albumin concentrations were measured merely to estimate the trans-capillary concentration difference at a given time, and not to make any contribution to the argument about the mechanism of albumin transport.

2.6.3. Dynamic Haematocrit in Control and Stimulated Glands

An important finding is that this tissue haematocrit is lower than the venous haematocrit; this is true in both control and stimulated glands but the haematocrit is higher in the stimulated glands. This finding is in agreement with the work of Klitzman and Duling (1979) who measured the haematocrit in individual capillaries of resting and stimulated skeletal muscle in hamsters. They found that the low microvessel haematocrit could not be fully explained by a high red cell flux through arteriovenous anastomoses, an interpretation which would also hold in the rabbit submandibular gland, where Fraser and Smaje (1977) failed to find any arteriovenous anastomoses.

Klitzman and Duling (1979) proposed that the low resting capillary haematocrit was the result of a difference in velocity between red cells and plasma, with a relatively slow moving plasma annulus surrounding the red cells. According to their theory, the resting tissue

haematocrit found in the present study can be accounted for by a red cell/plasma velocity ratio of 1.5 and a plasma annulus thickness of 0.4 μm, while in the stimulated gland either the velocity ratio decreases to unity or the annulus disappears

It is not clear whether these changes in microvessel haematocrit are of significance in determining the oxygen supply to a tissue, since it is red cell flux, not haematocrit, which determines oxygen supply. For the same red cell flux, however, an increased capillary haematocrit will mean more red cells in a capillary at any time. This may be important in maintaining the oxygen supply to contracting skeletal muscle, where the contraction stops the blood flow for a time comparable to the red cell transit time through the capillary. It is difficult to envisage an equivalent explanation in the salivary gland, and it may be that the increased tissue haematocrit is merely a reflection of a higher plasma velocity.

The importance of a low gland haematocrit in the present experiments is that allowance must be made for it in calculating intravascular volumes.

2.6.4. Intravascular Volume, Capillary Surface Area and Capillary Recruitment During Nerve Stimulation

Knowledge of intravascular volume in these experiments was important in order to calculate the extravascular volume of distribution of albumin and EDTA. Additionally, the value may be used to estimate capillary surface area, since

$$\text{Surface Area} = \frac{2 \times IVV}{r} \qquad 2.40$$

where IVV is intravascular volume and r is the capillary radius. Use of this relationship is valid only if the capillaries comprise all the intravascular volume of the gland.

Buran and Smaje (1982) used light microscopical analysis of 0.5 μm sections of rabbit submandibular gland and obtained values of 413 cm^2g^{-1} and 4.1 μm for capillary surface area and diameter respectively; Olive and Smaje (unpulished) found that capillaries occupied approximately 99% of the total vascular volume in the gland. More recently, Clough and Smaje (accepted for publication) have used electron microscopy on the same organ and have obtained values of 512 cm^2g^{-1} and 5.9 μm for capillary surface area and diameter respectively.

The estimates of intravascular volume obtained in the present studies yield surface area values of 366 cm^2g^{-1} for control glands and 407 cm^2g^{-1} for stimulated glands,

using the Buran and Smaje estimate for capillary diameter; when the Clough and Smaje estimate is used, the surface area values become 527 cm^2g^{-1} and 585 cm^2g^{-1} for control and stimulated glands, respectively. The average value from all these studies is approximately 470 cm^2g^{-1}, which is more than 6 times the value for skeletal muscle, but comparable to the figure found in cardiac muscle (Table 2.6).

The reason for such a large surface area is not entirely clear. It is possible that oxygen demands for secretion determine the number and spacing of capillaries and Henderson and Smaje (1984) have estimated that a cubic lattice with junctions 32 μm apart (giving a capillary surface area of 370 cm^2g^{-1}), cound account for the observed oxygen consumption of the gland during secretion. It is thus interesting to note that Fraser and Smaje (1977), using *in vivo* microscopy in the rabbit submandibular gland, found a meshwork of capillaries with juctions 25-40 μm apart in the acini and 15-20 μm apart around the intralobular ducts. However, since the venous Po_2 in the stimulated gland is higher than in the resting gland, it is clear that oxygen delivery to the gland is more than adequate to sustain secretion, and it may be that the need to transport a large volume of fluid out of the vasculature without a large increase in haematocrit is important in determining capillary surface area.

Organ	Capillary Surface Area ($cm^2 g^{-1}$)	Reference
Rabbit Heart	560	(a)
Rabbit Lung	3500	(b)
Rabbit Gastrocnemius	62	(b)
Rabbit Submandibular Gland	512	(c)

TABLE 2.6. Capillary surface areas in various organs of the rabbit.

References

a) Vargas and Johnson (1967)

b) Perry (1980)

c) Clough and Smaje (in press)

The 11% rise in capillary surface area during parasympathetic nerve stimulation suggests that there is capillary recruitment of this order. However, since blood flow increases approximately tenfold during stimulation the major mechanism for increased flow must still be an increased velocity. The results of Damon and Duling (1984) support this conclusion. Using *in vivo* microscopy of vessels in skeletal muscle, they found that at least 83% of the capillaries contained moving erythrocytes in resting tissues. The maximum recruitment would thus be approximately 20%.

2.6.5. Exclusion of Albumin in the Interstitium

The value for the EDTA volume of distribution agrees well with that found by Mann (1978) in the cat submandibular gland, but the value for the extravascular volume of distribution of albumin is much smaller than the EDTA volume. This implies that albumin is excluded from a portion of the interstitial space. The phenomenon of exclusion was first described in connective tissue polysaccharides by Ogston and Phelps (1961), following the proposal by Ogston (1958) that a random array of fibres would exclude a particle from a part of the volume occupied by the array. According to Ogston's theory, if such an array of fibres occupies a fractional volume$(1 - \varepsilon)$ of the total volume, and each fibre has a radius r_f, then the fractional volume available (K_{av}) for a sphere of

radius a is given by

$$K_{av} = \exp\left[\frac{-(1 - \varepsilon)}{r_f^2} \quad (a^2 + 2ar_f)\right]$$

The volume of distribution for albumin(a = 3.6 nm) obtained in the present study suggests that K_{av} = 0.15-0.25 However, there are difficulties in applying eqn. 2.41 directly to this data. The interstitium is a gel, consisting of an array of fibrils, composed mainly of collagen intermingled with hyaluronic acid and proteoglycans. McMaster and Parsons (1939) described preferential channels in the interstitium which they associated with collagen fibres; these could provide a low resistance pathway for transport of large solutes, with the hyaluronic acid and proteoglycan 'ground substance' creating a matrix with more restrictive properties. This arrangement resembles a gel chromatography column (Arturson, Groth and Grotte, 1972), and evidence for this arrangement has been provided by Watson, Bell and Renkin (1978) who found that larger molecular weight tracers approach equilibrium in lymph faster than small ones. However, to take the chromatography column analogy further might lead to difficulties, since it might be expected that much smaller molecular weight tracers would equilibrate even more slowly. This is clearly not the case in the present experiments, since EDTA had equilibrated 10 minutes after the intravenous injection; if lymph represents interstitial fluid, then

there will be equally rapid equilibration in the lymph. Rutili and Arfors (1976) found that FITC-dextran of molecular weight 2300 equilibrated in the interstitium and in lymph with the same time course as inulin (molecular weight $\sim$ 5500), and both had equilibrated within 2 hours. If the interstitium is the major barrier to solute transport (Watson, 1980), then the molecules used by Rutili and Arfors (1976) would have had different equilibration times.

Thus the interstitium cannot be considered simply as containing a random array of uniform fibres, and it is necessary to know the volume of 'free fluid' contained within the collagen fibres per unit volume of interstitium before the density of the ground substance matrix can be calculated. However, the least restrictive ground substance matrix may be estimated by assuming that there are no free fluid channels. With a matrix of hyaluronic acid (radius 0.3 nm) the aqueous volume (ε) for an excluded volume fraction of 0.25 is 0.99. The pore size distribution of a matrix with such properties is shown in Fig. 2.13; the frequency distribution of pore radii is given by (Ogston, Preston and Wells, 1973)

$$g(R) = \frac{(1 - \varepsilon)R}{r_f^2} \exp\left[-\frac{(1 - \varepsilon)}{r_f^2} R^2\right] \qquad 2.42$$

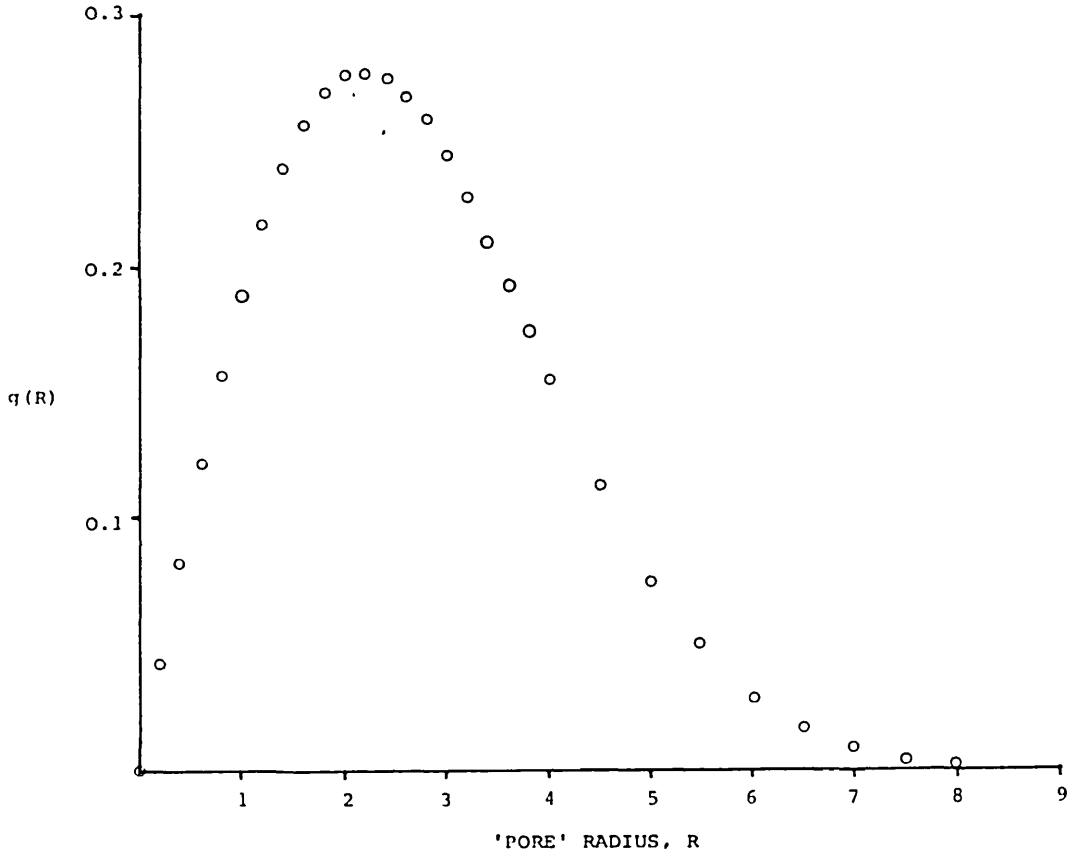


FIGURE 2.13. Pore size distribution of a fibre matrix according to Ogston, Preston and Wells (1973). Aqueous volume (ε) = 0.99; fibre radius (r_f) = 0.3 nm. g(R) is the fraction of pores with radius R.

$$g(R) = \frac{(1 - \varepsilon)}{r_f^2} \exp\left(- \frac{(1 - \varepsilon)R^2}{r_f^2}\right)$$

where g(R) is the fraction of pores of radius R. The maximum frequency is found at pore radii between 2 and 2.5 nm. Allowing preferential 'free fluid' channels would shift the distribution to even smaller pore radii. This would imply that albumin is almost completely excluded from the ground substance and equilibrates mainly in the channels. If this is the case in the submandibular gland then one would expect parasympathetic nerve stimulation, by causing an increase in convection, to ensure better mixing of albumin in the interstitium. The fact that stimulation did not increase the rate of equilibration of albumin strongly suggests that no gradient of concentration of albumin existed in the interstitium even in the resting gland, and that the capillary wall must be regarded as the major barrier to albumin movement.

2.6.6. Permeability and Reflexion Coefficients of Albumin

Perhaps the most important results of the experiments described in this Chapter are the high value of σ_{alb}^{cap} and the low value of PS_{alb}^{cap} predicted by the model. Previous experiments in the cat submandibular gland (Koo et al, 1980) suggested that σ_{alb}^{cap} was closer to 0.75 and PS_{alb}^{cap} was approximately 10^{-3} ml min^{-1} g^{-1}. These latter figures were based on estimates of lymph flow which were very uncertain, due to

1. the difficulty of cannulating a lymphatic vessel leaving the gland
2. the resistance of the cannula placed in the lymphatic, which may have been high enough to divert lymph flow into other vessels, and
3. the fact that there were other lymphatic vessels besides the one cannulated.

The value of σ_{alb}^{cap} may have been an underestimate, due to the possibility that lymph flow may not have been high enough to make the lymph:plasma albumin ratio independent of filtration (Granger and Taylor, 1980), but the errors in determination of lymph flow would lead to an underestimation of PS_{alb}^{cap}. The reason for the discrepancy between the results of Koo et al (1980) and the present results is not clear, but may be related to the increased dissection necessary in the former study in order to identify and cannulate a lymphatic vessel.

In recent years, evidence has been accumulating that fenestrae do not act as "giant pores"; rather that they are as selective as the "continuous" portions of endothelium in both fenestrated and continuous capillaries Grotte (1956) found that glomerular permeability to dextrans of various sizes was low, and decreased with increasing molecular size; Granger and Taylor (1980) found a reflexion coefficient to albumin of 0.9 in the cat ileum; Mann et al (1979a) found evidence of restricted diffusion even to small molecules in the cat submandibular gland; Bill (1977), using an isotope accumulation technique in various tissues of the rabbit, concluded that "the protein permeability of the capillary wall in most tissues with continuous or fenestrated capillaries may be similar".

The study which is perhaps most comparable to the present one is that of Bell, Pinter and Wilson (1978), who found a reflexion coefficient to albumin of greater than 0.998 in peritubular capillaries of the rat kidney. These authors measured the mean transit time of ^{125}I-labelled HSA from plasma to lymph in control animals and in animals which had received an infusion of hypo-osmotic fluid. Unidirectional clearance of labelled albumin was not significantly different in the two conditions, suggesting that convection plays a negligible role in albumin transport in these capillaries.

It is difficult to evaluate the results from this Chapter in terms of transport pathways. This aspect is discussed more fully in Chapter 4 where the data from all the experiments performed for this thesis are collected. Clearly the data from this chapter are incompatible with a single pore size, since the pore radius estimated by Mann et al (1979a) would lead to a much higher permeability-surface area product and lower reflexion coefficient than was found.

Teleologically, it is not unreasonable for albumin transport in the gland to be virtually independent of the volume flow. Fig. 2.7 suggests that an albumin reflexion coefficient even as high as 0.99 would lead to a rapid interstitial accumulation of albumin during nerve stimulation. When stimulation stops there would be an increased force favouring filtration. If salivation stops immediately, filtration will continue until the interstitial colloid osmotic pressure has returned to normal. The gland will thus become oedematous. There is no evidence to suggest that the gland gains weight at the end of stimulation, or that the albumin concentration of lymph increases, either of which would indicate extravascular concentration of albumin beyond the normal value.

The experiments described in this Chapter, although simple, have suggested that the fenestrated endothelium of the rabbit submandibular gland is more highly selective

to albumin than any other capillary endothelium for which published data is available. Whether the selectivity resides in the properties of a fibre matrix, in the tightness of the interendothelial junctions, or in the basement membrane, remains to be seen.

CHAPTER 3

A Model for Osmotically-Induced Weight Changes in the Submandibular Gland

A MODEL FOR OSMOTICALLY-INDUCED WEIGHT CHANGES IN THE SUBMANDIBULAR GLAND

3.1. Introduction

In 1964, Vargas and Johnson introduced a modification of the osmotic transient method of Pappenheimer et al (1951) which appeared to overcome some of the problems associated with the original technique. In particular, the venous pressure did not have to be adjusted during the course of the experiment, thus avoiding the error introduced by vascular compliance and the uncertainty associated with deciding whether or not the preparation was isogravimetric. Using the isolated, Ringer-perfused, rabbit heart Vargas and Johnson (1964) suddenly introduced a known concentration of an osmotically active test solute into the solution perfusing the previously isogravimetric organ. Fluid was drawn from the interstitium into the vasculature and the gland lost weight. No attempt was made to counter-balance the weight loss, but its magnitude was measured. Vargas and Johnson (1964) argued that, at time zero (ie when the test solute first enters the gland), the concentration difference of test solute across the capillary wall was equal to the concentration of test solute in the perfusate and so the initial rate of weight loss would be determined by $J_v^{cap} = K_f \sigma_{test}^{cap} RT\Delta C_{test}^{cap}$, where the subscript *test* refers to the properties of the test solute. K_f was previously determined using albumin as the test solute

assuming that $\sigma_{alb}^{cap} = 1$. Vargas and Johnson (1967) extended their work to the estimation of permeability-surface area products for the test solutes, arguing that as the solute crossed the capillary wall, the transcapillary concentration difference would be reduced and the rate of weight loss correspondingly lessened. They found that the rate of weight loss decreased monoexponentially with time, and that the slope of the log J_V^{cap} vs time graph was equal to PS_{test}^{cap}/V^{int}, where V^{int} is the interstitial volume of distribution of the test solute.

In their original experiments, Vargas and Johnson (1964, 1967) used a model which neglected such factors as solvent drag, lymph flow, interstitial compliance, "osmotic buffering" due to sieving of low molecular weight solutes (principally NaCl) and changes in cell volume. Some of these factors were discussed in the 1967 paper, and it was felt at that time that no serious errors would be introduced by their neglect. Between 1967 and 1976 very little work was published relating to the Vargas and Johnson technique, due perhaps to the criticisms that 'time zero' was difficult to estimate and that the transcapillary concentration difference of test solute would not be equal to the arterial concentration if the solute crossed the capillary wall.

Grabowski and Bassingthwaighte (1976) presented a detailed model of the osmotic transient experiment which included all the factors mentioned above. Their model

considered the organ to be divided into 5 adjacent segments of capillary, interstitium and cells. Changes in volume and solute concentrations in one segment determined what entered the next segment and so solute concentrations could change from arterial to venous end of the capillary. The model predicted that a substantial amount of water would leave the cells and would contribute to the weight loss incurred during the transient. Another important conclusion of their work is the prediction that sieving of low molecular weight 'resident' solutes (mainly NaCl) at the capillary wall could lead to large errors in the estimation of permeability, filtration and reflection coefficients.

Johnson and his colleagues (Bloom and Johnson, 1981; Johnson and Bloom; Johnson, Bloom, Anderson and McEvoy, 1981) developed a different model of the osmotic transient which represented the capillary, interstitium and cells each as single compartments. Although they recognised that the intracapillary concentration of the test solute could fall along the length of the capillary, they argued that this would be small because of the high perfusate flows employed in their studies. Their model also predicted a large transcellular water flux contribution to the total weight change during the transient, particularly for the low molecular weight test solute (NaCl). In contrast to the predictions of Grabowski and Bassingthwaighte (1976), however, they found that osmotic buffering had a negiligible effect on the estimation of the permeability coefficients. They attributed this to the rapid dissipation by diffusion

of any transcapillary concentration gradients which may have been established by sieving.

One feature of the model of Bloom and Johnson (1981) is the direct comparison of the model predictions with the methods of measuring reflexion and permeability used in the 1964 and 1967 papers. They concluded that "the zero time extrapolation ..... yields valid estimates of solute reflexion coefficients if ..... the flow is high and the volume of conduits leading to the capillaries is small". The situation for estimating PS products is more complicated; for molecules the size of inulin or larger, the slope of the ln J_v^{cap} vs time graph had to be modified by a factor related to interstitial elasticity, whereas for molecules smaller than NaCl, the correct PS product was found by equating the slope to $PS/(V^{int} + V^{cell})$, where V^{cell} is the intracellular volume, instead of PS/V^{int}. The modifications were valid "only if the parameters of the model are in the approximate range of those we have found in our system .... in which V^{int} undergoes little change. For molecules between inulin and NaCl in size the apparent rate constant is more complex and we have no way at this time of interpreting the slope to make it available for a permeability estimation".

The fenestrated capillaries of the submandibular gland are highly permeable to small solutes; this means that the perfusate flow rate cannot be made high enough to use the zero time extrapolation technique without altering

capillary pressure such that the gland could not be made isogravimetric before the test solute was introduced. This high permeability implies that the concentration of test solute will fall along the length of the capillary, and so the assumption of constant capillary concentration used by Bloom and Johnson (1981) is not valid. Also, there is a substantial pressure drop along the capillaries even though the vasculature is maximally dilated; assumption of a uniform capillary hydrostatic pressure would lead to errors in estimating the solvent drag component of solute flux, particularly if the intracapillary solute concentration is falling along the capillary. This effect would be less if the filtration coefficient increased from arterial to venous end of the capillary. The model of Grabowski and Bassingthwaighte allows for a fall in solute concentration along the capillary. However, since the interstitium and cells are divided into segments with no axial transfer between adjacent segments, a restricted mixing is built into the model. This would not occur with the small interstitial diffusion distances found in the submandibular gland.

Tissue hydrostatic pressure was assumed by both Bloom and Johnson (1981) and Grabowski and Bassingthwaighte (1976) to be a linear function of interstitial volume. Since their tissues were oedematous and tissue pressures were in the region of +15 mm Hg, this assumption was probably valid in their situation. However, the preparations described in Chapter 4 or this thesis did not tend to

gain much weight, partly because the perfusate contained bovine serum albumin as a colloid and partly because the perfusion pressure was lower. Although tissue pressures were not directly measured in the gland, it is unlikely that they were as high as those found by Bloom and Johnson.

Neither of the models currently available seems, therefore, to be suitable for direct application to the submandibular gland, and a model was developed which incorporated some of the features of each of the previous models as well as some new ones.

3.2. Description of the Model

3.2.1. Model System

A diagram of the components of the model is given in Fig. 3.1. It is essentially the same system as that used for modelling the extravascular accumulation of labelled albumin (Section 2.3.1.) but here the situation is much more complex because volume fluxes are not in a steady state.

The capillary is divided into a number (N) of segments. This allows hydrostatic pressures and solute concentrations to alter from arterial to venous ends of the capillary. Filtration, reflexion and permeability coefficients may also change along the capillary, but since no data for this are yet available in the salivary

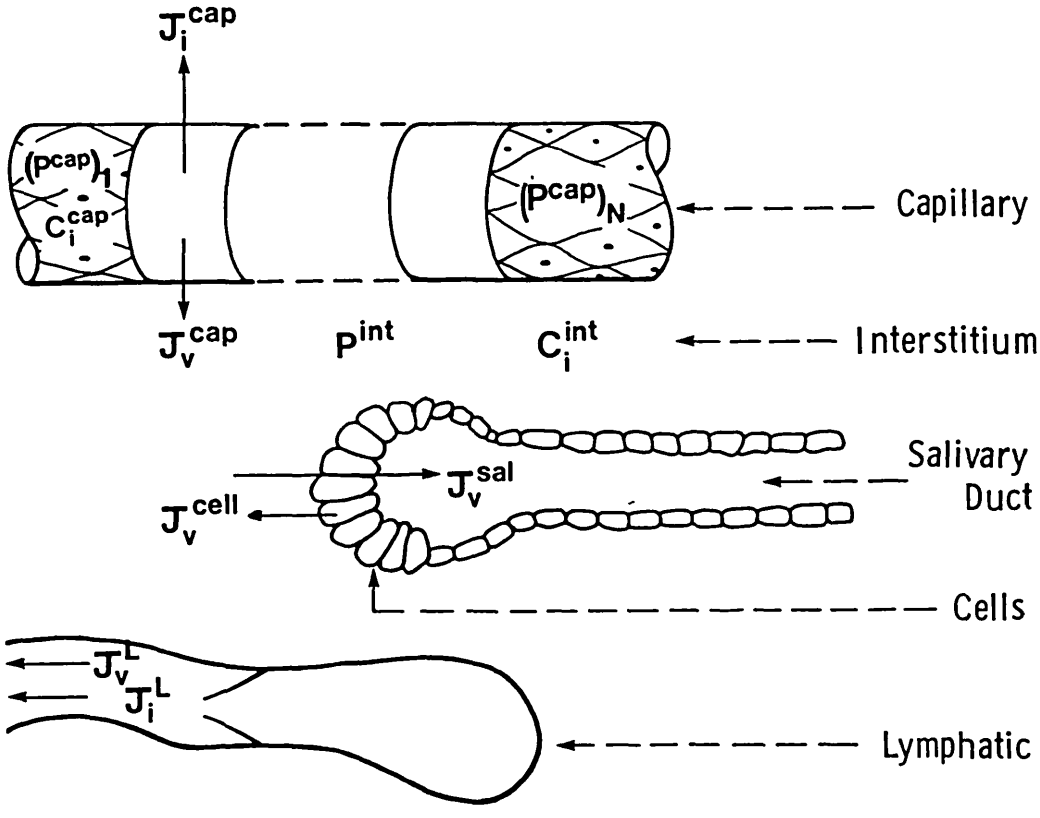


FIGURE 3.1. Schematic diagram of components of osmotic transient model. Volume and solute fluxes between compartments are depicted as arrows; the direction of the flux is taken as positive if it is in the direction of the arrow. See Section 3.2. for description of model, Table 3.1. for equations describing fluxes between specific compartments, and Appendix 1 for a list of symbols used.

gland, it was decided to use a single value for each of these coefficients.

3.2.2. Assumptions of the Model

To some extent, similar assumptions are made for the model of gland weight change as were made for the model of extravascular albumin accumulation. (Section 2.3.2, assumptions 1-6). Additionally, the following assumptions have been made:

1. The reflexion coefficient for all solutes across the cell membrane is 1.
2. The permeability coefficient for all solutes across the cell membrane is 0.
3. There is no hydrostatic pressure difference between the interstitium and the cell interior.
4. The cell acts as a perfect osmometer, ie its volume is inversely proportional to the osmotic pressure difference across the cell wall.
5. The elastic properties of the interstitium may be described by linear equations relating interstitial volume to pressure.
6. There is a linear hydrostatic pressure drop from the arterial to the venous end of the capillary.
7. When the test solute is introduced into the perfusate there is no axial diffusion of solute - ie the concentration of solute in the first capillary segment instantaneously reaches that in the perfusate.

8. In the resting state, salivary flow has a constant value, ie it is independent of interstitial pressure.

9. Lymph flow (J_v^L) is proportional to interstitial pressure if the latter is positive, ie $J_v^L = K_L.P^{int}$ where K_L is the hydraulic conductivity of the lymphatic vessels and P^{int} is interstitial hydrostatic pressure. If $P^{int} < 0$, then $J_v^L = 0$.

These assumptions will be discussed in Section 3.5.

3.2.3. Equations Used

The equation for volume flux across a membrane separating two compartments is an extension of the basic Starling-Landis formulation, including osmotic flows due to more than one solute. The general formulation is

$$J_v = K_f(\Delta P - \sigma_i \Delta \pi_i) \qquad 3.1$$

where J_v = net volume flux across membrane

K = hydraulic conductivity of membrane

ΔP = hydrostatic pressure difference across membrane

σ_i = reflexion coefficient of solute i

$\Delta \pi_i$ = osmotic pressure difference of solute i across membrane

The non-linear flux equation was used for solute flux, for similar reasons as in the albumin accumulation model. The general formulation for flux of solute i across

the capillary wall is

$$J_i^{cap} = J_v^{cap}(1 - \sigma_i^{cap})C_i^{cap} + \frac{J_v^{cap}(1 - \sigma_i^{cap})(C_i^{cap} - C_i^{int})}{e^{\lambda} - 1} \qquad 3.2$$

where J_i^{cap} = flux of solute across capillary wall

J_v^{cap} = volume flux across capillary wall

σ_i^{cap} = reflexion coefficient of capillary wall to solute

C_i^{cap} = concentration of solute i in capillary

C_i^{int} = concentration of solute i in interstitium

PS_i^{cap} = permeability-surface area product of solute i

$$\lambda = J_v^{cap}(1 - \sigma_i^{cap})/PS_i^{cap}$$

The equations used between specific compartments are shown in Table 3.1.

In reality, there are a number of solutes, each with its own fluxes, participating in the transient. To simplify the situation, it was assumed that the transient could be described in terms of 3 'representative' solute types:

1. Macromolecules - represented by albumin
2. Small solutes - represented by NaCl
3. Test solute - raffinose, inulin or albumin

Interstitial hydrostatic pressure is given by

$$P^{int} = P_o^{int} + E^{int}(V^{int} - V_o^{int}) \qquad 3.3$$

TABLE 3.1.

Compartments	Volume Flux	Solute Flux
Capillary → Interstitium	$K_f(P^{cap} - P^{int}) - \sigma_i^{cap}(\pi_i^{cap} - \pi_i^{int})$	$J_v^{cap}(1 - \sigma_i^{cap})C_i^{cap} + \frac{J_v^{cap}(1 - \sigma_i^{cap})(C_i^{cap} - C_i^{int})}{e^{\lambda} - 1}$
Interstitium → Cells	$K_{cell}\Sigma(\pi_i^{int} - \pi_i^{cell})$	0
Interstitium → Lymphatics	$K_L.P^{int}$	$J_v^L.C_i^{int}$
Interstitium → Salivary ducts	2×10^{-4} ml $min^{-1}g^{-1}$	0

TABLE 3.1. Equations describing volume and solute fluxes between compartments of model system depicted in Fig. 3.1.

where P_o^{int} is the initial interstitial hydrostatic pressure, E^{int} is the interstitial elasticity, V_o^{int} is the initial interstitial volume and V_t^{int} is the interstitial volume at time t. The value of E^{int} changed according to whether V_t^{int} was greater or less than V_o^{int}.

The osmotic pressure of a solution of albumin is not a linear function of its concentration. Several formulae have been produced to describe the relationship, but it appears that some of the earlier determinations of osmotic pressure may have been in error due to the characteristics of the osmometers used (Fraser, 1972). Also, there are problems with polymerization of the commercially available albumins, and so the concentration may not bear the expected relationship to the number of osmotically active particles. For the purposes of the model, the formula stated by Landis and Pappenheimer (1963) was employed:

$$\pi^{cap} = 2.8\ C_{alb}^{cap} + 0.18\ (C_{alb}^{cap})^2 + 0.012\ (C_{alb}^{cap})^3 \qquad 3.4$$

where π^{cap} is the intracapillary colloid osmotic pressure. The same equation was employed to determine π^{int}, the interstitial colloid osmotic pressure.

The intracapillary hydrostatic pressure was allowed to fall linearly from arterial to venous end of the capillary. Arterial pressure (P^{art}) and venous pressure (P^{ven}) were put into the model and the pressure in the r^{th} segment (P_r) calculated according to the relationship.

$$P_r = P^{art} - r(P^{art} - P^{ven}) \qquad 3.5$$

where N is the number of capillary segments.

The problem of determining interstitial volumes of distribution of solutes was mentioned in Chapter 2. For the purposes of the model, the interstitium was represented by a random fibre matrix with the initial values for ε (fractional aqueous volume) and r_f (radius fibre) taken to be those which gave the albumin distribution volume estimated from the experiments described in Chapter 2. The volume of the fibrous network was assumed to remain constant during changes in volume of the interstitial fluid, and so $(1 - \varepsilon)$ was inversely proportional to V^{int}. The interstitial volume of distribution of solute at time t, $(V_i^{int})_t$, is given by

$$(V_i^{int})_t = (V^{int})_t \exp\left[- \frac{(1 - \varepsilon)(V^{int})_o}{(V^{int})_t} (2ar_f + a^2) \right] \qquad 3.6$$

3.2.4. Iteration Procedure

The first step is to insert the chosen values for the various parameters needed (see Table 3.2). The initial value of tissue pressure is then calculated as that pressure required to maintain the gland in an isogravimetric state when test solute is absent from the perfusate.

Net filtration across capillary wall when the gland is isogravimetric = Lymph flow + Saliva flow:

$$\text{Net } J_v^{cap} = J_v^{L} + J_v^{sal} \qquad 3.7$$

Net J_v^{cap} may be calculated by determining the values of J_v^{cap} for each segment and summing over the N segments. However, since capillary hydrostatic pressure falls linearly from arterial to venous end, it is possible to use a mean value to calculate net J_v^{cap} from a single equation

$$\text{Net } J_v^{cap} = K_f \bar{P}^{cap} - P^{int} - \sigma_{int}^{cap}(\pi^{cap} - \pi^{int}) \qquad 3.8$$

where $\bar{P}^{cap}$ is the mean intracapillary hydrostatic pressure. Substituting 3.6 into 3.5 and noting that $J_v^{L} = P^{int}.K_L$, isogravimetric interstitial pressure P_{isog}^{int} is given by

$$P_{isog}^{int} = \frac{K_f \bar{P}^{cap} - \sigma_{alb}^{cap}(\pi^{cap} - \pi^{int}) - J_v^{sal}}{(K_f + K_L)} \qquad 3.9$$

Once isogravimetric conditions have been established, the osmotic transient is initiated by allowing the test solute to enter the first capillary segment at concentration C^{art}_{test} which is the concentration of test solute in the bulk of the perfusate.

With N identical capillary segments, each segment has an initial volume V^{seg}_o given by

$$V^{seg}_o = \frac{IVV}{N} \cdot W \qquad 3.10$$

where IVV (ml g^{-1}) is the intravascular volume and W (g) is the gland weight. As the perfusate flows through the gland at a rate F (ml $min^{-1}g^{-1}$) it will 'reside' in each segment for a short time Δt (min) given by

$$\Delta t = \frac{V^{seg}_o}{F} \qquad 3.11$$

During this time, volume and solute flux will occur across the capillary wall in each segment governed by the equations in Table 3.1, and both volume and solute concentrations in each segment have to be adjusted. After n iterations

$$(V^{seg})_n = (V^{seg})_{n-1} + (J^{seg}_v)_n \qquad 3.12$$

$$(C^{seg}_i)_n = (A^{seg}_i)_{n-1} + (J^{seg}_i)_n / (V^{seg})_n \qquad 3.13$$

where V^{seg} = volume of segment (ml)

J_v^{seg} = volume flux across segment wall (ml)

A_i^{seg} = amount of solute in segment (moles)

J_i^{seg} = flux of solute i across segment wall (moles)

C_i^{seg} = concentration of solute i in segment (moles/ml^{-1})

and the subscripts n-1 and n refer to the values after n-1 and n iterations respectively. The procedure is repeated for the remaining N-1 segments, and the volume and solute fluxes summed over all the segments for that iteration.

During the same period of time as the capillary fluxes are occurring, volume flux occurs across the cell wall into the interstitium, again governed by the equations given in Table 3.1. Intracellular volume and solute concentration have then to be adjusted according to the relationships.

$$(V^{cell})_n = (V^{cell})_{n-1} - (J_v^{cell})_n \qquad 3.14$$

$$(C_i^{cell})_n = \frac{(V^{cell})_o \cdot (C_i^{cell})_o}{(V^{cell})_n} \qquad 3.15$$

where V^{cell} = cell volume (ml)

J_v^{cell} = volume flux across cell membrane (ml)

C_i^{cell} = intracellular concentration of solute (moles ml^{-1})

b = volume of intracellular water not contributing to osmotic flow (ml)

Once the transcapillary and transcellular fluxes have been calculated, the volume and solute concentration in the interstitial space can be recalculated:

$$(V^{int})_n = (V^{int})_{n-1} - (J_v^{seg})_n + (J_v^{cell})_n - (J_v^L)_n \qquad 3.16$$

$$(C_i^{int})_n = \frac{(A_i^{int})_{n-1} + (J_i^{cap})_n - (J_i^L)_n}{(V_i^{int})_n} \qquad 3.17$$

V_i^{int} = interstitial volume of distribution for solute *i* (ml)

A_i^{int} = amount of solute *i* in interstitium (moles)

C_i^{int} = concentration for solute *i* in interstitium (moles ml^{-1})

The new interstitial volume necessitates a recalculation of the interstitial hydrostatic pressure, according to the compliance relationship Eqn 3.3.

Once the volume and solute fluxes have been calculated, and the volumes, solute concentrations and pressures in the various compartments adjusted, the perfusate can then move along to the next segment. This implies that the perfusate in segment 'N' is 'lost' as venous effluent, and the first segment is filled with solution with the same composition as the perfusate. Gland weight can then be calculated as the algebraic sum of all the volume fluxes into and out of the gland.

$$(W)_n = (W)_{n-1} + V^{segl} - V^{segN} - J_v^L - J_v^{sal} \qquad 3.18$$

In summary, steps in the iteration procedure are as follows:

1. Establish isogravimetric conditions.
2. Introduce test solute into first capillary segment.
3. Calculate volume and solute fluxes across each capillary segment.
4. Readjust segment volume and solute concentrations.
5. Sum segment fluxes.
6. Calculate volume flux across cell wall.
7. Readjust intracellular volume and solute concentrations.
8. Readjust interstitial volume, solute concentration and hydrostatic pressure, taking into account lymph and saliva flow.
9. Calculate gland weight.
10. Move perfusate along to next segment.
11. Repeat from Step 3.

Using the model it is possible, by varying the conditions, to simulate 3 types of experiment:

1. Venous pressure elevation - after isogravimetric conditions have been established, the hydrostatic pressure in the last capillary segment is altered; the computer program adjusts the hydrostatic pressure in the other segments so that there is still a linear pressure drop between the first and last segments. No test solute is introduced (the program achieves

this by putting $C^{art}_{test} = 0$)

2. Osmotic transient - the properties of the test solute (σ^{cap}_{test}, PS^{cap}_{test}, V^{cap}_{test}) are inserted into the program and at a known time after isogravimetric conditions have been established ('time zero'), a known concentration of test solute is introduced into the first capillary segment. Hydrostatic pressure in each capillary segment remains constant. The concentration of test solute introduced is one which has been found experimentally to give an easily measured weight loss.

3. Indicator dilution - the conditions are similar to those in the osmotic transient simulation, but the concentration of test solute is too small (10^{-3} mM) to produce any noticable change in gland weight. A step introduction and withdrawal of test solute is produced, and the interval between the introduction and withdrawal is 1 - 2 sec. Venous concentration of test solute (C^{ven}_{test}) is printed out and the extraction (E) after each time interval Δt is calculated by the relationship

$$E = 1 - \frac{C^{ven}_{test}}{C^{art}_{test}} \qquad 3.19$$

In all these simulations, values for the various coefficients (K_f, PS^{cap}_{test}, σ^{cap}_{test} etc) are inserted into the model. These would represent the 'true' values of

the coefficients, if these were known. The output of the program allows the coefficients to be estimated in a manner similar to that used in the experimental situation, and so compared with the values inserted into the model. For example, the 'true' value of σ^{cap}_{inulin} might be 0.4. If K_f = 2 ml min^{-1}100 $g^{-1}mm^{-1}$Hg and the perfusate concentration of inulin is 10 mM, the initial rate of weight loss would be expected to be approximately 1.36 ml min^{-1} for a gland weighing 1 g. If the weight vs time relationship generated by the model shows that the initial weight loss is only 1.0 ml min^{-1} then σ^{cap}_{inulin} is estimated at 1.0/1.36 x 0.4 = 0.29. The reasons for the discrepancy can then be elucidated by changing the values of some of the other parameters used in the model.

3.2.5. Testing the Model

Although the model does not employ complex analytical equations, the enormous number of arithmetic operations involved precludes checking even a small fraction of the calculations by hand. A number of 'extreme' conditions were set up which have predictable outcomes, and the results of these are shown in Table 3.2. In every instance, the computer output was the same as that expected.

TABLE 3.2.

	Conditions	Model Prediction	Type of Simulation
1.	$K_f = 0$	Gland Weight constant	(O.T., VPE)
2.	$K_{cell} = 0$	Cell volume constant	(O.T.)
3.	$E^{int} = \infty$	Interstitial pressure constant	(O.T.)
4.	$C^{cap}_{test} = 0$	Gland weight constant	(O.T.)
5.	$PS^{cap}_{alb} = 0; \sigma^{cap}_{alb} = 1$	$C^{seg}_{alb} \propto \frac{1}{V^{seg}}$	(Isograv)
6.	$\sigma^{cap}_{test} = 0; K_{cell} = 0$	Gland weight constant	(O.T.)
7.	$\sigma^{cap}_{test} = 0; V^{cell} = 0$	Gland weight constant	(O.T.)
8.	$PS^{cap}_{alb} = 0; \sigma^{cap}_{alb} = 1;$ $C^{int}_{alb} = 0; \sigma^{cap}_{buff} = 0;$ $K_{cell} = 0; PS^{cap}_{test} = 0;$ $E^{int} = \infty$	Wt vs time plot linear with slope = K_f; C^{int}_{alb} remains at 0; P^{int} constant; V^{cell} constant.	(VPE)
9.	As in 8 but with $PS^{cap}_{test} = 100$ ml $min^{-1} g^{-1}$ (ie very high)	Small, short-lived weight loss	(O.T.)

Table 3.2. continued

	Conditions	Model Predictions	Type of Simulation
10.	As in 9 but with $\sigma^{cap}_{test} = 0$	Gland weight constant	(O.T.)
11.	$PS^{cap}_{test} = 1.5$ ml $min^{-1}g^{-1}$; $\sigma^{cap}_{test} = 0$ $EVV_{test} = 0.5$ ml g^{-1} $F = 20$ ml $min^{-1}g^{-1}$	$PS^{cap}_{test} = 1.5$ ml $min^{-1}g^{-1}$	(I.D.)

TABLE 3.2. Tests of the model - results of inserting 'extreme' conditions for various parameters on the output of the program

O.T. - osmotic transient

VPE - venous pressure elevation

ID - indicator dilution

3.2.6. Values of Parameters Used in the Model

A large number of parameters are employed in the model, including filtration, reflexion and permeability coefficients, volumes of distribution and solute concentrations. The parameters used, and the values chosen for each, are presented in Table 3.3. Some of the numerical values chosen are taken from the present work (Chapters 2 and 4) or from the work of Mann et al (1979a) and Koo et al (1980) and are appropriately indicated in the Table. The values have been rounded to one or two significant figures. All the values given for volumes, concentrations and fluxes refer to the initial conditions.

No account is taken of vascular compliance, which is important in the early stages of a venous pressure elevation. Thus the change in gland weight is determined solely by the balance of volume fluxes across the capillary, lymphatic and salivary endo- and epithelia.

TABLE 3.3.

Parameter		Values Used	Units
K_f	(c)	2	ml min^{-1} 100 g^{-1} mm^{-1} Hg
K_{cell}		0.02, 0.2	"
K_L		0.5	"
σ_{alb}^{cap}	(b,c)	0.6, 0.95	
σ_{buff}^{cap}	(f)	0.05	
σ_{inulin}^{cap}	(c)	0.4	
σ_{raff}^{cap}		0.05	
PS_{alb}^{cap}	(b)	5×10^{-4}	ml min^{-1} g^{-1}
PS_{buff}^{cap}	(a)	15	"
PS_{inulin}^{cap}	(a)	1.5	"
PS_{raff}^{cap}	(a)	15	"
IVV	(b)	5	ml 100 g^{-1}
V_{alb}^{int}	(b)	4	"
V_{buff}^{int}	(b)	16.5	"
V_{inulin}^{int}	(b)	16.5	"
V_{raff}^{int}	(b)	16.5	"
V^{cell}		50	"
C_{alb}^{art}	(a)	6	g 100 ml^{-1}
C_{buff}^{art}	(c)	300	mM
C_{inulin}^{art}	(c)	10	mM
C_{raff}^{art}	(c)	50	mM

Parameter		Values Used	Units
C_{alb}^{int}	(d)	1.5	g 100 ml^{-1}
C_{buff}^{int}	(c)	300	mM
C_{inulin}^{int}	(c)	0	mM
C_{raff}^{int}	(c)	0	mM
F	(c)	4, 12	ml min^{-1} g^{-1}
J_v^L	(d)	10^{-3}	"
J_v^{sal}	(e)	2×10^{-4}	"
N		10	
p^{art}	(c)	30	mm Hg
p^{ven}	(c)	2	"

TABLE 3.3. List of Values Of Parameter Used in Model

a Mann, Smaje and Yudilevich (1979a)

b Present thesis - Chapter 2

c Present thesis - Chapter 4

d Koo et al (1980)

e Smaje (1973)

f Bloom and Johnson (1981)

3.3. Correction of Estimate of Solute Reflexion Coefficient Obtained by 'Initial Slope' Method

Diffusion of test solute into the interstitium, even before the solute 'front' has travelled from arterial to venous end of the capillaries, will lead to reduction of the transcapillary concentration gradient and hence to underestimation of the reflection coefficient if the arterial solute concentration is taken as the concentration difference.

According to Johnson et al (1981), the mean intracapillary solute concentration $\bar{C}^{cap}_{test}$ may be approximated by

$$\bar{C}^{cap}_{test} = \frac{C^{cap}_{test}(1 - e^{-PS^{cap}_{test}/F})}{PS^{cap}_{test}/F} \qquad 3.20$$

The amount of test solute leaving the capillary is thus the difference between the intracapillary amount if no solute had left and the mean intracapillary solute amount, ie

Amount leaving capillary =

$$C^{art}_{test}.IVV - \frac{IVV.C^{art}_{test}(1 - \exp\ (-\ PS^{cap}_{test}/F)}{PS^{cap}_{test}/F} \qquad 3.21$$

The extravascular concentration is given by amount leaving capillary/V^{int}

$$\text{ie}\quad C^{int}_{test} = \frac{C^{art}_{test}.IVV}{V^{int}_{test}}\left[1 - \frac{(1 - e^{-PS^{cap}_{test}/F})}{PS^{cap}_{test}/F}\right] \qquad 3.22$$

thus

$$\Delta C_{test} = \bar{C}^{cap}_{test} - C^{int}_{test} = C^{art}_{test} \left[1 + \frac{IVV}{V^{int}_{test}} \frac{(1 - e^{-\alpha})}{\alpha} - \frac{IVV}{V^{int}_{test}} \right]$$

where $\alpha = PS^{cap}_{test}/F$ 3.23

This value of ΔC_{test} occurs at the point when the gland begins to lose weight, ie zero time, and so if the initial slope of the weight vs time relationship can be obtained accurately, the correction may be performed easily.

3.4. Model Results

The results presented in this Section were obtained by inserting the appropriate values of the parameters listed in Table 3.3. and initiating the iteration procedure according to the type of simulation required. No attempt has been made to fit the output of the model to experimental data; rather the aim has been to compare estimations of the capillary coefficients obtained from the output to the values of those coefficients inserted into the model. In addition, some of the factors causing deviation of the estimated from the 'true' values have been investigated.

3.4.1. Venous Pressure Elevation

In order to determine solute reflexion coefficients it is clearly essential to have an accurate measurement of capillary filtration coefficient, K_f. This is usually achieved by raising venous (and therefore capillary) hydrostatic pressure and measuring the resulting change in weight of the organ. Fig. 3.2 shows the result of elevating venous pressure by 5 and 10 mm Hg on gland weight, assuming that σ_{alb}^{cap}= 0.95 and K_f = 2 ml min^{-1} 100 g^{-1} Hg. As expected, the gland gains weight at a rate which depends on the magnitude of the pressure elevation. Since the model does not take account of vascular compliance, at least the first 10 - 15 seconds would not be available for measurment experimentally. Although the model predicts a curvilinear weight-time relationship there would be little difficulty in drawing a straight line between 15 and 60 sec. The slope of this line represents $\Delta W/\Delta t$, and since J_v^L and J_v^{sal} are constant, this may be equated to J_v^{cap} . When the procedure is repeated for different pressure elevations a plot of J_v^{cap} vs ΔP^{cap} may be constructed, the slope of the resulting line being equal to K_f. Fig 3.3 shows such a plot using the results of Fig. 3.2 and also venous pressure elevations of 2.5 and 7.5 mm Hg. Mean capillary pressure elevation ($\bar{P}^{cap}$) is less than venous pressure elevation because arterial pressure remains constant With 10 segments, $\Delta\bar{P}^{cap} = 0.45\Delta P^{ven}$. Two important points emerge from Figs. 3.2 and 3.3:

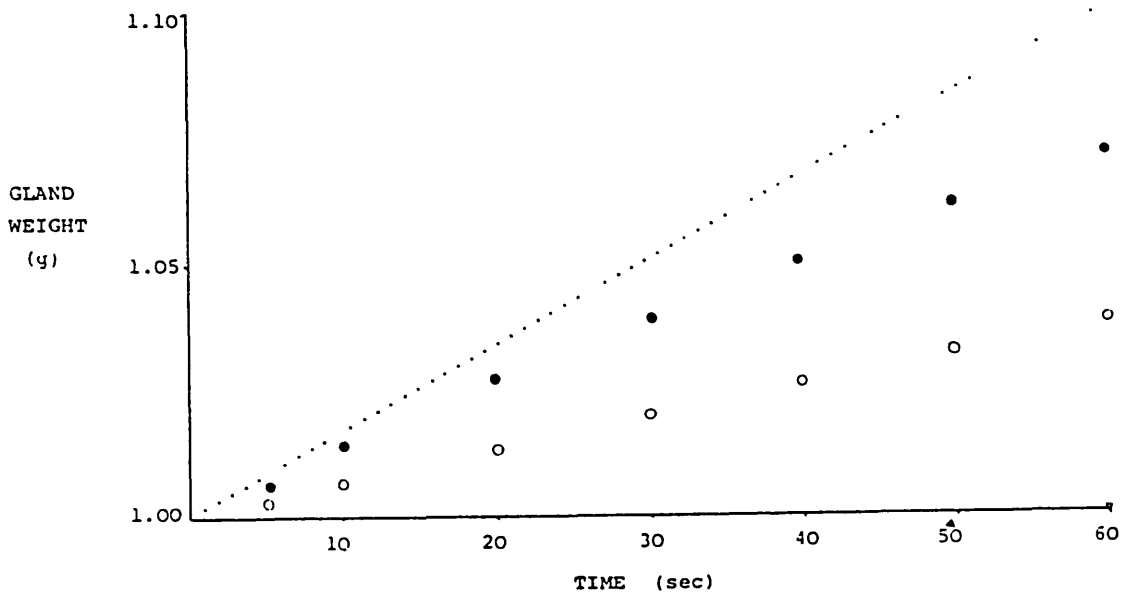


FIGURE 3.2. Plot of normalized gland weight vs time following venous pressure elevations of 5 (o) and 10 (●) mm Hg (P^{cap} increased by 2.25 and 4.5 mm Hg). In this and all subsequent figures in this Chapter, σ_{alb}^{cap} = 0.95, K_{cell} = 0.02 ml min^{-1}100 $g^{-1}mm^{-1}$Hg and perfusate flow = 12 ml $min^{-1}g^{-1}$ unless otherwise indicated. Other values are as in Table 3.3.
The dotted line indicates the relationship expected for a venous pressure elevation of 10 mm Hg if no counter-balancing forces were present.

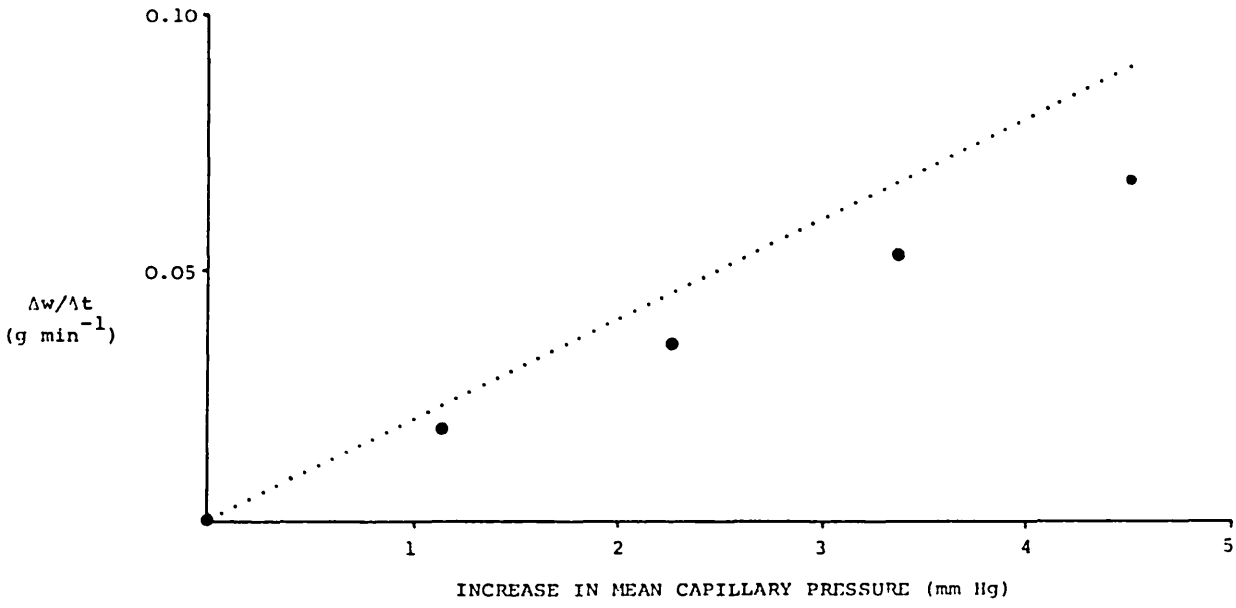


FIGURE 3.3. Rate of weight gain of gland ($\Delta w/\Delta t$) plotted against the increase in mean capillary pressure for venous pressure elevations of 2.5, 5, 7.5 and 10 mm Hg (●). $\Delta w/\Delta t$ was calculated from plots such as that illustrated in Fig. 3.2. using the slope drawn by eye between 15 and 30 seconds. The dotted line indicates the relationship expected if no counterbalancing forces were present.

1. The weight vs time relationship is not a straight line, ie J_v^{cap} falls with time.
2. The value of K_f estimated by the slope of the J_v^{cap} vs P^{cap} line is approximately 1.5 ml min^{-1} 100 g^{-1} mm^{-1} Hg, only 75% of the value inserted into the model.

Drake, Taylor and Gaar (1978) have recognised the problem of falling J_v^{cap} and have suggested that a better estimate of K_f may be obtained by extrapolating the graph of log J_v^{cap} vs time back to zero time. Fig. 3.4 is a plot of log J_v^{cap} vs time for the 10 mm Hg venous pressure elevation shown in Fig. 3.2, and clearly shows that J_v^{cap} falls with time; more importantly, it shows that J_v^{cap} falls fastest in the first 20 seconds, when the weight change due to vascular compliance will obscure changes in J_v^{cap}. The zero-time extrapolation gives an estimate of 1.8 ml min^{-1} 100 g^{-1} mm^{-1} Hg for K_f'. This is clearly closer to the 'true' value than the estimate given by the slope of the J_V^{cap} vs P^{cap} graph, but still is a 10% underestimate.

In the model runs illustrated by Figs. 3.2 - 3.4, interstitial compliance was set to ∞, and cellular hydraulic conductivity to a low value (0.02 ml min^{-1} 100 g^{-1} mm^{-1} Hg). The mechanisms which might account for the progressive reduction in J_v^{cap} are:

1. concentration of intracapillary albumin
2. 'osmotic buffering' by sieving of NaCl at the capillary wall

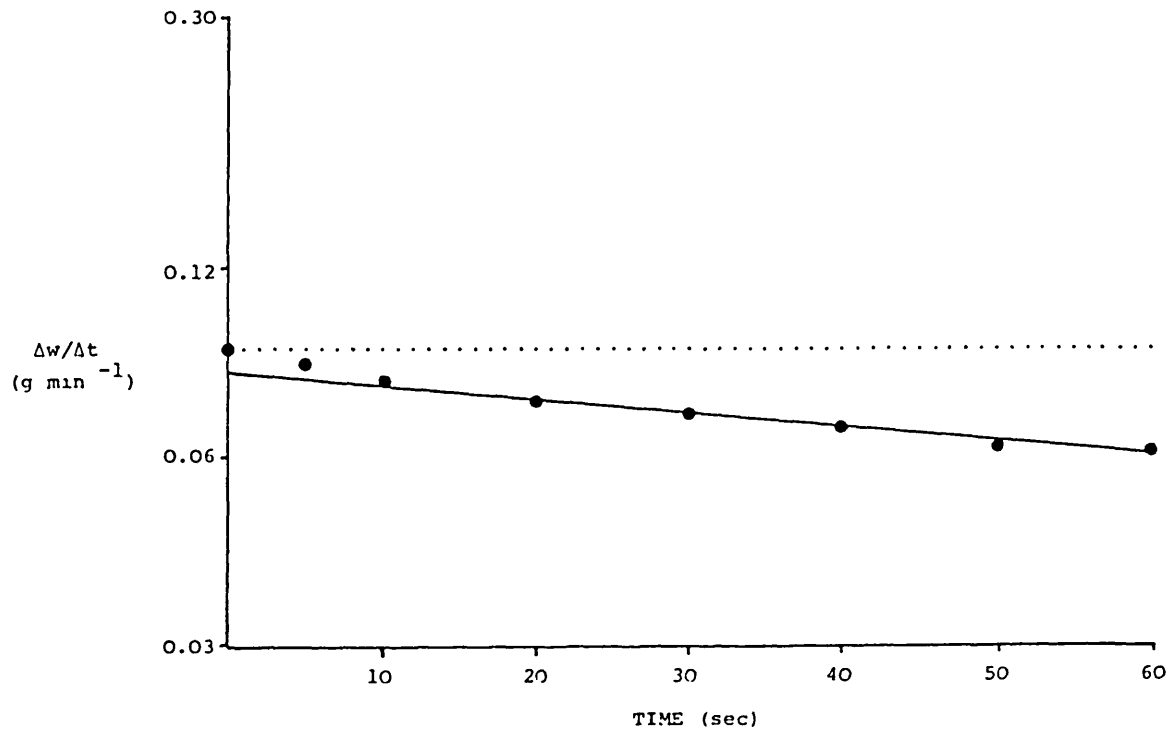


FIGURE 3.4. Rate of weight gain of gland (Δw /Δt) vs time for a venous pressure elevation of 10 mm Hg. (Δw/Δt) is plotted on a logarithmic scale to allow extrapolation to zero time according to the method of Drake et al (1978), shown by the solid line. The dotted line indicates the relationship expected if no counter-balancing forces were present.

3. dilution of interstitial albumin.

Since the computer output gives the intracapillary concentrations of albumin and NaCl in each segment, as well as the interstitial concentrations, the contributions of each of these mechanisms may be determined. Fig. 3.5 shows how the intracapillary concentrations of albumin and NaCl change early on in the course of a 10 mm Hg venous pressure elevation. An early time was chosen because J_v^{cap} is greatest and so the intracapillary concentrations would be expected to change by the greatest amount. The concentration changes are very small; for albumin the mean intracapillary change is approximately 0.04 g.100 ml^{-1}, which would increase the intracapillary colloid osmotic pressure by less than 0.2 mm Hg. The mean intracapillary concentration change for NaCl is 0.054 mM, and at this time the interstitial NaCl concentration has decreased by 0.03 mM; the combined effect of these changes is an inward osmotic pressure of less than 0.1 mm Hg. The total osmotic buffering of these mechanisms is thus approximately 0.3 mm Hg. When venous pressure is not elevated, intracapillary albumin concentration still rises, but then falls to reach the perfusate concentration by the end of the capillary. NaCl concentration rises then falls below perfusate concentration. The total effect of these concentration differences is approximately 0.15 mm Hg. The extra buffering effect due to the fluid movement is thus 0.15 mm Hg.

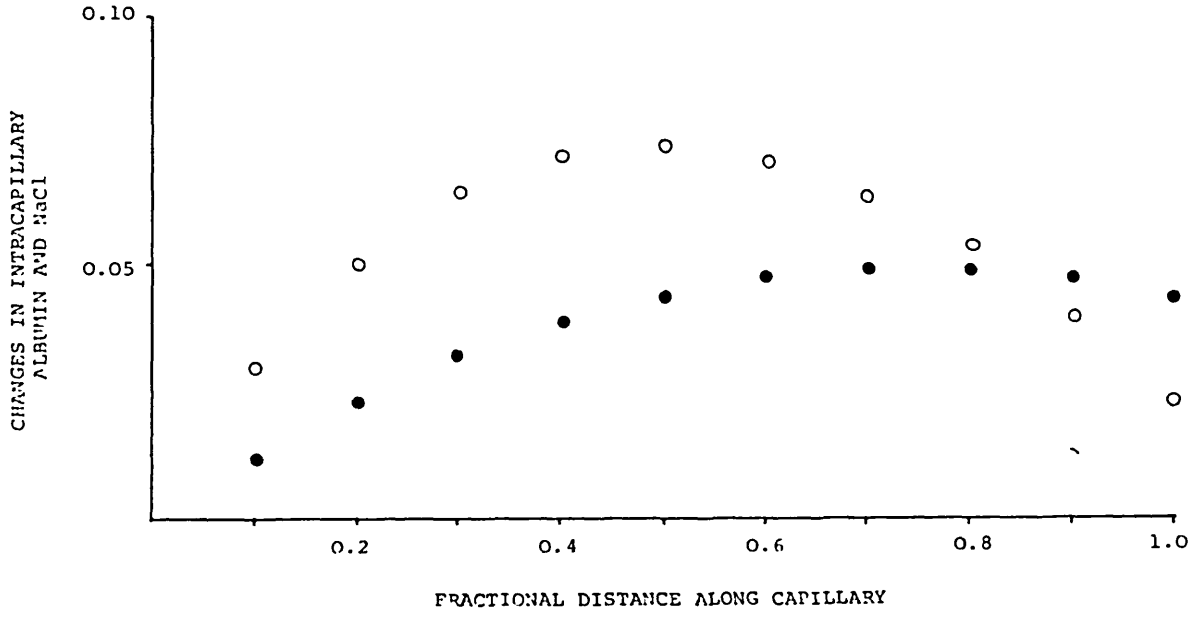


FIGURE 3.5. Changes in albumin (●) and NaCl (o) concentrations along the length of the capillary during the course of a 10 mm Hg venous pressure elevation. The concentration of each solute rises in the arterial (filtering) half of the capillary and falls in the venous (absorbing) half. As the perfusate leaves the capillary there remains an excess concentration of both solutes; the excess albumin concentration is almost exactly accounted for by a decrease in the volume of the capillary segment, consistent with a low albumin permeability.

Albumin concentration = g 100 ml^{-1}

NaCl concentration = mM

Fig. 3.6 illustrates how the fall in interstitial colloid osmotic pressure parallels the fall in J_v^{cap} for a venous pressure elevation of 10 mm Hg. After 60 sec, J_v^{cap} has fallen to 0.68 of its original value. The transcapillary pressure difference for filtration must therefore have fallen by (1 - 0.68) x 4.5 = 1.44 mm Hg. Fig. 3.6 shows that π^{int} has fallen by 1.4 mm Hg in 60 seconds.

Cell hydraulic conductivity has very little influence on the course of a venous pressure transient. For a 10 mm Hg venous pressure elevation and with K_{cell} = 0.02, the change in cell volume is 0.14 x 10^{-3} ml in 60 seconds. If K_{cell} were 20 times larger at 0.4 ml $min^{-1}100\ g^{-1}mm^{-1}Hg$, then the change in cell volume would still amount to only 4% of the total change in gland weight. At an interstitial pressure of 1.1 mm Hg and with K_L = 0.5 ml $min^{-1}100\ g^{-1}$ $mm^{-1}Hg$, lymph flow is 5.5 x 10^{-3} $ml.min^{-1}$. With a constant interstitial hydrostatic pressure, lymph flow is constant and so does not affect the weight change at different levels of venous pressure. However, if the interstitium is allowed to have some compliance, then lymph flow will increase as the interstitial hydrostatic pressure increases. This will buffer even further the weight change, as shown in Fig. 3.7, where interstitial elasticity is 7.7 mm Hg ml^{-1} if the interstitial volume is greater than 0.165 ml, and 15.4 mm Hg ml^{-1} if interstitial volume is less than 0.165 ml.

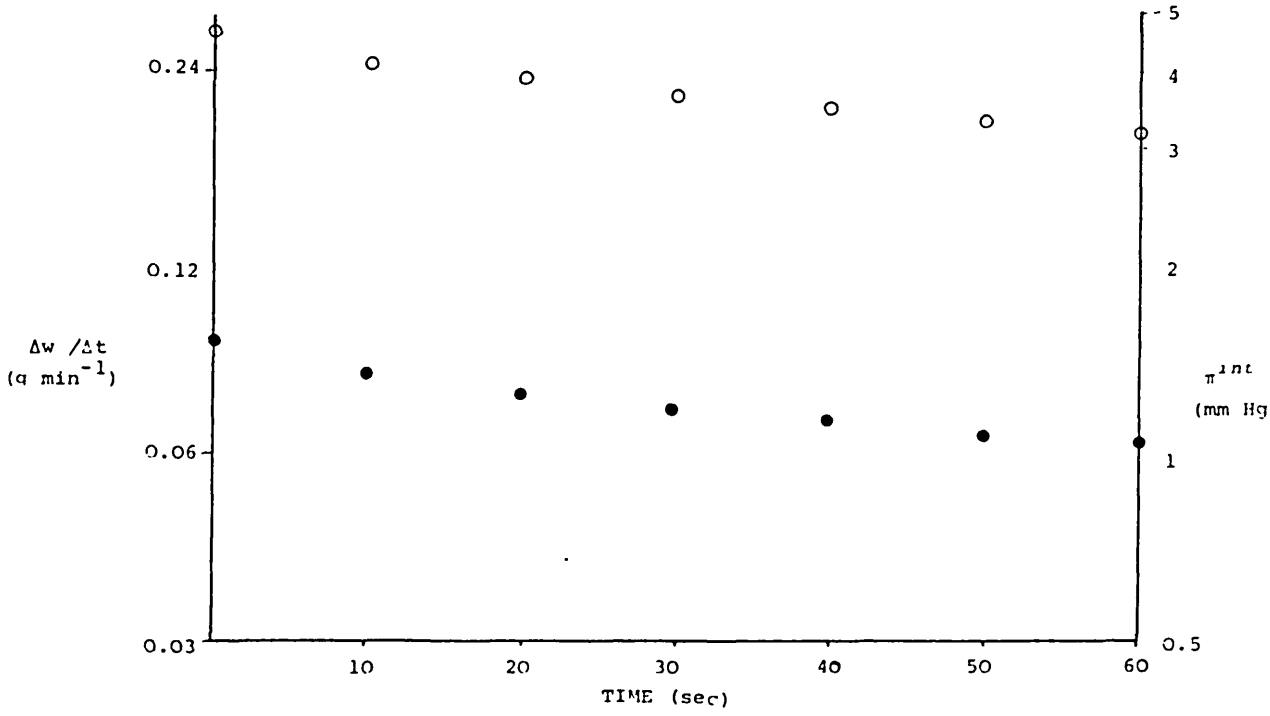


FIGURE 3.6. Changes in $\Delta w/\Delta t$ (●) and interstitial colloid osmotic pressure (π^{int}, o) with time following a 10 mm Hg venous pressure elevation. Both $\Delta w/\Delta t$ and π^{int} are plotted on a logarithmic scale.

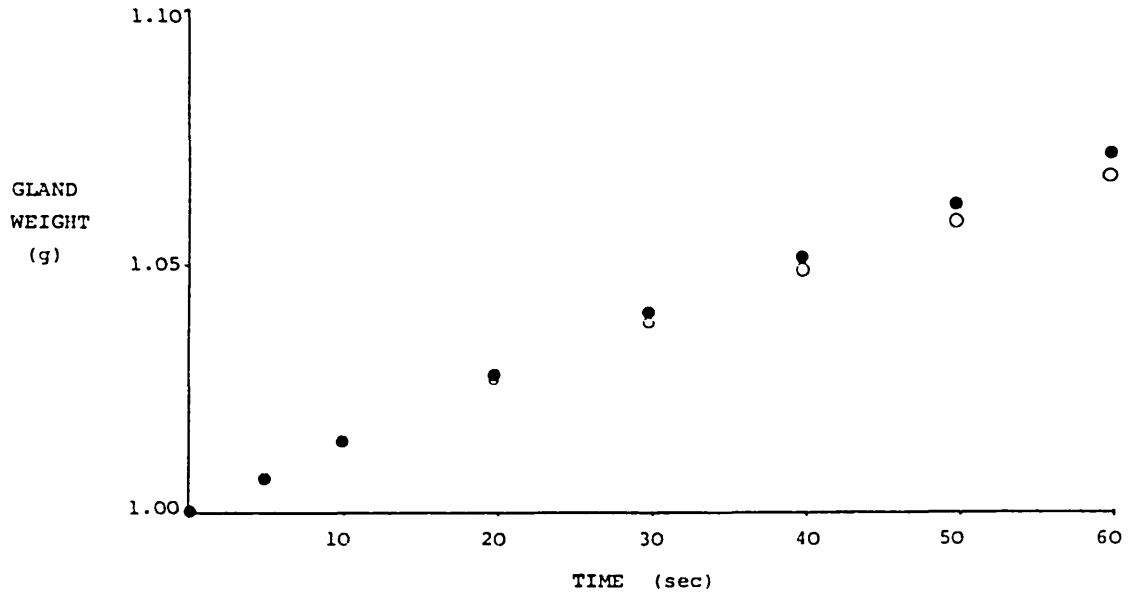


FIGURE 3.7. Effect of changing interstitial compliance on the time course of a 10 mm Hg venous pressure elevation

Interstitial compliance = ∞ (●)

" " = 0.13 ml mm^{-1}Hg (o)

Interstitial hydrostatic pressure itself has a small influence on the transient, as shown in Fig. 3.7. Since the gland gains approximately 7 x 10^{-2} g in 60 seconds, the increase in P^{int} will be about 0.5 mm Hg. Since the gland gains slightly less weight when P^{int} changes compared to when P^{int} is constant, the change in π^{int} is also less.

The above analysis suggests that reduction of interstitial colloid osmotic pressure is the main factor causing K_f to be underestimated, with elevation of interstitial hydrostatic pressure making a smaller contribution.

Thus far, the reflexion coefficient of albumin across the capillary wall has been assumed to be close to 1, as was found in the in vivo gland. If this is not the case, then the gland weight change in response to venous pressure elevation will be different. Fig. 3.8 shows the responses to a 10 mm Hg venous pressure elevation for σ_{alb}^{cap} = 0.95 and 0.6. It is at first sight surprising that the lower reflexion coefficient produces a greater weight change, but Fig. 3.9 shows that the reason for this is that interstitial albumin concentration does not fall. According to either the linear or the non-linear form of the equation for solute flux (Eqn. 1.2 and 1.3 respectively), lowering the reflexion coefficient will result in a higher albumin concentration in the filtrate. Neglecting diffusive albumin flux, the reflexion coefficient required to give a filtrate albumin concentration equal to that in the interstitium is

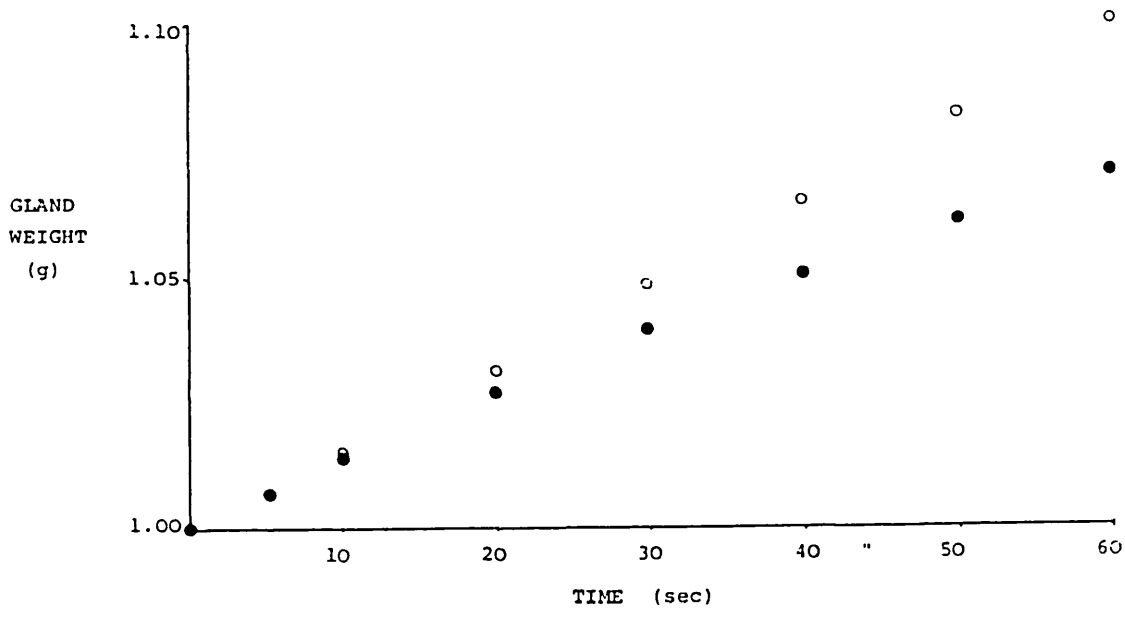


FIGURE 3.8. Effect of changing σ_{alb}^{cap} on the time course of a 10 mm Hg venous pressure elevation

$\sigma_{alb}^{cap} = 0.95$ (●)

$\sigma_{alb}^{cap} = 0.6$ (o)

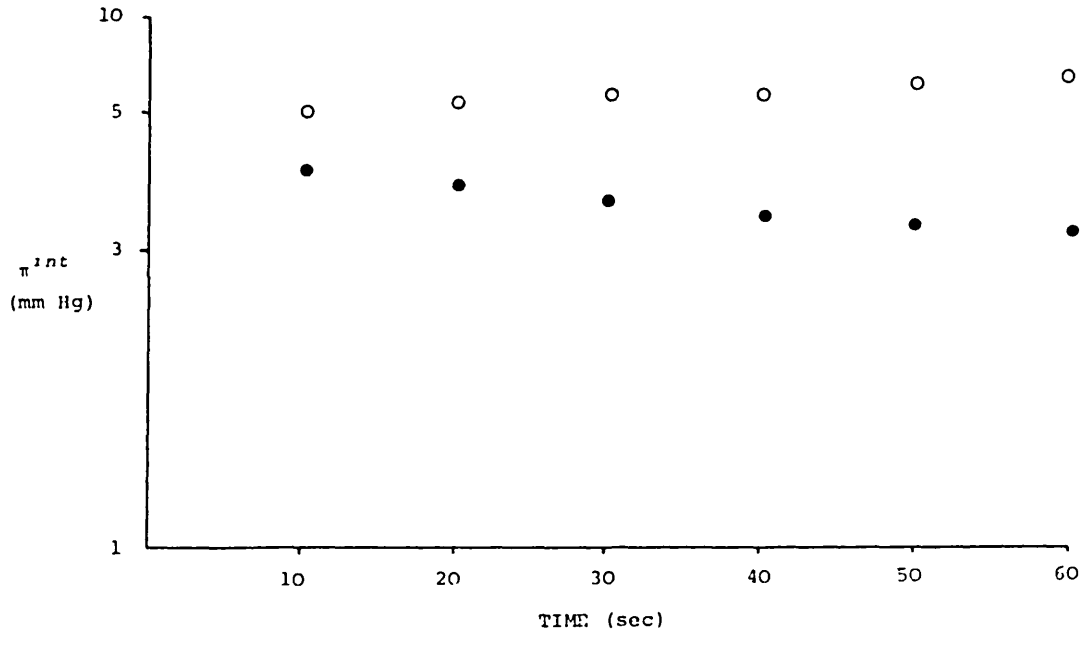


FIGURE 3.9. Effect of changing σ_{alb}^{cap} on the time course of interstitial colloid osmotic pressure (π^{int}) during a 10 mm Hg venous pressure elevation.

$\sigma_{alb}^{cap} = 0.95$ (●)

$\sigma_{alb}^{cap} = 0.6$ (o)

$$\sigma_{alb}^{cap} = \frac{(1 - R)}{(1 + R)}$$ for the linear equation, and

$$\sigma_{alb}^{cap} = (1 - R)$$ for the non-linear equation, where

$R = C_{alb}^{int}/C_{alb}^{cap}$. In the runs illustrated in Fig. 3.9, $R = 0.25$ and so $\sigma_{alb}^{cap} = 0.6$ or 0.75 for the linear and non-linear equations respectively. Using $\sigma_{alb}^{cap} = 0.6$ with the non-linear equation means that the interstitial albumin concentration will rise, and this is confirmed in Fig. 3.9.

3.4.2. Osmotic Transient using Albumin as the Test Solute

Fig. 3.10 shows the weight changes in response to alterations in the albumin concentration of the perfusate if $\sigma_{alb}^{cap} = 0.95$. Also shown are the weight changes expected for $K_f = 2$ ml.min^{-1}100 g^{-1}mm^{-1}Hg if no buffering factors are present. Fig. 3.11 shows the predicted values of J_v^{cap} plotted against π_{alb}^{cap}. The slope of the resulting line should be equal to $K_f\sigma_{alb}^{cap}$. One striking feature of Fig. 3.10 is the prediction of apparent rectification of volume flux, flow out of the capillary being greater than flow into it. The reason for this is that interstitial albumin is concentrated by fluid withdrawal faster that it is diluted by fluid addition, particularly with the low extravascular albumin volume of distribution used.

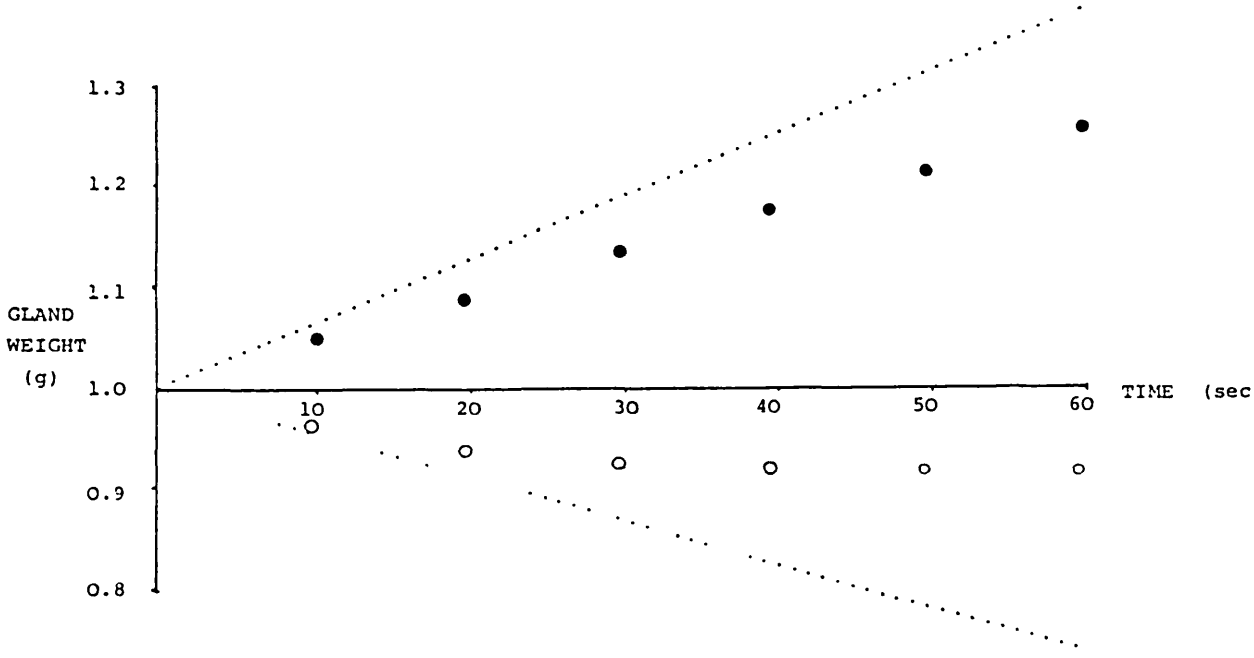


FIGURE 3.10. Weight changes induced in a 1 g gland by changing the concentration of albumin in the perfusate to 8 g 100 ml^{-1} (o) and 2 g 100 ml^{-1} (●). In each case the adjacent dotted line is the weight change expected if no counterbalancing forces were present.

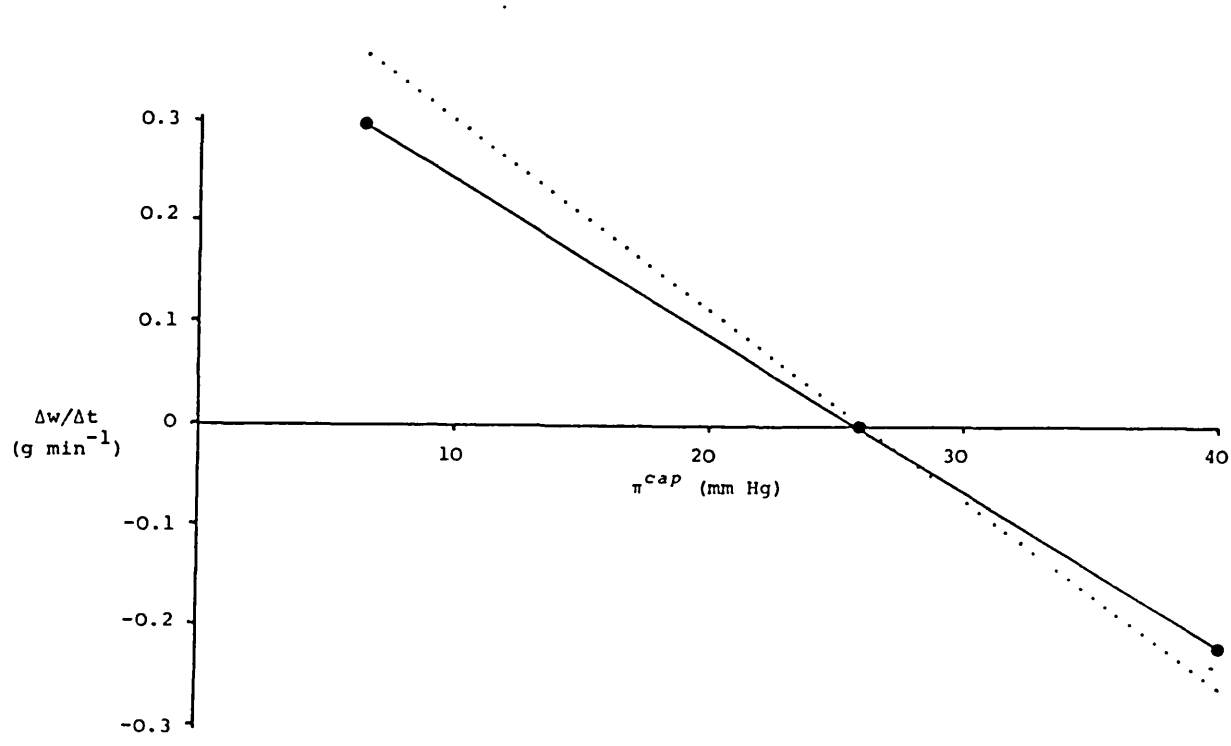


FIGURE 3.11. $\Delta w/\Delta t$ plotted against π^{cap} for the model runs shown in Fig. 3.10. $\Delta w/\Delta t$ was calculated using the slope drawn by eye between 0 and 10 seconds. The point for a perfusate albumin concentration of 6 g 100 ml^{-1} ($\Delta w/\Delta t = 0$) is also shown. The solid line is the line through the points generated; the dotted line is that expected for $\sigma_{alb}^{cap} = 0.95$, $K_f = 2$ ml min^{-1} 100 $g^{-1} mm^{-1} Hg$ if no counterbalancing forces were present.

However if the early times are considered, rectification is no longer apparent. Fig. 3.11 has been constructed using the first 10 seconds of the transient to calculate J_v^{cap} .

The slope of the line in Fig. 3.11 is 1.54. Taking the estimated value of K_f as 1.5 ml $min^{-1}100\ g^{-1}mm^{-1}Hg$ (Fig. 3.3), δ_{alb}^{cap} is estimated as 1.54/1.5 = 1.0 which compares very well with the value of 0.95 put into the model. If the zero-time extrapolation is used (Fig. 3.4) K_f is estimated at 1.8 $ml.min^{-1}100\ g^{-1}mm^{-1}Hg$ and σ_{alb}^{cap} at 1.8/1.5 = 1.14; the more accurate method for determining K_f thus appears to give a worse estimate of δ_{alb}^{cap}. The reason for this appears to be in the state of the interstitium when J_v^{cap} is calculated. The zero-time extrapolation attempts to estimate J_v^{cap} before any tissue adjustments have occurred, whereas the estimation of J_v^{cap} over the period 20-60 seconds after the pressure elevation allows such adjustments to take place. Approximately as much fluid has entered the interstitium in the 10 seconds following the introduction of perfusate containing 2 g $100\ ml^{-1}$ albumin as in the 60 seconds following a 10 mm Hg venous pressure elevation, so the tissue adjustments, and thus the errors in J_v^{cap} , are similar.

This suggestion is supported by the results illustrated in Fig. 3.12, which is a plot of the change in capillary pressure required to maintain the gland

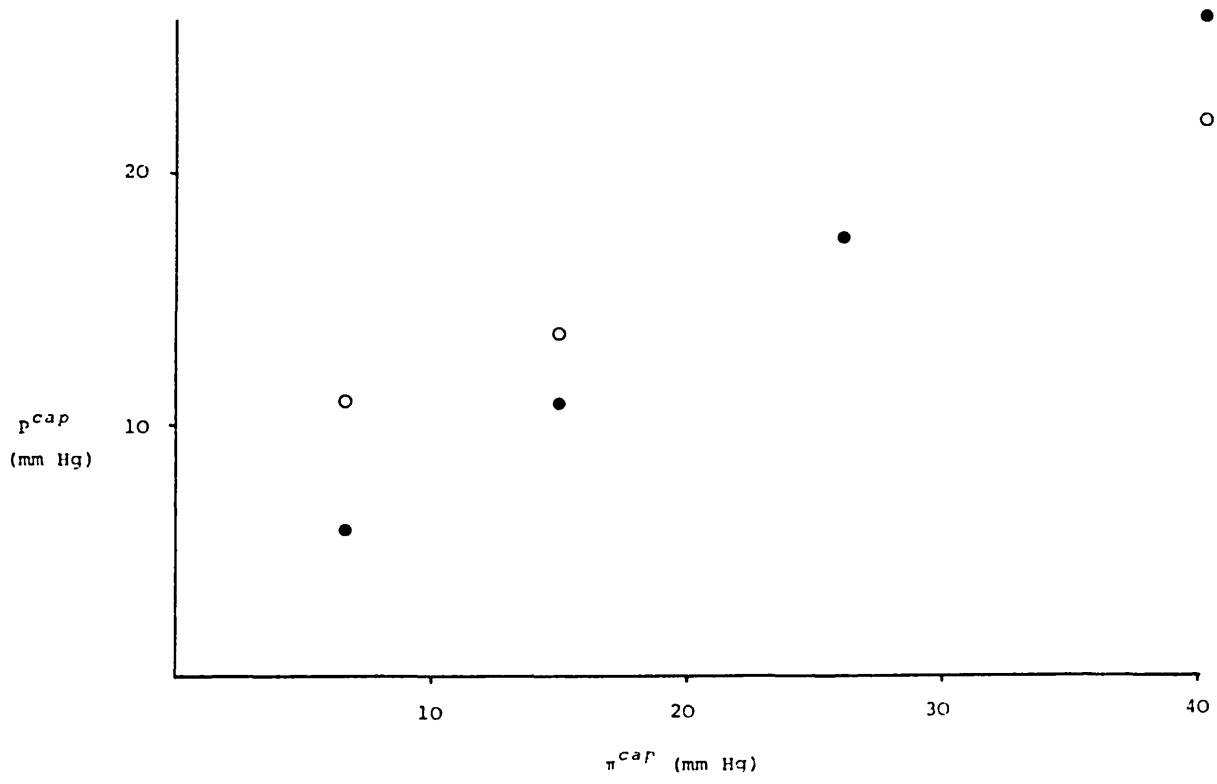


FIGURE 3.12. Capillary pressure required to keeep the gland isogravimetric when the albumin concentration of the perfusate is changed. The slope of the line is equal to the estimated σ_{alb}^{cap}. Two values of σ_{alb}^{cap} are illustrated.

$$\sigma_{alb}^{cap} = 0.6 \quad (\bullet)$$

$$\sigma_{alb}^{cap} = 0.3 \quad (o)$$

isogravimetric when the colloid osmotic pressure of the perfusate was changed. The procedure in the model was thus a combination of albumin osmotic transient and venous pressure elevation; the perfusate albumin concentration was altered, and hydrostatic pressure in the last capillary segement changed until the run showed that the gland was isogravimetric throughout the transient. Mean capillary pressure was calculated and this was plotted against the perfusate colloid osmotic pressure. The slope of the resulting line should be equal to σ_{alb}^{cap}. Fig. 3.12 illustrates the results obtained when σ_{alb}^{cap}= 0.6 and 0.3; the slopes of the lines are 0.6 and 0.3 respectively.

The fact that the gland may be maintained isogravimetric by a change in capillary pressure calculated on the basis of filtration equations alone suggests that diffusion of albumin plays a negligible part in the transient. This is in agreement with the results found in Chapter 2, hence the low value of PS_{alb}^{cap} used in the model.

3.4.3. Osmotic Transients Using Inulin as Test Solute

Fig. 3.13 shows the time course of the weight change when 10 mM inulin is introduced into the perfusate. In the model run illustrated in Fig. 3.13, K_f = 2 ml min^{-1} 100 $g^{-1}mm^{-1}Hg$. PS^{cap}_{inulin} = 1.5 ml $min^{-1}g^{-1}$ and σ^{cap}_{inulin} = 0.4. K_{cell} was assigned a low value, 0.02 ml $min^{-1}100\ g^{-1}mm^{-1}Hg$ and σ^{cap}_{alb} = 0.95. The initial rapid weight change soon starts to decrease, and with the values of the parameters used in this run, the gland starts to gain weight again after less than 10 seconds. It seems intuitively acceptable that the fall in rate of weight loss could be explained by diffusion of the inulin out of the capillary, but this could not explain a weight gain, since the concentration of inulin in the capillary would always be greater than that in the interstitium. In this section, some of the factors involved in determining the time course of the weight change are investigated. The factors considered are:

1. Hydraulic conductivity of cells
2. Interstitial compliance
3. Sieving of buffer solute
4. Changes in interstitial albumin concentration

Fig. 3.14 shows the changes in cell and interstitial volumes during the course of an inulin transient. With the low value of cell hydraulic conductivity used in this model run, changes in cell volume do not contribute much to the total gland weight change, particularly during the first 10 seconds. At 30 seconds, the cells contribute

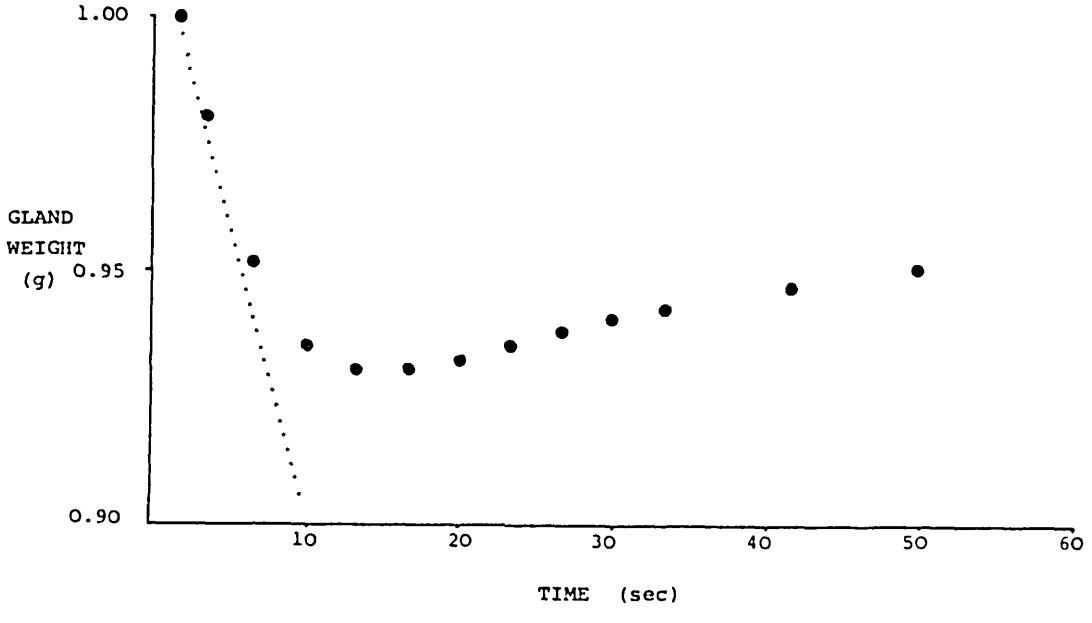


FIGURE 3.13. Time course of gland weight when 10 mM inulin is added to the perfusate.

Note 1. the gland does not immediately begin to lose weight after inulin is added

2. the gland weight reaches a minimum and then begins to rise, even though inulin is still present in the perfusate.

The dotted line indicates the slope of the initial part of the curve, drawn by eye.

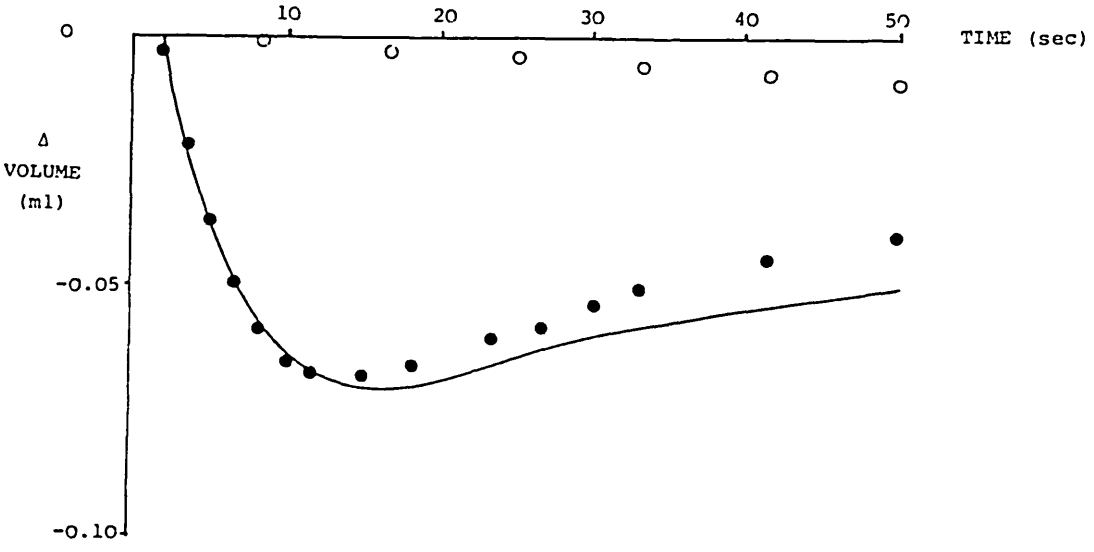


FIGURE 3.14. Time course of changes in interstitial (●) and cell (o) volumes during a 10 mM inulin transient. The total weight change (——) is also shown. Note that interstitial volume changes account for almost all the total weight changes incurred during the transient.

almost 20% of the total weight change. Changes in cell hydraulic conductivity would therefore, be expected to change the later part of the weight vs time curve while leaving the initial slope unaffected. This prediction is confirmed in Fig. 3.15 where the value of K_{cell} has been increased tenfold to 0.2 ml min^{-1} 100 $g^{-1}mm^{-1}Hg$. A secondary effect of an increase in K_{cell} is that the interstitial volume does not change as much, leading to a decrease in the elastic and osmotic buffering forces. The result is that the total weight loss is increased.

Buffering by molecular sieving of the 'resident' solute NaCl does not seem to contribute much to the time course of the osmotic transient. Fig. 3.16 shows the osmotic pressure differences across the capillary wall for albumin, NaCl and inulin as a function of time. In this figure $\sigma^{cap}_{NaCl} = 0.05$, and the maximum osmotic pressure exerted by the NaCl is 0.7 mm Hg at 2 seconds, which is less than 2% of that exerted by inulin at the same time. Even if σ^{cap}_{NaCl} were 0.1 the effect at early times would still be negligible. This is in agreement with the results of Johnson and Bloom (1981) but in contrast to those of Grabowski and Bassingthwaighte (1976). The difference probably lies in the way in which the importance of solute buffering was demonstrated; Johnson and Bloom (1981) varied σ^{cap}_{NaCl} while Grabowski and Bassingthwaighte (1976) varied the capillary and interstitial NaCl concentrations.

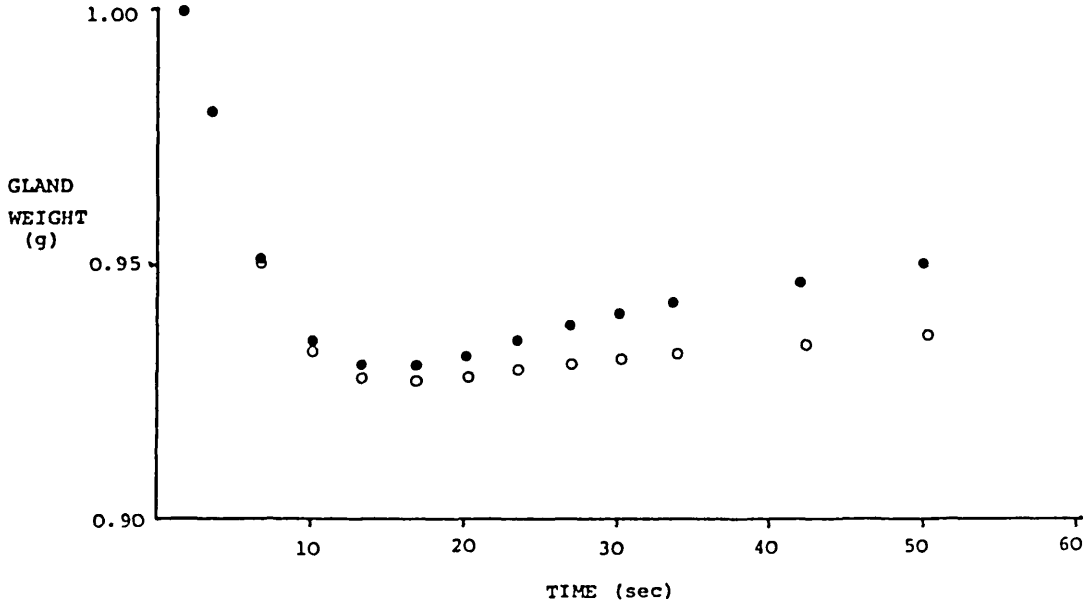


FIGURE 3.15. Effect of changing K_{cell} on the time course of a 10 mM inulin transient.

K_{cell}= 0.02 ml min^{-1}100 $g^{-1}mm^{-1}$Hg (●)

K_{cell}= 0.2 ml min^{-1}100 $g^{-1}mm^{-1}$Hg (o)

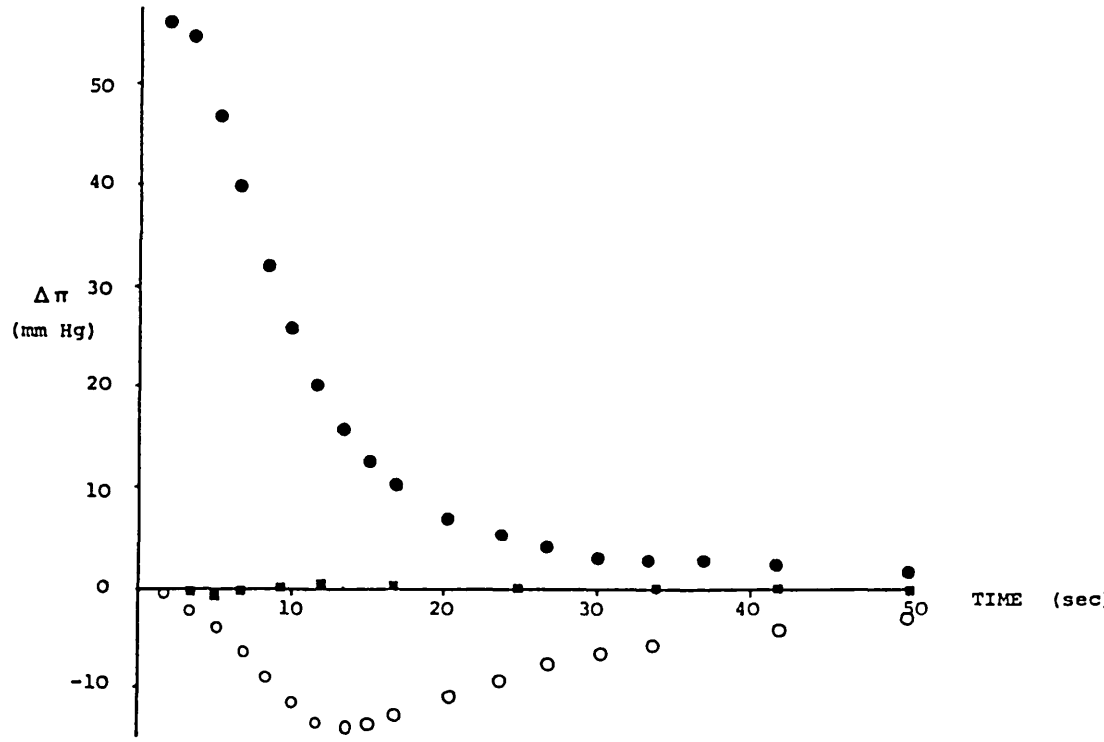


FIGURE 3.16. Transcapillary osmotic pressure differences ($\Delta\pi^{cap}$) due to inulin (●), albumin (o) and NaCl (■) during a 10 mM inulin transient. Positive numbers refer to a force tending to pull fluid into the capillary.

Changes in interstitial NaCl concentrations will also have an effect on water movement from the cells. With the values used in Fig. 3.13, the maximum interstitial NaCl concentration is 300.7 mM at 2 seconds. The additional 0.7 mM would lead to a water efflux of 0.04 µl s^{-1} with K_{cell} = 0.02 ml $min^{-1}100\ g^{-1}mm^{-1}Hg$. This is about 2% of the total rate of weight loss at the same time. The relative importance of NaCl-induced cell water efflux decreases as the transient progresses, due to the interstitial accumulation of inulin. If K_{cell} is increased tenfold to 0.2 ml $min^{-1}100\ g^{-1}mm^{-1}Hg$ then the rate of water movement out of the cells is increased initially. This however, tends to limit the rise in interstitial NaCl concentration and so the driving force for cellular water movement is reduced. In addition, the transcapillary NaCl concentration difference is reduced.

Fig. 3.16 shows that one of the major forces buffering the loss of interstitial fluid is the increased concentration of interstitial albumin. In fact, this appears to be the main factor involved in the reversal of the weight loss. Comparison of Figs. 3.13 and 3.16 shows that the transcapillary osmotic pressure due to inulin is balanced by that due to interstitial albumin at approximately 8.5 seconds, precisely when the gland stops losing weight. After this, interstitial albumin osmotic pressure is greater than the opposing inulin osmotic pressure, and the gland gains weight. This factor was not taken into account in the models of either Bloom

and Johnson (1981) or Grabowski and Bassingthwaighte (1976) and would seem to be of great importance.

Interstitial compliance also will to some extent limit the weight loss but the effect is not great. With a compliance of 15.4 mm Hg ml^{-1} for interstitial volumes less than 0.165 ml, a weight loss of 0.07 g (Fig. 3.13) would increase interstitial hydrostatic pressure by 1.1 mm Hg, about 8% of the transcapillary albumin osmotic difference. Interstitial hydrostatic pressure is a linear function of interstitial volume, whereas interstitial albumin colloid osmotic pressure is a function of:

a) interstitial albumin volume of distribution, which is itself an exponential function of interstitial volume.

b) interstitial albumin concentration, following a cubic relationship.

Both these factors tend to amplify the albumin colloid osmotic pressure increase at the larger volume changes. It would be expected, therefore, that the compliance effect would be relatively more important at smaller volume changes. This is true, but since the magnitude of all buffering effects is small relative to the effect of inulin in the first 3 seconds, this does not change the course of the transient to a measurable extent.

If $\sigma_{alb}^{cap} = 0.6$ then although interstitial volume falls, interstitial albumin concentration does not rise and there is little tendency for the gland to stop losing

weight, as shown in Fig. 3.17. Using these values in the model, the interstitial volume available for albumin due to exclusion becomes so small that the computer cannot deal with the numbers generated. Experimentally, the rate of weight loss does fall and so it is clear that other buffering forces, especially interstitial compliance, operate.

It is possible to estimate the reflexion coefficients of inulin (σ^{cap}_{inulin}) using the initial slope of the weight vs time curve. This can be done either by drawing a tangent to the weight vs time curve at zero time or by constructing a ln J_v^{cap} vs time curve and extrapolating this back to zero time. In both cases, "zero time" is taken as the time at which the gland begins to lose weight. Using the first method σ^{cap}_{inulin} is estimated at 0.375, and the correction described in Section 3.3. brings this up to 0.43 The ln J_v^{cap} vs time curve depicted in Fig. 3.18 allows extrapolation only from the first 3 seconds of the transient. Using this period, σ^{cap}_{inulin} is estimated at 0.38. Both these methods give values which correspond very well with the value of 0.4 inserted into the model. However, from a practical point of view, it may be difficult to make estimations of the tangents to the curves over the initial 3 seconds accurate enough to allow accurate calculations of σ^{cap}_{inulin}.

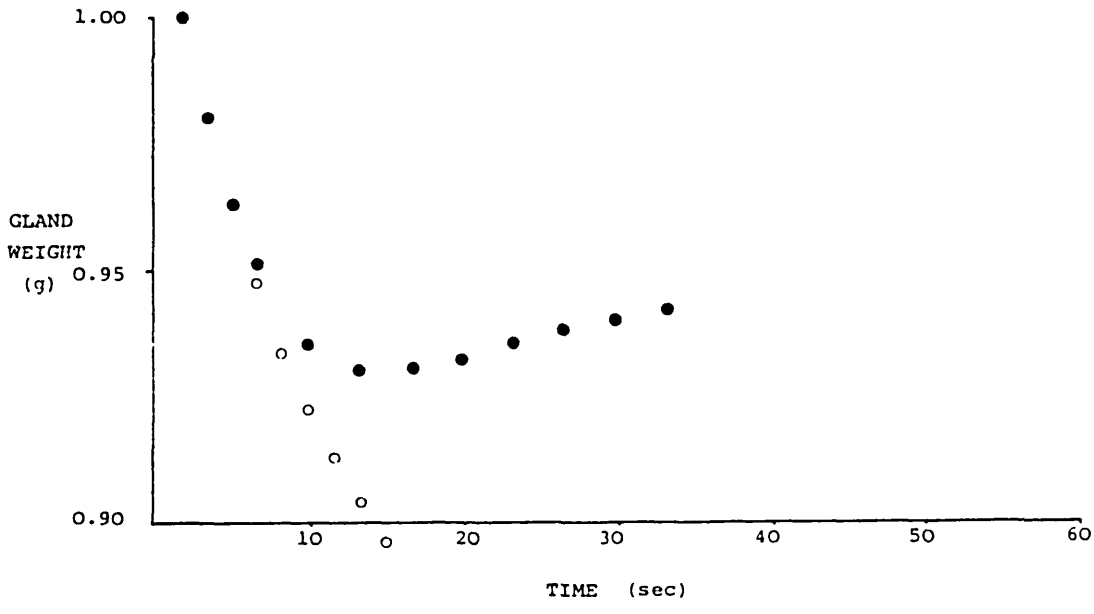


FIGURE 3.17. Effect of changing σ_{alb}^{cap} on the time course of a 10 mM inulin transient.

$\sigma_{alb}^{cap} = 0.95$ (●)

$\sigma_{alb}^{cap} \doteq 0.6$ (o)

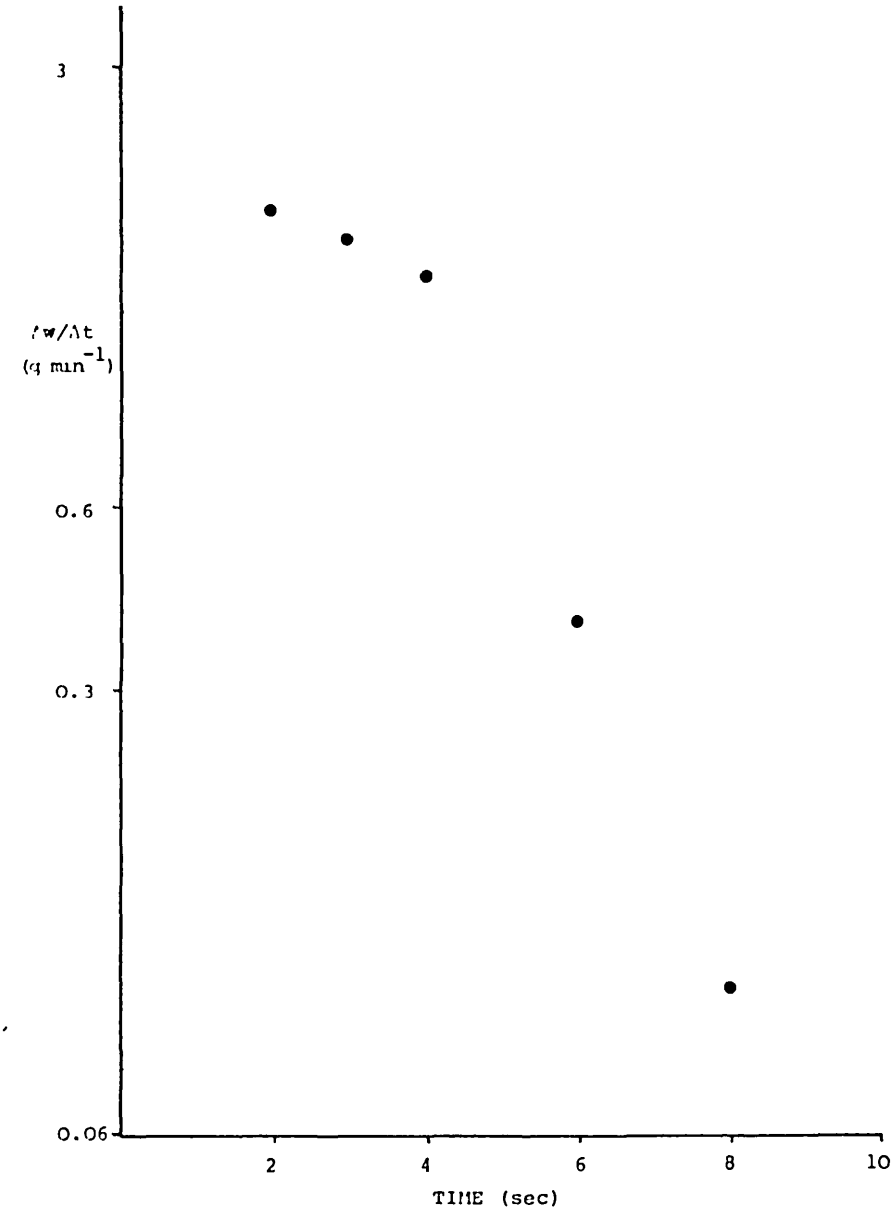


FIGURE 3.18. Rate of weight loss ($\Delta w/\Delta t$) vs time for a 10 mM inulin transient. $\Delta w/\Delta t$ is plotted on a logarithmic scale to enable extrapolation to zero time to be performed, according to the method of Vargas and Johnson (1967).

3.4.4. Osmotic Transient Using Raffinose as Test Solute

Fig. 3.19 shows the time course of the gland weight when 50 mM raffinose ($\sigma_{raff}^{cap} = 0.05$) is added to the perfusate. Two runs are illustrated, with K_{cell} equal to 0.02 or 0.2 ml $min^{-1}100\ g^{-1}mm^{-1}Hg$. In contrast to the predictions for inulin with the same values of K_{cell} the gland loses weight throughout the first 30 seconds of the transient. Fig. 3.20 shows that the cell loses a large quantity of water, even with the lower value of K_{cell}. This leads to an accumulation of solute-free water in the interstitium which occurs more quickly than the transcapillary fluid flux. The result is that the interstitium <u>increases</u> in volume, despite the fact that the gland is losing weight. An important consequence of this is that interstitial albumin concentration decreases leading to an increased transcapillary water flux. The same thing happens to the buffering solute NaCl. The net effect of all this is to <u>augment</u> the rate of weight loss. This is shown clearly in Fig. 3.21, where all the osmotic forces are tending to draw water from the interstitium into the capillary. Fig. 3.21 also shows that the contribution of the buffer NaCl is more important for raffinose than for inulin. Four seconds after the introduction of the solute, the transcapillary osmotic pressure due to raffinose has fallen to less than 2 mm Hg, the same as that due to NaCl. From 4 until 18 seconds NaCl provides the major osmotic force, after which albumin dominates. The effect is more pronounced with the higher

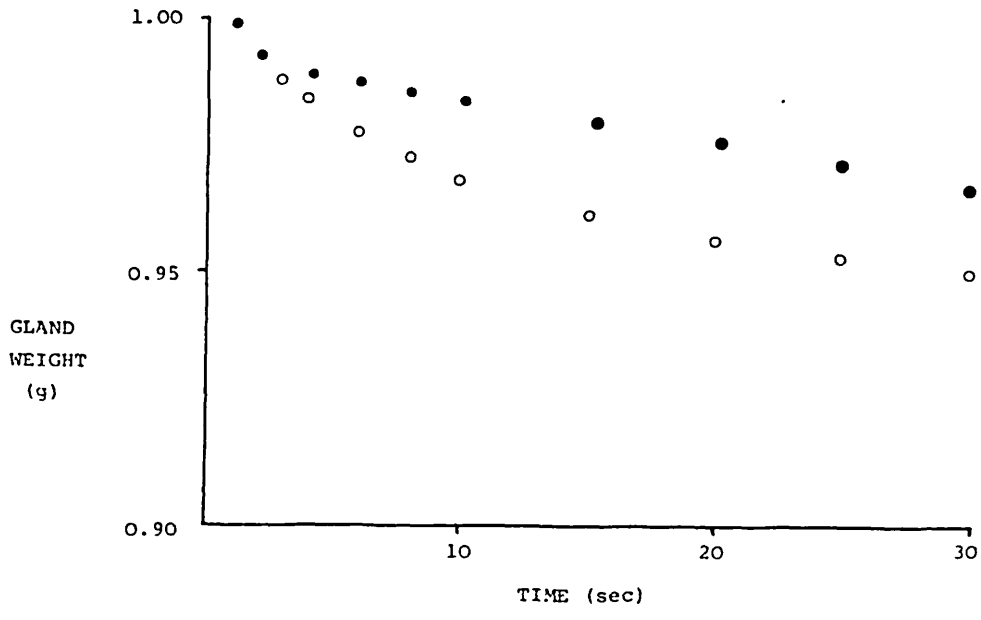


FIGURE 3.19. Time course of gland weight when 50 mM raffinose is added to the perfusate. Two values of K_{cell} are used.

K_{cell} = 0.02 ml min^{-1} 100 g^{-1} mm^{-1} Hg (●)

K_{cell} = 0.2 ml min^{-1} 100 g^{-1} mm^{-1} Hg (o)

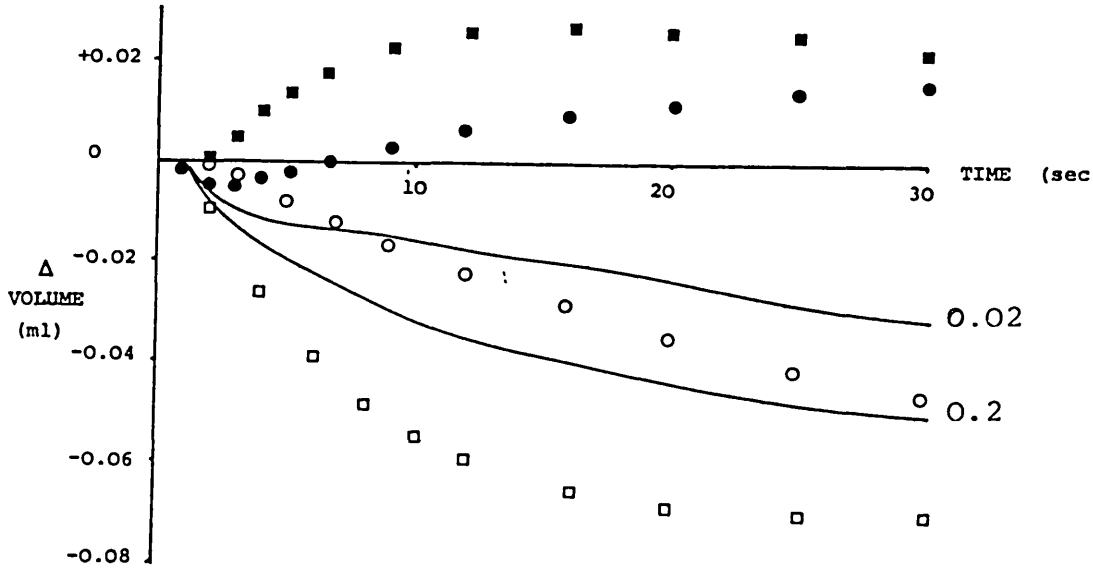


FIGURE 3.20. Time course of interstitial (filled symbols) and cell (open symbols) volumes during a 50 mM raffinose transient. The two values of K_{cell} used in Fig. 3.19. are both illustrated, as is the total weight change (solid lines - value of K_{cell} given next to the line). Note that, in contrast to the inulin transient (Fig. 3.14), changes in cell volume are greater than the total weight loss.

K_{cell} = 0.02 ml min^{-1} 100 $g^{-1}mm^{-1}Hg$ (● , ○)

K_{cell} = 0.2 ml min^{-1} 100 $g^{-1}mm^{-1}Hg$ (■ , □)

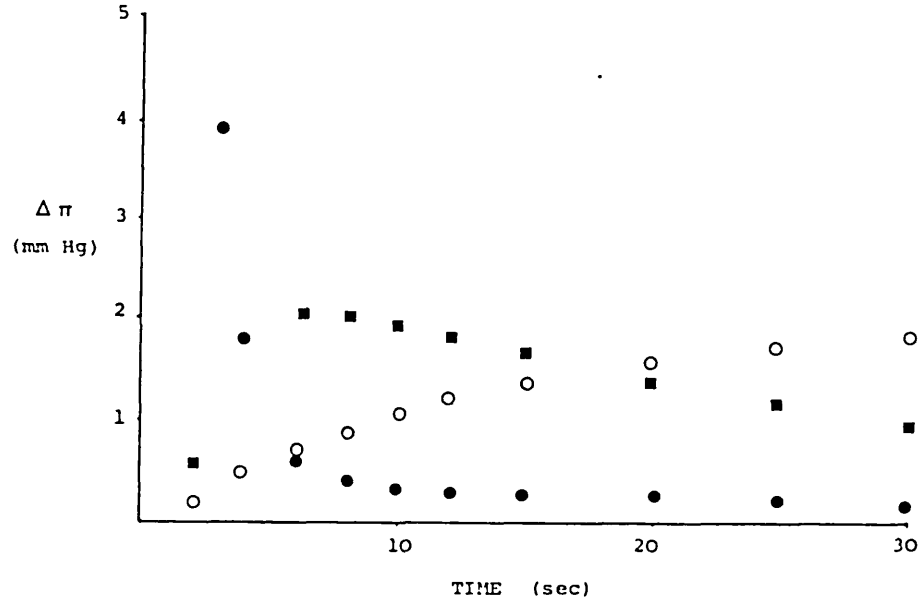


FIGURE 3.21. Transcapillary osmotic pressure differences ($\Delta\pi^{cap}$) due to raffinose (●), albumin (o) and NaCl (■) during a 50 mM raffinose transient. Positive numbers refer to a force tending to pull fluid into the capillary.

value of K_{cell} (not shown on Fig. 3.21) where at 4 seconds the contribution of NaCl is approximately 7.5 mm Hg.

Despite the interstitial dilution, the rate of weight loss does decrease, as shown in Fig. 3.22. The reason for this is that as water leaves the cells, the concentration of impermeant solutes inside the cells increases and buffers the cellular water loss. An equilibrium value will be reached when there is no osmotic pressure difference across the cells. An approximate value for this volume can be calculated from the initial intracellular osmolality (300 mOsm kg^{-1}) and volume (0.5 ml g^{-1}) and the interstitial osmolality at equilibrium (350 mOsm kg^{-1}). The volume is 0.429 ml g^{-1} in Fig. 3.20, the cell volume is approximately 0.43 ml g^{-1} at 30 seconds with K_{cell} = 0.2 ml $min^{-1}100\ g^{-1}mm^{-1}Hg$. Once the cells have reached this volume, water loss from the cells is governed by water loss from the interstitium and changing interstitial osmolality.

Interstitial compliance is of minor importance, but again tends to favour movement of fluid from interstitium to capillary. Fig. 3.20 shows that when K_{cell} = 0.2 ml $min^{-1}100\ g^{-1}mm^{-1}Hg$ the interstitium gains a maximum of approximately 0.03 ml. With a stiffness of 7.7 mm Hg ml^{-1} this would produce an increase of 0.23 mm Hg in interstitial hydrostatic pressure. The importance of increased interstitial hydrostatic pressure is greater when the cells have reached their equilibrium volume, since the transcapillary

NaCl concentration difference will quickly fall near zero.

Changing σ_{alb}^{cap} to 0.6 has very little effect on the early part of the weight transient, as shown in Fig.3.23. This is because interstitial volume has not changed much. However, more albumin leaves the interstitium and enters the capillary due to solvent drag, and so the interstitial albumin decreases more, than when σ_{alb}^{cap} = 0.95. This tends to augment the weight loss, more at the later times when the amount of albumin in the interstitium is progressively decreasing.

Comparison of the value of σ_{raff}^{cap} inserted into the model to that estimated by taking the initial slope of the weight vs time curve shows that by taking the slope within the first second of weight loss, σ_{raff}^{cap} is estimated at 0.02, and that the value of K_{cell} appears to have little influence on the estimate. Applying the correction explained in Section 3.3, σ_{raff}^{cap} is now estimated at 0.048.

Using the technique of extrapolating the J_v^{cap} vs time curve to zero time, however, shows that K_{cell} has a large influence on the estimate of σ_{raff}^{cap}. When K_{cell} = 0.2 ml $min^{-1}100\ g^{-1}mm^{-1}Hg$, the estimate of σ_{raff}^{cap} is 0.019, which increases to 0.046 using the correction; when K_{cell} = 0.02 ml $min^{-1}100\ g^{-1}mm^{-1}Hg$, σ_{raff}^{cap} is estimated at 0.032, which gives a value of 0.077 when corrected. It is clear that the slope of the J_v^{cap} vs time line has more to do with K_{cell} than PS_{raff}^{cap}, and that when K_{cell} is increased, the effective interstitial volume of distribution

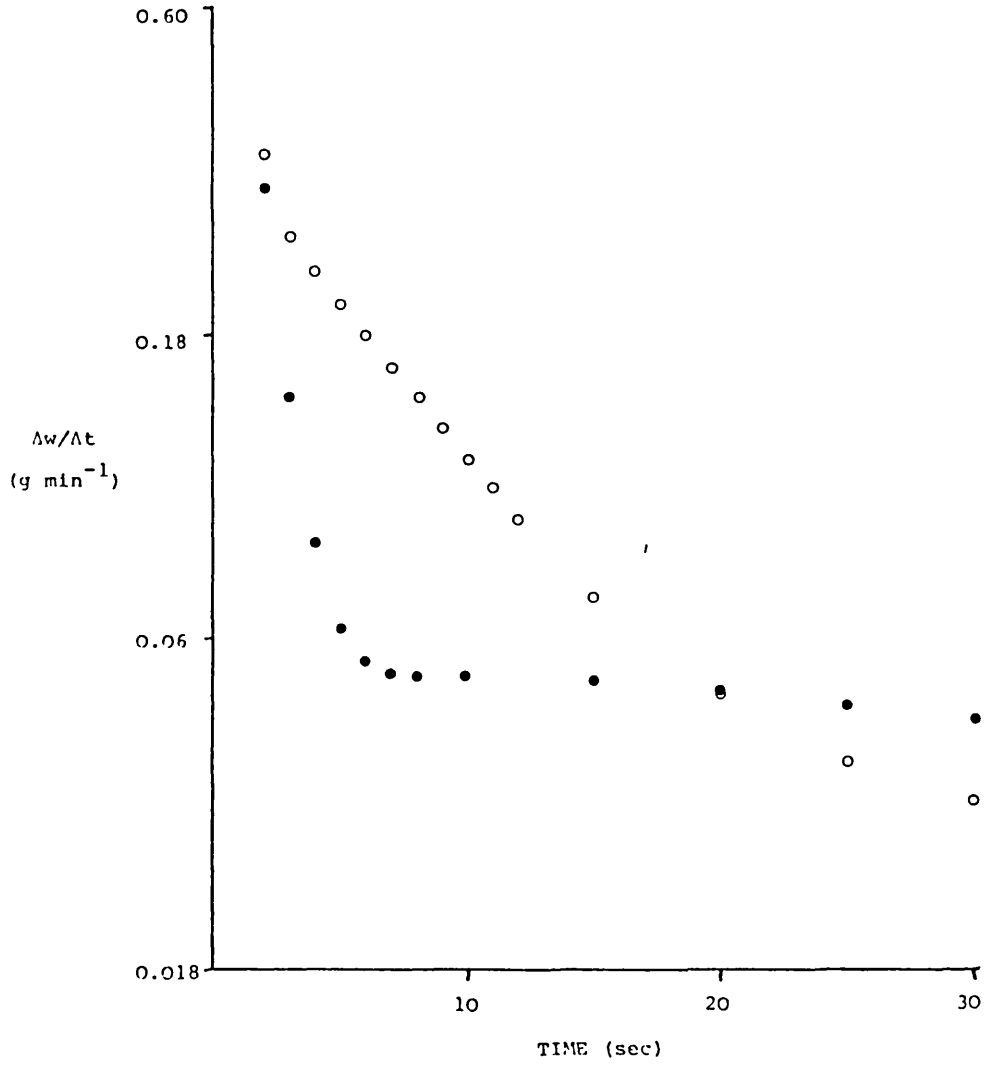


FIGURE 3.22. Rate of weight loss ($\Delta w/\Delta t$) vs time for a 50 mM raffinose transient. $\Delta w/\Delta t$ is plotted on a logarithmic scale to enable extrapolation to zero time to be performed.

$$K_{cell} = 0.02 \text{ ml min}^{-1} \text{ 100 g}^{-1}\text{mm}^{-1}\text{Hg} \quad (\bullet)$$

$$K_{cell} = 0.2 \text{ ml min}^{-1} \text{ 100 g}^{-1}\text{mm}^{-1}\text{Hg} \quad (\circ)$$

of raffinose is increased. This means that the transcapillary concentration difference of raffinose does not fall as quickly during the transient, thus reducing the slope of the ln J_v^{cap} vs time relationship and making the zero time estimate lower.

Surprisingly, the correction factor also becomes less, leading to a more serious underestimate of σ_{raff}^{cap} If the interstitial volume were infinite the correction formula (Eqn. 3.23) would reduce to

$$\Delta C = \frac{C_{raff}^{art} \; 1 - \exp(-\alpha)}{\alpha}$$

which is equal to 0.57 with the values used. The estimated value of σ_{raff}^{cap} must be multiplied by (1/0.57) ie 1.75, which would make the corrected value equal to 0.034.

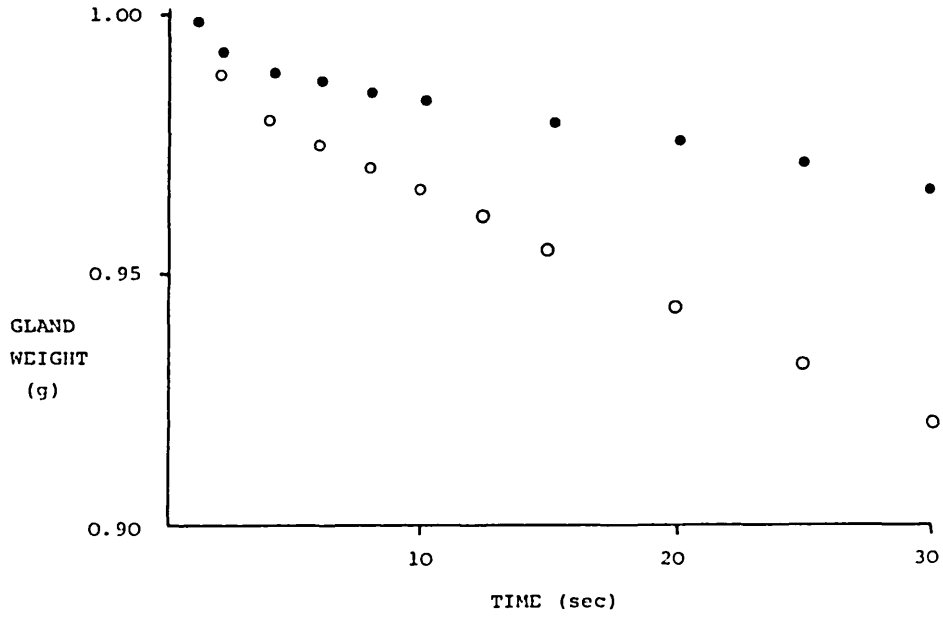


FIGURE 3.23. Effect of changing σ_{alb}^{cap} on the time course of a 50 mM raffinose transient.

$\sigma_{alb}^{cap} = 0.95$ (●)

$\sigma_{alb}^{cap} = 0.6$ (o)

3.5. Discussion

In the first paper of their series describing a model of osmotic transport in the rabbit heart, Bloom and Johnson (1981) state that "The utility of this model depends on whether it represents the preparation and its experimental perturbation in a useful form that provides new insights." Although the model developed in this chapter can hardly be said to provide a new conceptual approach to the osmotic transient technique, yet it can fairly claim to provide some "new insights" into the problems involved when the technique is applied to an organ whose capillaries are highly permeable to small solutes.

Some of the reasons for modifying the models of Bloom and Johnson (1981) and Grabowski and Bassingthwaighte (1976) have been outlined in the introduction to this chapter. One feature of the present model which is not taken into account in the Bloom and Johnson model is the change in interstitial albumin concentration. This seems to be of major importance in the venous pressure elevations, and albumin transients; the effect is large because the albumin is distributed in a small fraction of the total extravascular volume. This is true only if the gland is not oedematous, as in the in vivo experiments described in Chapter 2. The previous models have assumed that $\sigma_{alb}^{cap} = 1$ and that an albumin osmotic transient gives an accurate measurement of K_f. The effect of changing σ_{alb}^{cap} on the time course of both hydrostatic pressure elevations

and osmotic transients is seen in the present model to lead to significant differences in the estimations of K_f. Bloom and Johnson (1981) and Johnson and Bloom (1981) suggest that tissue elasticity is the main factor responsible for the return phase of a transient, a conclusion shared by Grabowski and Bassingthwaighte. The present model indicates that tissue pressure changes have a smaller effect than albumin, as long as σ_{alb}^{cap} is high. Grabowski and Bassingthwaighte used a value for interstitial elasticity of 16 mm Hg ml^{-1}, not very different from the value of 15.4 mm Hg ml^{-1} used in the present model for interstitial volumes below 0.165 ml, but twice the value taken by Bloom and Johnson.

3.5.1. Transcellular Water Flux

The relative contribution of the cellular water flux varies from one model to another. In a 50 mM NaCl transient, Grabowski and Bassingthwaighte conclude that at "t = 90 s, 53% of the weight loss has occurred from the cell." Bloom and Johnson, on the other hand, show that for a 50 mM NaCl transient the water loss from the cell is greater than the total weight loss of the organ, and the interstitium increases in volume, and a similar conclusion can be drawn from the present work. The differences between the models are not clear in this regard, but the cell equations used by Grabowski and Bassingthwaighte show that a decreased cell hydrostatic pressure would tend to buffer changes in cell volume. Also, the values of

K_{cell} used by Grabowski and Bassingthwaighte are much lower than that used by Bloom and Johnson; the values used in the present work fill the gap between the two.

3.5.2. Solute Buffering

Solute buffering (ie buffering of transcapillary water flux due to sieving of NaCl at the capillary wall) was considered by Grabowski and Bassingthwaighte to be an important factor modifying the time course of the weight change and causing errors in the determination of σ^{cap}_{test} and PS^{cap}_{test}. Bloom and Johnson relegate the solute buffering effect to a minor position, arguing that dissipation of concentration gradients by diffusion would tend to minimize any buffering and in the case of their NaCl transient would favour <u>increased</u> transcapillary water flux. The conclusion from the present work is that the importance of solute buffering depends on the conditions. The albumin and inulin transients are not affected to a great degree for different reasons; the albumin transient because the transcapillary volume flux is slow enough for diffusion to eliminate any concentration differences, while for the inulin transient the low NaCl reflexion coefficient means that the NaCl concentration in the transcapillary volume flux is 0.95 of its interstitial concentration, leading to relatively small changes in interstitial NaCl concentration. In a raffinose transient, however, solute-free water is entering the interstitium from the cells,

and so the interstitial NaCl concentration will fall, the magnitude of the fall being directly related to the cell hydraulic conductivity. Since the transcapillary concentration difference of raffinose falls rapidly, the NaCl and albumin osmotic pressure differences dominate. However, the effect of both of these is to favour movement of water from the interstitium into the capillary and so the weight loss is magnified and prolonged. If K_{cell} = 0 for a raffinose transient, the result is a small, short-lived weight loss reflecting the rapidity of raffinose diffusion.

3.5.3. Venous Pressure Elevation

The readjustment in tissue forces following an elevation of venous pressure has been discussed by Richardson, Granger and Taylor (1979), in their review of the measurement of capillary filtration coefficient. They made the point that "the time course of readjustment of tissue forces will vary depending on the hydration of the tissue and the true value of K_f ..... Tissue force changes in normally hydrated preparations with larger capillary hydraulic conductances will occur more rapidly .....".

This places the experimenter in a dilemma: it is important to measure the filtration coefficient as accurately as possible with the preparation in as normal

a state as possible. The objectives may not be reconcilable, if the more normal the tissue, the greater the error. This is especially important with venous pressure elevation, since vascular compliance dominates the weight changes at the very time that readjustment of tissue forces is of its greatest magnitude.

The zero time extrapolation (ZTE) technique was developed to try to overcome the problems of the initial tissue force readjustments (Drake et al, 1978). It was found that when J_v^{cap} was plotted semilogarithmically against time, two phases were evident; an initial rapid phase assumed to represent the time course of vascular compliance, and a slower phase assumed to represent filtration. The slow phase remained "linear" for 8-10 minutes enabling an extrapolation to zero time to be performed. According to Richardson et al (1979), "one should acquire a value for J_v^{cap} which theoretically represents K_f before readjustments in tissue forces have occurred." Although intuitively attractive, the theory behind this procedure is not as sound as one would perhaps like to believe. The major assumptions underlying the extrapolations are:

a) the slow phase of falling J_v^{cap} does indeed represent filtration rather than vascular compliance

b) filtration is falling with the same time course during the period covered by the extrapolation.

The first of these assumptions would seem to be justified by the fact that the blood volume changes are complete within about one minute. Johnson and Hanson (1966) found that the slow phase of volume response of dog intestine began in under 30 seconds, in agreement with Wallentin (1966) who monitored the activity of radiolabelled erythrocytes in cat intestine on elevating superior mesenteric venous pressure. In single capillaries, the vascular compliance response is much faster than this; Smaje and Swayne (1983) found that the fraction of the maximum compliance response that had occurred in 2 seconds was 0.8 in rat mesentery and 0.9 in frog mesentery. Some preliminary work in this laboratory (Gamble, unpublished data) suggests a similar time course for vascular compliance when the rabbit submandibular gland is perfused with a paraffin-silicone oil mixture and venous pressure elevated. However, the indication in these latter experiments was that the initial increase in weight when the gland was perfused with oil was much less than that when it was perfused with Krebs-albumin solution. Whether this is due to transcapillary fluid flux at the earliest times or to a difference in vascular response to the different perfusing solutions awaits further investigation.

The second assumption is more difficult to justify. There is no theoretical reason why J_v^{cap} should decrease monoexponentially with time; in order for this to be the

case, the net filtration pressure must be decreasing monoexponentially. If capillary hydrostatic and osmotic pressures are assumed to be constant, this implies that tissue hydrostatic and osmotic pressures are increasing at a monoexponentially decreasing rate, asymptotically approaching $(P^{cap} - \pi^{cap})$. In the analysis the time constants of the changes in P^{int} and π^{int} must be the same. This is unlikely, since tissue hydrostatic pressure is a non-exponential function of interstitial volume, and interstitial osmotic pressure depends upon the protein concentration (itself a complex function of the interstitial volume, due to exclusion effects) in a non-linear fashion. When these effects are considered, even in the relatively simple way in which the present model does, plotting J_v^{cap} semilogarithmically versus time does not give a straight line. Moreover, the greatest fall in J_v^{cap} occurs at the earliest times, so extrapolating back from even 30 seconds will underestimate K_f seriously. Oddly enough, reduction of σ_{alb}^{cap} to 0.6 gives an estimate of K_f closer to the value inserted into the model than if $\sigma_{alb}^{cap} = 0.95$; however, further reduction results in overestimation of K_f. The crucial element in this regard is the interstitial albumin concentration. This is difficult to measure directly and so has to be inferred from albumin concentration of lymph or from tracer studies. The tracer experiments described in Chapter 2 suggest that the extravascular albumin volume of distribution is about 25% of the total extravascular volume. With a

perfusate albumin concentration of 6 g 100 ml^{-1}, interstitial albumin concentration would be 1.5 g 100 ml^{-1} and this is the value used in the model. However, it is likely that local variations in concentration will occur, depending upon whether an individual region in the interstitial fibre matrix is large enough to accomodate an albumin molecule.

3.5.4. Assumptions of the Model

The success of any model depends to a large extent on the validity of its underlying assumptions. This is true even when a single equation is used. Unfortunately most of the assumptions listed in Section 3.2.2. have not been tested in the rabbit submandibular gland and so it is difficult to assess them; further work in this area is clearly required.

The numbers of the points listed here refer to the numbered assumptions in Section 3.2.2.

Assumptions 1 - 4. The problem of solute and volume fluxes across cells is discussed more fully in House (1974 - chapters 5 and 6). The animal cells most commonly studied are erythrocytes, and for these cells the ratio of water permeability to solute permeability is high even for a molecule as small as glycerol. Zaduniasky (1963) found that in skeletal muscle, the reflexion coefficient for both mannitol and sucrose at the cell wall was essentially unity, and according to House (1974; pp 195-196): "Probably it can be accepted quite safely that the reflexion coefficients of most osmotic solutes are close or equal to unity." It is unlikely that there is a hydrostatic pressure difference across the cell wall at equilibrium since the internal osmotic pressure of the cell at equilibrium appears to be identical to that of the surrounding fluid (eg Conway and McCormack, 1953). Robinson (1953) originally challenged this view

and proposed an active mechanism for water "secretion". However, Conway, Geohegan and McCormack (1955) showed that the apparent cellular hypertonicity found by Robinson (1953) was due to rapid intracellular breakdown of large molecules, such as glycogen. The model of Grabowski and Bassingthwaighte (1976) does allow for hydrostatic pressures to develop across the cell wall, and it is likely that under transient conditions there will be such a difference. However, the error involved in neglecting the resulting transcellular water flow will be negligible due to the small changes in tissue hydrostatic pressure and the low hydraulic conductivity of the cells.

The assumption that the cell is a perfect osmometer is an easy one to test for readily accessible cells such as erythrocytes. When this is done, however, (eg Cooke, 1967) it is found that a plot of cell water volume versus the reciprocal of the osmolality of the bathing fluid, although linear, does not pass through the origin. This implies that a certain fraction of the cell water does not take part in osmotic exchange. This conclusion has been confirmed in a number of different cell types but the fraction of "osmotically inactive" cell water varies (eg Cook, 1967; Blinks, 1965). An approximate value of 0.17 was taken for this fraction and the cell volume available for osmotic water flux estimated from the total cell volume (total gland volume - intravascular volume - interstitial volume) assuming that 75% of the cell volume is occupied by water (Cook, 1967).

Assumption 5. The studies of Guyton (1963) first demonstrated that interstitial hydrostatic pressure varied with the state of hydration of the tissue. Guyton also developed the concept that interstitial fluid pressure was subatmospheric, but conceded that "encapsulated organs, such as the kidney or eye, or tissues in firm cavities, such as the central nervous system, certainly have different fluid dynamics from those in loose tissue." The pressure-volume relationship for subcutaneous tissue found by Guyton (1963) shows a steep fall in hydrostatic pressure as the tissue is dehydrated below its normal volume, and a shallow rise in pressure as tissue volume increases. The tissue pressures in the submandibular gland have not been measured and so it is not possible to determine the compliance relationship in the gland. However, the values taken for interstitial compliance in the model are likely to be overestimates; the value of 0.13 ml $mm^{-1}Hg$ was taken from Bloom and Johnson (1981), but the rabbit heart interstitial space is much greater than that in the submandibular gland and the hearts used by Bloom and Johnson (1981) were oedematous.

A further complicating factor is that of stress-relaxation or delayed compliance. Guyton (1965) found that if the interstitial space of a dog's leg was increased, there was an initial rapid increase in pressure, but that pressure slowly declined to a steady level after several minutes. The point is discussed further by Guyton, Granger and Taylor (1975), but the transients described in Chapter

4 lasted only one minute, and stress-relaxation should not have a major influence during this period, particularly as tissue volume is continually changing.

It is difficult to see how to overcome these problems of tissue pressure until the pressure-volume relationship has been defined in the rabbit submandibular gland during a weight transient.

Assumption 6 "Capillary pressure" in the literature usually refers to a mean value which would be measured somewhere along the length of the capillary. However, it is obvious that for flow to occur, there must be a pressure drop between the ends of the capillary. Few studies have been directed towards determining the form of this pressure drop, but the figure given in the review by Landis and Pappenheirmer (1963 - Fig. 2.3) suggests that a linear fall may not be too far from the truth.

Assumption 7 Under experimental conditions it is clear that the test solute will not arrive at the capillary as a sharp 'front' of solute. Johnson et al (1981) provided an analytical solution for the concentration profile of test solute as it entered the capillary after a step change in perfusate composition. They concluded that the test solute concentration at the input end of the capillary was more than 95% of that in the bulk of the perfusate 2 seconds after the switch. Even with such a short time constant large errors would occur using this method with the small solutes. The use of the whole weight

vs time curve for estimating reflexion coefficients overcomes the problem to a certain extent.

Assumption 8 The assumption of a constant resting salivary flow rate is one which was experimentally verifiable and found to be reasonably valid. In any case, the resting salivary flow rate was so small as to make a negligible contribution to the weight change during a transient.

Assumption 9 Since tissue hydrostatic and osmotic pressures were not measured, it is not possible to determine how these influenced lymph flow. In other studies (eg Hogan, 1981; Mortillaro and Taylor, 1976; Granger, Mortillaro and Taylor, 1978), increased tissue pressure and/or increased capillary filtration produced increases in lymph flow, but the relationship between the two was not necessarily linear. The lymph flow found by Koo et al (1980) was 10^{-3} ml $min^{-1}g^{-1}$, which is about 1% of the initial rate of weight gain following a venous pressure elevation of 10 mm Hg. If lymph flow remained constant it would not affect the transient at all; if K_L = 0.5 ml $min^{-1}100\ g^{-1}mm^{-1}Hg$ a rise in interstitial pressure of 1 mm Hg would cause an increase in lymph flow of 5×10^{-3} ml $min^{-1}g^{-1}$, approximately 5% of the total rate of weight gain. In some of the initial runs of the model, tissue hydrostatic pressure in the isogravimetric gland was 0.2 mm Hg, and this, together with the lymph flow of 10^{-3} ml $min^{-1}g^{-1}$, gave the lymphatic hydraulic conductivity of 0.5 ml $min^{-1}100\ g^{-1}mm^{-1}Hg$ used in the model. Later runs

produced higher values for P^{int} under isogravimetric conditions and so the value of K_L would be smaller. The high value was kept as a maximum estimate of error in estimating weight changes, but even so the effect was small.

CHAPTER 4

Filtration and Reflexion Coefficients in the Isolated, Perfused Rabbit Submandibular Gland

FILTRATION AND REFLEXION COEFFICIENTS IN THE ISOLATED PERFUSED RABBIT SUMBANDIBULAR GLAND

4.1. Introduction

The main aim of this thesis, as set out in Section 1.5., was to extend previous work on the permeability properties of the submandibular gland capillaries. The work described in the previous two Chapters was initially intended to provide some tools for analysing and interpreting data obtained from the osmotic transient experiments described in this Chapter. However, it is evident from the discussions in Chapters 2 and 3 that there are still large areas in which experimental data and theoretical analysis are lacking, and that these deficiencies are major obstacles to the determination of membrane coefficients. This is particularly important in organs like the salivary glands, which have large fluxes of water and small solutes, and correspondingly high filtration and permeability coefficients.

In this Chapter, some of the osmotic transient experiments performed in this laboratory are described. There were some results which were puzzling, and possible explanations for these are discussed, both with the help of the osmotic transient model, and from preliminary results obtained in this laboratory relating to vascular compliance. It is clear, however, that the uncertainties mentioned in Section 3.5.4. remain to be resolved.

4.2. Methods

4.2.1. Animals and Anaesthesia

A total of 17 male New Zealand White rabbits, weighing between 1.47 and 2.58 kg (mean weight 1.79 ± 0.04 kg) were used. Anaesthesia was induced via a marginal ear vein with ethyl carbamate (Urethane; Sigma CHemical Co, St Louis, Missouri) made up to a concentration of 25 g 100 ml^{-1} in sterile 0.9 g 100 ml^{-1} NaCl. The initial dose given was approximately 1.8 g kg^{-1}. The trachea and a femoral vein were cannulated in each animal, and additional urethane administered as required via the venous cannula to maintain anaesthesia.

4.2.2. Isolation of the Submandibular Gland, and Transfer to Perfusion Circuit

Fig. 1.1 showed the vascular supply to the salivary glands of the rabbit. In order to maintain blood flow to the gland during the isolation procedure, the external maxillary artery was cannulated distal to the origin of the submandibular artery with a short length of 1.02 mm external diamter Portex nylon tubing. The nylon tubing was connected to a longer length of flexible silicone rubber tubing (Esco Rubber Ltd; Teddington, Middlesex) and a 50 ml reservoir containing perfusate equilibrated with 95% O_2 and 5% CO_2. During the arterial cannulation procedure, a clamp was placed around the external maxillary

artery between the cannula and the origin of the submandibular artery. The salivary duct was cannulated with a length of 0.63 mm external diameter nylon tubing. In order to check the patency of the duct and cannula, the duct was stimulated via platinum electrodes using square wave impulses of 2.0 msec duration at a stimulus strength of 10 V and frequency of 10 Hz. This usually resulted in a marked reddening of the gland and a copious flow of saliva through the duct cannula within a few seconds. If saliva did not flow, attempts were made to unblock the cannula and duct; if these attempts were unsuccessful, the gland was rejected.

After ligating and cutting all tributaries except that from the submandibular gland, the external jugular vein was cannulated with a short length of 1.65 mm external diameter nylon tubing connected to a longer length of flexible silicone rubber tubing.

After all cannulations had been completed, the animal was given 2000 iu heparin (Heparin sulphate; Paines and Byrne Ltd) intravenously. The reservoir on the arterial perfusion line was elevated to about 30 cm above the gland and the clamp on the external maxillary artery removed.

A small quantity of blood was forced up the arterial perfusion line. The external maxillary artery was then cut between ligatures close to its point of origin from the carotid artery.

The gland was immediately transfered to the perfusion circuit and the arterial cannula connected to the arterial limb of the circuit, care being taken to avoid introducing air bubbles into the cannula. The maximum time taken, from cutting the external maxillary artery to normal pressure in vitro perfusion was 4 minutes but was generally considerably less than this.

4.2.3. Perfusion Circuits

Two perfusion circuits were used, physically identical but containing different perfusing solutions, joining close to the arterial inflow of the gland. With this arrangement the solution perfusing the gland could be suddenly changed with very little delay between the instant of switching and the gland being perfused with the new perfusate.

One of the circuits is shown diagrammatically in Fig. 4.1. The perfusate was kept in a reservoir maintained at 37^{o}C by a water bath and impelled by a Watson-Marlow flow inducer via two 25 mm diameter, 0.8 µm filters (Diaflow) towards a membrane oxygenator (Biomedix; Pinner, Middlesex). This consisted of four narrow bore silicone rubber tubes arranged in parallel and enclosed in a glass tube which had an inlet and outlet port. Pre-warmed, humidified 95% O_2/5% CO_2 was passed through the outer tube, and the gas diffused through the ultrathin

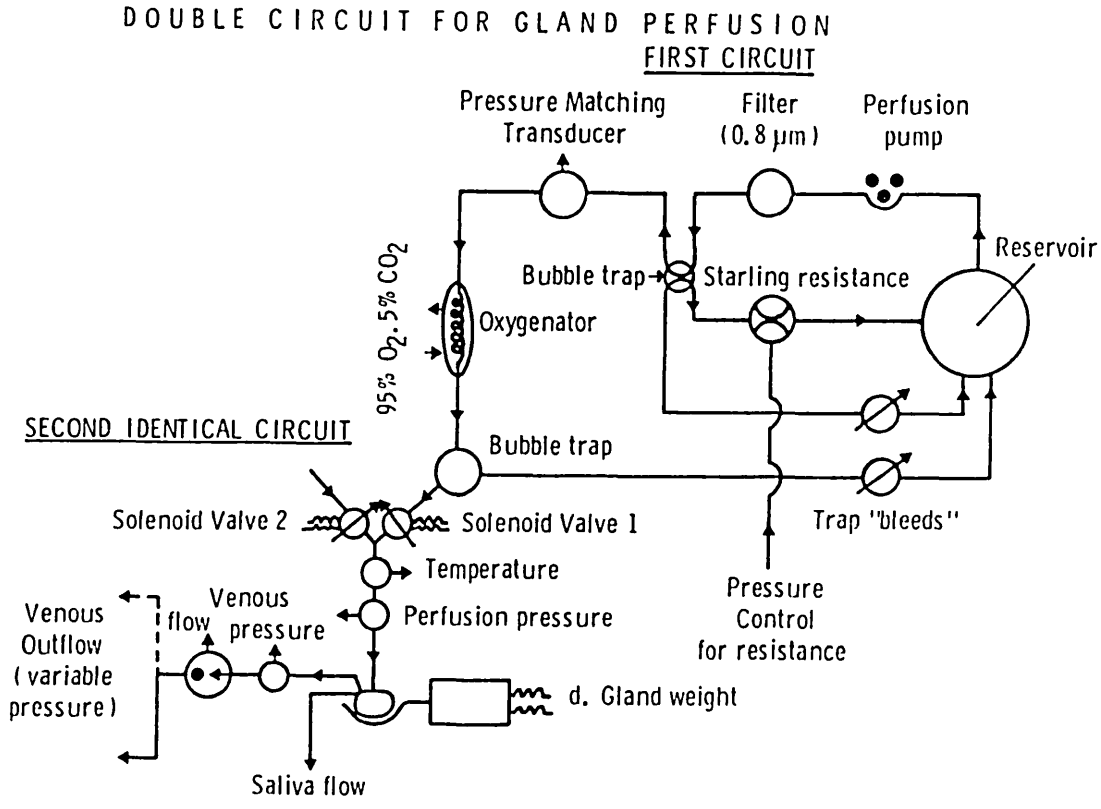


FIGURE 4.1. Schematic diagram showing one (of two) circuits used to perfuse the isolated rabbit submandibular gland. Both circuits, including the gland, are housed in a box at a constant temperature of 37°C. See Section 4.2.3. for details.

wall of the silicone rubber tubing. After passing through the oxygenator, the perfusate could either pass to the gland or back to the reservoir via a Starling resistor. The perfusion pressure could be set by adjusting the Starling resistor, and the resistances in the circuit were such that most of the perfusate returned to the reservoir to be recycled. A pressure transducer (Bell and Howell, type 4-422-0001) was incorporated into the circuit to allow the perfusion pressure to be measured; this was important to ensure that the pressure in the circuit not perfusing the gland was the same as that in the circuit perfusing the gland before a switch in perfusates was made. A series of bubble traps was included in the circuit to prevent air emboli from gaining access to the tissue.

The two perfusion circuits were housed in a perspex box whose internal temperature was maintained at 37^{o}C by means of an electrical fan heater. The two circuits merged after passing through electrically operated solenoid valves; in this way it was possible to switch rapidly from one perfusate to another by remote control. The Watson-Marlow pump and the 0.8 µm filters were located outside the cabinet; the use of two filters in parallel for each circuit enabled one of the filters to be isolated and replaced without interrupting the flow to the tissue.

Temperature and pressure of the solution entering the gland's arterial supply were measured just distal to

the point of junction between the two circuits by an Edale model C thermometer (Edale Instruments Ltd; Cambridge, England) and a Bell and Howell type 4-422-0001 physiological pressure transducer, respectively.

4.2.4. Perfusing Solutions

All perfusing solutions were made up from a modification of Krebs-Ringer solution which contained (m.mol.ℓ^{-1}): NaCl, 118; KCl, 4.8; KH_2PO_4, 1.2; $MgSO_4.7H_2O$, 1.2; $NaHCO_3$, 25; $CaCl_2$, 2.5; D-Glucose, 11.1. This solution, when bubbled with a gas mixture of 95% O_2 and 5% CO_2 at 37°C, had a pH of 7.4. The addition of albumin to the solution made it more acidic, and compensation was made by altering the concentration of $NaHCO_3$, the NaCl concentration being altered by an amount sufficient to maintain the osmolality of the final solution at approximately 320 mOsm. kg^{-1}.

The basic perfusate contained 6 g 100 ml^{-1} bovine serum albumin (6% BSA) (Cohn fraction V, Sigma Chemical Co). Test solutions contained either a different concentration of BSA (3 - 8 g 100 ml^{-1}) or had inulin (2.5 - 10 mM) or raffinose (30 - 120 mM) added to the basic perfusate.

The colloid osmotic pressure of the perfusate was determined using a membrane osmometer fitted with a Bell and Howell type 4-422-0001 physiological pressure transducer. The crystalloid osmotic pressure of the raffinose solutions

was checked by determining the depression of freezing point on an Advanced Digimatic Osmometer (Advanced Instruments Inc.
All osmotic pressure measurements were performed by Dr J Gamble.

In order to maintain maximum vasodilatation for the duration of the experiment, adenosine (Boehringer, Mannheim) was added to the Krebs-albumin solution to a final concentration of 0.3 mmol.ℓ^{-1}.

4.2.5. Measurement of Changes in Gland Weight

The gland was placed in a 5 ml plastic spoon attached to a Grass Isometer Force Transducer (FT03) and covered in cling film wrap to prevent dessication. Since the weight changes recorded were small, it was important to minimise the effects of tension in the perfusion lines. This was accomplished by supporting the perfusion lines just above the gland and by using very flexible silicone rubber tubing. The effectiveness of the system was checked by measuring the sensitivity of the recording system with and without the gland in place, by suspending known weights from a hook attached to the weighing platform.

4.2.6. Measurement of Venous Pressure and Flow Rate

Venous outflow pressure was measured close to the venous cannula by means of a Bell and Howell type 4-422-0001

physiological pressure transducer. The height of the venous outflow reservoir, and hence the venous outflow pressure, could be adjusted.

The rate of venous outflow was measured by passing the drops through the beam of a photoelectric counter (Devices, type 2611; Devices Instruments Ltd, Welwyn Garden City, Hertfordshire). The weight of a single drop was determined by weighing a known number of drops; this procedure was repeated at several different drop rates within the range of values expected and appropriate corrections made in calculating the volume flow rate.

The following quantities were measured and displayed on a Devices M19 pen recorder

1. Arterial perfusion pressure (mm Hg)
2. Venous outflow pressure (mm Hg)
3. Venous flow (drops)
4. Gland Weight (mg)

4.2.7. Experimental Protocol

This was divided into 3 stages:

a. determination of isogravimetric capillary pressure
b. determination of capillary filtration coefficient by venous pressure elevation
c. estimation of capillary reflexion coefficients of albumin, inulin and raffinose by osmotic transient method.

a. Isogravimetric capillary pressure was measured according to the method of Pappenheimer and Soto-Rivera (1948). Arterial and venous pressures were set so that the gland neither gained nor lost weight (the isogravimetric state). Arterial pressure was either raised or lowered and venous pressure adjusted in order to maintain the gland in the isogravimetric state at the same weight as that existing before the pressure alterations. Sufficient time was allowed between pressure alterations to allow vascular compliance effects to have ended. The pairs of arterial and venous pressures so obtained were then plotted against the perfusate flow rate pertaining to each pair of pressures, and the lines extrapolated back to zero flow. At this point, arterial and venous plots should coincide, the intercept representing the isogravimetric capillary pressure. The ratio of the slopes of the P^{art} vs flow and P^{ven} vs flow lines equals the pre- to post-capillary resistance ratio (R_{pre}/R_{post}).

b. The venous outflow reservoir was raised by known amounts and the resulting weight gain allowed to continue for approximately one minute, when the reservoir was returned to its original level. In some experiments, venous pressure was lowered first and then raised back to the original level after about 1 minute.

d. The perfusate was suddenly changed to one containing a known concentration of the test solute, and the gland allowed to change weight. After approximately one minute the perfusate was switched back to the original solution.

4.2.8. Statistical Comparisons

Values are expressed as mean and standard errors of mean (SEM). Where appropriate, statistical comparisons were made using Student's t-test for unpaired data.

4. 3. Results

4.3.1. Measurement of Capillary Filtration Coefficient (K_f)

The resting capillary pressure (P^{cap}) and changes in P^{cap} brought about by alterations in venous pressure were calculated following determinations of pre- and post-capillary resistances (Section 4.2). Fig. 4.2 shows the results in one gland of changing venous and arterial pressures with the gland isogravimetric. The pre- to post-capillary resistance ratio for the experiment shown in Fig. 4.2 was approximately 8.2, but the mean value in 17 experiments was approximately 8.7 (Table 4.1).

Fig. 4.2 shows that the extrapolated values for arterial and venous pressures at zero flow coincide at a

	R_a	R_v	K_f
	(mm Hg.min.100 $g.ml^{-1}$)		(ml.min^{-1}100 $g^{-1}mm^{-1}Hg$)
Mean	0.148	0.017	0.96
SEM	0.022	0.002	0.086
n	17	17	25

TABLE 4.1. Values of pre- and post-capillary resistance and filtration coefficient in all 17 animals. K_f was determined more than once in some experiments, hence n is greater than the number of animals. The mean pre- to post-capillary resistance ratio was 8.7.

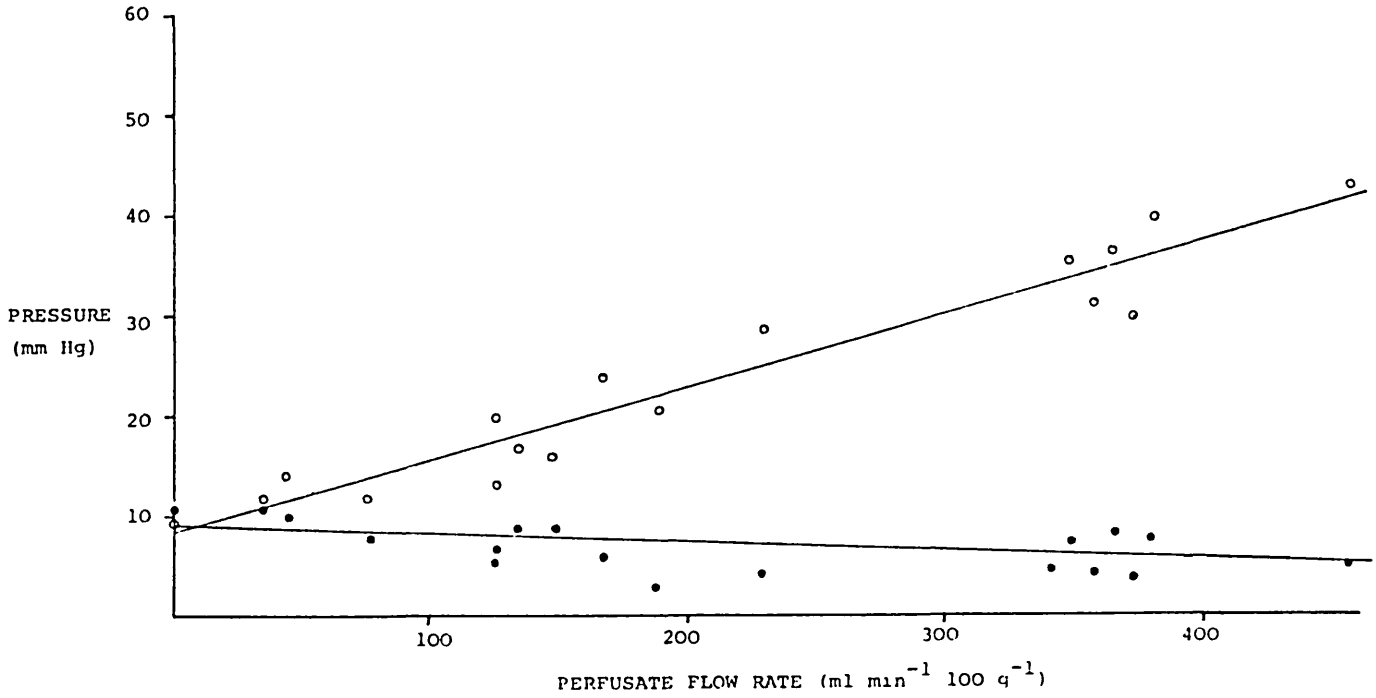


FIGURE 4.2. Determination of pre- and post-capillary resistances. Arterial and venous pressures were changed with the gland maintained in the isogravimetric state. The pairs of arterial (o) and venous (●) pressures were plotted against flow rate and the lines extrapolated to zero flow. The zero flow intercept is the isogravimetric capillary pressure, and the ratio of the slopes of the 'arterial' and'venous' lines is the pre- to post-capillary resistance ratio.

value of 8 mm Hg. Whilst in a number of experiments the "arterial" and"venous" lines did coincide at zero flow, thiswas not always the case; the mean discrepancy between isogravimetric capillary pressure measured by the arterial and venous pressure-flow relationships was 3.9 ± 0.56 mm Hg (n = 26). This problem has been noted previously, and may be a consequence of non-linear pressure-flow relationships at very low pressures. In experiments where differences in the intercepts did occur, the venous pressure intercept was taken as the capillary pressure for the purposes of calculations.

When venous pressure is raised by a known amount, capillary pressure changes by an amount related to the change in venous pressure and the pre- to post-capillary resistance ratio. Following the analysis of Pappenheimer and Soto-Rivera (1948), mean capillary pressure $\bar{P}^{cap}$ is given by

$$\bar{P}^{cap} = \frac{RP^{ven} + P^{art}}{1 + R} \qquad 4.1$$

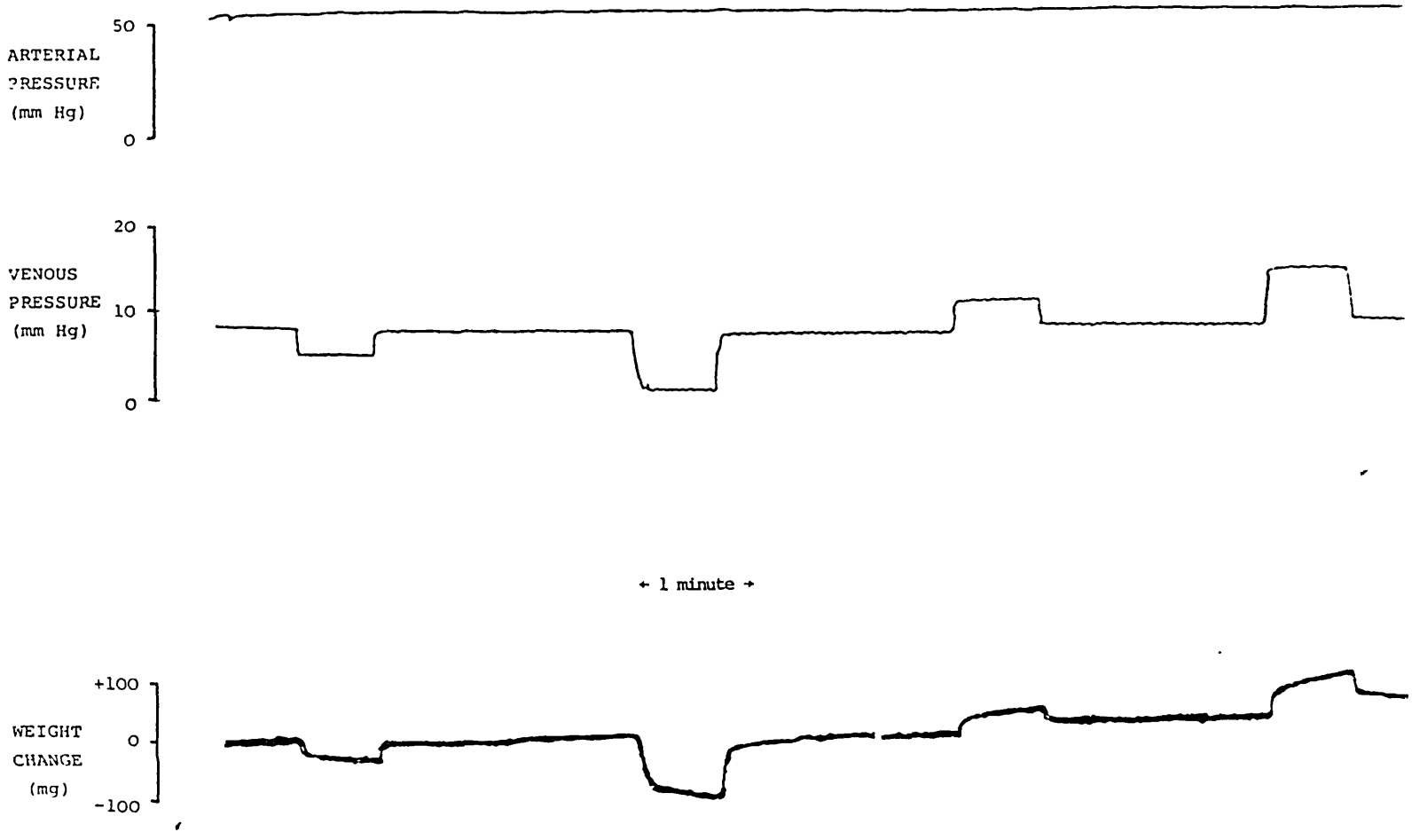
where R is the pre- to post-capillary resistance ratio, and P^{art} and P^{ven} are respectively arterial and venous perfusion pressures. Assuming that R remains constant whatever the arterial and venous pressures, a change in venous pressure, ΔP^{ven}, will cause a corresponding change, $\Delta\bar{P}^{cap}$, in mean capillary pressure, given by

$$\Delta\bar{P}^{cap} = \frac{R.\Delta P^{ven}}{1 + R} \qquad 4.2$$

The rise in venous pressure led to a two-phase increase in tissue weight, as shown in Fig. 4.3. The initial rapid weight gain is generally assumed to be the consequence of vascular compliance whilst the slower phase is attributed to capillary filtration (Richardson, Granger and Taylor, 1979). The slope of the slow phase is equal to the rate of fluid filtration (J_v^{cap}) and when this is plotted against the calculated change in mean capillary pressure, the resulting line has a slope equal to K_f. Fig. 4.4 shows such a plot for a single gland.

Inspection of Fig. 4.3 reveals an interesting phenomenon. When venous pressure is returned to its original value after a period of elevation, the rate of decline of tissue weight was slower than was the rate of increase on venous pressure elevation. This situation was mirrored when the venous pressure was first lowered and then raised back to the original level. The estimate of K_f is thus lower when fluid is being reabsorbed into the vasculature than during fluid filtration into the interstitium.

Table 4.1 summarizes the values obtained for pre- and post-capillary resistances and K_f in the gland perfused with 6% Krebs-albumin solution.


50
ARTERIAL
PRESSURE
(mm Hg)
0
20
VENOUS
PRESSURE
(mm Hg)
10
0
← 1 minute →
+100
WEIGHT
CHANGE
(mg)
0
-100

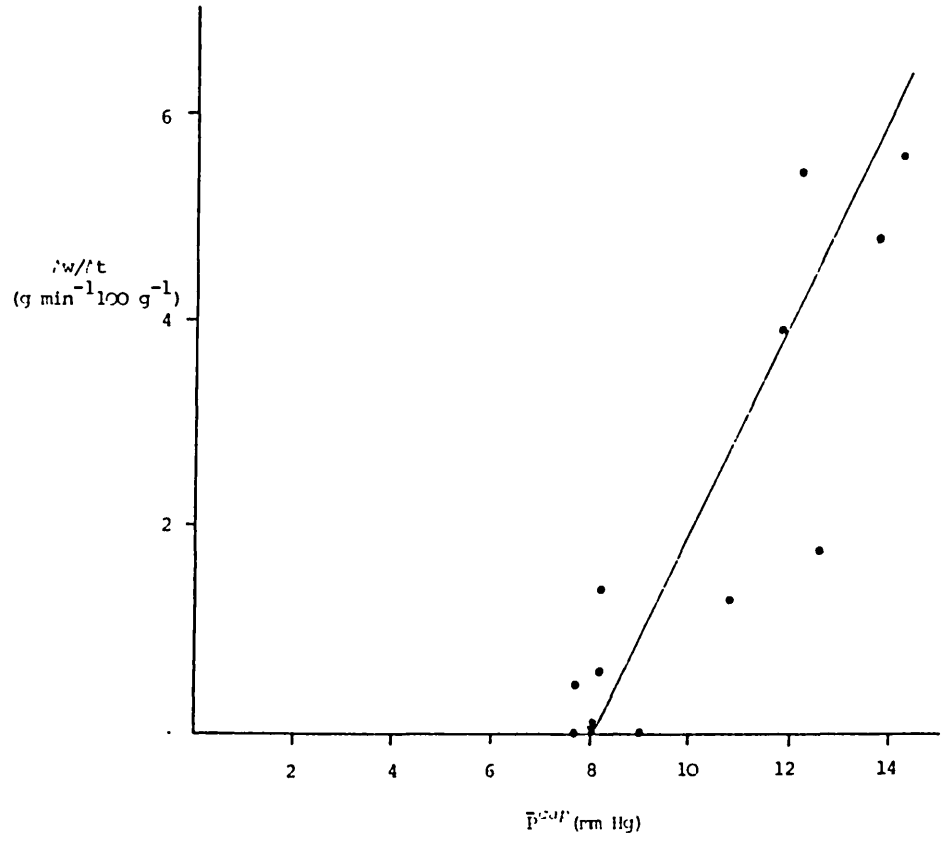


FIGURE 4.4. Plot of J_v^{cap} (taken to be the slope of the slow component of weight change in a record such as that depicted in Fig. 4.3.).against the mean capillary pressure. The slope of the line is equal to K_f

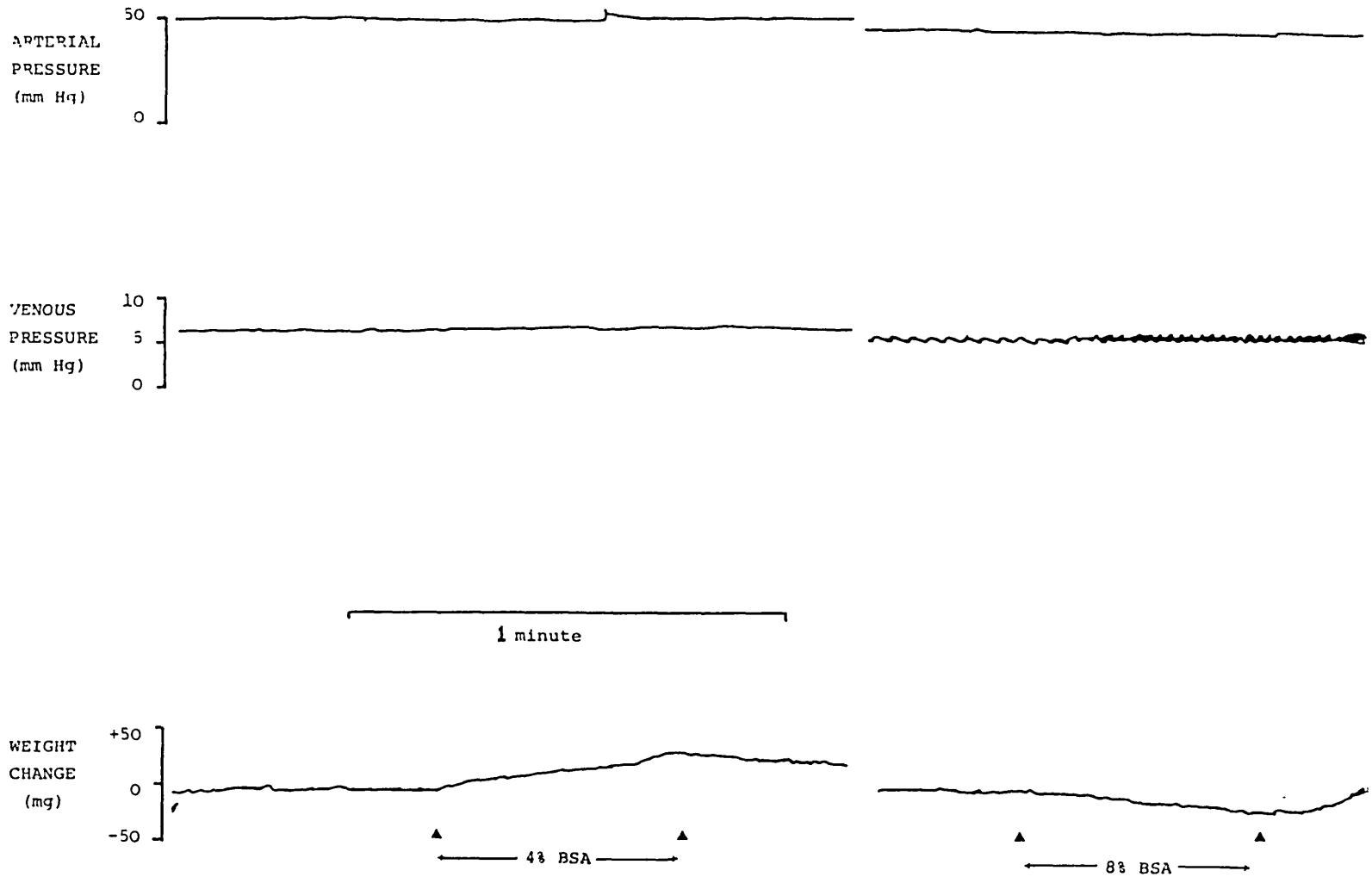
4.3.2. Reflexion Coefficient of Albumin

Fig. 4.5 illustrates the change in weight produced in one gland by an increase and a decrease in the albumin concentration of the perfusate (initial phase) and Fig. 4.6 shows the relationship between the change in perfusate colloid osmotic pressure (π^{cap}) and the initial fluid flux (J_v^{cap}) in that experiment. The slope of the resulting line is equal to $K_f\sigma_{alb}^{cap}$ from which σ_{alb}^{cap} can be calculated if K_f is known.

It was interesting to note that when perfusate with a low albumin concentration was replaced by the original perfusate containing 6 g 100 ml^{-1} albumin (return phase) the rate of weight loss was slower than the rate of weight gain when the low albumin perfusate was introduced. This phenomenon was mirrored when the test perfusate contained a higher albumin concentration than the control perfusate. However, whether the initial change in perfusate composition was to a high or to a low albumin concentration, the value for $K_f\sigma_{alb}^{cap}$ determined from the initial response was the same.

Thus for changes in both hydrostatic and colloid osmotic pressure, the measured rate of weight change for the return phase of the transient was different from that for the initial phase, and it appeared that fluid efflux from the vasculature was always faster than fluid influx. As indicated in Chapter 3, larger readjustments of tissue forces occur when the interstitium is losing fluid, and so the value of K_f will depend upon the direction of

FIGURE 4.5. Tracings of experimental record showing changes in gland weight produced by elevation (right hand trace) or depression (left hand trace) of perfusate albumin concentration. Note that both arterial and venous pressure remain constant, and the rate of weight change falls with time.


50
ARTERIAL
PRESSURE
(mm Hg)
0
10
VENOUS
PRESSURE
(mm Hg)
5
0
1 minute
+50
WEIGHT
CHANGE
(mg)
0
-50
4% BSA
8% BSA

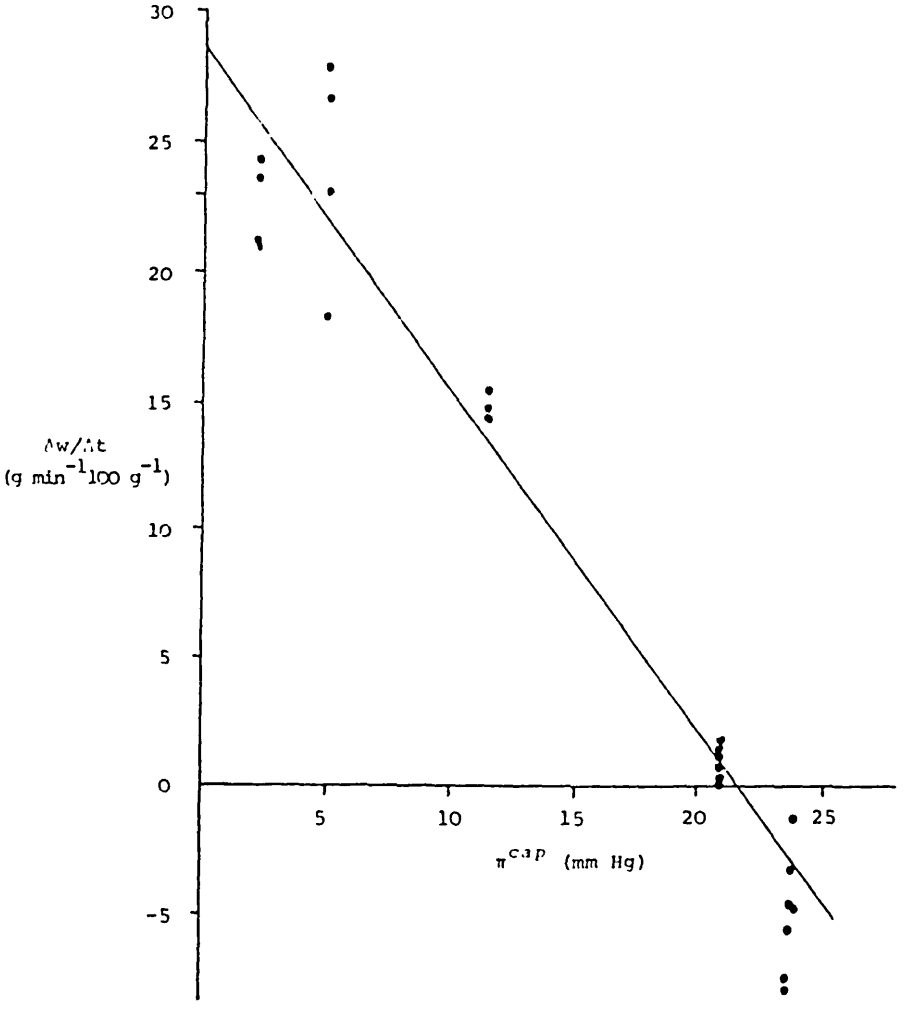


FIGURE 4.6. Plot of J_v^{cap} (taken as the slope of the initial 5 seconds of the weight vs time record) versus perfusate colloid osmotic pressure. The slope of the line is equal to $K_f\sigma_{alb}^{cap}$

fluid flux at the time of measurement of the slopes. For this reason, all comparisons between K_f and $K_f\sigma_{alb}^{cap}$ were made in seven experiments in which the glands were subjected to increases and decreases in both hydrostatic and osmotic pressures.

If the value of K_f measured by venous pressure elevation is a true representation of the filtration coefficient and the value $K_f\sigma_{alb}^{cap}$ is an accurate estimate of the changes produced during albumin osmotic transients, then σ_{alb}^{cap} may be obtained by dividing $K_f\sigma_{alb}^{cap}$ derived from osmotic transients by K_f derived from venous pressure elevations. From 13 experiments on albumin-perfused glands, a value of 1.123 ± 0.093 ml $min^{-1}100\ g^{-1}mm^{-1}$ Hg was obtained. The mean value is not significantly different from unity, but the fact that in some cases σ_{alb}^{cap} was estimated at greater than unity suggests either that $K_f\sigma_{alb}^{cap}$ was overestimated or that K_f was underestimated (or both).

In the experiments where K_f was determined by alterations in venous pressure, changes in weight due to vascular compliance made it impossible to make any assessment of transcapillary fluid flux until 12-24 seconds after the change in venous pressure (Fig. 4.3). On changing the intravascular colloid osmotic pressure (Fig. 4.5), there was a similar initial phase of rapid weight change followed by a slower phase, despite the fact that the osmotic transient is not influenced by vascular compliance effects.

The estimates of σ_{alb}^{cap} were originally made by taking the initial fast phase of the osmotic transient to determine $K_f\sigma_{alb}^{cap}$ (now designated $K_f\sigma_{alb}^{cap}(f)$) ; if, however, the slope was drawn 12-24 seconds after the initial osmotic pressure change, a lower value of $K_f\sigma_{alb}^{cap}$ was found (designated $K_f\sigma_{alb}^{cap}$ (s)). In 13 experiments, $K_f\sigma_{alb}^{cap}(s)$ was found to be 0.819 ± 0.098 ml min^{-1} 100 $g^{-1}mm^{-1}$Hg, which was significantly smaller than the value of $K_f\sigma_{alb}^{cap}(f)$ of 1.11 ± 0.102 (n = 13) ml min^{-1} 100 $g^{-1}mm^{-1}$Hg. Using $K_f\sigma_{alb}^{cap}$ (s) gave a value for σ_{alb}^{cap} (designated σ_{alb}^{cap} (s)) of 0.786 ± 0.041. The value of K_f which might have been obtained in the absence of a compliance component may be calculated from $K_f\sigma_{alb}^{cap}$ (s)/σ_{alb}^{cap} (s) and this procedure gives a value of 1.354 ± 0.136 ml min^{-1} 100 $g^{-1}mm^{-1}$Hg, indicating that the value of K_f determined by changing venous pressure is about 30% lower than the value that would have been obtained without the compliance component (Table 4.2).

Preliminary experiments designed to differentiate between the compliance and filtration components of gland weight change obtained immediately following a change in venous pressure have been performed in this laboratory. They indicate that there is indeed a rapid phase of filtration which is ordinarily swamped by the compliance effects.

	1	2	3	4	5	6
	K_f	$K_f\sigma_{alb}^{cap}(f)$	$\sigma_{alb}^{cap}(f)$	$K_f\sigma_{alb}^{cap}(s)$	$\sigma_{alb}^{cap}(s)$	K_f
Mean	1.020	1.117	1.123	0.819	0.786	1.354
SEM	0.087	0.102	0.093	0.098	0.041	0.136
n	13	13	13	13	13	13

TABLE 4.2. Filtration and albumin reflexion coefficients determined from the fast and slow components of the albumin osmotic transient records.

Column 1. venous pressure elevation
2. fast component of the albumin transient
3. $K_f\sigma_{alb}^{cap}(f)/K_f$
4. slow component of the albumin transient
5. $K_f\sigma_{alb}^{cap}(S)/K_f$
6. $K_f\sigma_{alb}^{cap}(f)/K_f$

Note that the figures in columns 3, 5 and 6 are not the same as those found by dividing the mean values from the other relevant columns. This is because the relevant ratio was obtained in each experiment, and the figures presented are the mean ratios (and not ratios of the means).

4.3.3. Reflexion Coefficients of Inulin and Raffinose

These solutes were investigated by introducing them into a perfusate previously lacking the solute, in a manner similar to that employed by Vargas and Johnson (1964, 1967). As discussed in Chapter 3 of this thesis, the high permeability of these solutes in the submandibular gland means that the transcapillary concentration difference will not be equal to the perfusate concentration, even at early times, and so calculating σ^{cap}_{test} using the initial slope of the weight vs time curve will lead to serious underestimation of the true values.

Fig. 4.7 illustrates how use of the osmotic transient model described in Chapter 3 may be used to provide a better estimate of σ^{cap}_{inulin}. In the experiment shown in Fig. 4.7, 6 mM inulin was used as the test solute. In the same gland, K_f had previously been estimated as 0.95 min^{-1} 100 $g^{-1}mm^{-1}$ Hg. Using the initial slope of the weight vs time curve, σ^{cap}_{inulin} was estimated at 0.13. When these values of K_f and σ^{cap}_{inulin} are inserted into the model, with PS^{cap}_{inulin} = 1.5 ml $min^{-1}g^{-1}$ and K_{cell} = 0.02 ml min^{-1} 100 $g^{-1}mm^{-1}$ Hg, it is clear that σ^{cap}_{inulin} = 0.13 will not fit the whole curve. The rate of weight loss predicted by this value of σ^{cap}_{inulin} rapidly diminishes and so the total weight loss is far less than is actually observed. Fig. 4.7 also shows the result of putting σ^{cap}_{inulin} = 0.35 into the model; a much closer fit to the experimental data is found.

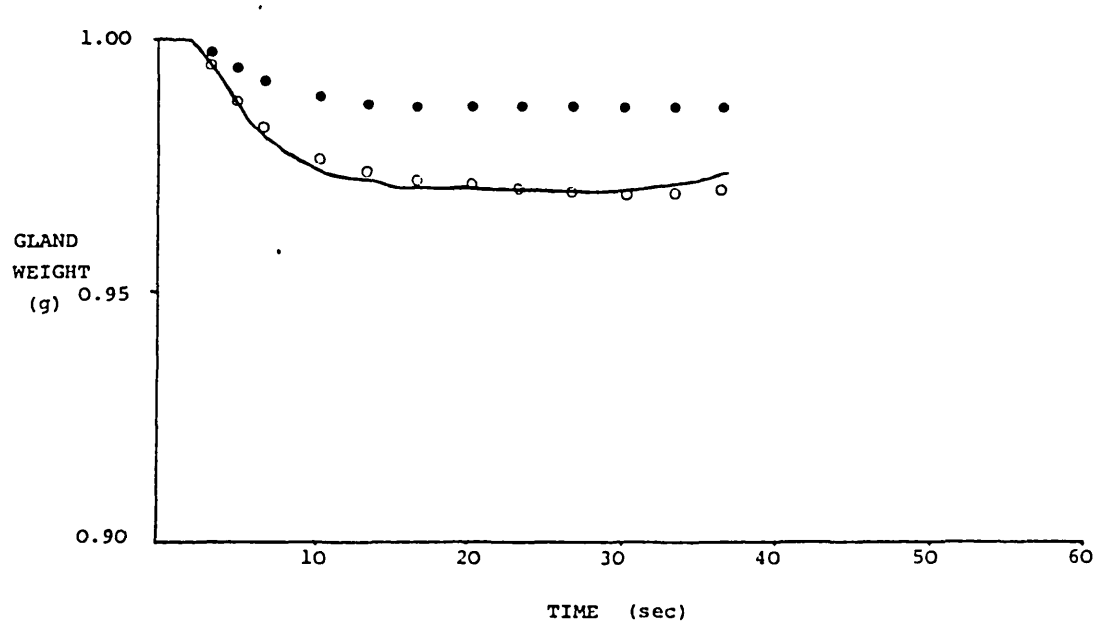


FIGURE 4.7. Tracing of weight record of a 6 mM inulin osmotic transient. The experimental record is shown as the solid line. Also shown are the predictions of the osmotic transient model when

1. σ^{cap}_{inulin} is taken as 0.13, the value obtained by taking the initial slope of the weight vs time record (●).
2. σ^{cap}_{inulin} = 0.35 (o).

Note that the 'initial slope' method seriously underestimates σ^{cap}_{inulin}.

In 5 experiments, σ^{cap}_{inulin} calculated by the initial slope method was found to be 0.134 ± 0.022. Using the model and the values given in Chapter 3 for the appropriate parameters, σ^{cap}_{inulin} was found to lie between 0.30 and 0.40 in these 5 experiments. It is not possible to give an exact mean and SEM for the model fits because

a) slight changes in the model parameters could cause changes in the value of σ^{cap}_{alb} required to give a reasonable fit.

b) the fits were judged by eye and only intervals of 0.01 in σ^{cap}_{inulin} were used.

When raffinose is used as the test solute, the situation is even less clear than in the case of inulin. Fig. 4.8 illustrates an osmotic transient using approximately 80 mM raffinose as the test solute. The crystalloid osmotic pressure of such a solution is over 1300 mm Hg and might be expected to have effects on capillary permeability, which would affect the estimation of its reflexion coefficient (see Discussion, Section 4.4.4). Even if this were not the case, it is still no easy matter to fit the experimental data by a single value of σ^{cap}_{raff}. Fig. 4.8 illustrates clearly that the value of σ^{cap}_{raff} estimated by the initial slope method (0.007) will not fit the experimental data when inserted into the model. Fig. 4.9 shows that widely differing values of σ^{cap}_{raff} can be made to fit the data, depending upon the values taken for the other parameters in the model.

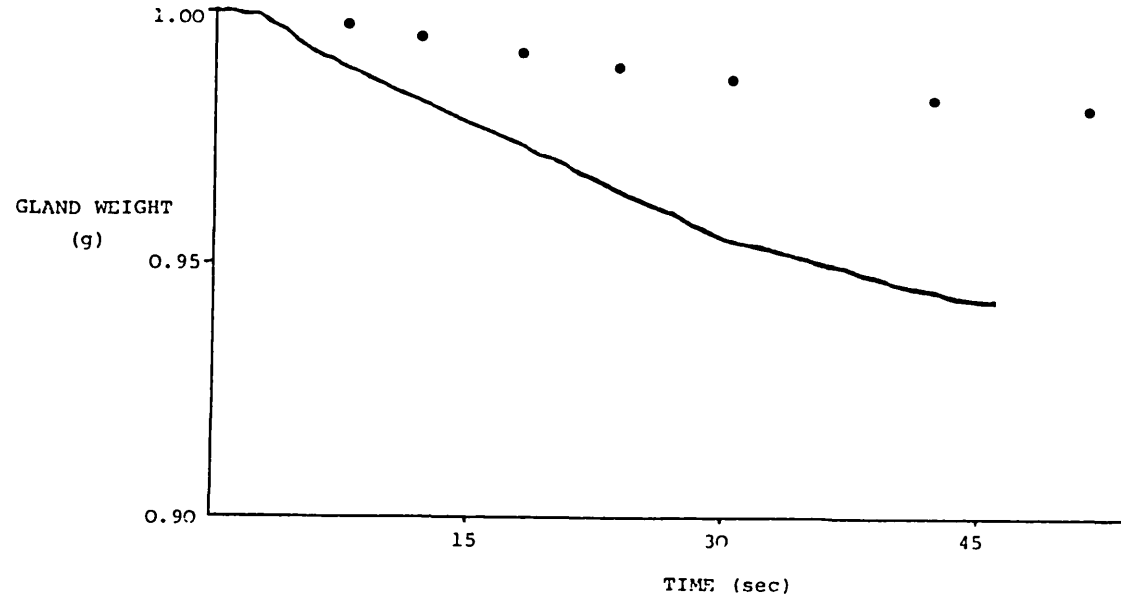


FIGURE 4.8. Tracing of weight record of an 80 mM raffinose osmotic transient. The experimental record is shown as the solid line. Also shown are the predictions of the osmotic transient model when σ_{raff}^{cap} = 0.007, the value obtained by taking the initial slope of the weight vs time record.

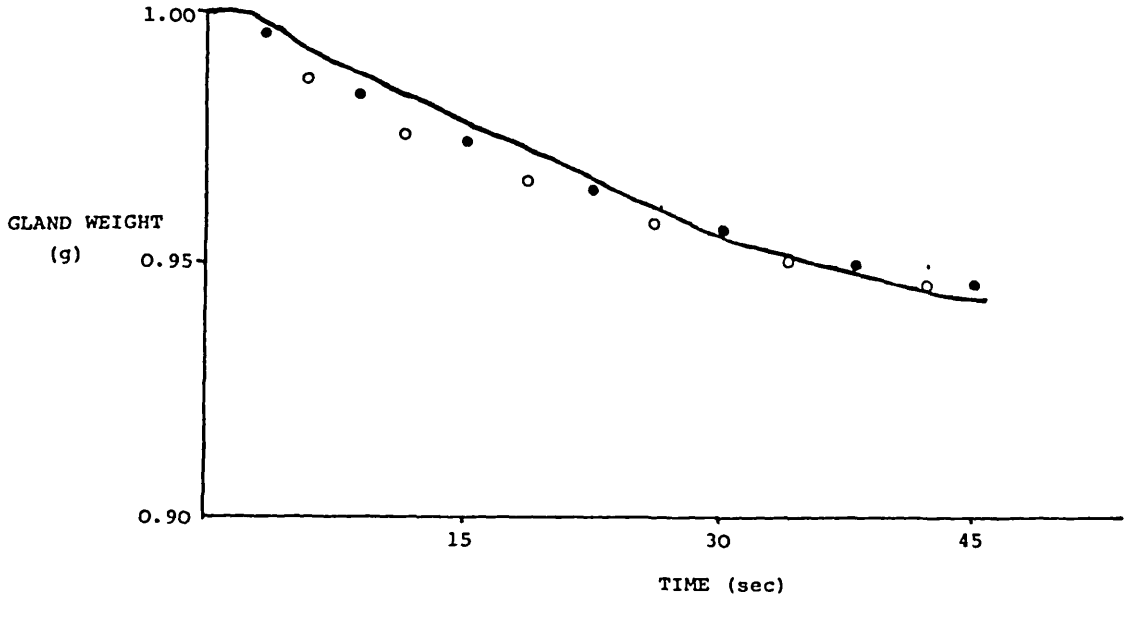


FIGURE 4.9. Same experimental record as in Fig. 4.8. Predictions of the osmotic transient model when various parameters are changed.

K_{cell} ml min^{-1} 100 g^{-1} mm^{-1} Hg	$PS^{cap.}_{raff}$ ml min^{-1} g^{-1}	σ^{cap}_{raff}	
0.02	8	0.15	(o)
0.2	15	0.2	(●)

There is little to be gained from trying to obtain an exact fit to the experimental data, given the uncertainty in the values of parameters such as K_{cell}, PS_{alb}^{cap}, and even K_f. What is clear, however, is that the actual value of σ_{raff}^{cap} is far higher than 0.007, and is probably at least one order of magnitude higher than this.

4.4. Discussion

4.4.1. Capillary Filtration Coefficients

The value of approximately 1 ml min^{-1} 100 g^{-1} $mm^{-1}Hg$ confirms the relatively high hydraulic conductivity expected in fenestrated capillaries and found in other organs with this type of endothelium. The experimental data confirm some of the model predictions, especially the underestimation of K_f produced by taking the slope of the weight vs time curve after the vascular compliance effect has ended. The magnitude of the error is not very different from that predicted by the model with the particular values of interstitial compliance and interstitial albumin concentration and volume of distribution used in Chapter 3. While this does not necessarily justify the use of those values, it does support the general concept that tissue readjustments occur rapidly.

Johnson and Hanson (1963) and Johnson and Richardson (1974) found that an isogravimetric state could be obtained in the dog intestine at different levels of venous pressure; and they attributed this finding particularly to a decrease in interstitial albumin concentration, as well as to an increase in lymph flow and tissue hydrostatic pressure when venous pressure was elevated. In the present experiments, elevation of venous pressure was not continued long enough for re-establishment of isogravimetric conditions at the higher pressure, and it was difficult to detect a continuously decreasing rate of weight gain.

Johnson and Hanson (1966) and Mortillaro and Taylor (1976) found that capillary filtration coefficient varied with the extent of venous pressure elevation. Granger, Richardson and Taylor (1979) used four different methods of determining K_f in the same preparation and found reasonable agreement between the methods with venous pressure elevations of up to 10 mm Hg. They also found that elevations of venous pressure of 10 mm Hg or less gave higher estimates of K_f than did larger elevations. Readjustment of tissue forces was discounted as an explanation for this finding since the authors reasoned that "the 'zero time extrapolation' method, which should theoretically, eliminate this problem, showed the same trend as each of the other methods." However, as mentioned in Chapter 3, the early part of the log J_v^{cap} vs time may not lie on the same straight line as the later part, and this is the portion of the curve which is likely to be most affected by rapid adjustments in tissue forces.

One possible way of overcoming the problem of changes in tissue forces is by the use of an albumin osmotic transient. Osmotic transients are not affected by compliance effects if the tissue is vasodilated (otherwise osmotic dilatation may occur) and so estimates of J_v^{cap} may be made very early in the transient. If the change in colloid osmotic pressure of the perfusate is comparable to the change in capillary pressure produced during a venous pressure elevation, then the time course

of tissue force readjustments should be similar in the two situations. It is thus reasonable to estimate the slope of the weight vs time curve for each type of transient at the same time after the beginning of the manoeuvre. The disadvantage of this method is that if $\sigma_{alb}^{cap} \neq 1$, then convective flux of albumin across the capillary will cause differences in the interstitial albumin concentration in the two situations, because the intracapillary albumin concentrations are different. However, since PS_{alb}^{cap} is very low and σ_{alb}^{cap} is high, the problem is not likely to be serious.

4.4.2. Apparent Rectification of Volume Flux

It was noted in Section 4.3.1. that J_v^{cap} was greater on elevating venous pressure than on its subsequent return to the control level; a similar phenomenon was noted for the albumin osmotic transients. However, it was also noted that the magnitude of the initial phase for an elevation of hydrostatic or osmotic pressure was similar to the initial phase produced by a decrease of pressure by the same amount.

The reason for these findings is not clear. If there were no readjustments in interstitial forces, then when intracapillary hydrostatic or osmotic pressure is returned from an altered level to its control value, the gland would remain at the weight that existed at the moment when the pressure was returned, ie the return value

of J_v^{cap} would be zero. It is relatively easy to explain why elevation of pressure should cause a greater J_v^{cap} than the subsequent return; changes in tissue forces are less than the change in applied pressure. In fact, if this is the correct explanation, it should be possible to estimate the amount of interstitial readjustment by comparing the return J_v^{cap} with the initial J_v^{cap} produced by a known change in capillary pressure.

Fig. 4.10 illustrates this point using the model developed in Chapter 3. Fig 4.10 shows the predictions of the model with a venous pressure elevation of 10 mm Hg, leading to a rise of 4.5 mm Hg in capillary pressure. The weight change is less than expected,for a filtration coefficient of 1 ml min^{-1} 100 g^{-1} mm^{-1} Hg, and would lead to an established K_f of 0.8 ml min^{-1} 100 g^{-1} mm^{-1} Hg. On return of venous pressure to control values, the slope of the weight vs time relationship is much less than that of the filtration phase. The ratio J_v^{cap} (filtration)/ J_v^{cap}(reabsorption) in this instance is approximately 5.5; the sum of the increases in interstitial hydrostatic and osmotic pressures during the filtration phase is approximately 0.8 mm Hg, which would just account for the return slope.

It is more difficult to explain why an initial decrease in pressure should cause a <u>greater</u> return J_v^{cap} than the initial value. If tissue force readjustments were the explanation, then they would have to be greater than

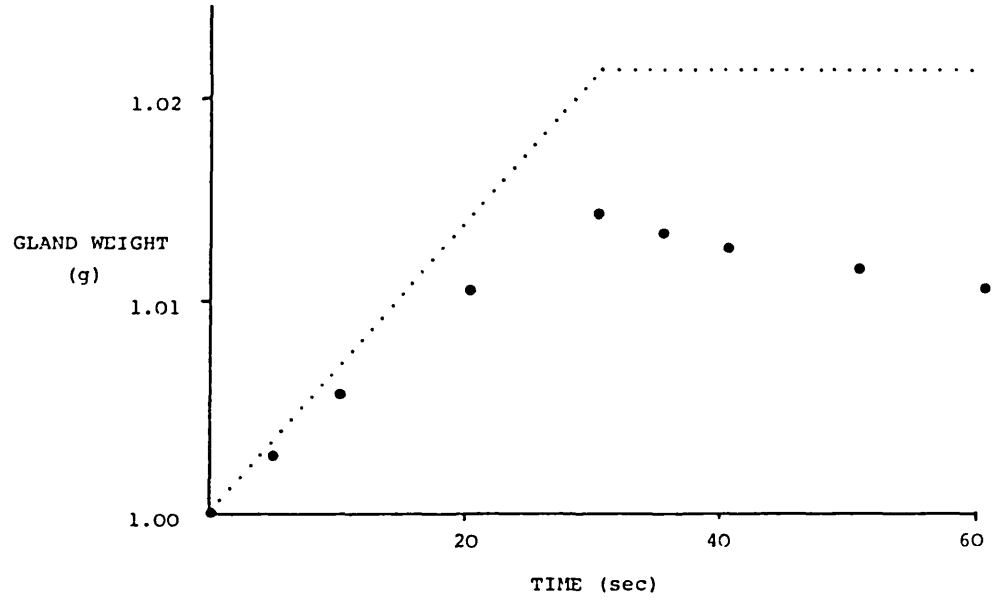


FIGURE 4.10. Predictions of the model (●) simulating the initial and return phases of a venous pressure elevation. Note that the return slope is much smaller than the initial slope, ie 'apparent rectification' is present. The dotted line shows the relationship expected if no counterbalancing forces were present; in this case there is no return phase.

the applied change in pressure. This would lead to a return of gland weight towards the original value even though intracapillary pressure was still lowered; none of the glands showed such a tendency.

In the model and the discussion so far, little account was taken of compliance effects except to emphasize the rapid fall in J_v^{cap} which occurred while the change in weight due to compliance was dominating the transient. In single venules of the rat mesentery, Swayne (unpublished results) found that the time course of the change in radius in response to a step pressure increase was faster than that found when the pressure was returned to the original level. It was also found that the difference in time courses was greater when smaller initial pressures were used. This latter finding appeared to be due to non-linearity and hysteresis in the stress-strain relationship of the vessels 15 seconds after the change in pressure. Swayne found that when capillary pressure was increased, over 80% of the total increase in vessel radius was complete in 2 seconds and over 95% complete in 10 seconds. In contrast, a step decrease in capillary pressure produced a change in radius which was only about 70% complete in 2 seconds and 85% complete in 10 seconds, there was then an approximately linear fall in radius between 10 and 30 seconds. These findings would suggest that vascular compliance could be a contributing factor to the venous pressure responses. It is thus important to determine how much of the weight change in the whole

gland is caused by compliance; however, this is difficult to do so experimentally. The gland has to be perfused with a fluid (usually silicone oil) which is immiscible with water, and differences in surface tension and viscosity of this fluid from that used in filtration experiments make comparisons between the two situations very uncertain. In some preliminary experiments, Gamble (unpublished results) has found that the initial 'fast' phase of weight change in response to venous pressure elevation appears to be smaller when perfusing with a silicone oil than when Krebs albumin is used, but it still is not clear whether there is hysteresis in the pressure-volume relationship in the whole gland.

Clearly, the apparent rectification of volume flux found during the albumin osmotic transients cannot be explained in terms of compliance effects. The arguments presented above for tissue force readjustments are also unlikely to explain why the return phase of an initial increase in intracapillary albumin concentration is faster than the initial phase. Rectification of volume (and solute) flux may occur in an assymmetrical double-membrane system, as described in detail by Kedem and Katchalsky (1963) and Patlak et al (1963). In this system, two membranes with different permeability characteristics are arranged in series, being separated by a central fluid compartment. When volume flux occurs, the solute concentration in the central compartment changes according to

the direction of volume flux and the relative permeabilities of the two membranes. This accumulation or depletion of solute leads to rectification of volume flux (see House, 1974, pp 70-76 and 148-151) If the capillary wall is considered to be analogous to this model, then the capillary endothelium (together with any endocapillary layer) might form one membrane and the basement membrane the other. Rectification of volume flux would be in the same direction as that observed experimentally if the basement membrane were less permeable than the endothelial layer.

The equations developed by Kedem and Katchalsky (1963) and Patlak et al (1963) apply to steady state volume flux, ie after the solute has accumulated or been depleted in the central compartment. Presumably the initial volume flux should be symmetrical with respect to transmembrane pressure differences, and this is what is found experimentally.

4.4.3. Reflexion Coefficient of Albumin

It was implied in Section 4.3.3. that there is uncertainty in the determination of σ_{alb}^{cap}. Taking the slope of the 'slow' phase of the weight vs time curve of an albumin transient yields a reflexion coefficient significantly less than that obtained by taking the 'fast' slope, but both values could be underestimates. If vascular

compliance contributes to the weight gain used for determining K_f during venous pressure elevation, then K_f will be overestimated. Vascular compliance is probably the most important factor causing uncertainty in K_f and reflexion coefficient determinations.

The capillary reflexion coefficient of albumin measured in the present experiments can thus be taken to be at least 0.8. This compares well with the minimum value of 0.75 found by Koo et al (1980) in the cat submandibular gland but is much lower than the value found in Chapter 2 of this thesis. The obvious differences between the experiments described in this Chapter and those in Chapter 2 are the amount of dissection and handling of the gland and the absence of blood in the perfusate of the isolated glands. Brace and Guyton (1967) found that isogravimetric capillary pressure in the isolated blood-perfused dog hindlimb was much lower when the limb was rapidly isolated than when a "previous isolation procedure" was used. Watson (1983) found that filtration coefficient in the cat hindlimb was doubled when a blood-free protein perfusate was used. Parker, Granger and Taylor (1981) found that capillary filtration coefficient in isolated, blood-perfused dog lungs was higher during alveolar hypoxia and concluded that this was "probably associated with changes

in vascular permeability rather than an increased surface area of the fluid exchange vessels." The effect of the isolation procedure on salivary gland permeability has not been investigated but is clearly of relevance in view of the discrepancy in estimates of σ_{alb}^{cap} by the two methods.

4.4.4. Reflexion Coefficients of Inulin and Raffinose

There have been very few measurements of small solute reflexion coefficients in organs with fenestrated capillaries. Granger, Granger, Brace, Parker and Taylor (1979) used an osmotic transient method to estimate reflexion coefficients of NaCl, urea, glucose, mannitol and maltose in the cat ileum, and estimated reflexion coefficients of less that 0.002 for the largest molecule used (maltose - molecular radius 0.52 nm). However, in the same preparation, they found a filtration coefficient of only 0.1 - 0.2 ml min^{-1} 100 $g^{-1}{}_{mm}{}^{-1}{}_{Hg}$ and a protein reflexion coefficient (using lymph/plasma protein concentration ratios) of 0.90. Granger et al (1979) found a large discrepancy between estimates of pore radii obtained from the osmotic transient studies and those obtained from the lymph analysis studies. Of the possible explanations for the discrepancy, three are of major importance in the work of Granger et al (1979) and in the present study. These are:

1. Errors in estimating K_f
2. Overestimation of $(\pi_{test}^{cap} - \pi_{test}^{int})$

3. Osmotically induced changes in capillary permeability.

The first two factors have been discussed in detail in Chapters 3 and 4 of this thesis, and may be corrected by using a suitable model and from vascular compliance measurements. The third factor is much more difficult to analyse. Evidence that the high osmolality used in the osmotic transient experiments does increase capillary permeability comes from both theoretical and experimental considerations. The test perfusate used by Granger and et al (1979) had osmolalities which were 40 - 175 mOsm ℓ^{-1} higher than that of the control blood perfusate. In the present experiments, the inulin concentrations were between 2.5 and 10 mmol ℓ^{-1} and the raffinose concentrations were between 30 and 120 mmol ℓ^{-1}. If the cellular hydraulic conductivity is taken as 2×10^{-2} ml min^{-1} 100 g^{-1} $mm^{-1}Hg$, and the intracellular volume 50 ml 100 g^{-1} in both series of experiments, then it is possible to make a crude estimate of the loss of cellular volume caused by the test solutes. For inulin in the rabbit submandibular gland the highest concentration used would produce a transcellular water flux of 3.4 ml min^{-1} 100 g^{-1}; thus the cells would lose approximately 6% of their volume during the course of a 1 minute transient. With even the lowest concentration of raffinose used, the cells would lose 20% of their volume, and with the maximum concentration of test solute employed by Granger et al (1979), the cells would lose all their water in under one minute! Clearly, the situation

is not as simple as this rough calculation implies, but the point is made that large volume reductions may occur in the cells, including the capillary endothelial cells. This could cause widening of endothelial cell junctions and possible distortion of the capillary wall, either of which might produce an increase in permeability.

Experimental evidence for the concept of osmotically induced changes in capillary permeability comes from the same paper of Granger et al (1979). The reflexion coefficient of plasma proteins under control conditions was found to lie between 0.87 and 0.92; when an osmotic transient was being performed at the same time, the protein reflexion coefficient fell to between 0.56 and 0.74. However, the equivalent pore radii calculated from even the lowest value of σ_{prot}^{cap} were far smaller than those predicted from the small solute reflexion coefficients suggesting that the discrepancy between the two sets of data could not be totally explained by an increased permeability.

4.4.5. Transport Pathways across Capillary Endothelium in the Submandibular Gland; Equivalent Pores and Fibre Matrix

Since the development of the concept of restricted diffusion by Pappenheimer et al (1951), a number of models have been established to account for experimentally

determined membrane coefficients in terms of transport pathways.

Drake and David (1978) have used an equation based on that developed by Levitt (1975) to estimate reflexion coefficients from the ratio of solute radius to pore radius (a/r)

$$\sigma = 16/3\ (a/r)^2 - 20/3\ (a/r)^3 + 7/3\ (a/r)^4 \qquad 4.3$$

Fig 4.11 shows the reflexion coefficient calculated from this equation plotted against molecular radius for a range of pore radii; the reflexion coefficients found in the present studies would appear to be reasonably well fitted by a pore radius of between 4 and 6 nm, even allowing for the difference in σ_{alb}^{cap} estimates found in Chapters 2 and 4.

The fibre matrix equation of Curry and Michel (1980) may be used to calculate the reflexion coefficient of a molecule of given molecular radius. Figs. 4.13 and 4.14 show the effects of varying the properties of a fibre matrix on the predictions of reflexion coefficient; the experimental data may be fitted by a fibre radius of approximately 0.5 nm and an aqueous volume of 0.91 - 0.95

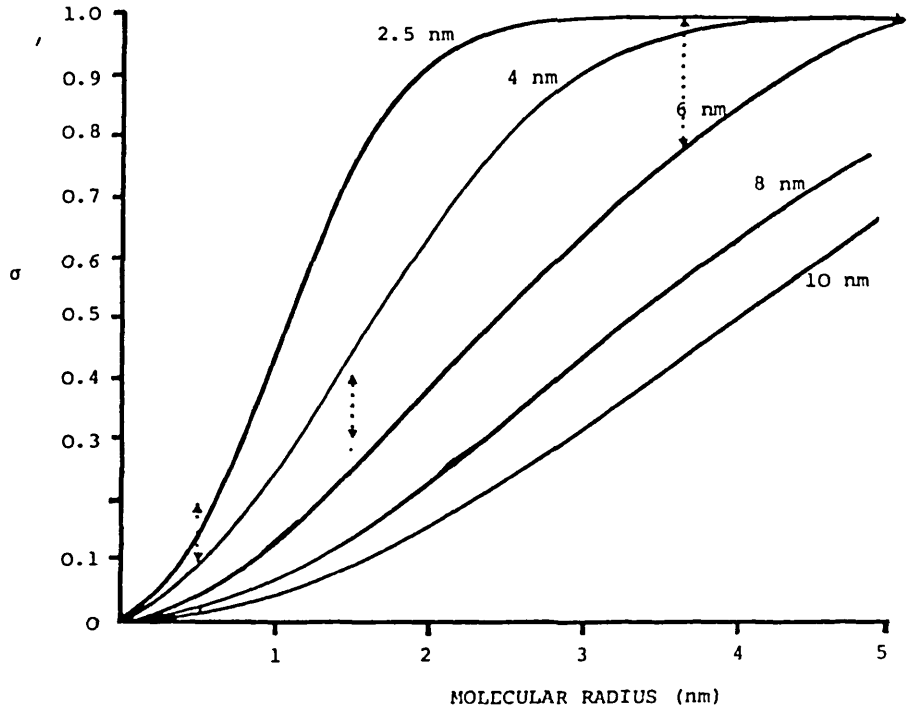


FIGURE 4.11. Theoretical relationship between solute reflexion coefficient and molecular radius according to the expression of Drake and David (1978) - Eqn. 4.3. The experimental data (▲) are superimposed on the theoretical lines. The uncertainty in estimating the reflexion coefficients is shown by the length of the dotted line for each molecule.

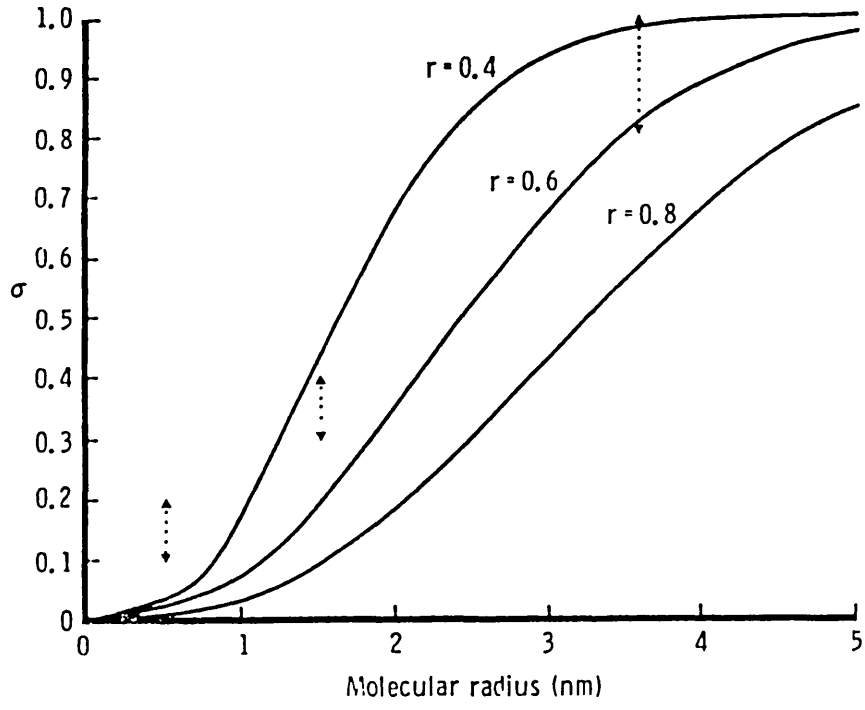


FIGURE 4.12. Theoretical relationship between solute reflexion coefficient and molecular radius for a fibre matrix, according to the equations of Curry and Michel (1980) and Curry and Huxley (1982). Effect of changing fibre radius (r_f). The experimental data (▲) are superimposed on the theoretical lines.

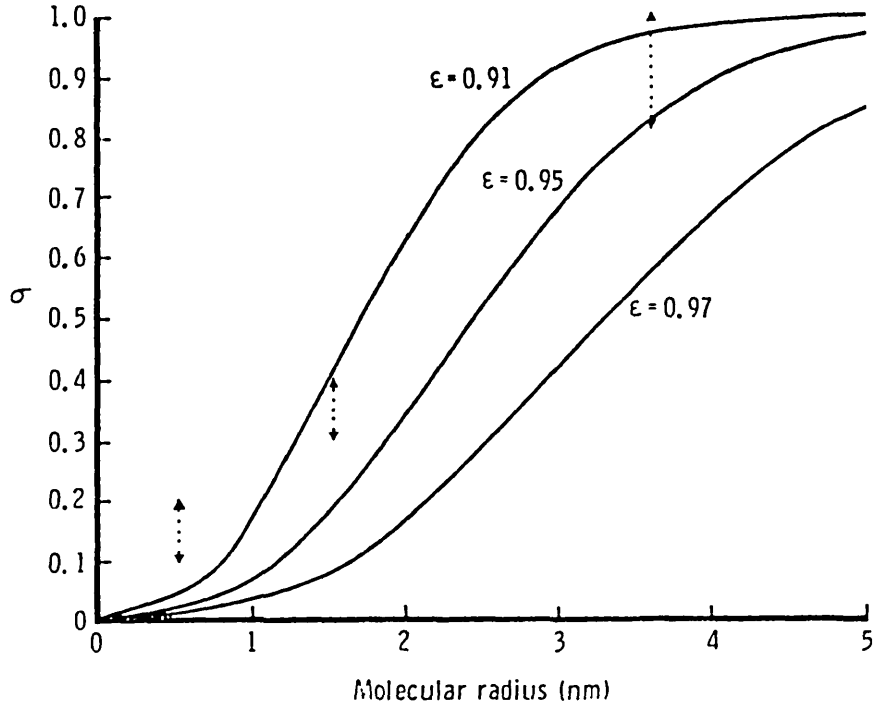


FIGURE 4.13. Theoretical relationship between solute reflexion coefficient and molecular radius for a fibre matrix. Effect of changing aqueous volume (ε). The experimental data (▲) are superimposed on the theoretical lines.

Is there any way of distinguishing which analysis is the correct one? Curry and Huxley (1982) have compared the pore and fibre matrix models using filtration, permeability and reflexion coefficients in whole organs and single capillaries. They define a quantity termed the specific hydraulic conductivity, which calculated as $K_f \eta D_{test}/PS^{cap}_{test}$, where η is the viscosity of the intracapillary solution, and D_{test} is the free diffusion coefficient of the test solute. The specific hydraulic conductivity and the osmotic reflexion coefficient of albumin are calculated from either the pore or fibre matrix theory and plotted against each other. When experimental measurements for both these quantities are introduced into the graphs, it was found that a single pore size could not account for both quantities but that a fibre matrix provided a good fit for data from both single capillaries and whole organs.

In one sense, the analysis of Curry and Huxley (1982) does not give the pore theory a fair chance. In deriving the specific hydraulic conductivity separate equations were used for K_f and PS. These are

$$K_f = \frac{A_w}{\Delta x} \cdot \frac{r^2}{8\eta} \qquad 4.4$$

$$PS = \frac{A_p}{\Delta x} \cdot \emptyset D'_{test} \qquad 4.5$$

where A_w is the area of cylindrical channels of radius r available for water flux, A_p is the pore area available for solute flux and Δx is the thickness of the membrane. $\emptyset$ and D'_{test} are defined by

$$\emptyset = (1 - a/r)^2 \qquad 4.6$$

$$D'_{test} = D_{test}\left[1 - 2.104\ (a/r) + 2.088\ (a/r)^3 - 0.95\ (a/r)^5\right] \qquad 4.7$$

It appears from their analysis that A_w has been equated to A_p, implying that all the water and solute traverse the capillary by the same route. If there is an 'exclusive' water pathway, a suggestion developed by Curry himself (Curry, Mason and Michel, 1976), then A_w should greater than A_p. If $A_w = 2.A_p$, then the data given by Curry and Huxley would be fitted very well by the pore theory equations.

The data for PS^{cap}_{alb} obtained in Chapter 2 are difficult to reconcile with a single pore model. Even with a small pore radius of 5 nm (Taylor and Granger, 1983) the observed restriction to diffusion is much greater than would be predicted from the restricted diffusion coefficient (eqn. 4.7) and the data of Mann et al (1979a). The fibre matrix theory makes it much easier to account for a very low large solute permeability while retaining a high small solute permeability, and the present data can be reconciled with those of Mann et al (1979a) by using a fibre radius of 0.5 nm and an

aqueous volume of 0.9. These values also provide a reasonable fit for the reflexion coefficient data presented in this Chapter.

The experiments described in this Chapter have shown that the conventional method of estimating solute reflexion coefficients using the osmotic transient technique has some serious limitations in an organ whose capillaries are highly permeable to the test solutes. Some of the problems were predicted and partially overcome using the model described in Chapter 3, but others (notably vascular compliance and osmotically induced alterations in capillary permeability) still require elucidation.

CHAPTER 5

Summary

and

Concluding Remarks

SUMMARY AND CONCLUDING REMARKS

Two approaches were used to investigate the permeability properties of the capillary endothelium in the rabbit submandibular gland

1. Transcapillary passage of radiolabelled albumin in the in situ gland. This study yielded the following information

σ_{alb}^{cap}	=	> 0.999	
PS_{alb}^{cap}	=	10^{-4} - 10^{-5}	ml $min^{-1} g^{-1}$
V_{EDTA}^{int} (∞)	=	16.7 ± 0.4	ml 100 g^{-1}
V_{alb}^{int} (∞)	=	2 - 4	ml 100 g^{-1}
IVV (control)	=	5.35 ± 0.12	ml 100 g^{-1}
IVV (stimulated)	=	6.03 ± 0.11	ml 100 g^{-1}

2. Osmotic weight transients induced by albumin, inulin and raffinose in the isolated gland perfused with Krebs-Albumin solution. The following values were obtained using this method.

K_f	=	1.354 ± 0.136 ml min^{-1} 100 $g^{-1} mm^{-1}$ Hg
σ_{alb}^{cap}	=	0.79 ± 0.041
σ_{inulin}^{cap}	=	0.3 ~ 0.4
σ_{raff}^{cap}	=	> 0.007 but probably < 0.2

These results extend the work of Mann et al (1979a) in an organ all of whose capillaries are fenestrated. There are, however, several problems of methodology and

interpretations which require highlighting:

1. In order to follow the passage of albumin into the tissue, a label must be attached, and this may alter the properties of the molecule. However, it is still safe to interpret the results in terms of the labelled molecule.

2. Since the value of K_f is essential to the estimation of solute reflexion coefficient, it is important to explore in detail the errors which could arise experimentally in its determination. A 10% error in K_f may be acceptable within the framework of a theory of transcapillary exchange, but the same error in σ_{alb}^{cap} would radically alter the relative importance of convection and diffusion for albumin exchange. Future work should concentrate on determining the time course of vascular compliance during the "filtration" phase of a venous pressure elevation so that a more accurate extrapolation to zero time may be made.

3. Some of the problems associated with an osmotic weight transient were predicted by the model developed in Chapter 3, particularly for the small solutes. If an accurate estimation of small solute reflexion coefficient is to be made, then it is necessary to know the cell hydraulic conductivity and the interstitial compliance. This information would mean that curve fitting could be carried out with more

confidence. However, it is unlikely that the reflexion coefficient of a solute as small as raffinose could be determined accurately, since the concentration required to produce a measurable weight change would lead to alterations of capillary permeability which would be difficult to correct for.

Despite the difficulties outlined above, a picture emerges of an endothelium which is highly permeable to small solutes yet perhaps more restrictive to macromolecules than continuous endothelium. This is in keeping with other recent work on fenestrated capillaries in the kidney and intestine. Perhaps it is the continuous capillaries that should be regarded as having "giant pores".

REFERENCES

ALVAREZ, O.A. and YUDILEVICH, D.L. (1967). Capillary permeability and tissue exchange of water, and electrolytes in stomach. Am. J. Physiol., 213, 315-322.

AMSTERDAM, A., OHAD, I. and SCHRAMM, M. (1969). Dynamic changes in the ultrastructure of the acinar cell of the rat parotid gland during the secretory cycle. J. Cell Biol., 41, 753-773.

ARCHER, F.L. and KAO, V.C.Y. (1968). Immunohistochemical identification of actomyosin in myoepithelium of human tissues. Lab. Invest., 18, 669-674.

ARTURSON, G., GROTH, T. and GROTTE, G. (1972). The functional ultrastructure of the blood-lymph barrier. Computer analysis of data from dog heart-lymph experiments using theoretical models. Acta. Physiol. Scand. Suppl. 374, 1-30.

BARCROFT, J. (1914). The Respiratory Function of the Blood. Cambridge: Cambridge University Press

BELL, D.R., PINTER, G.G. and WILSON, P.D. (1978). Albumin permeability of the peritubular capillaries in rat renal cortex. J. Physiol., 279, 621-640.

BENNETT, H.S., LUFT, J.H. and HAMPTON, J.C. (1959). Morphological classification of vertebrate capillaries. Am. J. Physiol., 196, 381-390.

BERNARD, C. (1858). De l'influence de deux ordres de nerfs qui determinent les variations de couleur du sang veineux dans les organes glandulaires. C. R. Acad. Sci.(Paris), 47, 245-253.

BILL, A. (1977). Plasma protein dynamics: albumin and IgG capillary permeability, extravascular movement and regional blood flow in unanaesthetised rabbits. Acta Physiol. Scand., 101, 28-42.

BLAIR-WEST, J.R., COGHLAN, J.P., DENTON, D.A., NELSON, J., WRIGHT, R.D. and YAMAUCHI, A. (1969). Ionic, histological and vascular factors in the reaction of the sheep's parotid to high and low mineralocorticoid status. J. Physiol., 205, 563-579.

BLINKS, J.R. (1965). Influence of osmotic strength on cross-section and volume of isolated single muscle fibres. J. Physiol., 177, 42-57.

BLOOM, G. and JOHNSON, J.A. (1981). A model for osmotically induced weight transient in the isolated rabbit heart. Microvasc. Res., 22, 64-79.

BRACE, R.A., GRANGER, D.N. and TAYLOR, A.E. (1978). Analysis of Lymphatic Protein Flux Data III. Use of the Nonlinear Flux Equation to Estimate σ and PS. Microvasc. Res., 16, 297-303.

BRACE, R.A. and GUYTON, A.C. (1976). Effect of hindlimb isolation procedure on isogravimetric capillary pressure and transcapillary fluid dynamics in dogs. Circ. Res., 38, 192-196.

BRANDTZAEG, P., GAUTVIK, K., NUSTAD, K. and PIERCE, J.V. (1976). Rat submandibular gland kallikreins: purification and cellular localization. Brit. J. Pharmacol., 56, 155-167.

BURAN, J. and SMAJE, L.H. (1982). The surface area of capillaries in the rabbit submandibular salivary gland. Microvasc. Res., 24, 238-239.

BURGEN, A.S.V. and SEEMAN, P. (1958). The role of the salivary duct system in the formation of the saliva. Canad. J. Biochem. Physiol., 36, 119-143.

CHAMBERS, R. and ZWEIFACH, B.W. (1947). Intercellular cement and capillary permeability. Physiol. Revs., 27, 436-463.

CHINARD, F.P., VOSBURGH, G.J. and ENNS, T. (1955). Transcapillary exchange of water and other substances in certain organs of the dog. Am. J. Physiol., 183, 221-234.

CLEMENTI, F. and PALADE, G.E. (1969). Intestinal capillaries. I. Permeability to peroxidase and ferritin. J. Cell. Biol., 41, 33-58.

CLOUGH, G.F. and SMAJE, L.H. (1984). Exchange area and surface properties of the microvasculature of the rabbit submandibular gland following duct ligation. J. Physiol., (in press).

COMPER, W.D. and LAURENT, T.C. (1978). Physiological function of connective tissue polysaccharides. Physiol. Revs., 58, 255-315.

CONWAY, E.J., GEOGHEGAN, H. and McCORMACK, J.I. (1955). Autolytic changes at zero Centigrade in ground mammalian tissues. J. Physiol., 130, 427-437.

CONWAY, E.J. and McCORMACK, J.I. (1953). The total intracellular concentration of mammalian tissues compared with that of the extracellular fluid. J. Physiol., 120, 1-14.

COOK, J.S. (1967). Nonsolvent water in human erythrocytes. J. Gen. Physiol., 50, 1311-1325.

CRONE, C. (1963). The permeability of capillaries in various organs as determined by use of the 'Indicator Diffusion Method'. Acta physiol. scand., 58, 292-305.

CRONE, C. and LEVITT, D.G. (1983). Capillary permeability to small solutes. In: "Handbook of Physiology - Cardiovascular System IV". Amer. Physiol. Soc., Washington DC.

CURRY, F.E. and HUXLEY, V.H. (1982). Comparison of the capillary membrane properties determining fluid exchange in single capillaries and whole organs. Int. J. Microcirc: Clin. Exp., 1, 381-391.

CURRY, F.E., MASON, J.C. and MICHEL, C.C. (1976). Osmotic reflexion coefficients of capillary walls to low molecular weight hydrophilic solutes measured in single perfused capillaries of the frog mesentery. J. Physiol, 261, 319-336.

FRASER, P.A. and SMAJE, L.H. (1977). The organization of the salivary gland microcirculation. J. Physiol., 272, 121-136.

FOX, J.R. and WAYLAND, H. (1979). Interstitial diffusion of macromolecules in the rat mesentery. Microvasc. Res., 18, 255-276.

FRIEDMAN, J.J. (1957). Vascular-extravascular equilibration of radioactive iodinated albumin in mice. Amer. J. Physiol., 191, 115-118.

GAMBLE, J., HAWKINS, J.D., PENN, W.P. and SPENCER, P.D. (1982a). Observations on the difference in movement of rat serum albumin (RSA) and human serum albumin (HSA) during peritoneal dialysis in the rat. J. Physiol., 325, 42P.

GAMBLE, J., HAWKINS, J.D., PENN, W.P. and SPENCER, P.D. (1982b). The effect of chloramine-T on the in vivo and in vitro behaviour of serum albumin. Microvasc. Res., 24, 238.

GAMBLE, J., SMAJE, L.H. and YOUNG, J.A. (1983). The effect of changed vascular pressures on salivation in the isolated rabbit submandibular gland. J. Physiol., 334, 79-80P.

GARRETT, J.R. (1972). Neuro-effector sites in salivary glands. pp. 83-97, In:"Oral Physiology", eds. N. Emmelin and Y. Zotterman, Oxford and New York: Pergamon Press.

GRABOWSKI, E. and BASSINGTHWAIGHTE, J.B. (1976).An osmotic weight transient model for estimation of capillary transport parameters in myocardium. In: "Microcirculation", eds. J. Grayson and W. Zingg, Vol 2, pp 29-50. Plenum, New York.

GRANGER, D.N. and BARROWMAN, J.A. (1983). Microcirculation of the alimentary tract. I Physiology of transcapillary fluid and solute exchange. Gastroenterology, 84, 846-868.

CURRY, F.E. and MICHEL, C.C. (1980). A fiber matrix model of capillary permeability. Microvasc. Res., 20, 96-99.

DAMON, D.H. and DULING, B.R. (1984). Distribution of capillary blood flow in the microcirculation of the hamster - an *in vivo* study using epifluorescent microscopy. Microvasc. Res., 27, 81-95.

DARKE, A.C. and SMAJE, L.H. (1972). Dependence of functional vasodilatation in the cat submaxillary gland upon stimulation frequency. J. Physiol., 226, 191-203.

DIAMOND, J.M. and BOSSERT, W.H. (1967). Standing-gradient osmotic flow. A mechanism for coupling of water and solute transport in epithelia. J. Gen. Physiol., 50, 2061-2083.

DOREY, G. and BHOOLA, K.D. (1972). I. Ultrastructure of acinar cell granules in mammalian submaxillary glands. Z. Zellforsch., 126, 320-334.

DRAKE, R. and DAVID, E. (1978). A corrected equation for the calculation of reflection coefficients. Microvasc. Res., 15, 259.

DRAKE, R.E., GAAR, K.A. and TAYLOR, A.E. (1978). Estimation of the filtration coefficient of pulmonary exchange vessels. Amer. J. Physiol., 234, H266-H274.

EMMELIN, N., GARRETT, J.R. and OHLIN, P. (1968). Neural control of salivary myoepithelial cells. J. Physiol., 196, 381-396.

FERREIRA, S.H. and SMAJE, L.H. (1976). Bradykinin and functional vasodilatation in the salivary gland. Br. J. Pharmac. 58, 201-209.

FRASER, P. (1972) The Relationship Between Plasma Protein Concentration and Colloid Osmotic Pressure. MSc Thesis, University of London.

FRASER, P.A. (1976). Microvascular flow in the submandibular salivary gland. PhD Thesis, University of London.

GRANGER, D.N., GRANGER, J.P., BRACE, R.A., PARKER, R.E. and TAYLOR, A.E. (1979). Analysis of the permeability characteristics of cat intestinal capillaries. Circ. Res., 44, 335-344.

GRANGER, D.N., MORTILLARO, N.A. and TAYLOR, A.E. (1978). Interactions of intestinal lymph flow and secretion. Amer. J. Physiol., 232, E13-E18.

GRANGER, D.N., RICHARDSON, P.D.I. and TAYLOR, A.E. (1979). Volumetric assessment of the capillary filtration coefficient in the cat small intestine. Pflug. Arch, 381, 25-33.

GRANGER, D.N. and TAYLOR, A.E. (1980). Permeability of intestinal capillaries to endogenous macromolecules. Amer. J. Physiol., 238, H457-H464.

GREENWOOD, F.C., HUNTER, W.M. and GLOVER, J.S. (1963). The preparation of ^{131}I-labelled human growth hormone of high specific radioactivity. Biochem. J. 89, 114-123.

GROTTE, G. (1956). Passage of dextran molecules across the blood-lymph barrier. Acta. Chir. Scand., 211, 1-84.

GUYTON, A.C. (1963). A concept of negative interstitial pressure based on pressures in implanted perforated capsules. Circ. Res., 12, 399-414.

GUYTON, A.C. (1965). Interstitial fluid pressure II. Pressure-volume curves of interstitial space. Circ. Res., 16, 452-460.

GUYTON, A.C., TAYLOR, A.E. and GRANGER H.J. (1975). Circulatory Physiology III. Dynamics and control of body fluids. W.B. Saunders Co., Philadelphia, Pa.

HARVEY, W. (1628). An anatomical disputation concerning the movement of the heart and blood in living creatures. (G. Whitteridge, Trans. 1976) Blackwell, Oxford.

HEIDENHAIN, R. (1872). Ueber die Wirkung eininger Gifte auf die Nerven der glandula submaxillaris. Pflugers Arch. ges. Physiol., 5, 309-318.

HILL, A. (1979). Osmosis. Quart. Rev. Biophys., 12, 67-99.

HILTON, S.M. and LEWIS, G.P. (1955a). The cause of the vasodilatation accompanying salivation in the submandibular salivary gland. J. Physiol. 128, 235-248.

HILTON, S.M. and LEWIS, G.P. (1955b). Mechanism of functional hyperaemia in the submandibular salivary gland. J. Physiol., 129, 253-271.

HOGAN, R.D. (1981). The initial lymphatics and interstitial fluid pressure. In "Tissue Fluid Pressure and Composition". ed A.R. Hargens, Williams and Wilkins Co., Baltimore, MD.

HOUSE, C.R. (1974). "Water Transport in Cells and Tissues". Arnold, London.

ICHIKAWA, A. (1965). Fine structural changes in response to hormonal stimulation of the perfused canine pancreas. J. Cell. Biol., 24, 369-385.

JOHANSSON, B.R. (1979). Capillary permeability to interstitial microinjections of macromolecules and influence of capillary hydrostatic pressure on endothelial ultrastructure. Acta.Physiol. Scand., Suppl.463, 45-50.

JOHNSON, J.A. (1966). Capillary permeability, extracellular space estimation, and lymph flow. Amer. J. Physiol., 211, 1261-1263.

JOHNSON, J.A. and BLOOM, G. (1981). Permeability and reflection coefficients from somotic transients - extravascular factors. Microvasc. Res., 22, 80-94.

JOHNSON, J.A., BLOOM, G., ANDERSON, S. and McEVOY, K. (1981). Intracapillary events in osmotic weight transients. Microvasc. Res., 22, 93-109.

JOHNSON, J.A., LEVITT, D.G., WANGENSTEEN, D. and BLOOM, G. (1975). A distributed pore size model for capillaries. Microvasc. Res., 10, 217-219.

JOHNSON, P.C. and HANSON, K.M. (1963). Relation between venous pressure and blood volume in the intestine. Amer. J. Physiol., 204, 31-34.

JOHNSON, P.C. and HANSON, K.M. (1966). Capillary filtration in the small intestine of the dog. Circ. Res., 19, 766-773.

JOHNSON, P.C. and RICHARDSON, D.R. (1974). The influence of venous pressure on filtration forces in the intestine. Microvasc. Res., 7, 296-306.

KARNOVSKY, M.J. (1967). The ultrastructural basis of capillary permeability studied with Peroxidase as a tracer. J. Cell. Biol., 35, 213-236.

KARNOVSKY, M.J. (1970). Morphology of capillaries with special reference to muscle capillaries. pp 341-350, In: "Capillary Permeability", Alfred Benzon Symposium II, eds. C. Crone and N.A. Lassen, Copenhagen: Munksgaard.

KATCHALSKY, A. and CURRAN, P.F. (1965). "Nonequilibrium Thermodynamics in Biophysics" 1st Ed., Cambridge, Mass: Harvard University Press.

KATZ, M.A. (1980). Dependency of permeability-surface area product upon solute concentration, and its significance in the interpretation of lymph flow data. Microvasc. Res., 20, 212-222.

KEDEM, O. and KATCHALSKY, A. (1958). Thermodynamic analysis of the permeability of biological membranes to non-electrolytes. Biochem. Biophys. Acta., 27, 229-246.

KEDEM, O. and KATCHALSKY, A. (1963). Permeability of composite membrane. Part 3. Series array of elements. Trans. Faraday Soc., 59, 1941-1953.

KETY, S.S. (1951). Theory and applications of the exchange of inert gas at the lung tissue. Pharmac. Rev., 3, 1-41.

KLITZMAN, B. and DULING, B.R. (1979). Microvascular haematocrit and red cell flow in resting and contracting striated muscle. Amer. J. Physiol., 237, H481-H490.

KNAUF, H. (1972). The isolated salivary duct as a model for electrolyte transport studies. Pflugers Arch., 333, 82-94.

KOO,A., SMAJE, L.H., DZIELGIELEWSKA, K.A., SPENCER, P.D. and PENN, W.P. (1980). Low permeability to macromolecules of the fenestrated capillaries in the cat mandibular salivary gland. Microvasc. Res., 20, 256-257.

KOWALEWSKY, N. (1885). Ueber das Blutgefasssystem der Speicheldrusen. Arch. Anat. Physiol. Anat. Abt., 385-395.

LANDIS, E.M. (1927). Micro-injection studies of capillary permeability. II. The relation between capillary pressure and the rate at which fluid passes through the walls of single capillaries. Amer. J. Physiol., 82, 217-238.

LANDIS, E.M. and PAPPENHEIMER, J.R. (1963). Exchange of substances through the capillary walls. In: "Handbook of Physiology, Circulation Vol. II, Section 2, pp 961-1034 Amer. Physiol. Soc., Washington DC.

LASSEN, N.A., PARVING, H.H. and ROSSING, N. (1974). Filtration as the main mechanism of transcapillary protein escape from the plasma. Microvasc.Res., 7, i-iv.

LEE, C.Y. and RYAN, R.J. (1973). Interaction of ovarian receptors with human luteinizing hormones and human chorionic gonadotropin. Biochemistry, 12, 4609-4615.

LEESON, C.R. (1959). Histological, histochemical and electron microscopic studies on the rat submaxillary gland, with special reference to its post-natal development. MD Thesis, Cambridge University.

LEVITT, D.G. (1970). Quantitation of the error in the E_o method of measurement of capillary permeability for certain capillary and organ models. In "Capillary Permeability", pp 81-103. Alfred Benzon Symposium II, Eds. C. Crone and N.A. Lassen, Copenhagen: Munksgaard.

LEVITT, D.G. (1975). General continuum analysis of transport through pores. I: Proof of Onsager's reciprocity postulate for uniform pores. Biophys. J., 15, 533-551.

LUFT, J.H. (1966). Fine structure of capillary and endocapillary layer as revealed by ruthenium red. Fedn. Proc., 25, 1773-1783.

LUNDBERG, J.M. (1981). Evidence for coexistence of vasoactive intestinal polypeptide (VIP) and acetylcholine in neurons of cat exocrine glands. Acta Physiol. Scand., Suppl. 496, 1-57.

LUNDVALL, J. and HOLMBERG, J. (1978). Dynamics of saliva secretion and tissue volume changes during parasympathetic stimulation in the constant flow perfused cat submandibular gland. Acta Physiol. Scand., 102, 382-384.

MANGOS, J.A., McSHERRY, N.R., IRWIN, K. and HONG, R. (1973). Handling of water and electrolytes by rabbit parotid and submaxillary glands. Amer. J. Physiol., 225, 450-455.

MANN, G.E. (1978). Capillary and epithelial exchange in the cat submandibular gland. PhD Thesis, University of London.

MANN, G.E., SMAJE, L.H. and YUDILEVICH, D.L. (1979a). Permeability of the fenestrated capillaries in the cat submandibular gland to lipid-insoluble molecules. J. Physiol., 297, 335-354.

MANN, G.E., SMAJE, L.H. and YUDILEVICH, D.L. (1979b). Transcapillary exchange in the cat salivary gland during secretion, bradykin infusion and after chronic duct ligation. J. Physiol., 297, 355-367.

MARANDA, B., RODRIGUES, J.A.A., SCHACHTER, M., SCHNITKA, T.K., and WEINBERG, J. (1978). Studies on kallikrein in the duct systems of the salivary glands of the cat. J. Physiol., 276, 321-328.

MARTIN, C.J., FROMTER, E., GEBLER, B., KNA , H., and YOUNG, J.A. (1973). The effects of carbachol on water and electrolyte fluxes and transepithelial electrical potential differences of the rabbit submaxillary main duct perfused in vitro. Pflugers Arch, 341, 131-142.

MARTIN DE JULIAN, P. and YUDILEVICH, D.L. (1964). A theory for the quantification of transcapillary exchange by tracer dilution curves. Amer. J. Physiol., 207, 162-168.

MATERAZZI, G., BONDI, A.M., BALDONI, E. and MARALDI, N. (1976). The ultrastructure of the rabbit submandibular gland. Anat. Anz., 140, 154-161.

MATSUDA, Y., MORIWAKA, C., PERET, M.W., SCHACHTER, M. and SCHNITKA, T.K. (1979). Localization of kallikrein in duct cells of submandibular gland in cat, dog, guinea-pig and man using immunocytochemical techniques. J. Physiol., 296, 84-85P.

MAYERSON, H.S., WOLFRAM, C.G., SHIRLEY, H.H. Jr and WASSERMAN, K. (1960). Regional differences in capillary permeability. Amer. J. Physiol., 198, 155-160.

MOHAMED, A.H. (1975). Ultrastructural permeability studies in capillaries of rabbit oral mucosa and salivary glands. Microvasc. Res., 9, 287-303.

MORTILLARO, N.A. and TAYLOR, A.E. (1976). Interaction of capillary and tissue forces in the cat small intestine. Circ. Res., 39, 348-358.

McMASTER, P.D. and PARSONS, R.J. (1939). Physiological conditions existing in the connective tissue. I. The spread of vital dyes. J. Exp. Med., 69, 247-264.

NOER, I. and LASSEN, N.A. (1979). Evidence of active transport (filtration?) of plasma proteins across the

capillary walls in muscle and subcutis. Acta. Physiol. Scand., Suppl. 463, 105-109.

OGSTON, A.G. (1958). The spaces in a uniform random suspension of fibres. Trans. Faraday Soc. 54, 1754-1757.

OGSTON, A.G. and MICHEL, C.C. (1978). General descriptions of passive transport of neutral solute and solvent through membranes. Prog. Biophys. Molec, Biol., 34, 197-217.

OGSTON, A.G. and PHELPS, C.F. (1961). The partition of solutes between buffer solutions containing hyaluronic acid. Biochem. J., 78, 827-833.

OGSTON, A.G., PRESTON, B.N. and WELLS, J.D. (1973). On the transport of compact particles through solutions of chain polymers. Proc. Roy. Soc. Lond. A., 333, 297-309.

OHTANI, O., KIKUTA, A., OHTSUKA, A., TAGUCHI, T., and MURAKAMI, T. (1983). Microvasculature as studied by the microvascular corrosion casting/scanning electron microscope method. I. Endocrine and digestive system. Arch. histol. jap., 46, 1-42.

OHTANI, O., OHTSUKA, A., LIPSETT, J., and GANNON, B. (1983). The microvasculature of rat salivary glands. A scanning electron microscopic study. Acta. Anat., 115, 345-356.

OPRESKO, L, WILEY, H.S. and WALLACE, R.A. (1980). Proteins iodinated by the chloramine-T method appear to be degraded at an abnormally rapid rate after endocytosis. Proc. Natl., Acad. Sci. USA, 77, 1556-1560.

OWEN, M. and TRIFFIT, J.T. (1976). Extravascular albumin in bone tissue. J. Physiol., 257, 293-307.

PAASKE, W.P. (1983). Microvascular exchange of albumin. Microvasc. Res., 25, 101-107.

PALADE, G.E., SIMIONESCU, M. and SIMIONESCU, N. (1979). Structural aspects of the permeability of the microvascular endothelium. Acta Physiol. Scand., Suppl. 463, 11-32.

PAPPENHEIMER, J.R., RENKIN, E.M.and BORRERO, L.M. (1951) Filtration, diffusion and molecular sieving through peripheral capillary membranes. A contribution to the pore theory of capillary permeability. Amer. J. Physiol., 167, 13-46.

PAPPENHEIMER, J.R. and SOTO-RIVERA, A. (1948). Effective osmotic pressure of the plasma proteins and other quantities associated with the capillary circulation in the hindlimbs of cats and dogs. Amer. J. Physiol., 471-491.

PARKER, R.E., GRANGER, D.N. and TAYLOR, A.E. (1981). Estimates of isogravimetric capillary pressures during alveolar hypoxia. Amer. J. Physiol., 241, H732-H739.

PATLAK, C.S., GOLDSTEIN, D.A. and HOFFMAN, J.F. (1963). The flow of solute and solvents across a two membrane system. J. Theor. Biol., 5, 426-442.

PEASE, D.C. (1956). Infolded basal plasma membranes found in epithelia noted for their water transport. J. Biophys. Biochem. Cytol., 2 (Suppl), 203-209.

PERL, W. (1975). Convection and permeation of albumin between plasma and interstitium. Microvasc. Res., 10, 83-94.

PERRY, M.A. (1980). Capillary filtration and permeability coefficients calculated from interendothelial cell junctions in rabbit lung and skeletal muscle. Microvasc. Res., 19, 142-157.

QUINTARELLI, G. (1963). Histochemical identification of salivary mucins. Ann. N.Y. Acad. Sci., 106, 339-363.

RENKIN, E.M. (1959). Transport of potassium-42 from blood to tissue in isolated mammalian skeletal muscles. Amer. J. Physiol., 197, 1205-1210.

RENKIN, E.M. (1964). Transport of large molecules across capillary walls. The Physiologist, 7, 13-28.

RENKIN, E.M. (1979). In "Pulmonary Edema" pp 145-159. Eds. A.P. Fishman and E.M. Renkin. Amer. Physiol. Soc., Bethesda, Maryland.

RENKIN, E.M., JOYNER, W.L., SLOOP, C.H. and WATSON, P.D. (1977). Influence of venous pressure on plasma-lymph transport in the dog's paw: convective and dissipative mechanisms. Microvasc. Res., 14, 191-204.

RICHARDSON, P.D.I., GRANGER, D.N. and TAYLOR, A.E. (1979). Capillary filtration coefficient: the technique and its application to the small intestine. Cardiovasc. Res., 13, 547-561.

ROBINSON, J.R. (1953). The active transport of water in living systems. Biol. Revs., 28, 158-194.

SCHACHTER, M. (1980). Kallikreins (kininogenases) - a group of serine proteases with bioregulatory actions. Pharmacol. Revs., 31, 1-17.

SCHACHTER, M., MARANDA, B. and MORIWAKA, C. (1978). Localization of kallikrein in the coagulating and submandibular glands of the guinea-pig. J. Histochem. Cytochem., 26, 318-321.

SELINGER, Z., SHARONI, Y. and SCHRAMM, M. (1974). Modification of the secretory granule during secretion in the rat parotid gland. In "Advances in Cytopharmacology". Vol. 2, pp 23-28. Eds. B. Ceccarelli, F. Clementi and J. Meldolesi. Raven Press, New York.

SELKURT, E.E. (Ed.) (1976). "Physiology", 4th Edition. Little Brown Co., Boston, Mass.

SHACKLEFORD, J.M. and WILBORN, W.H. (1968). Structural and histochemical diversity in mammalian salivary glands. Ala. J. med. Sci., 5, 180-203.

SHANNON, I.A., SUDDICK, R.P. and DOWD, F.J. (1974) "Saliva; Composition and Secretion". Basel: Karger.

SIMIONESCU, N., SIMIONESCU, M. and PALADE, G.E. (1972). Permeability of intestinal capillaries. Pathway followed by dextrans and glycogen. J. Cell. Biol., 53, 365-392.

SIMIONESCU, N., SIMIONESCU, M. and PALADE, G.E. (1973). Permeability of muscle capillaries to exogenous myoglobin. J. Cell. Biol., 57, 424-454.

SIMIONESCU, N., SIMIONESCU, M. and PALADE, G.E. (1975). Permeability of muscle capillaries to small heme-peptides. Evidence for the existence of patent trans-endothelial channels. J. Cell. Biol., 64, 586-607.

SIMSON, J.A.V., CHAO, J. and MARGOLIUS, H.S. (1978). Cytochemical localization and secretagogue-induced release of kallikrein and nerve growth factor from rodent salivary glands. Anat. Rec., 190, 542-543.

SMAJE, L.H. (1973). Spontaneous salivation in the rabbit submandibular gland. J. Physiol., 231, 179-193.

SMAJE, L.H. and HENDERSON, J.R. (1984). Microcirculation of the exocrine glands. In: "Physiology and Pharmacology of the Microcirculation".

SMAJE, L.H. and SWAYNE, G.T.G. (1983). Distensibility of single capillaries in the frog mesentery. J. Physiol., 343, 73-74P.

STARLING, E.H. (1896). On the absorption of fluids from the connective tissue spaces. J. Physiol., 19, 312-326.

STAVERMAN, A.J. (1951). The theory of measurement of osmotic pressure. Rec. Trav. Chim. des Pays-Bas et de la Belgique, 70, 344-352.

STUDER, R. and POTCHEN, J. (1971). The radioisotopic assessment of regional microvascular permeability to macromolecules. Microvasc. Res., 3, 35-48.

SUDDICK, R.P. and DOWD, F.J. (1969). The microvascular architecture of the rat submaxillary gland: possible

relationship to secretory mechanisms. Arch. oral. Biol., 14, 567-576.

SVIRIDOVA, I.K. (1970). Intraorganic lymphatic bed of the human parotid salivary gland (trans). Arkh. Anat. Gistol. Embriol., 59, 10-18.

TAMARIN, A. (1966). Myoepithelium of the rat submaxillary gland. J. Ultrastruct. Res., 16, 320-338.

TANDLER, B. and POULSEN, J.H. (1977). Ultrastructure of the cat sublingual gland. Anat. Rec., 187, 153-159.

TAYLOR, A.E. and GRANGER, D.N. (1983). Equivalent pore modeling: vesicles and channels. Fedn. Proc., 42, 2440-2445.

TENLAND, T. (1982). On laser doppler flowmetry. Methods microvascular applications. Linkoping Studies Sci. Technol. Dissertations No 83, Linkoping University, Sweden.

TERROUX, K.G., SEKELJ, P. and BURGEN, A.S.V. (1959). Oxygen consumption and blood flow in the submaxillary gland of the dog. Can. J. Biochem. Physiol., 37, 5-15.

THAYSEN, J.H., THORN, N.A. and SCHWARTZ, I.L. (1954). Excretion of sodium, potassium, chloride and carbon dioxide in human parotid saliva. Amer. J. Physiol., 178, 155-159.

THOMAS, S.R. and MIKULECKY, D.C. (1978). Transcapillary solute exchange. A comparison of the Kedem-Katchalsky convection-diffusion equations with the rigorous non-linear equations for this special case. Microvasc. Res., 15, 207-220.

UNGAR, G. and PARROT, J-L. (1936). Sur la presence de la callicreine dans la salive, et la possibilite de son intervention dans la transmission chimique de l'influence nerveux. C. R. Soc. Biol. (Paris), 122, 1052-1055.

VARGAS, F and JOHNSON, J.A. (1964). An estimate of reflexion coefficients for rabbit heart capillaries. J. Gen. Physiol., 47, 667-677.

VARGAS, F. and JOHNSON, J.A. (1967). Permeability of rabbit heart capillaries to non-electrolytes. Amer. J. Physiol., 213, 87-93.

VIRCHOW, R. (1859). Cellular pathology. (F. Chance, trans. 1860). Re-issued 1971, Dover, New York.

WALLENTIN, I. (1966). Importance of tissue pressure for the fluid equilibrium between the vascular and interstitial compartments in the small intestine. Acta. Physiol. Scand., 68, 304-315.

WATSON, P.D. (1980). The interstitial matrix as a barrier in blood-to-lymph solute movement. The Physiologist, 23, 86-89.

WATSON, P.D., BELL, D.R. and RENKIN, E.M. (1978). The equilibration of macromolecules in dog leg lymph. Microvasc. Res., 15, 273.

WATSON, P.D., BELL, D.R. and RENKIN, E.M. (1980). Early kinetics of large molecule transport between plasma and lymph in dogs. Amer. J. Physiol., 239, H525-H531.

WIEDERHIELM, C.A. and BLACK, L.L. (1976) Osmotic interaction of plasma proteins with interstitial macromolecules. Amer. J. Physiol., 231, 638-641.

YOUNG, J.A. and van LENNEP, E.W. (1978a). Transport in Salivary and Salt Glands. In "Membrane transport in Biology" Vol. IV. Eds. G. Giebisch, D.C. Tosteson, H.H. Ussing. Springer, New York.

YOUNG, J.A. and van LENNEP, E.W. (1978b) "The Morphology of Salivary Glands". Academic Press, London.

YOUNG, J.A. and SCHNEYER, C.A. (1981). Composition of saliva in Mammalia. Aust. J. Exp. Biol. Med. Sci., 59, 1-53.

ZADUNIASKY, J.A., PARISI, M.N. and MONTOREANO, R. (1963). Effect of antidiuretic hormone on permeability of single muscle fibres. Nature, 200, 365-366.

Additional References

RUTILI, G., and ARFORS, K-E. (1976). Fluorescein-labelled dextran measurement in interstitial fluid in studies of macromolecular permeability. Microvasc. Res., 12, 221-230

WATSON, P.D. (1983). Effects of blood-free and protein-free perfusion of CFC in the isolated cat hindlimb. Amer. J. Physiol., 245, H911-H919.

APPENDIX 1 - LIST OF SYMBOLS

Main Symbols

K_f - hydraulic conductivity of capillary wall

K_{cell} - hydraulic conductivity of cell wall

K_L - hydraulic conductivity of lymphatics

PS - permeability-surface area product

σ - reflexion coefficient

J - flux

C - concentration

V - volume

R - universal gas constant; lymph:plasma ratio; pre to post-capillary resistance ratio.

T - absolute temperature

P - hydrostatic pressure

π - osmotic pressure

Δ - difference

E - elasticity; extraction

t - time

N - number of capillary segments (for osmotic transient model)

ε - aqueous volume

r_f - fibre radius

a - molecular radius

IVV - intravascular volume

W - weight

A - amount

Main Symbols cont.

Σ - sum

F - perfusate flow

H - haematocrit

Δx - path length

Superscripts - refer to compartments within which, or barrier across which, the main symbol pertains.

cap - capillary

int - interstitium

L - lymphatic

sal - saliva

*seg*1 - 1st capillary segment (osmotic transient model)

*seg*N - Nth capillary segment (osmotic capillary model)

ven - venous effluent

art - arterial inflow

pl - plasma

Subscripts - refer to molecular species, the property of which is defined by the main symbol

alb - albumin

inulin - inulin

raff - raffinose

test - test molecule

Subscripts cont.

i	-	general solute
prot	-	protein
buff	-	buffer
v	-	volume (relating to flux)
B	-	blood
g	-	gland

Other Symbols

λ	-	$J_v(1 - \sigma)/PS$
α	-	PS/F
o, t, ∞	-	value of main parameter at time O, t or ∞
τ	-	time constant
η	-	viscosity
$\emptyset$	-	partition coefficient
n outside brackets	-	value of quantity inside brackets after n iterations of the computer program

APPENDIX 2

Computer program for model of extravascular albumin accumulation

```
10 PRINTER 3
20 C0=100
30 C2=0
40 A2=0
50 T1=0
60 INPUT"REFLEXION COEFFICIENT.....",S
70 INPUT"LYMPH FLOW (ML/MIN/G).....",L
80 INPUT"EXTRAVASCULAR VOL (ML/G)..",V2
90 INPUT"SALIVARY FLOW (ML/MIN/G)..",S2
100 INPUT"SHORT PLASMA TIME CONSTANT",H1
110 INPUT"INTERCEPT OF FAST EXPONENTIAL",A1
120 A2=1-A1
130 INPUT"LONG PLASMA TIME CONSTANT.",H2
140 INPUT      "UPPER LIMIT OF PS PRODUCT (ML/MIN/G)",X
150 INPUT"PS PRODUCT STEP INTERVAL",Y
160 F=S2+L
170 FORP=0.00001TOXSTEPY
180 LPRINTTAB(10);"PS PRODUCT";TAB(25);"SIGMA";TAB(40);"FILTRATION"
190 LPRINTTAB(10);P;TAB(25);S;TAB(40);F
200 LPRINT
210 LPRINT
220 LPRINTTAB(10);"TIME";TAB(25);"IV CONC.";TAB(40);"EV CONC.";TAB(55);"SPACE"
230 T1=0
240 FORB=1TO360
250 C1=C0*(A1*EXP(-T1/H1)+A2*EXP(-T1/H2))
260 T1=T1+1
270 Z=F*(1-S)/P
280 J=F*(1-S)*(C1-C2*EXP(-Z))/(1-EXP(-Z))
290 A2=A2+J
300 C2=A2/V2
```

```
310 FORD=10TO360STEP10
320 IFT1=DGOTO350
330 NEXTD
340 NEXTB
350 LPRINTTAB(10);T1;TAB(25);C1;TAB(40);C2;TAB(55);C2*V2/C1
360 IFB<360GOTO340
370 A2=0
380 C2=0
390 LPRINT
400 LPRINT
410 LPRINT
420 LPRINT
430 LPRINT
440 NEXTP
450 STOP
460 END
```

APPENDIX 3

Computer program for osmotic transient model

```
10 REM THIS PROGRAM IS CALLED CAP 2
20 CLEAR2000
30 PRINTER3
40 DIMH(30),C1(30),C2(30),C3(30)
50 DIMJ1(30),K1(30),K2(30),K3(30)
60 DIMV1(30),A1(30),A2(30),A3(30)
70 INPUT"NAME OF TEST SOLUTE",T$
80 LPRINTTAB(50);"TEST SOLUTE=  ";T$
90 LPRINT
100 LPRINT
110 LPRINT "INPUT PARAMETERS"
120 LPPINT
130 LPRINT
140 LPRINT TAB(40);"CONDUCTANCES (ML/MIN/100G/mmHg)"
150 LPRINTTAB(20);"CAPILLARY";TAB(40);"CELL";TAB(60);"LYMPH"
160 PRINT"TYPE IN CAPILLARY ,CELL,AND LYMPH CONDUCTANCES (ML/MIN/100G/mmHg)"
170 INPUTK1,K2,K3
180 LPRINTTAB(22);K1;TAB(40);K2;TAB(60);K3
190 LPRINT
200 LPRINT
210 LPRINT
220 LPRINTTAB(20);"REFLEXION COEFFICIENTS";TAB(80);"PS PRODUCTS (ML/MIN/G)"
230 LPRINTTAB(15);"ALB";TAB(30);"BUFFER";TAB(45);"TEST SOLUTE";TAB(75)"ALB";TAB(90);"BUFFER";TAB(105);"TEST SOLUTE"
240 PRINT"TYPE IN REFLEXION COEFFICIENTS FOR ALBUMIN, BUFFER AND TEST SOLUTE"
250 INPUTS1,S2,S3
260 PRINT"TYPE IN PS PRODUCTS(ML/MIN/G) FOR ALBUMIN, BUFFER AND TEST SOLUTE"
270 INPUTP1,P2,P3
280 LPRINTTAB(17);S1;TAB(32);S2;TAB(50);S3;TAB(77);P1;TAB(92);P2;TAB(110);P3
290 LPRINT
300 LPRINT
310 LPRINTTAB(15);"INTRAVASCULAR CONCENTPATIONS";TAB(90);"EXTRAVASCULAR CONCENTRATIONS"
320 LPRINTTAB(15);"ALB";TAB(30);"BUFFER";TAB(45);"TEST SOLUTE";TAB(75);"ALB";TAB(90);"BUFFER";TAB(105);"TEST SOLUTE"
330 PRINT"TYPE IN INTRAVASCULAR CONCENTRATIONS OF ALBUMIN (g/100ml),BUFFER (mM) AND TEST SOLUTE (mM)"
340 INPUTC1,C2,C3
350 PRINT"TYPE IN EXTRAVASCULAR CONCENTPATIONS OF ALBUMIN (g/100ml),BUFFER (mM) AND TEST SOLUTE (mM)"
360 INPUTE1,E2,E3
370 LPRINTTAB(16);C1;TAB(31);C2;TAB(49);C3;TAB(76);E1;TAB(91);E2;TAB(109);E3
380 LPPINT
390 LPRINT
400 LPPINT
410 LPRINTTAB(20);"TIME";TAB(40);"WEIGHT";TAB(60);"ISF VOL";TAB(80);"ISF PRESSUPE";TAB(100);"CELL VOL";TAB(115);"PERF. FLOW RATE"
420 LPRINT
430 LPRINT
440 PRINT"TYPE IN PERFUSATE FLOW RATE,LYMPH FLOW AND SALIVA FLOW (ML/MIN/G)"
450 INPUTQ0,L,Q1
460 INPUT"GLAND WEIGHT",W
470 INPUT"INTEPSTITIAL STIFFNESS (mm Hg/ml) FOR VOLUMES ABOVE INITIAL",E6
480 INPUT"INTERSTITIAL STIFFNESS (mm Hg/ml) FOR VOLUMES BELOW INITIAL",E7
490 INPUT MOLECULAP RADIUS OF TEST SOLUTE",R6
500 N2=40
```

```
510 N4=200
520 V0=0.06*W
530 V2=0.165*W
540 V1=V2*EXP(-1.68)
550 C5=1.5
560 C6=300
570 V9=0.5*W
580 V8=V9
590 C7=C5
600 C8=C6
610 V3=V2*EXP(-R6*(0.6+R6)/9)
620 INPUT"NO. OF CAPILLAPY SEGMENTS",N1
630 INPUT"NO. OF DATA POINTS",N3
640 INPUT"ARTERIAL PRESSURE (mm Hg)",H1
650 INPUT"VENOUS PRESSURE (mm Hg)",H2
660 FORZ=1TON1
670 H(Z)=H1-(Z-1)*(H1-H2)/N1
680 C1(Z)=C1
690 C2(Z)=C2
700 V1(Z)=V0/N1
710 NEXTZ
720 FORJ=1TON1
730 B=H(J)+B
740 NEXTJ
750 H4=(K1*B/N1-100*(S0+L)-K1*S1*(2.8*(C1-E1)+.18*(C1^2-E1^2)+.012*(C1^3-E1^3)))/(K1+K3)
760 PRINTH4
770 DIM W(250),T(250),D1(250),D2(250),D3(250),S1(250),S2(250),L(250)
780 DIME1(250),E2(250),E3(250),X1(250),X2(250),X3(250)
790 T1=(V0*60)/(N1*Q0)
800 M=T1*W/6000
810 V4=V2
820 INPUT"DO YOU WANT A VENOUS PRESSURE ELEVATION (TYPE P) OR A TEST SOLUTE ADDITION (TYPE A)?",U$
830 IFU$><"P"GOTO870
840 INPUT"HOW MUCH (mm Hg) IS THE PRESSURE STEP ?",D
850 C3=0
860 GOTO880
870 D=0
880 FOR Y=2 TO 4
890 IF Y><2 GOTO 940
900 N2=N2
910 F=1
920 C4=0
930 GOTO 1100
940 IF Y><3 GOTO 1020
950 F=N2+1
960 N2=N2+N3
970 C4=C3
980 FORZ9=1TON1
990 H(Z9)=H1-(Z9-1)*(H1-H2-D)/N1
1000 NEXTZ9
```

```
1010 GOTO 1100
1020 GOTO1030
1030 F=N2+1
1040 N2=N2+N4
1050 C4=0
1060 FORZ9=1TON1
1070 H(Z9)=H1-(Z9-1)*(H1-H2)/N1
1080 NEXTZ9
1090 GOTO 1100
1100 FOR X=F TO N2
1110 FORZ=1TON1
1120 J1(Z)=P1*M*(H(Z)-H3)-M*K1*17.02*(S2*(C2(Z)-E2)+S3*(C3(Z)-E3))-S1*M*K1*(2.8*(C1(Z)-E1)+.18*(C1(Z)^2-E1^2)+.012*(C1(Z)^3-E1^3)
1130 J1(Z)=J1(Z)/N1
1140 G1=J1(Z)*(1-S1)/P1
1150 G2=J1(Z)*(1-S2)/P2
1160 G3=J1(Z)*(1-S3)/P3
1170 K1(Z)=J1(Z)*(1-S1)*(C1+(C1-E1)/(EXP(-G1)-1))
1180 X1=X1+S1*(2.8*(C1(Z)-E1)+.18*(C1(Z)^2-E1^2)+.012*(C1(Z)^3-E1^3))
1190 K2(Z)=J1(Z)*(1-S2)*(C2+(C2-E2)/(EXP(-G2)-1))
1200 K3(Z)=J1(Z)*(1-S3)*(C3+(C3-E3)/(EXP(-G3)-1))
1210 J1=J1+J1(Z)
1220 C7=C5*V9/V8
1230 C8=C6*V9/V8
1240 P1=P1+K1(Z)
1250 P2=P2+K2(Z)
1260 P3=P3+K3(Z)
1270 A1(Z)=C1(Z)*V1(Z)/6.9
1280 A2(Z)=C2(Z)*V1(Z)
1290 A3(Z)=C3(Z)*V1(Z)
1300 V1(Z)=V1(Z)-J1(Z)
1310 C1(Z)=(A1(Z)-K1(Z))*6.9/V1(Z)
1320 C2(Z)=(A2(Z)-K2(Z))/V1(Z)
1330 C3(Z)=(A3(Z)-K3(Z))/V1(Z)
1340 IFX>20THENGOTO1360
1350 PRINTTAB(15);C1(Z);TAB(30);C2(Z);TAB(45);C3(Z);TAB(60);V1(Z)
1360 NEXTZ
1370 IFX>20THENGOTO1390
1380 PPINT
1390 J2=K2*M*((E1-C7)/6.9+(E2-C8)+E3)*17.02
1400 V8=V8-J2
1410 IF H3<0 THEN L=0 ELSE L=H3*P3*M
1420 P=J1+J2-(L+S0)*100*M
1430 B1=(E1*V1-L*E1*100*M)/6.9
1440 B2=E2*V2-L*E2*100*M
1450 B3=E3*V3-L*E3*100*M
1460 V1=V2*EXP(-0.2772/V2)
1470 V2=V2+P
1480 V3=V2*EXP(-0.0183*P6*(0.6+P6)/V2)
1490 IFV2>0.165THENH3=H4+E6*(V2-0.165)ELSEH3=H4+E7*(V2-0.165)
1500 E1=(E1+P1)*6.9/V1
```

```
1510 E2=(E2+R2)/(V2)
1520 E3=(E3+P3)/V3
1530 W=W-V1(N1)-100*M*(L+S0)+V0/N1
1540 U=40
1550 IFX/U><INT(X/U)THEN1690
1560 X1(X/U)=X1/N1
1570 X2(X/U)=X2/N1
1580 X3(X/U)=X3/N1
1590 W(X/U)=W
1600 D1(X/U)=C1(N1)
1610 D2(X/U)=C2(N1)
1620 D3(X/U)=C3(N1)
1630 S1(X/U)=J1
1640 S2(X/U)=J2
1650 L(X/U)=L
1660 E1(X/U)=E1
1670 E2(X/U)=E2
1680 E3(X/U)=E3
1690 J1=0
1700 J2=0
1710 P1=0
1720 R2=0
1730 R3=0
1740 X1=0
1750 X2=0
1760 X3=0
1770 FOR P=N1 TO 2 STEP -1
1780 V1(P)=V1(P-1)
1790 C1(P)=C1(P-1)
1800 C2(P)=C2(P-1)
1810 C3(P)=C3(P-1)
1820 NEXT P
1830 V1(1)=V0/N1
1840 C1(1)=C1
1850 C2(1)=C2
1860 C3(1)=C4
1870 T=T+T1
1880 IFX/U><INT(X/U)THEN1910
1890 T(X/U)=T
1900 LPRINTTAB(20);T;TAB(40);W;TAB(60);V2;TAB(80);H3;TAB(100);V8;TAB(120);V1(N1)*60/T1
1910 NEXT X
1920 NEXT Y
1930 LPRINT
1940 LPRINT
1950 LPRINT
1960 LPPINT
1970 LPPINTTAB 10);"TIME (SEC)";TAB(25);"WEIGHT (G)";TAB(50);"VENOUS CONCENTPATIONS";TAB(85);"VOLUME FLUX COMPONENTS"
1980 LPRINTTAB(40);"ALBUMIN ";TAB(55);"BUFFER ";TAB(70);"TEST";TAB(85);"CAPILLARY ";TAB(100);"CELL";TAB(115);"LYMPH
1990 FORI=1TON2/U
2000 LPRINTTAB 10);T(I);TAB(25);W(I);TAB(40);D1(I);TAB(55);D2(I);TAB(70);D3(I);TAB(85);S1(I);TAB(100);S2(I);TAB(115);L(I)
```

```
2010 NEXTI
2020 LPRINT
2030 LPRINT
2040 LPRINT
2050 LPRINTTAB(55)"- - - - - - - - - - - - - - - - - - - - - "
2060 LPRINT
2070 LPRINT
2080 LPPINTTAB(20);"TIME (sec)";TAB(40);"RATE OF WT. LOSS";TAB(80);"EXTRAVASCULAR CONCENTPATIONS (mM)"
2090 LPRINTTAB(44)"(Mg/sec)";TAB(60);"ALBUMIN";TAB(80);"BUFFER";TAB(100);"TEST"
2100 LPRINT
2110 FORI=1TON2/U
2120 LPPINTTAB(20);T(I);TAB(42);1000*(W(I)-W(I-1))/(U*T1);TAB(60);E1(I);TAB(80);E2(I);TAB(100);E3(I)
2130 NEXTI
2140 LPRINT
2150 LPPINT
2160 LPRINTTAB(50);"OSMOTIC PPESSURE DIFFERENCES"
2170 LPRINTTAB(20);"TIME";TAB(40);"ALBUMIN";TAB(60);"BUFFEP";TAB(80);"TEST SOLUTE"
2180 LPRINT
2190 FORI=1TON2/U
2200 LPRINTTAB(20);T(I);TAB(40);X1(I);TAB(60);X2(I);TAB(80);X3(I)
2210 NEXTI
2220 END
```